68 Topics in Current Chemistry
Fortschritte der chemischen Forschung

Theory

Springer-Verlag
Berlin Heidelberg New York 1976

This series presents critical reviews of the present position and future trends in modern chemical research. It is addressed to all research and industrial chemists who wish to keep abreast of advances in their subject.

As a rule, contributions are specially commissioned. The editors and publishers will, however, always be pleased to receive suggestions and supplementary information. Papers are accepted for "Topics in Current Chemistry" in either German or English.

ISBN 3-540-07932-7 Springer-Verlag Berlin Heidelberg New York
ISBN 0-387-07932-7 Springer-Verlag New York Heidelberg Berlin

Library of Congress Cataloging in Publication Data. Main entry under title: Theory. (Topics in current chemistry; 68). Includes bibliographical references and index. CONTENTS: Chapuisat, X. and Jean, Y. Theoretical chemical dynamics: a tool in organic chemistry. – Papoušek, D. and Špirko, V. A new theoretical look at the inversion problem in molecules. – Schneider, H. Ion solvation in mixed solvents. 1. Chemistry, Physical and theoretical – Addresses, essays, lectures. I. Chapuisat, Xavier, 1946 – Theoretical chemical dynamics. 1977. II. Papoušek, Dušan. A new theoretical look at the inversion problem in molecules. 1977. III. Schneider, Hermann. Ion solvation in mixed solvents. 1977. IV. Series. QD1.F58 vol. 68 [QD455] 540'.8s [541] 76-44447

Printed in Germany

Typesetting and printing: Schwetzinger Verlagsdruckerei GmbH, 6830 Schwetzingen. Bookbinding: Konrad Triltsch, Graphischer Betrieb, 8700 Würzburg

Contents

Theoretical Chemical Dynamics: A Tool in Organic Chemistry
Xavier Chapuisat and Yves Jean 1

A New Theoretical Look at the Inversion Problem in Molecules
Dušan Papoušek and Vladimír Špirko 59

Ion Solvation in Mixed Solvents
Hermann Schneider 103

Author Index Volumes 26–68 149

Theoretical Chemical Dynamics: A Tool in Organic Chemistry

Dr. Xavier Chapuisat and Dr. Yves Jean

Laboratoire de Chimie Théorique*, Université de Paris XI – Centre d'Orsay, Faculté des Sciences, F-91405 Orsay, France

Contents

Foreword 3

A. Trajectory Studies in Chemical Dynamics 4
1. Introduction 4
2. Trajectory Studies of Small Molecular Systems 6

B. A General Framework for Chemical Dynamics Studies in Organic Chemistry 11
I. The Cubic Splines for Expression of the Potential Energy Function . 12
1. Introduction 12
2. One Dimensional Cubic Splines 14
3. Cardinal Splines 17
4. Supplementary Indications for Practical Use 20
a) Reduction in the Case of Equal Intervals 20
b) Differentiation 21
c) The Cubic Spline Functions in Classical Dynamical Studies . . . 21
5. Conclusion 23
II. A Formulation of Classical Mechanics for Constrained Molecular Systems in Chemical Dynamics 23
1. Introduction 23
2. Classical Mechanics of Constrained Systems within Lagrangian and Hamiltonian Formalisms 24
3. Discussion 27
4. Conclusion 28
III. Some Remarks on How to Select Initial Conditions 28
1. Introduction 28
2. Physical Observables and Phase Variables 29
3. Unimolecular Reactions 30

* The Laboratoire de Chimie Théorique is associated to the C. N. R. S. (ERA n°549).

C. Applications: Optical and Geometrical Isomerizations of Cyclopropane . . 32
I. Experiments and Previous Theoretical Investigations 32
II. Potential Energy Surface 34
III. Dynamical Study 38
1. Equations of Motion and Initial Conditions 38
2. Dynamical Results 41
a) Synchronous Conrotatory Motion 41
b) Synchronous Disrotatory Motion 47
c) General Motion 47
3. Conclusion 50

General Conclusion 51

References 52

Foreword

Obtaining the rate of a chemical reaction from the knowledge of the collisional elementary processes governing it, defines approximately the field of Chemical Dynamics. In most cases the investigation is restricted to molecular systems including a few atoms for the following reasons:

(i) the experiments for analyzing a flux of molecules in various intramolecular states are limited for technical reasons;

(ii) it is only in the case of small systems that "ab initio" potential energy surfaces can be computed over a wide range of coordinates where the dynamic can be studied rigorously.

The present article is a contribution for extending the scope of Chemical Dynamics in Organic Chemistry. In the first Chapter (A), previous trajectory studies in Chemical Dynamics are reviewed. The second Chapter (B) presents a general but elementary method for undertaking the dynamical study of any chemical reaction. This method seems to be applicable in a straightforward way to rather large molecular systems in Organic Chemistry. An application of this method is presented in the third Chapter (C): the optical and geometrical isomerizations of cyclopropane are treated dynamically[a]. It makes use of an ab initio potential energy surface[2-4]. The results are, as far as possible, compared with experimental results[b].

It should be emphasized that classical trajectories methods at present can be considered as fairly standard techniques for studying the dynamical behaviour of small molecular systems (either triatomic or tetraatomic). As a consequence many technical points have already been discussed in great detail in the literature[7-9] and they will not be discussed here. Such technical questions are, for instance:

(i) should a parameter defining an initial state be either scanned or sampled in a random way (Monte-Carlo methods)? ;

(ii) should the sampled points have uniform density or be distributed according to some weighting function?;

(iii) should quantized values of the initially observable quantities be exclusively selected? etc . . .

Other important topics related to the technology of trajectories will not be discussed either, for instance:

(iv) which integrator should be used to obtain the best compromise between stability and efficiency?[10-12];

(v) what are suitable tests to stop a trajectory integration according to the type of outcome produced?[7]

(vi) what type of semi-empirical potential should be preferentially used for a given reaction?[8] etc . . .

We will restrict this article to developing in detail our original contribution to the study of Chemical Dynamics in the field of Organic Chemistry. Consequently we will not say much about the connection between our work and semi-empirical statis-

---

a) This study was previously published in the Journal of the American Chemical Society[1,2].

b) More details on the subject can be found in our two "Thèses de Doctorat d'Etat": Yves Jean, Orsay (1973)[5] and Xavier Chapuisat, Orsay (1975)[6].

tical methods of chemical reactivity, such as the transition state method or the Rice-Ramsperger-Kassel-Marcus (RRKM) theory of unimolecular reactions[13–15]. The two points of view, dynamical and semi-empirical, differ greatly. Once again, the comparison is only meaningful in the case of small molecular systems for which complete and rigorous results have been obtained within both methodologies.

Finally, in view of all the restrictions above, the title of this article could as well be: "What can we do with trajectories in Organic Chemical Dynamics and under what kind of restrictions (drastic or not) is it possible?"

A. Trajectory Studies in Chemical Dynamics

1. Introduction

In this chapter we define the scope of this article, mention some studies relevant to it and give references where these studies are dealt with.

It is quite simple to say that this article deals with Chemical Dynamics. Unfortunately, the simplicity ends here. Indeed, although everybody feels that Chemical Dynamics lies somewhere between Chemical Kinetics and Molecular Dynamics, defining the boundaries between these different fields is generally based more on surmisal than on knowledge. The main difference between Chemical Kinetics and Chemical Dynamics is that the former is more empirical and the latter essentially mechanical. For this reason, in the present article we do not deal with the details of kinetic theories. These are reviewed excellently elsewhere[16–21]. The only basic idea which we retain is the reaction rate. Thus the purpose of Chemical Dynamics is to go beyond the definition of the reaction rate of Arrhenius (activation energy and frequency factor) for interpreting it in purely mechanical terms.

This field of research is subject to rapid expansion at present because the improvement of sophisticated experimental methods coincides with an increase of the computational possibilities for the theoretical investigation of both the mechanical study of the nuclear motion and the quantum mechanical study of the electron potential governing this motion.

The experimental situation has been the subject of several recent review papers, either general[22–24] or more specialized (molecular beams[25–32], infrared chemiluminescence[33], reactions of small molecules in excited states[34], etc . . .). The quantum mechanical theoretical approaches of Chemical Dynamics were also reviewed recently[8, 35, 36].

Since the scope of this article is purely theoretical, we just outline below the state of the experimental situation. The ideal experiment in Chemical Dynamics would be that in which starting with reactants in definite intramolecular quantum-states and running towards each other in a definite way (relative velocity and orbital angular momentum) the distribution of the products over the various intramolecular quantum-states and the state of the relative motion (direction and velocity) would be measured. Such an experiment would show whether there is a preferential molecular orientation at the heart of the collision, what the lifetime of the intermediate complex is, how the excess energy is distributed over the various degrees of freedom of

this complex, etc. . . Unfortunately, this experiment has not been carried out yet, but there are experiments which fulfill one part or the other of the ideal experiment. In crossed-molecular-beams experiments, the reactants are prepared in perfectly defined states[37–53]. For instance a laser can select a given rotation-vibration intramolecular state[54, 55]. The products are analyzed by means of one of the following techniques:

(i) the laser-induced fluorescence[56–58];
(ii) the infrared chemiluminescence[33, 59–63];
(iii) the electric resonance spectroscopy[64–67] and
(iv) the chemical laser[59, 68–74].

We do not insist on stating details of these experiments. Let us just mention the recent work of Herschbach and collaborators which is a very impressive achievement[75, 76]. These authors have studied, by means of molecular beams, the very details of "termolecular" reactions involving van der Wall's bonds among halogen molecules, such as:

$$\begin{aligned} Cl_2 \ldots Cl_2 + Br_2 \longrightarrow\ & (1)\ Cl_2 + 2\ BrCl; \\ & (2)\ BrCl \ldots Cl_2 + BrCl \text{ and} \\ & (3)\ Br_2 \ldots Cl_2 + Cl_2. \end{aligned}$$

In particular, to channel (1) and (2) mechanisms involving formations of the same cyclic six-center intermediate complex can be attributed whereas channel (3) only requires Br_2 to interact with the nearer Cl_2 molecule of the dimer within a noncyclic molecular conformation. Thus channel (3) dominates at low collision energies (< 9 kcal/mol), but declines rapidly at higher collision energies and becomes much less probable than collision-induced dissociation to form $Br_2 + 2\ Cl_2$, this applies also to both channels (1) and (2).

In Chemical Dynamics the direct comparison between experiments (more precise than simple kinetic measurements of reaction rates) and theoretical results is in general rather subtle. As far as we know, it has been restricted to reactions in which a halide is produced. The most studied reaction, both theoretically[77, 80] and experimentally[47, 48, 69, 81], is

$$F + D_2 \longrightarrow DF + D,$$

or its isotopic variants

$$F + H_2 \longrightarrow HF + H \text{ and}$$
$$F + HD \longrightarrow HF + D.$$

Thus the activation energy for the formation of DF is minimal when F and D_2 collide colinearly. At low collision energy most molecules DF are observed backwards, in vibrational states $v = 2$, 3 and 4, at weak total angular momentum, etc. . . All the theoretical studies of this reaction, but one[80], use classical trajectories.

2. Trajectory Studies of Small Molecular Systems

Since theoretical Chemical Dynamics resort practically to classical trajectories, we briefly review below some previous works in this field[c].

The first chemical reaction studied by means of classical trajectories was $H_2 + H \longrightarrow H + H_2$ within the *collinear collision model*[84–87]. This pioneering work states the following: For any system driven by a bent potential valley, the reaction proceeds through a gradual transformation of the collision energy into vibrational energy of the product molecule. The first 3-dimensional trajectories were for the same reaction[88]. Since then, much important work has been undertaken. For instance, the way in which an empirical modification of the potential modifies the reaction-probability, the intramolecular states of the products, the deflection angle, etc. . . all these were the subject of many studies[89–95] and also of a review article[96].

The first "a priori" study (by Karplus, Porter and Sharma) of a chemical reaction undertaken on a large scale was again for $H_2 + H$, described by a London-Eyring-Polanyi-Sato (LEPS)-type potential[97–100]. All the standard concepts and techniques were introduced for this investigation[101]: 3-dimensional model, restricting the intramolecular states of the reactants to quantized states, obtaining the reaction total cross-section[d] as a function of the collision energy and of the intramolecular states of the reactants by averaging over the impact parameter (pseudo-random Monte-Carlo method), integrating these cross-sections with the collision energy to obtain the *rate constant* of the reaction, etc. . .

The main results of this study are[101]:

(i) the total reaction cross section is an increasing function of the collision energy that rises smoothly from a threshold to an asymptotic value;

(ii) the zero-point vibrational energy of the molecule contributes to the energy required for reaction, but the rotational energy does not;

(iii) the reaction probability is a smoothly decreasing function of the impact parameter;

(iv) for temperatures between 300 °K and 3000 °K the theoretical rate constant can be expressed by the form $K(T) = AT^{\alpha} \exp\{-E^{\ddagger}/kT\}$ where A, $E^{\ddagger}$ and α ($\simeq 1.18$) are constants;

(v) there is no evidence of a long-lived intermediate complex.

The model was extended to the general atom-diatom exchange reaction $A + BC \longrightarrow AB + C$[102, 103], for which Polanyi and Wong studied in *3 dimensions* the relative influence of both initial translational energy and vibrational energy. This depends largely on the location of the top of the potential barrier, either along the approach coordinate (case I) or along the retreat coordinate (case II). In case I translation is more effective than vibration in promoting reaction. Moreover, at low collision energy, a major part of the available energy transforms into vibration of the product molecule (at higher collision energy this fraction decreases). In case II the opposite situation is observed: vibration is more effective than translation. Moreover, for low vibra-

---

c) There are several more detailed review articles on the subject[7–9, 82, 83].

d) The cross section of an elementary collision process is roughly a measure of the reaction efficiency of this process.

tional energy of the reactants only a small part of the available energy appears as vibration in the product (at higher vibrational energy this fraction increases). This confirms the conclusion obtained within the collinear collision model. In both cases I and II most product molecules are scattered backwards at low collision energy (the peak of the distribution shifts forward at increased reactant energy, even in case II for an increase of reactant vibration).

Then the Karplus *et al.* model was extended to more complex reactions[104, 105], such as

$$K + CH_3I \longrightarrow KI + CH_3$$ [92, 93, 99, 100, 106]

and finally to the general *thermal bimolecular* reaction in the gas-phase: $A + B \rightleftharpoons C + D$[107, 114]. For the latter it is possible to obtain the forms for the theoretical rate constants[19, 82, 101, 115–120] for the forward ($\vec{K}$) and the backward ($\overleftarrow{K}$) reactions [defined by[e]: $-d(A)/dt = \vec{K}(A)(B) - \overleftarrow{K}(C)(D)$] as functions of the temperature. If the gas phase is homogeneous the temperature is introduced through maxwellian distribution functions. The result is:

$$\vec{K} = \sum_{\chi_A, \chi_B, \chi_C, \chi_D} F_A(\chi_A) F_B(\chi_B) \int d\vec{v}_A F_A(\chi_A; \vec{v}_A) \int d\vec{v}_B F_B(\chi_B; \vec{v}_B)$$

$$v\, \sigma(\chi_A, \chi_B, \chi_C, \chi_D; E_{col})$$

$$\overleftarrow{K} = \sum_{\chi_A, \chi_B, \chi_C, \chi_D} F_C(\chi_C) F_D(\chi_D) \iint d\vec{v}_A\, d\vec{v}_B\, F_C(\chi_C; \vec{v}_C) F_D(\chi_D; \vec{v}_D)$$

$$v\, \sigma(\chi_A, \chi_B, \chi_C, \chi_D; E_{col})$$

where χ_I (I = A, B, C, D) denotes the set of all the quantum numbers defining the intramolecular state of molecule I (rotations and vibrations) $F_I(\chi_I)$ is the distribution function of the intramolecular quantum states of molecule I, $\vec{v}_I$ is the velocity of molecule I, $F_I(\chi_I; \vec{v}_I)$ is the normalized distribution function of the velocity of molecule I in the state χ_I, v is the initial relative velocity and E_{col} the collision energy:

$$v = |\vec{v}_A - \vec{v}_B| = (2E_{col}/\mu)^{1/2}$$

where μ is the reduced mass of A and B.

$$\sigma(\chi_A, \chi_B, \chi_C, \chi_D; E_{col})$$

is the reaction cross section of the elementary collision process $[A(\chi_A) + B(\chi_B) \longrightarrow C(\chi_C) + D(\chi_D)]$ at collision energy E_{col}. It is this quantity which is obtained by means of trajectories.

---

[e] This definition is for low concentrations and implies that the rate constants depend neither on the concentrations nor on the time.

This result is purely statistical. Replacing the distribution function by particular expressions, depending on the temperature, is the last operation[f]. When a dynamical process occurs the equilibrium distribution function (maxwellian) should be modified, and the greater the reaction rate compared to the relaxation rates of both the velocities and the intramolecular states, the greater the modification[121–123]. Thus it is only for low reaction rates that equilibrium distribution functions can be inserted in the formulas above, and that the reaction rate depends on the temperature, but neither on the time nor on the concentrations.

Now a question must be raised: which connection is there between classical trajectories results and results obtained through Quantum Mechanical calculations?

The Quantum Mechanical study of molecular collisions and of the chemical reaction is itself an important topic[124]. There are several review papers[35, 36, 125–129] and textbooks[130–139] on the subject. Unfortunately, there are no exact quantum results within a realistic model of a chemical reaction yet, not even for the simplest 3-atoms exchange. Thus the comparison is limited to particular cases.

For instance, $H + H_2 \longrightarrow H_2 + H$ was studied in 3-dimensions within a model where the vibrational states were reduced to a single one for each of the three possible product molecules[140]. At low collision energy (less than the classical energy threshold) the reaction cross section is non zero because of tunnelling. For the same reaction studied colinearly the following conclusions emerge[141–143]:

(i) for great values of the collision energies the quantum mechanical reaction probability slightly oscillates around the classical probability, because of the gradual "opening of excited vibrational states" in the products;

(ii) the reaction probability extends below the threshold by tunnelling. Thus, at low temperature and for the phenomenon of a pronounced quantum nature (such as the exchange of a light atom between two heavy groups), the classical trajectory reaction rate may be an underestimated approximation of the true reaction rate.

On the basis of such results and, more convincingly, on the strength of semiclassical investigations (classical S-matrix of Miller and Marcus[144–150]) it can be asserted that the classical description of the nuclear motion in the course of a molecular collision (either reactive or not) is not in itself a severe restriction. Thus, McCullough and Wyatt[151–152] have shown that for collinear $H + H_2 \rightarrow H_2 + H$ the agreement is quite good between the classical and the time-dependent quantum-mechanical descriptions during the greatest part of the reaction. A slight discrepancy appears only near the end of the reaction; the classical reaction is completed somewhat faster than the quantum-mechanical one. Nevertheless, all the dynamical effects such as the centrifugal force pushing the representative point of the reaction towards the outer part of the bent reaction valley and the whirlpool turbulence effects close to the saddle point, are surprisingly well described classically.

---

f) In the case of a complete equilibrium distribution, the result is:

$$K(T) = (8/\pi\mu kT)^{1/2}/kT \int_0^\infty dE_{col}\, \sigma'(E_{col})\, E_{col} \exp(-E_{col}/kT),$$

where: $\sigma'(E_{col}) = \sum_{x_A, x_B, x_C, x_D} F_A(x_A)\, F_B(x_B)\, \sigma(x_A, x_B, x_C, x_D; E_{col})$.

To wind up this chapter, we enumerate below the various fields of application of classical trajectories in Chemical Dynamics.

Many trajectories were integrated to obtain either total reaction cross sections for comparison with molecular beams experiments[79, 105, 153–171], or rotational and vibrational relaxation times of the products of chemical reactions, or intermolecular energy transfers[103, 107–111, 172–185], etc. . .

As seen previously, the chemical reactions studied most often are the exchange ones. Those requiring several potential energy surfaces of excited states (diabatic reactions) are worth special mention, since they most certainly define a domain of application with a future for classical trajectories. An electron jump from one surface to another requires either to be given a statistical probability of occurence by the Landau Zener formula[186, 187] (or one of its improved versions[188–192]) or to be described by means of complex-valued classical trajectories as a direct and gradual passage in the complex-valued extension of the potential surfaces (generalization of the classical S-matrix[193–197]).

Some atomic recombinations catalized by a rare gas atom[198–205] and some reactions involving a long-lived intermediate complex[112, 113, 206–208] were also studied classically. *Unimolecular* reactions are quite advantageous for trajectory studies since the potential is generally easy to express and the total energy is sufficiently great for reasonably neglecting the discreteness of vibrational levels of the reactant[7]. Until recently only triatomic decomposition has been studied extensively: $ABC \longrightarrow AB + C$[209–211]. The main concern is for the distribution of molecular lifetimes (the time elapsed before decomposition occurs) and for the variation of this distribution when varying the total energy and the particle mass. This can be compared directly with semiempirical predictions. Thus, it is well established for triatomic systems that the RRKM rate coefficients[13] satisfactorily agree with trajectory results. Another important advantage of trajectory methods is to provide the final energy partitioning between AB and C.

More recently, the unimolecular isomerization $CH_3NC \longrightarrow CH_3CN$ gave rise to elaborated studies by Bunker and collaborators[212–215]. The pressure dependence of the thermal reaction rate constant is well explained by the RRKM theory, applying the simple concept of the geometry and vibrations of the activated molecule[216]. However, the fact that the hot-atom displacement reactions

$$T^* + CH_3NC \longrightarrow CH_2TNC + H$$

and

$$T^* + CH_3CN \longrightarrow CH_2TCN + H$$

both result at the very end in CH_2TCN (observed by trajectories) is indicative of a failure of the RRKM theory for the unimolecular isomerization of nascent molecules[217]. In particular, CH_3NC is not a good RRKM molecule under non-thermal conditions, because the vibrational modes of CH_3NC are too far from being equally coupled to one another and also to the mode of isomerization. For unimolecular reactions it should be kept in mind that, since many vibrations (and not only the single translation) may play important roles, trajectory studies are always delicate and require much caution.

There have been a number of interesting trajectory studies of organic reactions that have used *empirical* potential energy surfaces. $CH_3NC \longrightarrow CH_3CN$ is the first example. The second example is

$K + C_2H_5I \longrightarrow KI + C_2H_5$ (studied by Raff)[218]

where the ethyl group is treated as a two-body system. The main results are:

(i) the total reaction cross section for this reaction is less than that for $K + CH_3I \longrightarrow KI + CH_3$, due to the increased steric hindrance;

(ii) KI is predominantly scattered backwards;

(iii) the C–C stretch of the ethyl absorbs an important part (15%) of the heat of reaction;

(iv) the reaction can occur by two mechanisms, either directly or through formation of a collision complex.

In the first mechanism most of the reaction energy transforms into rotation-vibration energy of KI, while in the second mechanism the energy distribution between the products is more random. A third example of organic reaction studied dynamically is that of a "hot" tritium atom on a methane molecule (studied by Polanyi and collaborators[219] on the one hand and by Bunker and collaborators[220–221] on the other hand). The main findings of several studies (using various potential energy surfaces) are:

(i) both abstraction of H by T ($T^* + CH_4 \longrightarrow TH + CH_3$) and T-for-H substitution ($T^* + CH_4 \longrightarrow H + CH_3T$) are direct (non complex) and concerted (non sequential) reactions;

(ii) substitution is favoured at intermediate collision energy (90–160 kcal/mol collision energy);

(iii) substitution with Walden inversion is an important fraction of overall substitution at low collision energy (40–100 kcal/mol);

(iv) the greatest part of the collision energy transforms into translational energy of the products;

(v) at 45–90 kcal/mol the product molecule is scattered sideways, following abstraction and backwards following substitution;

(vi) for abstraction, replacing T by D, the abstracted H by D, or CH_3 by a heavier radical results in a decrease of the reaction cross section;

(vii) for substitution, replacing T by D or the abstracted H by D results in a decrease of the reaction cross section while the latter increases when replacing CH_3 by a heavier radical.

We have kept the dynamical study of organic reactions by means of classical trajectories and based on semi-empirical and ab initio potential energy surfaces for the end. These studies are rare and constitute most likely a research subject with a future. The difficulty is to obtain forces acting on a large numbers of atoms. Constructing a potential whose partial derivatives provide reasonable forces is more and more difficult when the number of atoms and the directionality of valence forces increase[7, 9]. Except for the reaction study presented in the 3rd chapter of the present article, (in which an ab initio potential energy surface is interpolated and differentiated to give the forces) and as far as we know, these studies are reduced to a single one by Wang

and Karplus[222]. It deals with the insertion of singlet methylene into the hydrogen molecule:

$CH_2 + H_2 \longrightarrow CH_4$.

Here the forces are derived directly from matrices associated with SCF–MO calculations (at the semi-empirical $CNDO_2$ level). The results for the heat of reaction are accurate. The methylene is shown to be inserted into the hydrogen molecule for a wide range of initial conditions. But the most significant conclusion is that the analysis of the reaction in terms of the static reaction-path alone is largely insufficient, compared with the more realistic dynamical conclusions about the mechanism which is very complicated.

B. A General Framework for Chemical Dynamics in Organic Chemistry

The theoretical investigation of a chemical reaction is essentially a two-step study. The first step is *static.* It consists of computing the potential energy of the reaction system as a function of the different geometrical parameters. Hence, some information on the reaction mechanism can be obtained, such as

(i) the *minimum-energy path* to go from reactants to products and consequently the shape of the *reaction coordinate;*

(ii) the difference between the calculated energies for the reactants and for the system at the *transition state,* which is compared to the *activation energy* of the reaction as a first approximation. In recent years, the growth of scientific computers, as well as the realization of fast programs for quantum mechanical calculations has made the extensive investigation of potential-energy surfaces possible for many organic reactions involving rather complex molecules.

The second step is of a *dynamical* nature. It consists of obtaining dynamical trajectories on the potential surface. Classical Mechanics are supposed to describe correctly the atomic motion. In certain cases such a study, at the end, allows one to obtain the rate constant of the reaction[101]. In other respects the dynamical study brings new information on the mechanism of the reaction[102–103], which cannot be derived only from the study of the static potential surface. Moreover, the dynamical study is sometimes clearly indispensable for the elucidation of the reaction mechanism. Thus, the reaction $H_2 + I_2 \longrightarrow 2$ HI was considered for a long time to be a simple bimolecular reaction. Semi-empirical calculations of the potential-barrier height for a bimolecular process gave a result of 42 kcal/mol[179, 223], an excellent agreement with the experimental value of the activation energy (41 kcal/mol). However, dynamical trajectories calculations have shown that the mechanism is much more complicated than previously thought. In particular the conflict between two possible channels ($H_2 + I_2 \longrightarrow H_2 + 2\,I \longrightarrow I + H_2I$ (collinear) $\longrightarrow 2$ HI on the one hand[7, 224–226], and direct $H_2 + I_2 \longrightarrow 2$ HI on the other hand[227]) has not yet been resolved. Nevertheless, the dynamical study of the first channel gave reaction rates of recombination of $H_2 + 2\,I$ in good agreement with the experiment[228].

Complete dynamical studies, including the calculation of macroscopic reaction rates, have been restricted, until now, to small molecular systems[7, 9]. They require a preliminary knowledge of all the regions of the potential surface that are accessible for a given total energy. In addition, very many dynamical trajectories must be computed for suitably selected sets of initial conditions. For larger systems – even the smallest systems of interest in organic chemistry – it is impossible to obtain reaction rates by means of a complete dynamical study. Too many degrees of freedom have to be taken into account to obtain the full potential surface. Simplified assumptions are required to scan the surface. In general, only those geometrical parameters which contribute notably to the reaction path are varied. The secondary parameters are either held constant or varied in a conventional way. There is no choice but to carry these constraints over into the dynamical calculation. Then the system is said to be *constrained.* Consequently, the vibrational excitation of purely nonreactive modes is ignored. From a static point of view, this is not a severe restriction, if the important parameters have been carefully selected. On the contrary, from a dynamic point of view, the *a priori* neglect of any energy transfer between reactive and nonreactive modes (as well as the possible dissipation of a part of the energy over various nonreactive modes) can play a crucial role, in particular near the middle of the reaction where the final outcome of the reaction is decided.

Nevertheless, the dynamical study of the elementary processes occuring in the course of a reaction remains useful and complementary to the static study of the potential surface, even though it is incomplete and does not lead to the reaction rate. In particular, the comparison of dynamical trajectories with the static minimum-energy path is very instructive. As we mentioned in Chap. A for $CH_2 + H_2 \longrightarrow CH_4$[222], the initial conditions seem to play a crucial part in the shape of dynamical trajectories; only certain specific initial conditions lead to trajectories close to the minimum energy path; most dynamical trajectories are much more complex than this path. Furthermore, deviations may result from the fact that for a given potential surface in several dimensions the optimum path is most often drawn approximately under the assumption that the evolution of the system can be represented by the sliding of a mass point on the potential surface. This model is generally unsuitable for constrained systems[6, 19].

I. The Cubic Splines for Expression of the Potential Energy Functions

1. Introduction

Quantum chemical calculations provide the values of a multi-dimensional potential at the mesh points of a grid. Several coordinates are varied step by step and to each set of all these coordinates there is a corresponding number. However, we need a potential energy function which is analytic if possible, continuous and differentiable in any order. At the mesh points of the grid the values of this function are to be as close as possible to the computed ones. In addition, the values of the derivatives of this function with respect to any coordinate must be physically possible on the limiting contour surrounding the region of the potential surface studied. This is very im-

portant in order to avoid starting the numerical propagation of a trajectory the wrong way in a limiting region; after the propagation this would lead to an incorrect result in the opposite limiting region.

Different procedures can be envisaged. Most commonly used for small systems is a simple analytical formula which is derived from a physical basis[7–9]. Each parameter in such a formula has a specific physical meaning and can be optimized (for instance by a least squares fit). The main advantage of this procedure is that the parameters may be varied independently (this is the origin of many physical studies, see for instance Ref.[218]). But there are two drawbacks in doing this. Firstly, varying a parameter modifies the whole surface (for instance, modifying the height of a gaussian barrier at a constant parameter of steepness, implies a change in the width of the barrier). Secondly, in a strict sense, such a formula is hardly exact anywhere, since it is not an interpolation formula. However, this procedure is to be used as often as possible because of the high speed in computing the numerical values of simple expressions. We are not discussing here which analytical formula is the most suitable for a given molecular system. The treatment of these topics can be found in the literature[7, 9].

Many problems can be found in large systems in which most of the degrees of freedom are artificially frozen. Then the potential energy, as a function of the coordinates over a wide range, can become very complex. An alternative procedure is to use interpolation techniques. By the common polynomial techniques all the values of either the potential or its derivatives can be exactly fitted whenever it is necessary; but this leads to polynomials of a very high degree (hundreds of mesh points may have to be considered). Consequently, instabilities can appear, especially on the sides of the region studied (see Fig. 1 for a one dimensional case).

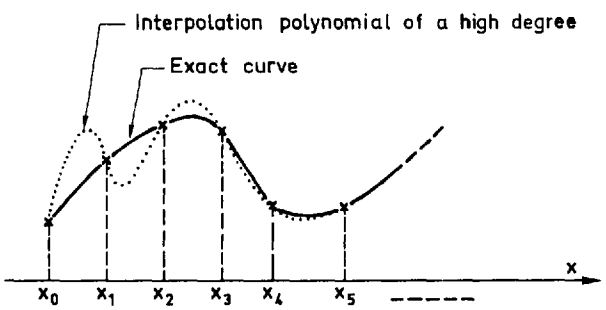

Fig. 1. An example of a possible behavior of an interpolation polynomial of high degree, as compared with the exact function. This is what we call an instability on the sides of the range of interpolation

Therefore, we must search for an analytical expression or the potential energy which exactly fits the calculated values at each mesh point of the grid, which avoids divergence on the sides of the physically interesting region and which has, nevertheless, a rather simple form. The aim of the present section is to use a procedure which

provides an expression fulfilling all these requirements by means of cubic spline functions[g].

In order to avoid any mathematical sophistication, we restrict ourselves to the construction of only those functions that are of interest in the application. Many more details can be found in the pioneering work of Ahlberg, Nilson and Walsh[233,234] and in various textbooks on the subject[235,236]. Some authors already applied spline techniques to various problems in Chemical Physics, either to interpolate ab initio potential surfaces[114,237,238] or experimental data[239] or to analytically expand atomic orbital functions[240–242] or to solve bound state Schrödinger equations[243].

2. One Dimensional Cubic Splines

On an interval $[x_{j-1}, x_j]$ of a variable x, there exists one cubic function $S_j(x)$ and only one such that:

$$\begin{aligned} &(1) \quad S_j(x_{j-1}) = y_{j-1} \text{ and } [dS_j(x)/dx]_{x_{j-1}} = m_{j-1}; \\ &(2) \quad S_j(x_j) \quad = y_j \quad \text{and } [dS_j(x)/dx]_{x_j} \quad = m_j. \end{aligned} \tag{1}$$

A convenient expression for this function is for instance:

$$S_j(x) = (\bar{y}_j - h_j M_j/8) + (3\,Y_j - h_j \bar{m}_j)\,X_j/2 + h_j M_j X_j^2/2 + 2\,(h_j \bar{m}_j - Y_j)\,X_j^3 \tag{2}$$

where: $X_j = (x - \bar{x}_j)/h_j$ lies within $[-1/2, +1/2]$

and: $\bar{x}_j = (x_j + x_{j-1})/2$, $\bar{y}_j = (y_j + y_{j-1})/2$, $\bar{m}_j = (m_j + m_{j-1})/2$,

$h_j = x_j - x_{j-1}$, $Y_j = y_j - y_{j-1}$, $M_j = m_j - m_{j-1}$.

Now we consider an interval $[a, b]$ of the variable x, which is subdivided by a mesh of points:

$$\Delta \equiv \{a = x_0 < x_1 < \ldots\ldots x_{N-1} < x_N = b\}.$$

We associate a set of ordinates with this set of abcissas;

$$y \equiv \{y_0, y_1 \ldots\ldots y_{N-1}, y_N\}$$

and with the extremal abcissas we associate two slopes: m_0 and m_N. We look for a function $S_\Delta(x)$, which is continuous on $[x_0, x_N]$ (as are its first and second derivatives), which coincides with a cubic in each $[x_{j-1}, x_j]$ and satisfies:

$$\begin{aligned} &S_\Delta(x_j) = y_j \quad (j = 0, 1 \ldots N) \\ &S'_\Delta(x_j) = m_j \quad (j = 0, N) \end{aligned} \tag{3}$$

---

g) An alternative analytical and stable interpolation technology has recently been extensively used: the continued fraction[194,195,229–232].

We call this function a cubic spline on Δ. The definition of such a function requires a knowledge of the intermediate slopes:

$$m_j = [dS_\Delta(x)/dx]_{x_j} \qquad (j = 1, 2 \ldots N-1)$$

From the continuity requirement imposed on $S''_\Delta(x)$ at x_j $(j = 1, 2 \ldots N-1)$ the set of linear equations results[2,3,4]:

$$\lambda_j m_{j-1} + 2\, m_j + \mu_j m_{j+1} = c_j \qquad (j = 1, 2 \ldots N-1) \tag{4}$$

where: $\lambda_j = h_{j+1}/(h_j + h_{j+1})$

$\mu_j = h_j/(h_j + h_{j+1}) = 1 - \lambda_j$

$c_j = 3\,\lambda_j (y_j - y_{j-1})/h_j + 3\,\mu_j (y_{j+1} - y_j)/h_{j+1}$

In matrix notation:

$$\begin{bmatrix} 2 & \mu_1 & 0 & \ldots 0 & 0 & 0 \\ \lambda_2 & 2 & \mu_2 & \ldots 0 & 0 & 0 \\ \vdots & \vdots & \vdots & \vdots & \vdots & \vdots \\ 0 & 0 & 0 & \ldots \lambda_{N-2} & 2 & \mu_{N-2} \\ 0 & 0 & 0 & \ldots 0 & \lambda_{N-1} & 2 \end{bmatrix} \times \begin{bmatrix} m_1 \\ m_2 \\ \vdots \\ m_{N-2} \\ m_{N-1} \end{bmatrix} = \begin{bmatrix} c_1 - \lambda_1 m_0 \\ c_2 \\ \vdots \\ c_{N-2} \\ c_{N-1} - \mu_{N-1} m_N \end{bmatrix} =$$

$$= \begin{bmatrix} \gamma_1 \\ \gamma_2 \\ \vdots \\ \gamma_{N-2} \\ \gamma_{N-1} \end{bmatrix} \tag{5}$$

Standard algorithms exist to solve such a band system in an efficient and stable way. The solution spline function $S_\Delta(x)$ exists and is unique. Moreover, it is an excellent interpolation function which converges to $f(x)$ when $N \to \infty$, if $\lim_{N\to\infty}(h_j) = 0$.

An important special case is that of equal intervals. Then, $\lambda_j = \mu_j = \frac{1}{2}$ $(j = 1, 2 \ldots N-1)$ and the matrix in Eq. (5) – which we then call $\underset{\sim}{B}$ – is easily inverted. The result is (see Table 1):

$$[\underset{\sim}{B}^{-1}]_{i,j} = (-1)^{i+j} B_{i-1}\, B_{N-j-1}/(2^{j-i} B_{N-1}) \quad (1 \leqslant i \leqslant j \leqslant N-1) \tag{6}$$

where:

$$B_n = [(1 + \sqrt{3}/2)^{n+1} - (1 - \sqrt{3}/2)^{n+1}]/\sqrt{3}$$

$\underset{\sim}{B}$ is symmetric with respect to its two diagonals. The same remains true for $\underset{\sim}{B}^{-1}$:

$$[\underset{\sim}{B}^{-1}]_{j,i} = [\underset{\sim}{B}^{-1}]_{i,j}$$

$$[\underset{\sim}{B}^{-1}]_{N-i-1,N-j-1} = [\underset{\sim}{B}^{-1}]_{i,j}$$

Table 1. $\underset{\sim}{B}^{-1}$ matrices in the case of equal intervals for $N = 4, 7, 10$ and $N \to \infty$. All of these matrices are symmetric with respect to their two diagonals so that only the upper quarter is reproduced here. In the case $N \to \infty$ ($\underset{\sim}{C}$), the upper half is reproduced. The infinite matrix is cut when the elements on each line parallel to the main diagonal have reached a constant value.
All the numbers in this table are given with a precision of 10^{-6}

$N = 4$

.535714	−.142857	.035714	
	.571429		

$N = 7$

.535898	−.143593	.038475	−.010306	.002748	−.000687
	.574373	−.153899	.041223	−.010993	
		.577121	−.154586		

$N = 10$

.535898	−.143594	.038476	−.010310	.002762	−.000740	.000198	−.000053	.000013
	.574374	−.153903	.041238	−.011050	.002961	−.000793	.000211	
		.577137	−.154643	.041436	−.011103	.002974		
			.577335	−.154696	.041450			
				.577348				

$N \to \infty$

.535898	−.143594	.038476	−.010310	.002762	−.000740	.000198	−.000053	.000014	−.000004	.000001	−	−	−
	.574374	−.153903	.041238	−.011050	.002961	−.000793	.000213	−.000057	.000015	−.000004	.000001	−	−
		.577137	−.154643	.041437	−.011103	.002975	−.000797	.000214	−.000057	.000015	−.000004	.000001	−
			.577335	−.154696	.041451	−.011107	.002976	−.000797	.000214	−.000057	.000015	−.000004	.000001
				.577349	−.154701	.041452	−.011107	.002976	−.000797	.000214	−.000057	.000015	−.000004
					.577350	−.154701	.041452	−.011107	.002976	−.000797	.000214	−.000057	.000015
						.577350	−.154701	.041452	−.011107	.002976	−.000797	.000214	−.000057

Let us define a new quantity: $\sigma = \sqrt{3} - 2 = -0.267949\ldots$ Then:

$$B_n = (1 + \sqrt{3}/2)^n\ (1 - \sigma^{2n})/\sqrt{3}$$

and:

$$[\underset{\sim}{B}^{-1}]_{i,j} = [(\sigma^{j-i} - \sigma^{j+i})/\sqrt{3}]\ (1 - \sigma^{2(N-j)})/(1 - \sigma^{2N})\quad (1 \leqslant i \leqslant j \leqslant N-1) \qquad (7)$$

We can now write down an explicit expression for the slope m_i at the ith mesh point of the grid ($i = 1, 2 \ldots N-1$):

$$m_i = (3/2\,h) \sum_{j=1}^{N-1} [\underset{\sim}{B}^{-1}]_{i,j}\,(y_{j+1} - y_{j-1}) - ([\underset{\sim}{B}^{-1}]_{i,1}\,m_0 + [B^{-1}]_{i,N-1}\,m_N)/2 \qquad (8)$$

It should be emphasized that the quantities $[\underset{\sim}{B}^{-1}]_{i,j}$ decrease rapidly as j departs from i. Only a few terms centered around x_i are to be kept in the sum, in Eq. (8).

We now study the equal intervals cubic spline function for $N \to \infty$. This limiting case is of general interest, since it affords a considerable simplification in the applications of the spline theory. $|\sigma|$ being less than 1, we have:

$$\underset{\sim}{C}_{i,j} = \lim_{N\to\infty} [\underset{\sim}{B}^{-1}]_{i,j} = (\sigma^{|j-i|} - \sigma^{j+i})/\sqrt{3} \quad (1 \leqslant i \text{ and } j \leqslant N-1) \qquad (9)$$

This is the current element of the infinite symmetric matrix $\underset{\sim}{C}$ (see Table 1), the elements of which decay rapidly apart from the diagonal and tend to be constant values on each line parallel to the diagonal. If this line is marked by k such that $|i - j| = k$, the limiting value for large i and j is:

$$\lim_{i\to\infty} \underset{\sim}{C}_{i,\,i\pm k} = \sigma^k/\sqrt{3} \qquad (10)$$

Thus, for sufficiently large i, the slope m_i can be expressed as:

$$m_i = (\sqrt{3}/2\,h) \sum_{k=-l}^{+l} \sigma^{|k|}\,(y_{i+k+1} - y_{i+k-1}) \qquad (11)$$

The integer constant l is defined according to the precision required.

3. Cardinal Splines

Let us introduce the cardinal splines. They are a set of $N + 3$ independent one-dimensional cubic splines $\{A_\Delta^{(k)}(x), k = 0, 1 \ldots N; B_\Delta^{(k)}(x), k = 0, N\}$ forming a complete basis on which to expand any cubic spline on Δ. We define them as follows:

$$A_\Delta^{(k)}(x_i) = \delta_{ik}\ \ (i = 0, 1 \ldots N) \text{ and } [dA_\Delta^{(k)}(x)/dx]_{x_i} = 0 \qquad (i = 0, N)\ (k = 0, 1 \ldots N);$$
$$B_\Delta^{(k)}(x_i) = 0 \quad (i = 0, 1 \ldots N) \text{ and } [dB_\Delta^{(k)}(x)/dx]_{x_i} = \delta_{ik} \quad (i = 0, N)\ (k = 0, N). \qquad (12)$$

δ_{ik} is the Kronecker delta.

It is readily verified that the spline function defined by the set of conditions (3) can be expanded in the form:

$$S_\Delta(x) = \sum_{j=0}^{N} y_j A_\Delta^{(j)}(x) + m_0 B_\Delta^{(0)}(x) + m_N B_\Delta^{(N)}(x) \tag{13}$$

This expansion will be of great interest in the following.

In the case of equal intervals the slopes of the cardinal splines at the mesh points have a simple form; from Eq. (8) ($i = 1, 2 \ldots N-1$):

$$m_i \{A_\Delta^{(k)}(x)\} = (3/2\,h)([\underset{\sim}{B}^{-1}]_{i,k-1} - [\underset{\sim}{B}^{-1}]_{i,k+1}) \quad (k = 2, 3 \ldots N-2) \tag{14}$$

For $k = 0, 1, N-1$ or N this relationship is still valid under the condition that the $[\underset{\sim}{B}^{-1}]_{i,j}$ that do not exist (*i.e.* $[\underset{\sim}{B}^{-1}]_{i,-1}$, $[\underset{\sim}{B}^{-1}]_{i,0}$, $[\underset{\sim}{B}^{-1}]_{i,N}$ and $[\underset{\sim}{B}^{-1}]_{i,N+1}$) are regarded as being equal to zero. In addition:

$$m_i \{B_\Delta^{(0)}(x)\} = -[\underset{\sim}{B}^{-1}]_{i,1}/2 \text{ and } m_i \{B_\Delta^{(N)}(x)\} = -[\underset{\sim}{B}^{-1}]_{i,N-1}/2 \tag{15}$$

From the expressions (1), (7), (14) and (15) one deduces the following properties of the cardinal splines: (1) the cardinal splines $A_\Delta^{(k)}(x)$ and $A_\Delta^{(N-k)}(x)$ are mutually symmetric with respect to the center of the range Δ; (2) the cardinal splines $B_\Delta^{(0)}(x)$ and $B_\Delta^{(N)}(x)$ are antisymmetric; (3) The A-type cardinal splines are oscillating functions with a peak just a bit greater than 1 for a value of x very close to x_k (or rigorously equal to 1 at $x = x_k$ for the case of symmetric function) which rapidly damp out for the values of x apart from x_k; (4) the B-type cardinal splines are oscillating functions with a peak close to the middle of the end interval and which rapidly damp out away from that interval; (5) The absolute values of the cardinal splines

$$A_\Delta^{(k)}\left(\frac{x}{h}\right) \quad (k = 0, 1 \ldots N)$$

do not depend on h; (6) The absolute values of the cardinal splines $B_\Delta^{(k)}\left(\frac{x}{h}\right)$ ($k = 0$, N) are proportional to h.

In the case $N \to \infty$, the B-type cardinal splines can be considered to vanish unless x is close to $x_0 \cdot x_0$ however, can always be removed far from the range of x, which is of interest. In other words, whenever h is reduced (tends to zero), the two terminal terms in the r.h.s. of Eq. (13) become negligible compared with the first one, because of the properties (5) and (6) above. Moreover, the complete set of the A-type cardinal splines reduces to a unique symmetric function called $A_\infty(X)$; this function is to be translated ($hX = x - x_k$), in such a way that it possesses the maximum of unit height at $x = x_k$ in order that it may represent $A_\infty^{(k)}(x)$. The intermediate slopes characterizing this unique function are evaluated using Eq. (11):

$$\begin{aligned} m_{i-k} &= m_i \{A_{N\to\infty}^{(k)}(x) = A_\infty((x - x_k)/h)\} \\ &= (\sqrt{3}/2\,h)(\sigma^{|i-k+1|} - \sigma^{|i-k-1|}) = \alpha_{i-k}/h \end{aligned} \tag{16}$$

Table 2. To obtain the intermediate slopes characterizing the function $A_\infty(X)$, where $X = \frac{|x - x_k|}{h}$, the integer indices and values given here are to be inserted in the formula:

$[m\{A_\infty(X)\}]_{X=i} = \frac{\alpha_i}{h}$, where $\alpha_{-i} = -\alpha_i$

Otherwise: $\beta_i = \alpha_i + \alpha_{i-1}$ and $\gamma_i = \alpha_i - \alpha_{i-1}$

Hence: $\beta_{1-i} = -\beta_i$ and $\gamma_{1-i} = \gamma_i$

i	0	± 1	± 2	± 3	± 4	± 5	± 6	± 7	± 8	± 9	± 10	± 11
α_i	.0	∓.803847	±.215391	∓.057714	±.015465	∓.004143	±.001110	∓.000299	±.000080	∓.000021	±.000006	∓.000002
β_i	+.803847	−.803847	−.588456	+.157677	−.042249	+.011322	−.003033	+.000811	−.000219	+.000059	−.000015	+.000004
		+.588456	−.157677	+.042249	−.011322	+.003033	−.000811	+.000219	−.000059	+.000015	−.000004	+.000002
γ_i	−.803847	−.803847	+1.019238	−.273105	+.073179	−.019608	+.005253	−.001409	+.000379	−.000101	+.000027	−.000008
		+1.019238	−.273105	+.073179	−.019608	+.005253	−.001409	+.000379	−.000101	+.000027	−.000008	+.000002

The α's are given in Table 2. The function A_∞ is drawn in Fig. 2. Consequently, the spline expression of any function defined by a sufficiently large set of values $\{y_i\}$ regularly spaced, is now very simple:

$$S_{N\to\infty}(x) = \sum_j y_j A_\infty(|x - x_j|/h) \tag{17}$$

The sum is to be limited to a few terms, depending on the precision desired. This only presupposes that one knows the accurate values of y_j that are sufficiently far away from the x considered. From Fig. 2 one sees that four steps further away suffice since $A_\infty(X)$ is negligible, for $|X| > 4$, within 0.25% (for $|X| > 5$, within 0.09%).

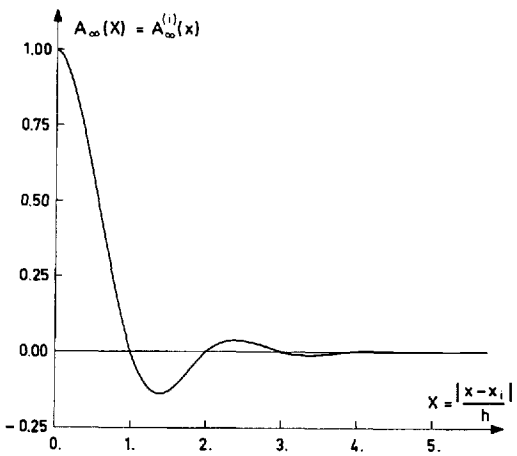

Fig. 2. The $A_\infty(X)$ function. $A_\infty\left(\frac{|x - x_k|}{h}\right)$ is the same as $A_\infty^{(k)}(x)$

Generalizing the one dimensional spline theory in relation to the two dimensional case is very straightforward. The explicit expressions of the multidimensional splines are beyond the scope of the present article. They can be found in the literature[2 3 4)] and have been used by one of us previously[1, 5, 6, 24 4)].

4. Supplementary Indications for Practical Uses

a) Reduction to the Case of Equal Intervals. We know a function $y(x)$ by the data set: $\{\tilde{x}_i$ and $\tilde{y}_i$ $(i = 0, 1 \ldots N); \tilde{m}_i$ $(i = 0, N)\}$, where the $\tilde{x}_i$'s are irregularly distributed. We define Δ, the mesh of regularly spaced abscissas: $\{x_i = \tilde{x}_0 + i(\tilde{x}_N - \tilde{x}_0)/N$ $(i = 0, 1 \ldots N)\}$. We reorder the expression of the spline – which is unique on $[x_0, x_N]$ – in the following way:

$$\sum_{i=1}^{N-1} y_i A_\Delta^{(i)}(x) = S(x) - [\tilde{y}_0 A_\Delta^{(0)}(x) + \tilde{y}_N A_\Delta^{(N)}(x) + \tilde{m}_0 B_\Delta^{(0)}(x) + \tilde{m}_N B_\Delta^{(N)}(x)] \tag{18}$$

Here the y_i's are $(N-1)$ unknowns, which are obtainable by imposing the $N-1$ conditions that $S(\tilde{x}_i) = \tilde{y}_i$ $(i = 1, 2 \ldots N-1)$ and then resolving a linear system of equations. The above reduction is of importance because of the high stability and simplicity of the cardinal splines on a mesh of regularly spaced abscissas.

b) Differentiation[234]. The flexibility of spline functions is very useful in the field of differentiation. Noting $\tilde{m}_j$ the average slope over the jth interval: $\tilde{m}_j = (y_j - y_{j-1})/h_j$ and $\underset{\sim}{W}$ the matrix in Eq. (5), after reordering the current derivative m_i is expressed as:

$$m_i = \lambda_1 [\underset{\sim}{W}^{-1}]_{i,1} (3\,\tilde{m}_1 - m_0) + 3 \sum_{j=2}^{N-1} \tilde{m}_j (\lambda_j [\underset{\sim}{W}^{-1}]_{i,j} + \mu_{j-1} [\underset{\sim}{W}^{-1}]_{i,j-1})$$
$$+ \mu_{N-1} [\underset{\sim}{W}^{-1}]_{i,N-1} (3\,\tilde{m}_N - m_N) \qquad (i = 1, 2 \ldots N-1) \qquad (19)$$

The structure of this formula is interesting. The λ's and μ's lying by definition between 0 and 1, $\underset{\sim}{W}$ is a band matrix with a dominant diagonal ($W_{i,i} = 2$). The same is approximately true for $\underset{\sim}{W}^{-1}$ ($[W^{-1}]_{i,i}$ close to 0.5). This shows that the m_i's are refinements of the $\tilde{m}_i$'s.

Now, from Eq. (2) we have $(x_{j-1} \leqslant x \leqslant x_j)$:

$$dS(x)/dx = (3\,\tilde{m}_j - \bar{m}_j)/2 + M_j X_j + 6\,(\bar{m}_j - \tilde{m}_j)\,X_j^2 \qquad (20)$$

(remember that: $\bar{m}_j = (m_j + m_{j-1})/2$ and $M_j = m_j - m_{j-1}$). Near to the center of the interval $\{S'(\bar{x}_j) = (3\,\tilde{m}_i - \bar{m}_j)/2\}$, it is noticeable that the derivative depends three times as much on the given quantity $\tilde{m}_j$ (directly related to the data) than on the computed one $\bar{m}_j$.

c) The Cubic Spline Functions in Classical Dynamical Studies. Consider a molecular system as a mechanical system to which no limitation to the free motion is imposed (symmetries excepted), i.e. no bond and no angle are frozen. Then the hamiltonian is expressed as:

$$H = T(P) + V(Q) \qquad (21)$$

where Q and P are two sets of suitable dynamical variables (respectively, coordinates and conjugate momenta) and the kinetic energy is:

$$T(P) = (\sum_k P_k^2/\mu_k)/2 \qquad (22)$$

μ_k is the mass associated with the coordinate Q_k. The first type hamiltonian equations of motion are simple:

$$\dot{Q}_1 = \partial H/\partial P_1 = \partial T/\partial P_1 = P_1/\mu_1 \qquad (23)$$

The second type equations:

$$\dot{P}_1 = -\partial H/\partial Q_1 = -\partial V/\partial Q_1 \qquad (24)$$

are generally more difficult to obtain, because the potential energy is a function of natural coordinates $x, y \ldots u \ldots$:

$$V(Q) = \mathrm{V}(x, y \ldots u \ldots) \tag{25}$$

where $x = x(Q), y = y(Q), \ldots u = u(Q) \ldots$

Thus the chain rule is used:

$$\dot{P}_1 = -(\partial \mathrm{V}/\partial x)(\partial x/\partial Q_1) - (\partial \mathrm{V}/\partial y)(\partial y/\partial Q_1) \ldots\ldots -(\partial \mathrm{V}/\partial u)(\partial u/\partial Q_1) \ldots\ldots \tag{26}$$

Suppose now, that the potential V is spline fitted[h]. We consider the general polydimensional case and that the number of mesh points in all directions are equivalent to infinity ($N \to \infty$). This situation is always attainable from a polydimensional grid of computed values in a sufficient quantity by subdivision of the step in each direction and preliminary interpolation of purely numerical supplementary values to be used in the spline expression, which therefore is:

$$\mathrm{U}(x, y \ldots u \ldots) = \sum_{i,j,\ldots n \ldots} \mathrm{V}_{i,j \ldots n \ldots} A_\infty[(x - x_i)/h_x] A_\infty[(y - y_j)/h_y] \ldots\ldots$$
$$A_\infty[(u - u_n)/h_u] \ldots\ldots \tag{27}$$

The partial derivatives required by Eq. (26) then are very simply expressed for instance:

$$\partial \mathrm{U}/\partial u = \sum_{i,j,\ldots n \ldots} \mathrm{V}_{i,j,\ldots n \ldots} A_\infty[(x - x_i)/h_x] A_\infty[(y - y_j)/h_y] \ldots\ldots$$
$$dA_\infty[(u - u_n)/h_u]/du \ldots\ldots \tag{28}$$

where, if $\mathrm{u}_{q-1} \leqslant \mathrm{u} \leqslant \mathrm{u}_q$:

$$dA_\infty[(u - u_n)/h_u]/du = [3\,\delta^*_{q-n}(1/2 - 2\,U_q^2) + \beta_{q-n}(3\,U_q^2 - 1/4) + \gamma_{q-n}U_q]/h_u \tag{29}$$

and: $\beta_k = \alpha_k + \alpha_{k-1}$, $\gamma_k = \alpha_k - \alpha_{k-1}$ and $\delta^*_k = \begin{cases} 1 \text{ if } k = 0 \\ -1 \text{ if } k = 1 \\ 0 \text{ otherwise} \end{cases}$

The local variable $U_q = \dfrac{u - \bar{u}_q}{h_u}$ lies within the limits $-\dfrac{1}{2}$ and $+\dfrac{1}{2}$. Values of β's and γ's are given in Table 2.

The algorithm is readily programmed. It allows for dynamical studies with non empirical potentials whatever the dimensionality of the problem under consideration.

---

h) In the two-dimensional case, McLaughlin and Thompson[114] recently used an elegant and convenient matrical method given by Jordan and de Boor[245].

5. Conclusion

The advantages of the spline functions as an interpolation technique are essentially threefold:

(1) they are general and directly related to the results of quantum chemistry calculations as they are produced by the specialists (grids of numerical values);

(2) the obtained potential energy surface can be modified locally without noticeably changing the rest of the surface. This allows for a great flexibility in the course of studies on the influence of local potential properties on whatever phenomenon is dependent on them;

(3) their flexibility makes them a tool with a future in the field of dynamical studies in theoretical chemistry.

The drawback of the method is that one does not obtain parameters that are of significance to the whole surface. To wind up this section, let us assert that the first application has shown the spline technique to be useful and advantageous[1, 2, 114, 244].

II. A Formulation of Classical Mechanics for Constrained Molecular Systems in Chemical Dynamics

1. Introduction

On generally restricts a Chemical Dynamics study to the framework of Classical Mechanics[7, 9, 82, 83, 246]. This is quite justified as long as no trajectory passes close to a crossing point or to a symmetry-avoided-crossing point[i) 247, 248] (the range of validity of classical trajectory studies can be extended to this last case by specific devices[186, 193–197, 246]). At the present time all the Classical Chemical Dynamics studies using adiabatic surfaces have been restricted to small molecular systems (including no more than six atoms)[7, 9, 104, 112, 222]. Indeed, a realistic dynamical study of a greater system is not a straightforward matter. In particular, the usual formulation of Classical Mechanics is relevant to mass points interacting through forces. For nuclear motion this formulation is well adapted to systems in which all the intramolecular degrees of freedom (plus the degrees of relative motion in the case of bimolecular encounters) are explicitly taken into account and therefore may change in the course of the motion. Such a system is called a *free system*. The inclusion of overall rotation, *i.e.* three supplementary degrees of freedom, is optional. Unfortunately, most studies in Chemistry concern systems in which the atoms are too numerous to allow a complete investigation of the entire potential energy surface. Thus many degrees of freedom must be held constant. For instance, some bond lengths which are not sensibly modified in the course of the reaction are fixed *a priori*.

---

i) Classical Mechanics is known to hold for the description of nuclear motions on a static potential surface from various semiclassical investigations[144, 148–150] and from direct comparison with quantum-mechanical results for small systems[140, 141, 143].

Similarly, when the atoms in a substituent group (an alkyl group for instance) do not participate in a reaction as individuals but only as a group, the geometry of the group is frozen. Such systems will be referred to as *constrained systems*, and we search for a suitable formulation of Classical Mechanics for them.

Indeed, the mechanical counterpart to a constrained system is a set of solids (frozen groups) articulated with each other through idealized hinges. The motion of the solids is driven by forces which derive from a potential depending on the remaining degrees of freedom. Below we present a method which executes the required job by introducing a matrix called the *constraint matrix*. This constraint matrix is built up with the mass like-coefficients appearing in the non-diagonal kinetic energy. It depends on generalized coordinates only, *i.e.* not on conjugate momenta. The equations of motion are simply obtained by inverting the matrix and by differentiating its elements with respect to generalized coordinates.

2. Classical Mechanics of Constrained Systems within Lagrangian and Hamiltonian Formalisms

We consider an N-particle mechanical system. A set of K constraints applied to it is holonomic[250] whenever all the relationships connecting the natural coordinates $\{Q_i, i = 1, 2 \ldots 3N\}$ of the particles in the system plus the time t – and which are a mathematical counterpart to the existence of constraints inside the system – are of the form:

$$g_l(Q_1, Q_2 \ldots Q_{3N}, t) = 0 \qquad (l = 1, 2 \ldots K) \tag{30}$$

The elimination of K dependent coordinates results in the introduction of a set of generalized coordinates $\{q_j, j = 1, 2 \ldots n\}$ where $n = 3N - K$, in terms of which the natural coordinates are expressed parametrically[j]:

$$Q_i = Q_i(q_1, q_2 \ldots q_n, t) = Q_i(q, t) \qquad (i = 1, 2 \ldots 3N) \tag{31}$$

Any conservative mechanical system which is either free or subject to holonomic constraints and whose potential does not depend on the generalized velocities is described by standard equations of motion (either Lagrangian or Hamiltonian).

The kinetic energy of the N-particle system is:

$$T = \frac{1}{2} \sum_{i=1}^{N} m_i (\dot{x}_i^2 + \dot{y}_i^2 + \dot{z}_i^2) \tag{32}$$

where x, y and z are cartesian coordinates. The introduction of $3N$ "natural" coordinates:

---

j) On the scale of molecules, all the constraints to be taken into account are mathematically idealized and of the holonomic type. Moreover, the defining transformation Eq. (31) do not depend on time explicitly.

$$Q_1 = m_1^{1/2} x_1,\ Q_2 = m_1^{1/2} y_1, \ldots\ldots\ Q_{3N} = m_N^{1/2} z_N \tag{33}$$

results in a simplified expression for T:

$$T = \frac{1}{2} \sum_{i=1}^{3N} \dot{Q}_i^2 \tag{34}$$

Then the natural coordinates Q_i ($i = 1, 2 \ldots 3N$) are expressed as functions of the independent generalized coordinates q_j ($j = 1, 2 \ldots n$). As an immediate consequence the analytical expression of the potential V is modified:

$$V(Q) = \mathrm{U}(q) \tag{35}$$

The natural velocity $\dot{Q}_i$ (the total differential of Q_i with respect to time) is:

$$\dot{Q}_i = \sum_{j=1}^{n} \frac{\partial Q_i(q)}{\partial q_j} \dot{q}_j \qquad (i = 1, 2 \ldots 3N) \tag{36}$$

Insertion of (36) into (34) provides the expression of the kinetic energy in terms of generalized coordinates:

$$T(q, \dot{q}) = \frac{1}{2} \sum_{j,k=1}^{n} A_{jk}(q)\, \dot{q}_j\, \dot{q}_k \tag{37}$$

where:

$$A_{jk}(q) = \sum_{i=1}^{3N} \frac{\partial Q_i(q)}{\partial q_j} \frac{\partial Q_i(q)}{\partial q_k} \tag{38}$$

$A_{jk}(q)$ is the current element of a matrix $\underset{\sim}{A}(q)$ called the *constraint-matrix*. $\underset{\sim}{A}(q)$ is a real symmetric matrix whose diagonal elements are positive; it depends on the generalized coordinates as variables and parametrically on the constraints. This matrix possesses an inverse since $\det \underset{\sim}{A}(q) = 0$ is not possible; it would correspond to a supplementary relationship between the coordinates only, *i.e.* a supplementary holonomic constraint.

The expressions of the generalized momenta in terms of the generalized velocities are:

$$p_i = \sum_{k=1}^{n} A_{ik}(q)\, \dot{q}_k \qquad (i = 1, 2 \ldots n) \tag{39}$$

The inversion of the matrix $\underset{\sim}{A}(q)$ results in:

$$\dot{q}_i = \sum_{k=1}^{n} A_{ik}^{-1}(q)\, p_k \qquad (i = 1, 2 \ldots n) \tag{40}$$

which is a convenient form of the Hamilton equations of the first type for constrained systems.

Insertion of Eq. (40) into Eq. (37) leads to the expression of the kinetic energy in terms of generalized coordinates and momenta:

$$T(q, p) = \frac{1}{2} \sum_{i,j=1}^{n} A_{ij}^{-1}(q)\, p_i p_j \tag{41}$$

$\underset{\sim}{A}^{-1}(q)$ exists; moreover, it is real and symmetric. It is important to note that obtaining $T(q, p)$ is no more difficult than an inversion of $\underset{\sim}{A}(q)$. The Hamilton equations of motion of the second type then are:

$$\dot{p}_i = -\frac{1}{2} \sum_{j,k=1}^{n} \frac{\partial A_{jk}^{-1}(q)}{\partial q_i} p_j p_k - \frac{\partial \mathcal{U}(q)}{\partial q_i} \quad (i = 1, 2 \ldots n) \tag{42}$$

since $H(q, p) = T(q, p) + \mathcal{U}(q)$.

On the basis of Eqs. (40) and (42), one may state that – once the constraint matrix $\underset{\sim}{A}(q)$ is known – using the hamiltonian formalism to study the dynamics of a constrained system amounts to

(i) inverting $\underset{\sim}{A}(q)$ and

(ii) obtaining the partial derivatives of all the elements of $\underset{\sim}{A}^{-1}(q)$ with respect to all generalized coordinates.

The Lagrange equations of motion are:

$$\sum_{j=1}^{n} A_{ij}(q)\, \ddot{q}_j = \sum_{k,l=1}^{n} \left[\frac{1}{2} \frac{\partial A_{kl}(q)}{\partial q_i} - \frac{\partial A_{ik}(q)}{\partial q_l} \right] \dot{q}_k \dot{q}_l - \frac{\partial \mathcal{U}(q)}{\partial q_i} \tag{43}$$

$$(i = 1, 2 \ldots n)$$

since $L(q, \dot{q}) = T(q, \dot{q}) - \mathcal{U}(q)$.

In order to solve numerically this set of coupled second order differential equations, it is generally the practice to use numerical integrators adapted to coupled first order differential equations only and, consequently, Eq. (43) must be transformed into:

$$\dot{q}_i = \pi_i \tag{44}$$

$$\dot{\pi}_i = -\sum_{j=1}^{n} A_{ij}^{-1}(q) \left[\sum_{k,l=1}^{n} \left(\frac{\partial A_{jk}(q)}{\partial q_l} - \frac{1}{2} \frac{\partial A_{kl}(q)}{\partial q_j} \right) \pi_k \pi_l + \frac{\partial \mathcal{U}(q)}{\partial q_j} \right] \tag{45}$$

$$(i = 1, 2 \ldots n)$$

It should be noticed that the bracket in Eq. (45) is independent of i and depends on j only. Using the Lagrangian formalism to study the dynamics of a constrained system amounts to

(i) inverting $\underset{\sim}{A}(q)$ and

(ii) obtaining the partial derivatives of all the elements of $\underset{\sim}{A}(q)$ with respect to all generalized coordinates.

3. Discussion

At this stage, we must stress one point: the more constrained the system, the smaller the dimension of the reduced problem and the more involved the matrix elements $A_{ij}(q)$. In other words, the reduction of a great number of natural degrees of freedom to a small number of privileged ones by imposing constraints to the system – which results in a shortening of quantum chemical calculations and a simplification of the potential energy surface – happens to introduce supplementary intricacies when dealing with dynamical problems. However, the requirement that a system retains the same symmetry along a reaction path does not appear as a constraint, although it is a restriction to free motion. In fact, a symmetry-constrained system can always be viewed as a free system with a smaller number of dimensions.

Now a qualitative distinction between two classes of constrained systems is discussed. The first class corresponds to a highly constrained system, that is to say a molecule in which at least two frozen groups of atoms are related by means of a hinge located at the atom in common with the two groups. Nothing more than what is in strict conformity with the general treatment presented above can be said for such a system. A preliminary difficulty is generally to express the constraints in a convenient way. A simple solution is to take as generalized coordinates those degrees of freedom that are of physical interest on the basis of either experimental or theoretical information. Expressing the cartesian and natural coordinates as functions of the generalized coordinates results in trigonometrical calculations. An important point is then to ascertain the fixity of the center of mass and, if necessary, the zero value of the total angular momentum. The last operation consists in applying the standard procedure exposed in paragraph 2. The whole work can be very long but is always feasible[1, 2].

The second class includes the minimally constrained systems, *i.e.* molecular systems in which certain groups are still frozen but are individually treated as solids interacting only through a position dependent potential. A quite simple example in this category is a rigid diatomic rotor moving in an external static field. For such systems, mechanical developments that are not possible in the general treatment can often be achieved[170].

Finally, the advantages of respectively, the Lagrangian and Hamiltonian methods, are compared below. Two points should be emphasized:

(i) the Hamiltonian equations are more balanced that the Lagrangian equations. Indeed, there appears a simple summation in Eq. (40) and a double one in Eq. (42) whereas, in Eq. (45) the summation in the expression of $\dot{\pi}_i$ is a triple one. Consequently, the numerical integration (by means of usual integrators) of Hamiltonian equations is somewhat faster and more stable than the integration of Lagrangian equations;

(ii) obtaining Hamiltonian equations requires differentiation of the matrix $\underset{\sim}{A}^{-1}(q)$ whereas, for Lagrangian equations, it is $\underset{\sim}{A}(q)$ which is differentiated. Since the matrix elements $A_{ij}(q)$ are often rather complicated, the matrix-elements $A_{ij}^{-1}(q)$ are even more complicated and their differentiation can result in very large and intricate expressions. Consequently, for highly constrained system, the Lagrangian integration often appears more suitable. The definitive choice for either one method or the other depends in fact on the particular system treated.

4. Conclusion

The present method is applicable to large constrained molecular systems in a streightforward way. Its main advantage is to allow the direct resolution of dynamical problems in those generalized coordinates in terms of which the potential energy functions are expressed, obtained through quantum-chemical calculations. Its main drawback is that the derivation of the analytical constraint-matrix can be quite tedious in some intricate cases of highly constrained systems. The illustration of such a case is presented in the next chapter. To wind this formal section up, let us mention that an alternative technique to resolve mechanical problems involving constrained systems is that of the Lagrange multipliers[k].

III. Some Remarks on How to Select Initial Conditions

1. Introduction

To start the mathematical integration of the equations of motion for one particular trajectory, a set of initial values of coordinates and either velocities or momenta must be specified. These, however, are dependent on the experimental conditions which need be reproduced, such as collision energy, intramolecular vibrational energies etc. . . In addition, some other variables, for instance intramolecular instantaneous elongations, molecular orientations, impact parameter, etc. . ., are necessarily specified in classical mechanics but are not observable microscopically because of the Uncertainty Principle. The ensemble of these result in a set of trajectories associated with a given set of observable initial conditions.

Many trajectories are necessary to describe all the different events that are summed up to form a unique wave describing the global chemical reaction under observable conditions in quantum mechanics. In this respect, a set of classical trajectories which spread around a mean trajectory in classical mechanics corresponds roughly to the quantum mechanical spreading (through space or time) of the density probability function around its center.

Since the number of trajectories is necessarily limited (in particular when computing the forces requires a great amount of computer time), good criteria for selecting the initial conditions are of prime interest. The problem is so important that it was discussed at length several times before[7, 101]. In this section we just consider what can be done in the case of constrained systems. The approximation of the "constraints" is so rough as to eliminate the need for any of the refined corrections that allowed to get very accurate results for small free molecular systems (cf. Chapter A).

Several domains of application need to be distinguished. In the thermal chemistry of unimolecular reactions, a complex process, which is not known to us, leads to the

---

k) By the Lagrange multipliers technique[250] the differential equations are integrated in the natural coordinates and the Lagrange multipliers are used to keep constant the constraints at each step of integration.

initial energy of the reacting molecule (activated molecule). All the possible sets of initial conditions should therefore be studied in order to determine which sets of those initial conditions favour the reaction. To have a statistic weight for each set of initial conditions is desirable but not always possible to obtain. In photochemistry the intramolecular activation energy originates through a photon impact, *i.e.* a well-defined and instantaneous process. From a knowledge of the Franck-Condon principle, it is possible to ascribe to each individual trajectory a statistical weight[189, 191] from which average values of different quantities can be derived.

In the thermal chemistry of bimolecular reactions studied within the framework of trajectories calculations, it is normally possible to obtain the rate constant of the reaction as a function of temperature[116] (cf. Chapter A). However, this can require rather tedious calculations, because of the necessity of averaging the results over a large distribution of individual trajectories. We do not discuss further the problem of bimolecular reactions.

2. Physical Observables and Phase Variables

At the beginning of any trajectory one must specify either the coordinates and the velocities $[q_0, \dot{q}_0]$ or the coordinates and the momenta $[q_0, p_0]$. It is physically desirable that the initial conditions describe an observable situation of the reactants. We denote by G the set of all the experimentally observable quantities (called *physical observables*) which must be reproduced. Such quantities are, for instance, the collision energy, the quantum numbers defining the intramolecular state (vibrations and the principal quantum number of rotation), the total angular momentum etc. . . However, there are other dynamical variables which have a clear meaning in Classical Mechanics but correspond to no physical observable because of the Uncertainty Principle. We call them *phase variables* and denote them globally by g. The phase variables must be given particular values to obtain, at given G, a particular trajectory. Such variables are, for instance, the various intramolecular normal vibrational phases, the intermolecular orientation, the secondary rotation quantum numbers, the impact parameter, etc. . . Thus we look for relationships of the type $q_0 = q_0\,(G, g)$ and either $\dot{q}_0 = \dot{q}_0\,(G, g)$ or $p_0 = p_0\,(G, g)$

To reproduce the results of a given experiment whose theoretical specification is G we must obtain a set of trajectories for various g. Then the theoretical results (the energy transfer, the reaction probability, etc. . .) are obtained as averages over g. Thus an observable quantity F, observable at the end of the reaction, is calculated for given G as

$$F(G) = \sum_{i=1}^{N} F_i(G)/N$$

where:

$$F_i(G) = F(G, g_i) = F(q_0\,(G, g_i), \dot{q}_0\,(G, g_i)) \qquad (i = 1, 2 \ldots N).$$

N is the total number of trajectories. Here g_i is implicitly selected pseudo randomly[251, 252].

Sometimes an additional average over G is required to obtain the theoretical value of a macroscopic experimental quantity. Then one uses a normalized distribution function $P(G)$ of all the components of G, so that in application of the basic principles of Statistical Mechanics: $F = \int_\Gamma P(G)\, F(G)\, dG$ where Γ denotes the subspace of all the possible values of G under the given experimental conditions.

The integral is most often transformed into a finite sum. If the selected values G_j of G are regularly distributed over Γ, then:

$$F = \sum_{j=1}^{M} P(G_j)\, F(G_j) / \sum_{j=1}^{M} P(G_j)$$

where M is the total number of the G_j's. If they are selected pseudorandomly over Γ according to $P(G)$ as weighting function, then

$$F = \sum_{j=1}^{M} F(G_j)/M.$$

These expressions represent the most general theoretical results for whatever macroscopic experimental quantity F.

3. Unimolecular Reactions

In an unimolecular *thermal* reaction, *i.e.* a reaction whose mechanism is a pure intramolecular rearrangement (either isomerization or dissociation), the initial energy distribution among the various degrees of freedom of the system is unknown. Indeed, in a preliminary step the molecule acquires activation energy through a complex process (a collision or, rather, a sequence of collisions) which is in general badly elucidated experimentally. In addition the energy exchange between distortion modes of the activated molecule is very fast[14, 15].

Whenever the reaction involves a few atoms only, both the activation phase of the reaction and the subsequent unimolecular rearrangement can be studied dynamically[210–215]. Then it is possible to ascribe a statistical weight to a given trajectory. As soon as the reactant molecule includes numerous atoms (as is often the case in Organic Chemistry) one just cannot study the overall dynamics of the reaction. In particular, if one must renounce the investigation of the activation phase of the reaction, one must also renounce the attribution of statistical weights to individual trajectories. Then one must postulate, on the basis of either experimental information or physical intuition, initial activated states of the reactant system and study only its subsequent dynamical evolution. Thus the work is restricted to sample in a random way all the possible initial conditions with no attempt to obtain at the end theoretical values of experimental quantities. Nevertheless, this context is not too restrictive. The trajectory study of thermal unimolecular reactions allows one

(i) to discover which initial energy distributions favour completion of the reaction, which others disfavour or prevent it, and to relate these "a posteriori" observations to experimental facts;

(ii) to observe qualitatively the microscopic dynamical paths of the reactions;

(iii) to obtain the statistical distribution of the molecular lifetimes and thus to have a feeling for the reaction times at various total energies. Such a dynamical study of a unimolecular thermal reaction (isomerization of cyclopropane) is the subject of the next Chapter (C).

The situation just described is not inherent in all unimolecular reactions. In certain cases (for instance unimolecular *photochemical* reactions, *i.e.* non photosensitized) an equilibrium energetic distribution (that of the fundamental state in the case of photochemical reaction) is warranted. Then a statistical weight can be attributed to each trajectory, either classically or semi-quantally.

In the classical approach[253], the probability to find the ith normal coordinate of the system within $[q, q + dq]$ is proportional to the time elapsed in it:

$$P_i(E; q) = 2/\{T_i(E - k_i q^2/2)^{1/2}\}$$

where k_i and T_i are respectively the force constant and the period of the ith normal mode; E is the total energy in the mode (physical observable) and q is the phase variable. Thus the classical probability is minimal at equilibrium and infinite at the turning points of the vibration. Finally, the statistical weight of a set of initial conditions $\{G = E_1, E_2 \ldots; g = q_1, q_2 \ldots\}$ is the product of the partial probabilities for the various modes:

$$P(G; g) = \prod_{i=1,2\ldots} P_i(E_i; q_i)$$

In the semiquantal approach (theory of Wigner functions)[253–255], Statistical Mechanics is corrected according to quantum mechanical criteria. The statistical probability of finding the coordinate of the ith normal mode within $[q, q + dq]$ and its conjugate momentum within $[p, p + dp]$ is proportional to $\exp\{-[p^2/m_i + k_i q^2]/2\,kT\}$, where m_i and k_i and respectively the reduced mass and force constant of the ith mode, k is the Boltzmann constant and T is the temperature. There is no counterpart to this probability in Quantum Mechanics because of the Uncertainty Principle. However, since the normalized wave function $\Psi_i^v(p)$ of the ith normal mode in its vth vibrational state is known, the separate probabilities for q and p are entirely defined: $\Pi_i^v(q) = |\Psi_i^v(q)|^2$ and $\tilde{\Pi}_i^v(p) = |\Phi_i^v(p)|^2$ where $\Phi_i^v(p)$ is the Fourier transform of $\Psi_i^v(q)$. The meaning of these probabilities is the following: although it is impossible to predict the results of the simultaneous measurements of both q and p, it is nevertheless possible to predict the average results of measurements on a numerous set of identical systems if all of them are in the same quantum state. Thus it is quantum mechanically sound to look for a pseudo-distribution function $P_i(v; q, p)$ which would result in $\Pi_i^v(q)$ when integrated over p and in $\tilde{\Pi}_i^v(p)$ when integrated over q. Among all the mathematical functions fulfilling these two requirements, Wigner[254] has selected the very simple one:

$$P_i(v, q, p) = (\pi h)^{-1} \int_{-\infty}^{+\infty} \Psi_i^v(q + Q)\, \Psi_i^v(q - Q) \exp(2\,\mathrm{i}pQ/\hbar) dQ$$

$$= P_i(v; \xi_i^2) = (\pi h)^{-1} (-1)^v \exp(-\xi_i^2)\, L_v(2\,\xi_i^2)/(\pi\hbar v!)$$

where: $\xi_i^2 = \alpha_i^2 q^2 + p^2/(\alpha_i^2 h^2)$, α_i is a constant and L_v denotes a Laguerre polynomial. Here v is a physical observable and ξ^2 a phase variable. This function is real but not everywhere positive. For this reason it cannot be viewed as a true probability distribution function. Nevertheless, it can be used qua a distribution function since it fulfils all the requirements which would characterize this function if it existed. When $v = 0$, and only then,

$$P_i(v = 0; q, p) = \Pi_i^0(q) \times \tilde{\Pi}_i^0(p)$$

as it would be the case if p and q where simultaneously measurable[253]. When $v \neq 0$ the probability of a given p depends on q, and vice versa. In the classical limit (great values of v) this situation is consistent with the Correspondence Principle; indeed, in Classical Mechanics, the values of q and p are related to each other.

Finally, for a reactant system including several vibrational modes, the Wigner function is simply a product of one dimensional functions:

$$P(G = v_1, v_2 \ldots, g = \xi_1^2, \xi_2^2 \ldots) = \prod_{i=1,2\ldots} P_i(v_i, \xi_i^2)$$

One of us has personally applied the theory of Wigner functions to obtain statistical weights for individual trajectories in the study of the photochemical dissociation of the water molecule in its second singlet excited state[244, 256]:

$$H_2O(\tilde{B}\ ^1A_1) \longrightarrow H(^2S) + OH(^2\Sigma_+)$$

to account for the abnormally excited rotation of the OH fragment which is observed experimentally[257, 258].

C. Application: Optical and Geometrical Isomerizations of Cyclopropane

1. Experiments and Previous Theoretical Investigations

The pyrolysis of substituted cyclopropane leads to three types of unimolecular isomerizations (see Fig. 3). The first kinetic study of the conversion of cyclopropane into propylene (reaction a) was undertaken by Trautz and Winkler in 1922[l) 259]. The geometrical isomerization (reaction b) was discovered by Rabinovitch, Schlag, and Wiberg in 1958[m) 261]; reaction b is faster than structural isomerization in propylene (a). Finally, the optical isomerization was observed, independently by Crawford and Lynch[268], by Berson and Balquist[269], by Bergmann and Carter[270, 271], and by Willcott and Cargle[272]; their common conclusion states that geometrical (b) and optical (c) isomerizations are competitive reaction processes. If only the sub-

l) For a more recent experimental work on the mechanism of this reaction, see Ref.[260].

m) For later studies on *cis-trans* isomerization in substituted cyclopropanes, see Refs.[262–267].

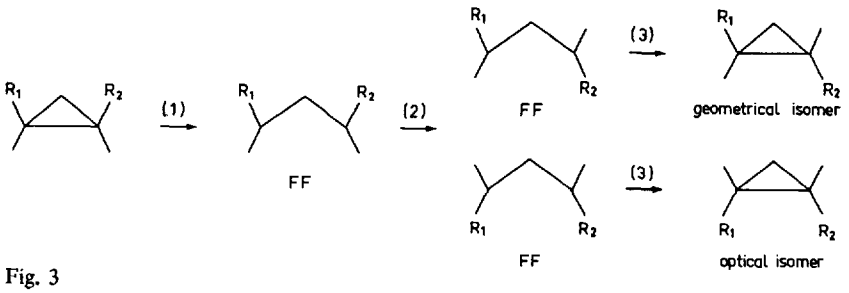

Fig. 3

stituted bond breaks, this result implies that the single-rotational process, required for geometrical isomerization, and the double-rotational process, required for optical isomerization, are competitive rotational processes. This was confirmed by Doering and Sachdev[273]. However, Berson, Pedersen and Carpenter have recently shown that in substituted cyclopropanes in which the three C–C bonds can break equally (*i.e.*: 1-phenylcyclopropane-2-d), the major pathway is a synchronous rotation of both terminal groups[274, 275]. Most mechanisms for the geometrical and optical isomerizations invoke a trimethylene diradical species (for a complete review, see Ref.[276]).

These reactions have aroused a great deal of interest among theoretical chemists. Indeed, they lie within the simplest reactions in organic chemistry; formally, they require only a rotation of 180° in one or both methylene groups. Hoffmann, in his

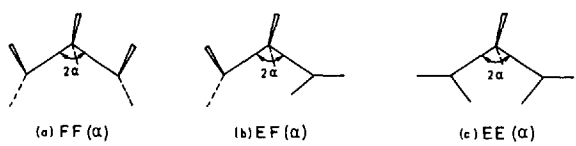

Fig. 4. Definition of the geometries of the three diradicals face-to-face [FF(α)], edge-to-face [EF(α)] and edge-to-edge [EE(α)]

pioneering search of the potential energy surface for isomerization of cyclopropane, found that synchronous (conrotatory) motion of the terminal groups, through an edge-to-edge (EE) diradical (Fig. 4-c) is the easiest path on the surface[277]. This prediction was recently confirmed by the kinetic analysis of the isomerization of trans-cyclopropane-1,2-d_2 by Berson and Pedersen[275]. Afterwards, several groups undertook nonempirical quantum-mechanical calculations on

(i) the ring opening of the cyclopropane and

(ii) the rotations of the terminal groups in the face-to-face (FF) diradical (Fig. 4-a) thus obtained[3, 4, 278–280]. The results of these calculations confirm the competition experimentally observed between the two isomerization reactions: the diradical EE is slightly more stable than the edge-to-face (EF, Fig. 4-b) diradical (ΔE = 1–2 kcal/mol). Moreover, no potential energy barrier is found in the ring closure of the diradical toward the cyclopropane. This result, inconsistent with thermodynamic pre-

dictions[281], is in agreement with the results of recent ESR study of 1,3-cyclopentadiyl diradical[282]. Finally, the geometry of the transition state for geometrical isomerization has been resolved in 21-dimensional space, and that for optical isomerization obtained approximately. Static reaction paths were proposed for both reactions b and c[3, 4].

II. Potential Energy Surface

The static study requires consideration of three main geometrical parameters: the angle of ring opening $\widehat{CCC}$ (= 2 α) and the rotation angles for both terminal methylene groups (θ_1 and θ_2). The other (secondary) parameters are either held constant or varied in a conventional way.

The potential energy function $V(\alpha, \theta_1, \theta_2)$ can be re-written as a sum of two terms:

$$V(\alpha, \theta_1, \theta_2) = V(\alpha, 0, 0) + [V(\alpha, \theta_1, \theta_2) - V(\alpha, 0, 0)] \tag{46}$$

The first term corresponds to the potential energy of a cyclopropane molecule in the FF configuration with the ring angle $\widehat{CCC}$ = 2 α (Fig. 4-a). The calculated energy curve is pictured in Fig. 5: there appears no barrier to the reclosure motion of the diradical FF (α). This curve will be analytically approximated by means of one-dimensional cubic spline functions.

The second term denotes the amount of energy required for rotations of the terminal groups, with angular amplitude of θ_1 and θ_2, at constant α. For each value of α, the potential energy of the diradical as a function of the two rotation angles is

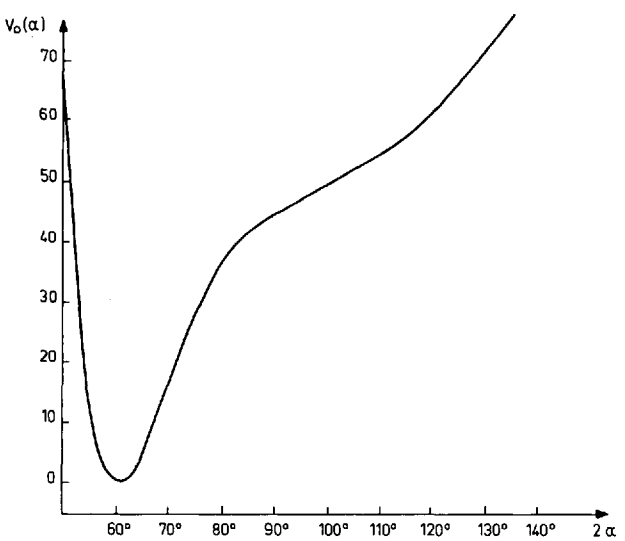

Fig. 5. Potential energy curve for the ring opening from cyclopropane to the face-to-face diradical. The energies are in kcal/mol

described by an analytical expression, which is simple but yet retains the essential features of the surface[1]. There are four main features of the rotational surfaces that the analytic formula must reproduce accurately: the energies of the half-way points EF(α) and EE(α); the potential-barrier heights, $h_C(\alpha)$ and $h_D(\alpha)$ for conrotatory and disrotatory motions (Fig. 6). The following analytic formula is somewhat arbitrary; it is selected because it abides by the law of symmetry and takes into account the four parameters independently:

$$\begin{aligned} V(\alpha,\theta_1,\theta_2) - V(\alpha,0,0) = {} & a(\alpha)\sin^2(\theta_1+\theta_2)\sin^2(\theta_1-\theta_2) \\ & + b(\alpha)\sin^2(\theta_1-\theta_2)\cos^2(\theta_1+\theta_2) \\ & + c(\alpha)\sin^2(\theta_1+\theta_2)\cos^2(\theta_1-\theta_2) \\ & + d(\alpha)\sin^2\theta_1\sin^2\theta_2 \end{aligned} \tag{47}$$

$a(\alpha)$ denotes the potential energy of the molecule in the configuration EF(α) ($\theta_1 = 90°$, $\theta_2 = 0°$) minus the potential energy of EF(α) ($\theta_1 = \theta_2 = 0°$). Similarly, $d(\alpha)$ is the potential energy of the molecule in the configuration EE(α) ($\theta_1 = \theta_2 = 90°$). $b(\alpha)$ and $c(\alpha)$ are simple functions of the potential energy barriers to the synchronous disrotatory motion [$h_D(\alpha)$] and the synchronous conratatory motion [$h_C(\alpha)$] respectively (see Fig. 6)

$$b(\alpha) = [h_D(\alpha) + (h_D^2(\alpha) - h_D(\alpha)\,d(\alpha))^{1/2}]/2 \tag{48}$$

$$c(\alpha) = [h_C(\alpha) + (h_C^2(\alpha) - h_C(\alpha)\,d(\alpha))^{1/2}]/2 \tag{49}$$

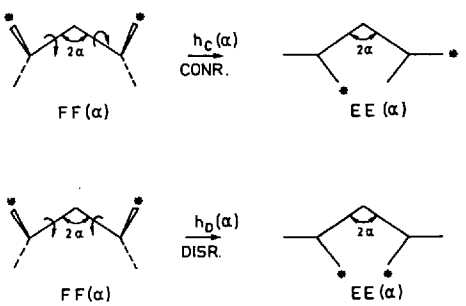

Fig. 6

Calculations of the energies were performed with a 3 x 3 CI version of Gaussian 70, at the STO-3G level[283]. For sixteen values of 2 α, regularly spaced form 50.1° = 0.875 rd to 136.1° = 2.375 rd, the potential energy curves which drive

(i) the synchronous conrotatory motion of both terminal methylene groups,

(ii) the synchronous disrotatory motion and

(iii) the rotation of a single methylene group (the other being held fixed) were computed. The computed values of $a(\alpha)$, $b(\alpha)$, $c(\alpha)$ and $d(\alpha)$ are interpolated by means of one-dimensional cubic spline functions.

The detailed results of these calculations have been given elsewhere[2]. Then we shall only recall the main features of the three-dimensional potential energy surface,

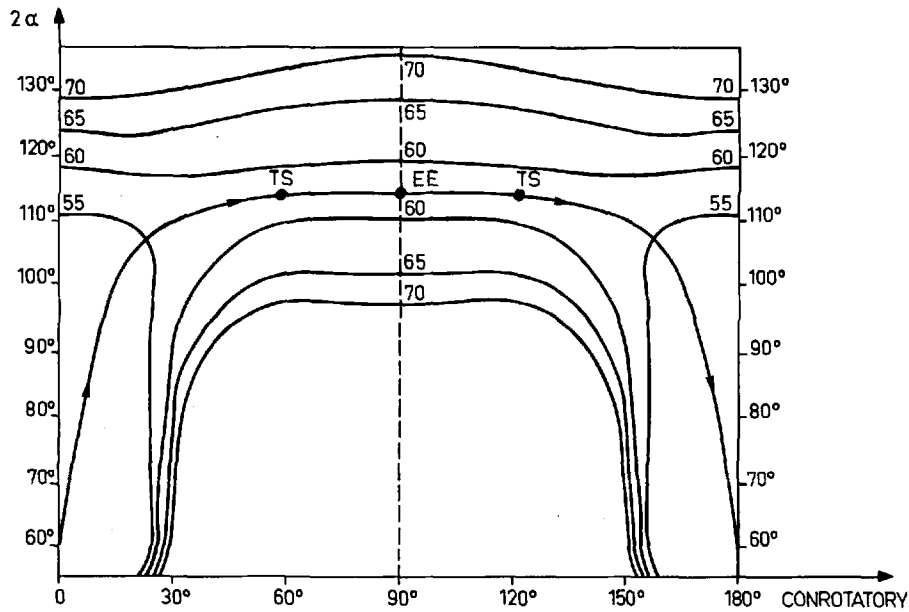

Fig. 7. Two-dimensional potential energy surface and static reaction path for the synchronous conrotatory motion of the terminal methylene groups. 2α represents the value of the carbon ring angle. The abcissa gives the common value of both rotational angles: $\theta = \theta_1 = \theta_2$. TS denotes the position of a transition state. The energies are in kcal/mol

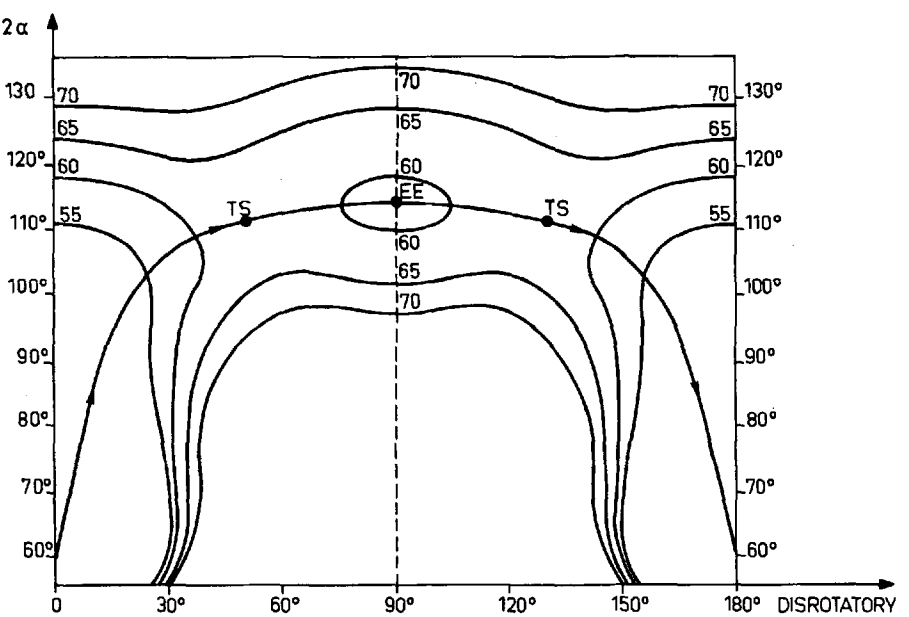

Fig. 8. Two-dimensional potential energy surface and static reaction path for the synchronous disrotatory motion of the terminal methylene groups. 2α represents the value of the carbon ring angle. The abcissa gives the common absolute value of both rotational angles: $\theta = \theta_1 = -\theta_2$. TS denotes the position of a transition state. The energies are in kcal/mol

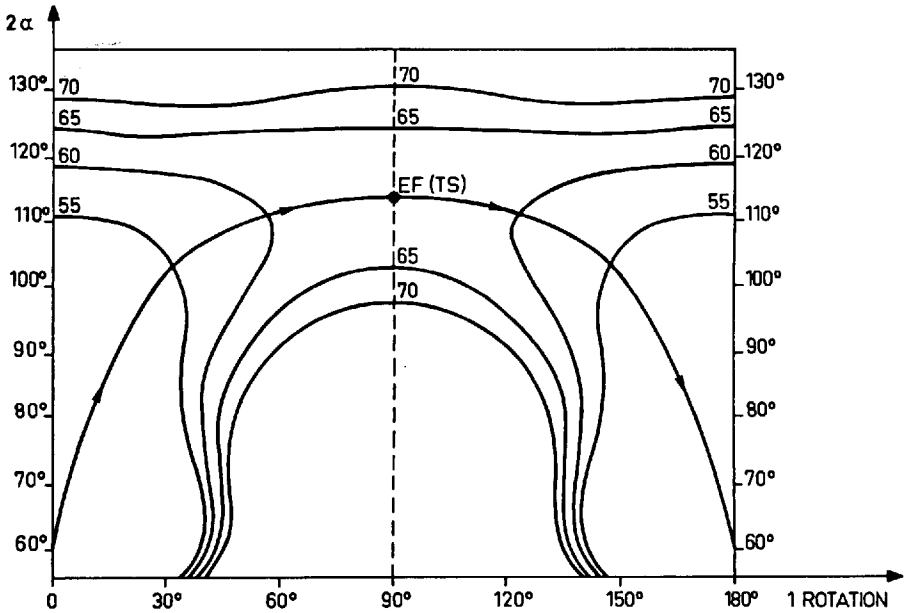

Fig. 9. Two-dimensional potential energy surface and static reaction path for the rotational motion of a single terminal methylene group. 2α represents the value of the carbon ring angle. The abcissa gives the value of the rotational angle: $\theta = \theta_1$ along with $\theta_2 = 0$. TS denotes the position of a transition state. The energies are in kcal/mol

by means of two-dimensional cuts obtained in the following three limiting cases:

(i) synchronous conrotatory motion ($\theta_1 = \theta_2 = \theta$; cf. Fig. 7);

(ii) synchronous disrotatory motion ($\theta_1 = -\theta_2 = \theta$; cf. Fig. 8);

(iii) rotation of a single methylene group ($\theta_1 = 0$, $\theta_2 = \theta$; cf. Fig. 9). The minimum energy paths are drawn approximately and the positions of the transition states (TS) are specified.

The main features of the overall surface appears clearly in these two-dimensional cuts: in a first step, the reaction coordinate is almost identical with a pure ring-opening motion; the rotation of the terminal groups occurs at almost constant angle $\widehat{CCC}$, and finally the ring recloses and the isomer molecule is formed. The optical isomer is most easily formed via a purely conrotatory process (see Fig. 7). The transition state is close to EE (α) with $2\alpha = 113°$ and is energetically located at 59.8 kcal/mol above cyclopropane. In Fig. 8, the diradical EE (α) with $2\alpha = 113°$ appears to be a secondary minimum along the synchronous disrotatory reaction path. In fact, it is not a true minimum, since a conrotatory distortion (here, the hidden third coordinate) requires practically no activation energy. The optical isomerization via a synchronous disrotatory process requires an activation energy of 61.9 kcal/mol. At last, the transition state for geometrical isomerization (cf. Fig. 9) is the diradical EF (α) with $2\alpha = 113°$ whose potential energy is 61.6 kcal/mol above that of cyclopropane.

III. Dynamical Study

1. Equations of Motion and Initial Conditions

The equations of motion are established within the following simplification: the kinetic energy of the system is written for a model in which the terminal methylene groups remain trigonal throughout the reaction (see Fig. 10). Then, the $\underset{\sim}{A}$ matrix, defined in a previous section, is diagonal and the expression of the kinetic energy is a diagonal quadratic form of the angular velocities:

$$T = \frac{1}{2} A_{\alpha\alpha} \dot{\alpha}^2 + \frac{1}{2} I (\dot{\theta}_1^2 + \dot{\theta}_2^2) \tag{50}$$

where: $A_{\alpha\alpha} = S \sin^2\alpha + C \cos^2\alpha + I(\sin^2\theta_1 + \sin^2\theta_2)$ (51)

and: $$S = \frac{2}{M + 2m_1} \left\{ \frac{1}{1 + 2\rho} [L(M + 2m_1) + 2m_1\lambda]^2 + M 2m_1\lambda^2 \right\}$$

$$C = 2[ML^2 + 2m_1(L + \lambda)^2]$$

$$I = 2m_1\mu^2$$

$$\rho = \frac{M + 2m_1}{M + 2m_2}$$

$$\lambda = l\cos\frac{\gamma}{2}, \quad \mu = l\sin\frac{\gamma}{2}$$

L is the CC length, l the CH length and γ the $\hat{HCH}$ angle in the terminal groups, M the mass of a carbon atom, m_1 and m_2 the masses of the substituents on $C_1(C_2)$ and C_3 respectively. In the present study $m_1 = m_2 = 1$ and $\rho = 1$; I is the moment of inertia of the rotor which is formed of the two hydrogen atoms in a terminal methylene group. Eq. (51) leads to the partial derivatives:

$$\frac{\partial A_{\alpha\alpha}}{\partial\alpha} = (S - C)\sin 2\alpha \tag{52}$$

$$\frac{\partial A_{\alpha\alpha}}{\partial\theta_i} = I\sin(2\theta_i) \qquad (i = 1, 2) \tag{53}$$

Finally, the three Lagrangian equations of motion are:

$$\ddot{\alpha} = -\frac{1}{A_{\alpha\alpha}} \left[\frac{1}{2} \frac{\partial A_{\alpha\alpha}}{\partial\alpha} \dot{\alpha}^2 + \dot{\alpha} \left(\frac{\partial A_{\alpha\alpha}}{\partial\theta_1} \dot{\theta}_1 + \frac{\partial A_{\alpha\alpha}}{\partial\theta_2} \dot{\theta}_2 \right) + \frac{\partial V}{\partial\alpha} \right] \tag{54}$$

$$\ddot{\theta}_i = \frac{1}{I} \left[\frac{1}{2} \frac{\partial A_{\alpha\alpha}}{\partial\theta_i} \dot{\alpha}^2 - \frac{\partial V}{\partial\theta_i} \right] \qquad (i = 1, 2) \tag{55}$$

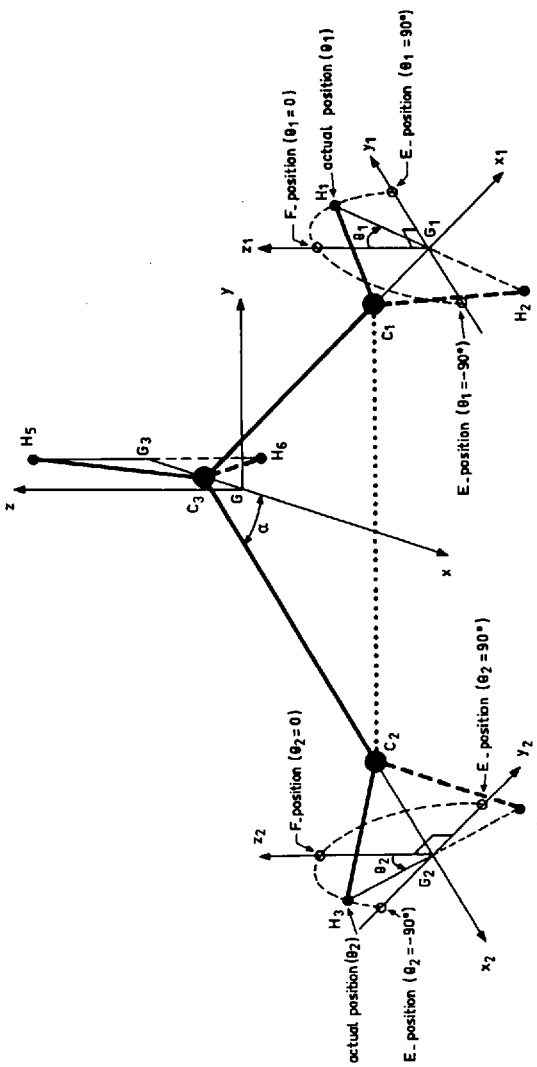

Fig. 10. Definition of the dynamical variables α, θ_1 and θ_2. Particular molecular conformations are explicitly indicated

where:

$$\frac{\partial V}{\partial \alpha} = \frac{dV_0}{d\alpha} + \frac{da}{d\alpha}\sin^2(\theta_1+\theta_2)\sin^2(\theta_1-\theta_2) + \frac{db}{d\alpha}\sin^2(\theta_1-\theta_2)\cos^2(\theta_1+\theta_2)$$
$$+ \frac{dc}{d\alpha}\sin^2(\theta_1+\theta_2)\cos^2(\theta_1-\theta_2) + \frac{dd}{d\alpha}\sin^2\theta_1\sin^2\theta_2 \qquad (56)$$

$$\frac{\partial V}{\partial \theta_i} = 2\sin(2\theta_i)\ \pm a(\alpha)\sin(\theta_1+\theta_2)\sin(\theta_1-\theta_2) \pm b(\alpha)\sin(\theta_1-\theta_2)\cos(\theta_1+\theta_2)$$
$$+ c(\alpha)\sin(\theta_1+\theta_2)\cos(\theta_1-\theta_2) + \frac{1}{2}d(\alpha)\sin^2\theta_{i'}$$
$$(i = 1, 2 \text{ and } i' \neq i) \qquad (57)$$

The + alternative should be used for $i = 1$ and the − alternative for $i = 2$ respectively.

The numerical integration of the three coupled second order differential Eq. (54), (55) requires six initial conditions. These are (i, ii, iii) the three values $2\alpha^\circ$, θ_1° and θ_2°, which determine the molecular geometry at the starting point (all the trajectories in the present study start with the cyclopropane molecule in its equilibrium geometry, *i.e.* $2\alpha^\circ = 60^\circ$, $\theta_1^\circ = \theta_2^\circ = 0$); (iv) the total internal energy in the molecule, E_{tot}; (v) the fraction E_{rot}° of initial energy attributed to the "rotation" (at starting point, this is actually vibration energy); (vi) the manner in which E_{rot}° is distributed among the two "rotors". This is defined by an angle (δ°) such that:

$$\mathrm{tg}\delta^\circ = \dot{\theta}_1^\circ/\dot{\theta}_2^\circ \qquad (58)$$

where $\dot{\theta}_1^\circ$ and $\dot{\theta}_2^\circ$ are the initial rotational velocities of the two groups. Then the relationship:

$$\dot{\theta}_2^\circ = \cos\delta^\circ\,[2I^{-1}E_{rot}^\circ]^{1/2} \qquad (59)$$

is used. It is not restrictive to have $\dot{\theta}_2^\circ > 0$ since $\dot{\theta}_1^\circ$ can be either positive or negative. A third relationship:

$$\dot{\alpha}^\circ = \pm\{2\,[E_{tot} - E_{rot}^\circ - V(\alpha^\circ, \theta_1^\circ, \theta_2^\circ)]/A_{\alpha\alpha}(\alpha^\circ, \theta_1^\circ, \theta_2^\circ)\}^{1/2}, \qquad (60)$$

is necessary to define the initial $\widehat{CCC}$ angular velocity. The present study has been arbitrarily limited to $\dot{\alpha}^\circ > 0$, *i.e.* to initial extensions of the CC bond.

Five different values of E_{tot} have been studied, namely 61, 62, 63, 64 and 65 kcal/mol. For $E_{tot} = 61$ kcal/mol, the only available channel is the synchronous conrotatory motion (transition state at 59.8 kcal/mol). For $E_{tot} \geqslant 62$ kcal/mol, the rotation of a single group (transition state at 61.6 kcal/mol) and the concerted disrotatory motion (transition state at 61.9 kcal/mol) both become feasible motions, at least in principle. For each value of E_{tot}, E_{rot}° has been varied stepwise from 2 to 50 kcal/mol, with a step of 2 kcal/mol. In addition, for given values of E_{tot} and E_{rot}°, δ° has been varied from 45° (conrotatory motion, *i.e.* antisymmetric vibra-

tion of the methylene groups) to −45° (disrotatory motion, *i.e.* symmetric vibration), with a step of 10°. All things considered, about 1500 trajectories have been run.

In our model, no fraction of the total energy in the molecule can be transferred to nonreactive intramolecular modes; nor can any fraction be exchanged with the medium. Under this assumption the computed trajectories are endless: a given set of initial conditions leads to an infinite sequence of ring openings, rotations and ring closures. The integration of a trajectory is stopped the first time the representative point of the molecule moving on the surface enters a prescribed narrow region around the absolute minimum, *i.e.* the representative point of cyclopropane in its equilibrium geometry. This is consistent with the analysis of the reaction given by Doering and Sachdev[273] within the RRK-model[13]. Their conclusion was that "the best trap for a diradical is its own reclosure to a covalent bond", because there the energy "is rapidly dissipated by distribution among other, non-reactive modes. The larger the number of atoms . . . in the molecule, the more nearly true this statement is".

2. Dynamical Results

We first treat separately the trajectories corresponding to the particular values $\delta° = 45°$ and $-45°$. Indeed, the total symmetry of the problem is such that, whenever the motion of both rotors at the starting point is either purely conrotatory or purely disrotatory, it keeps this particularity throughout the trajectory. Then the trajectory can be drawn on a two-dimensional potential energy surface such as that pictured in Fig. 7 and 8.

a) Synchronous Conrotatory Motion ($\delta° = 45°$). For a very weak amount of excess energy (1.2 kcal/mol) with respect to the conrotatory transition state (59.8 kcal/mol), a rather striking phenomenon occurs: reactive trajectories are observed

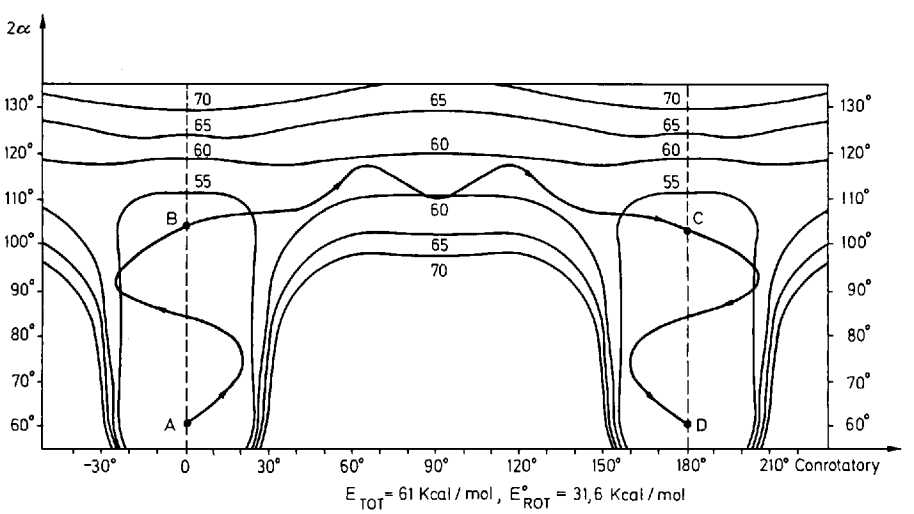

Fig. 11. A low total energy (61 kcal/mol) reactive trajectory leading from cyclopropane to the optical isomer via a purely conrotatory process ($\delta° = 45°$)

only when E°_{rot} – initial "rotational" energy here exclusively in the antisymmetric twisting vibration of the methylene groups – lies between 30.4 and 32.4 kcal/mol (see Fig. 11). Thus, in order to observe the optical isomer formed in a purely conrotatory fashion, one half of the total molecular internal energy must be placed in the methylene groups. The other half of the total energy (28.6 to 30.6 kcal/mol) remains in the stretching vibrational mode of the carbon-carbon bond. At first sight, this would seem insufficient to bring about the opening of the carbon ring. However, during the first part of the reaction (from point A to point B in Fig. 11), the ring opening motion and a complete oscillation of both terminal groups (with an amplitude of 20°) go on simultaneously. Hence, an important energy transfer occurs from the methylene groups to the carbon-carbon bond. Then only, the carbon ring can open. Afterwards, the methylene groups rotate by 180° (from B to C in Fig. 11); in the meantime the value of the $\hat{CCC}$ angle oscillates weakly around the optimum value 113°. The reaction ends with a motion of ring closure (from C to D in Fig. 11).

When the total intramolecular energy increases ($E_{tot} \geqslant 62$ kcal/mol), the reactive trajectories are more numerous. Below we analyze in detail the set of trajectories for $E_{tot} = 62$ kcal/mol (see Fig. 12). Depending on the value of E°_{rot}, several distinguishable motions are observed:

$E^{\circ}_{rot} \leqslant 10$ kcal/mol: the trajectories are non reactive. As shown in Fig. 12a, the carbon ring opens and recloses without reaching the transition state. This is simply due to a lack of twisting energy in the methylene groups at the starting point.

$12 \text{ kcal/mol} \leqslant E^{\circ}_{rot} \leqslant 20$ kcal/mol: within these limits the trajectories are reactive (see Fig. 12b, c and d). They are quite different from the trajectories in Fig. 11: only one half of an oscillation of the methylene groups occurs during the ring-opening phase. In Fig. 12b the first reactive trajectory of this type is pictured: during the rotation of the methylene groups the carbon ring angle oscillates many times around the optimum value 113° and, consequently, the duration of the phase of rotation is long (3.3×10^{-13} second). This means, that the way in which the representative point reaches the upper valley is far from being ideal. The ideal situation occurs when $E^{\circ}_{rot} = 16$ kcal/mol (see Fig. 12c); then, the methylene groups rotate very easily in 2.2×10^{-13} second. Finally, for $E^{\circ}_{rot} = 20$ kcal/mol (see Fig. 12d) the rotational process is again difficult and lengthy (4.4×10^{-13} second). It is quite important to note that all these trajectories include only a *single rotation of 180°* by each terminal group. This result is all the more surprising since the energy in the rotational motion can only be transferred, in our model, to the vibration of the carbon-carbon bond, and not to a non reactive mode.

$22 \text{ kcal/mol} \leqslant E^{\circ}_{rot} \leqslant 32$ kcal/mol: the trajectories are non-reactive, as pictured in Fig. 12e and 12f. When the ring opens the energy is badly distributed among the different possible modes and the transition state cannot be reached. In Fig. 12e, the representative point, after a half oscillation of the methylene groups, bounces off the edge of the lower potential energy bump towards the upper part of the figure. In Fig. 12f, the same thing occurs, but after a complete oscillation.

$32.4 \text{ kcal/mol} \leqslant E^{\circ}_{rot} \leqslant 35.2$ kcal/mol: within these limits the trajectories are again reactive (see Fig. 12g) and of the same type as that pictured in Fig. 11. As previously, each terminal group rotates by only 180°. It should be emphasized that this second "reactive band" of initial rotational energies is much more narrow than the

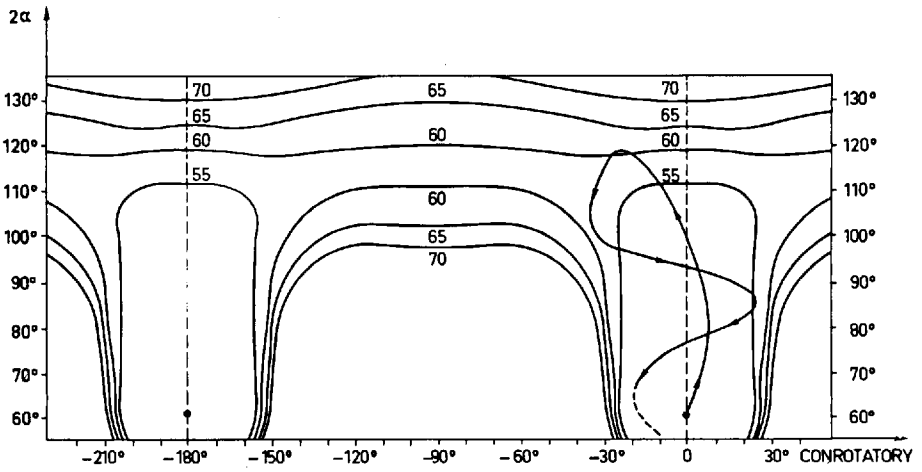

(a) E°_{ROT} = 6 Kcal/mol

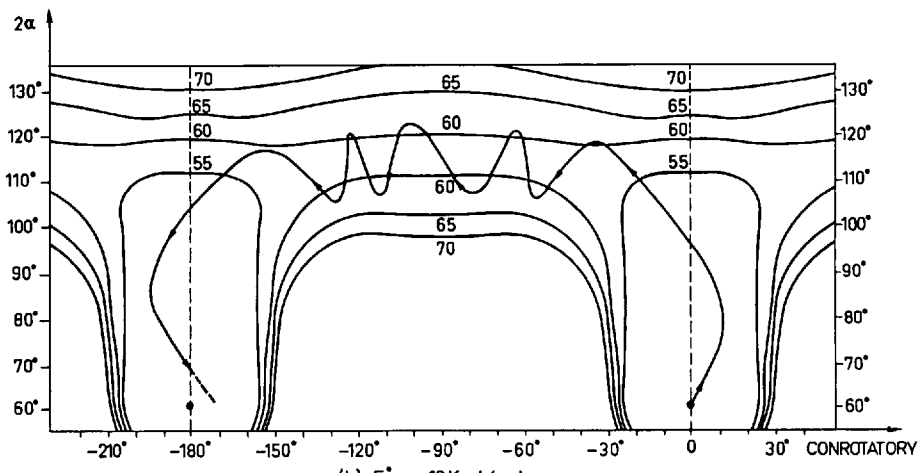

(b) E°_{ROT} =12 Kcal/mol

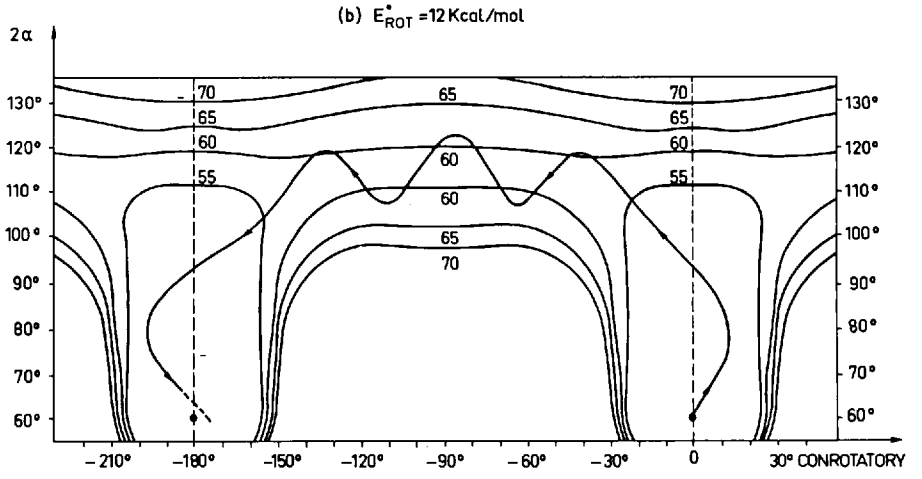

(c) E°_{ROT} = 16 Kcal / mol

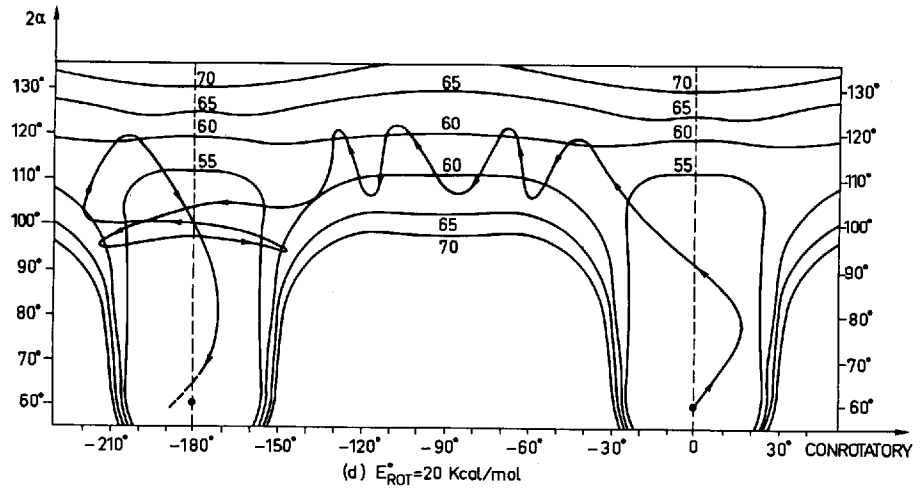

(d) E°_{ROT}=20 Kcal/mol

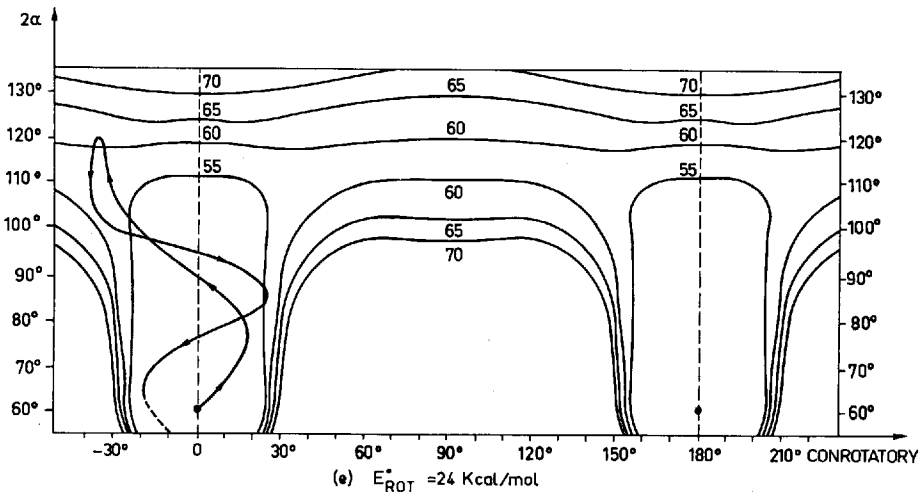

(e) E°_{ROT} =24 Kcal/mol

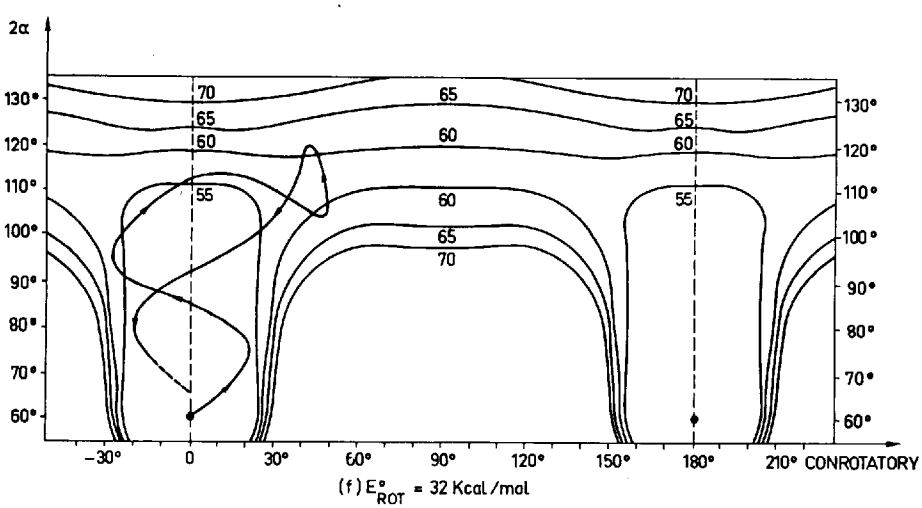

(f) E°_{ROT} = 32 Kcal/mol

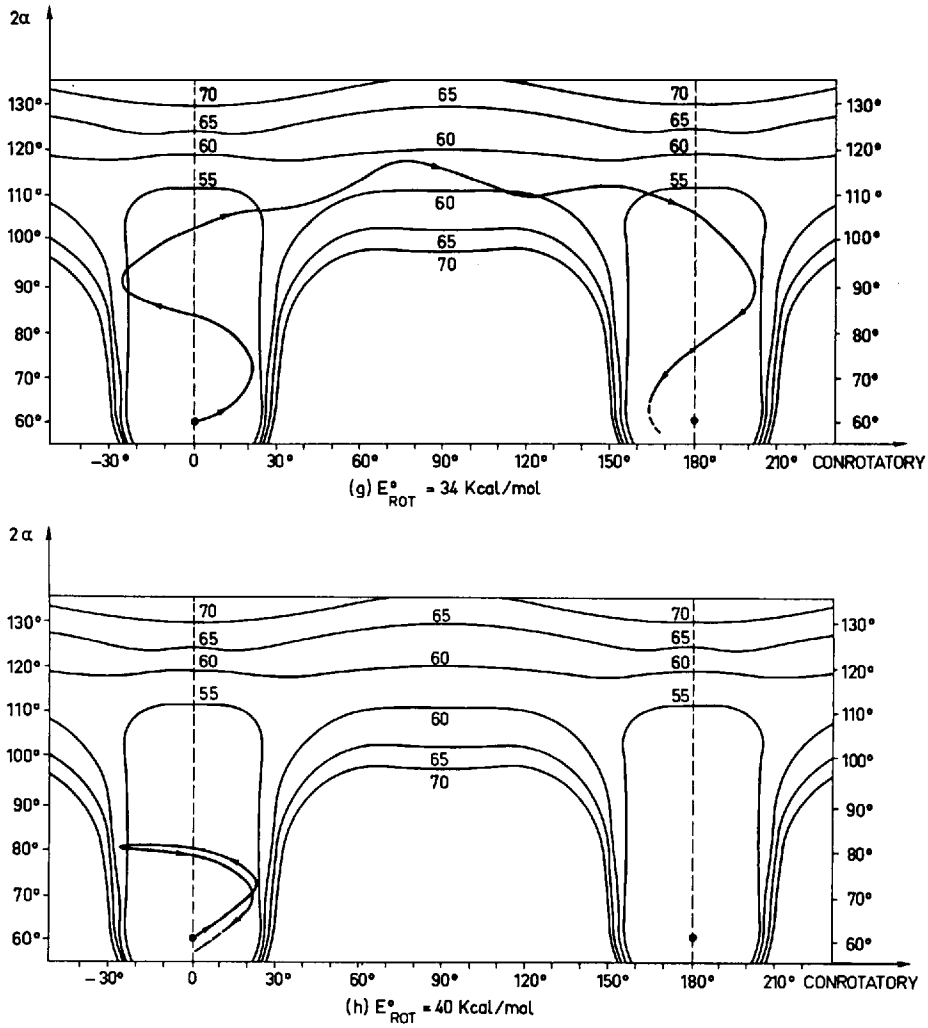

Fig. 12. Typical conrotatory trajectories at E_{tot} = 62 kcal/mol for different initial "rotational" (vibrational) energies

first one. This can be explained as follows: the rotations occur after a complete oscillation of the methylene groups. As a consequence, this first part of the reaction (ring opening) lasts longer in the trajectories of the second band (32.4 to 35.2 kcal/mol) than in the trajectories of the first "reactive band" (12 to 20 kcal/mol). Then the reactive trajectories are much more "focused" around the ideal trajectory: a slight modification can lead to large deviations and rapidly to non reactive trajectories.

$E^{\circ}_{rot} \geqslant 36$ *kcal/mol:* these trajectories are non reactive (see Fig. 12h). The energy initially concentrated in the stretching mode of the carbon-carbon bond is too small ($\leqslant$ 26 kcal/mol) to allow a sufficient opening of the carbon ring.

For total intramolecular energies greater than 62 kcal/mol, (E°_{tot} = 63, 64, 65 kcal/mol), the two "reactive bands" of initial E°_{rot} values still exist (see Fig. 13a) and even become larger and larger with increasing E_{tot}[n) 285)]. This is due to the fact that, the greater the excess energy, the easier it is for the representative point of the molecule to step over the transition state, even if the approach coordinate is not favourable. Moreover, the second reactive band shifts slightly towards higher values of E°_{rot}, so that the first phase of the reaction (ring opening along with a complete oscillation of the methylene groups) always results in a face-to-face diradical with a $\widehat{CCC}$ angle close to 105°.

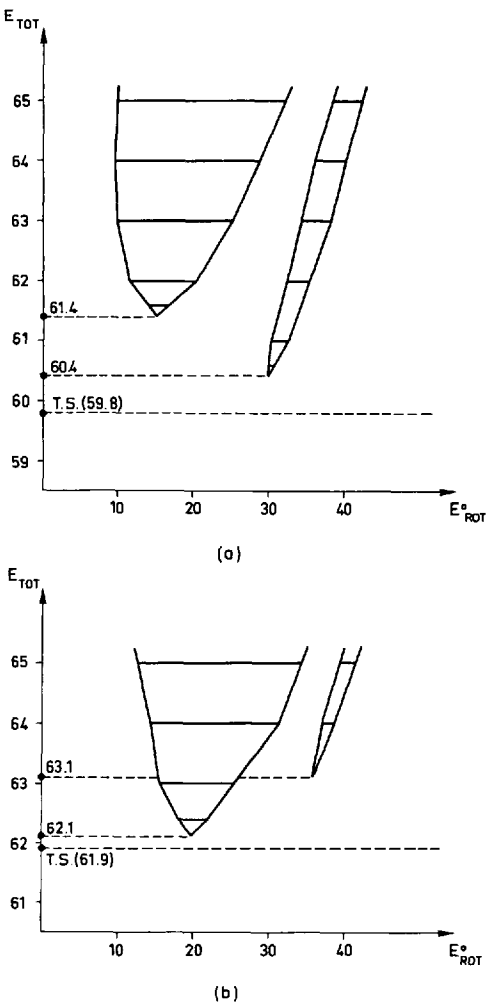

Fig. 13. Evolution of the "reactive bands" versus E_{tot} and E°_{rot} for (a) a conrotatory motion of the terminal groups and (b) a disrotatory motion

n) A long time ago, Wall and Porter[90)] have mentioned the existence of upper energy bounds for H + H_2 collinear reactions. More recently, Wright *et al.*[284)] have observed quite similar reactive and unreactive "bands" for exchange reactions resulting from collinear atom-molecule collisions.

The results presented in this section all depend strongly on the assumption which allowed us to terminate the trajectories. For instance, certain "reactive" trajectories, if they were free to go on, could come back to the starting point of the reaction. Conversely, certain "non-reactive" trajectories, after the first process of ring opening and closure, could yield a cyclopropane molecule possessing a more suitable amount of CH_2 vibration energy and the isomerization reaction could now be possible (Fig. 12a). Furthermore, the treatment of the dynamical problem in its *full dimensionality* might well make the unreactive region between the two reactive bands disappear.

b) Synchronous Disrotatory Motion ($\delta° = -45°$). The main results of the previous section for conrotatory trajectories remain true in the case of disrotatory trajectories. According to the value of E°_{rot} (here the initial CH_2 symmetric vibration energy), two reactive bands are still observed and exhibit the same characteristics as above; the first band corresponds to values of E°_{rot} of the order of 20 kcal/mol and the second band to values of E°_{rot} of the order of 40 kcal/mol. Most of the reactive trajectories involve a single concerted rotation of the terminal groups.

The only noticeable difference concerns the nature of the reactive trajectories when the total energy is only weakly in excess of that of the transition state. For the lowest total intramolecular energy studied (E_{tot} = 63 kcal/mol, *i.e.* $E_{tot} - E_{T.S.}$ = 1.1 kcal/mol), we observed reactive trajectories in the first band only, *i.e.* for E°_{rot} lying between 16 and 26 kcal/mol. This is exactly opposite to what happens in the case of a synchronous conrotatory motion at E_{tot} = 61 kcal/mol ($E_{tot} - E_{T.S.}$ = 1.2 kcal/mol) where reactive trajectories are observed in the second band only. The difference is probably due to the disrotatory transition state lying closer to the entrance valley than the conrotatory transition state (the top of the rotational barrier is at $\theta_1 = -\theta_2 = 50°$ presently, instead of $\theta_1 = \theta_2 = 58°$ before). Moreover, the entrance valley which drives the ring opening is wider in the disrotatory case than in the conrotatory case because disrotatory distortions require a smaller amount of energy than conrotatory distortion, as long as $2\alpha < 95°$.

More precise calculations indicate that the first reactive band appears at E_{tot} = 62.1 kcal/mol and the second reactive band at E_{tot} = 63.1 kcal/mol. The evolution of the reactive band widths versus the total energy is represented in Fig. 13b.

The small secondary minimum (well depth: 2.3 kcal/mol) at the edge-to-edge half-way point does not affect the trajectories very much even for the lowest total energy. However, there are some rare exceptions where the representative point of the molecule spends rather a long time in this region of the potential energy surface (for certain trajectories, the integration was stopped after $1.5\ 10^{-12}$ second and the molecule was still trapped into the well). Then, the final outcome of the reaction is quite a random phenomenon.

c) General Motion (General $\delta°$). When $\delta°$ differs from $\pm 45°$, the coupling between the rotations of both methylene groups results, at anytime, in an energy transfer from one to the other. Then the first question arises: for a given value of $\delta°$ characterizing the distribution of the initial methylene "rotation" (vibration) energy, what is the actual value of $\delta = \mathrm{tg}^{-1}(\dot{\theta}_1/\dot{\theta}_2)$ after the ring-opening phase of the reaction is terminated?

Table 3. Nature of the half-way point for reactive trajectories, depending on the values of $\delta°$ and $E°_{rot}$, when E_{tot} = 62 kcal/mole. The blank terms of the array correspond to non reactive trajectories

$\delta°$	$E°_{rot}$																								
	2	4	6	8	10	12	14	16	18	20	22	24	26	28	30	32	34	36	38	40	42	44	46	48	50
−45°																									
−35°																									
−25°																									
−15°																									
−5°																									
5°																									
15°																									
25°							EE_C	EE_C	EE_C								EE_C								
35°						EE_C	EE_C	EE_C	EE_C	EE_C		EE_C					EE_C								
45°						EE_C	EE_C	EE_C	EE_C	EE_C							EE_C								

Table 4. Nature of the half-way point, depending on the values of δ° and E°_{rot}, when E_{tot} = 63 kcal/mole. The blank terms of the array correspond to non reactive trajectories. Several rotations within the diradical lead either to the starting molecule (1) or to the geometrical isomer (2)

δ°	E°_{rot}																							
	2	4	6	8	10	12	14	16	18	20	22	24	26	28	30	32	34	36	38	40	42	44	46	48	50
−45°								EE_D	EE_D	EE_D	EE_D	EE_D	EE_D												
−35°								EE_D	EE_D	EE_D	EE_D	EE_D	EE_D												
−25°								EF	EF	$EF^{(1)}$	$EE_D^{(1)}$	EE_D	EE_D				EF	EF							
−15°								EF	EF	EF	EF	EF	EE_D					$EF^{(2)}$							
−5°								$EF^{(2)}$	EF	EF	EF	EF						EE_D	$EF^{(2)}$						
5°								EE_C	EE_C	EF	EF							EF	EE_D						
15°							$EE_C^{(1)}$	EE_C	EE_C	EE_C	EE_C							EF	EF						
25°						EE_C	EE_C	EE_C	EE_C	EE_C	EE_C							EE_C							
35°						EE_C	EE_C		EE_C		EE_C	EE_C	EE_C					EE_C							
45°					EE_C	EE_C	EE_C		EE_C	EE_C		EE_C						EE_C	EE_C						

In Ref.[1], we noted that the process of ring-opening is much faster than the rotations of the terminal groups whatever the type of cyclopropane molecules, either substituted or not. Consequently, energy transfer between the two oscillating terminal groups does not have time to operate significantly while the carbon ring opens. The opened molecule is rather similar to a FF-type diracial whose CH_2 rotational energy – which is possibly very different from E°_{rot} – is nevertheless distributed among both rotors in almost the same way as that defined by δ° at starting point. A careful study of the relative variations with time of θ_1 and θ_2 leads to the following conclusion. Whatever, the value of δ°, the corresponding trajectory, when reactive, closely resembles the reactive trajectory obtained for the same value of δ° on the rotational potential energy surface at constant $\widehat{CCC}$ angle (see Ref.[1], Fig. 7). Thus, if $\delta^{\circ} > 0$, the rotation of the terminal groups most frequently leads, *via* a conrotatory process, to a molecular conformation close to that of an edge-to-edge diradical (EE_C). If $\delta^{\circ} < 0$, we observe either the rotation of a single terminal group (EF), or within a narrow range close to -45°, the formation via a disrotatory process of an edge-to-edge diradical (EE_D). It should be emphasized that, whatever the value of δ°, both reactive bands (corresponding to values of E°_{rot} of the order of 20 and 40 kcal/mol respectively) are still observed. At low total energy (62 kcal/mol), all the reactive trajectories lead to the formation of the diradical EE_C via a *synchronous* conrotatory motion of both terminal methylene groups (cf. Table 3). The amount of excess energy above the potential energy of the transition state is weak (2.2 kcal/mol), so that it is only within the range $\delta^{\circ} \geqslant 25^{\circ}$ that the reaction is possible. The ring reclosure occurs after only a single concerted 180° rotation of the terminal groups. For $E_{tot} \geqslant 63$ kcal/mol, the three distinct rotational processes within the diradical species are now possible (cf. Table 4). When δ° varies from 45° to -45°, we observe successively the concerted conrotatory process, the rotation of a single group and, last, the concerted disrotatory process. Reactive trajectories involving several rotations in the diradical appear. They correspond, most frequently, either to limits (on the reactive side) between "reactive" and "non reactive" bands, or within a reactive band, to limiting values of δ° and E°_{rot} beyond which there is a change in the nature of the isomer formed.

3. Conclusion

The dynamical study of the coupling between the modes of ring opening (and closure) and the modes of rotation of the methylene groups of a cyclopropane molecule in the course of isomerization reactions confirms essentially the two main conclusions of the static study:

(i) an isomerization involves, at least approximately, three sequential steps: ring opening, methylene rotation(s) and ring closure;

(ii) the concerted conrotatory motion of the terminal groups is the easiest reaction path.

This study also brings new information which could not be derived from the only study of the potential surface:

(i) the amount of methylene "rotation" (vibration) energy required for the reaction to be possible is much larger than was previously estimated;

(ii) in general, a single rotation of 180° of one or both terminal groups occurs within the diradical species.

General Conclusion

The dynamical study of mechanistic details in organic reactions is complementary to the static study of the potential energy surface. It furnishes a supplement of information which cannot be obtained from the static surface alone.

The question which must be raised now is: "Is this type of study called for and will it be of common use in the future?" A first limitation is of a technical nature: the dynamical study may be of interest only when the potential energy surface driving the reaction is known with sufficient accuracy. Thus the range of application is restricted to reaction systems involving rather simple molecules. A second limitation is that such a dynamical study is almost necessarily incomplete; for instance, in most cases this precludes the obtaining of the reaction rates of organic reactions.

The purpose of such dynamical studies is mainly the development of a dynamical intuition among chemists. Once the potential energy surface of reaction is known, this intuition could allow qualitative predictions of

(i) possible deviations of the actual trajectories compared to the static minimum energy path;

(ii) those energy distributions in reagents which favour completion of the reaction, etc. . .

In this respect, dynamical studies of a limited number of typical reactions are highly desirable. The rapid improvement of both the means of calculation and the experimental techniques which result in having access to more and more tiny details of reaction mechanisms, should stimulate research work in this direction.

Acknowledgements. We gratefully acknowledge the assistance of Professor L. Salem who introduced us to the dynamical study of the isomerization of cyclopropane, Professor J. M. Lehn who suggested to us to write the present article, Dr. G. Bergeron who read the manuscript, Professor F. Fiquet-Fayard, Dr. M. Sizun and Dr. S. Goursaud who made available to us part of their work and Dr. F. Flouquet for helpful discussions.

References

[1] Jean, Y., Chapuisat, X.: J. Amer. Chem. Soc. *96*, 6911 (1974).
[2] Chapuisat, X., Jean, Y.: J. Amer. Chem. Soc. *97*, 6325 (1975).
[3] Jean, Y., Salem, L., Wright, J. S., Horsley, J. A., Moser, C., Stevens, R. M.: Pure Appl. Chem., Suppl. *1*, 197 (1971).
[4] Horsley, J. A., Jean, Y., Moser, C., Salem, L., Stevens, R. M., Wright, J. S.: J. Amer. Chem. Soc. *94*, 279 (1972).
[5] Jean, Y., Thesis: Isomerisation géométrique du cyclopropane. Orsay 1973.
[6] Chapuisat, X., Thesis: Etude dynamique des réactions chimiques: isomerisations optique et géométrique du cyclopropane. Orsay 1975.
[7] Bunker, D. L.: Meth. Comp. Phys. *10*, 287 (1971) and references therein.
[8] Secrest, D.: Ann. Rev. Phys. Chem. *24*, 379 (1973).
[9] Porter, R. N.: Ann. Rev. Phys. Chem. *25*, 317 (1974) and references therein.
[10] Gear, C. W.: J. Siam Num. Anal. *2B*, 69 (1964).
[11] Gear, C. W.: Numerical initial value problems in ordinary differential equations. Prentice-Hall 1971.
[12] Brumer, P., Thesis: Harvard University 1972.
[13] Marcus, R. A., in: Chemische Elementarprozesse (ed. Hartmann). Berlin-Heidelberg-New York: Springer 1968 and references therein.
[14] Robinson, P. J., Holbrook, K. A.: Unimolecular reactions. Wiley 1972.
[15] Forst, W.: Theory of unimolecular reactions. Acad. Press 1973.
[16] Present, R. D.: Kinetic theory of gases. McGraw-Hill 1958.
[17] Benson, S. W.: The foundations of chemical kinetics. McGraw-Hill 1960.
[18] Rice, O. K., in: Energy transfer in gases. 12th Solvay Congress. Interscience Pub. 1962.
[19] Laidler, K. J.: Chemical kinetics. McGraw-Hill 1965.
[20] Bunker, D. L.: Theory of elementary gas reaction rates. Pergamon Press 1966.
[21] Benson, S. W.: Thermochemical kinetics. Wiley 1968.
[22] Troe, J., Wagner, H. G.: Ann. Rev. Phys. Chem. *23*, 311 (1972).
[23] Westenberg, A. A.: Ann. Rev. Phys. Chem. *24*, 77 (1973).
[24] Farrar, J. M., Lee, Y. T.: Ann. Rev. Phys. Chem. *25*, 357 (1974) and references therein.
[25] Herschbach, D. R.: Disc. Faraday Soc. *33*, 149 (1962).
[26] Ross, J., Greene, E. F., in: Energy transfer in gases. 12th Solvay Congress. Interscience Pub. 1962.
[27] Toennies, J. P., in: Chemische Elementarprozesse (ed. Hartmann). Springer-Verlag 1968.
[28] Ramsay, N. R.: Molecular beams. Clarendon Press 1969.
[29] Kinsey, J. L.: Reaction kinetics (ed. Polanyi). M.T.P. Int. Rev. Sci. Med. Tech. Publ. Butterworth 1972.
[30] Toennies, J. P.: Physical chemistry, an advanced treatise, kinetics of gas reactions *4*. Acad. Press 1973.
[31] Molecular beam scattering. Disc. Faraday Soc. *55* (1973).
[32] Toennies, J. P.: Centenary lecture. Chem. Soc. Rev. *3*, 407 (1974).
[33] Carrington, T., Polanyi J. C.: Reaction kinetics (ed. Polanyi). MTP Int. Rev. Sci. Med. Tech. Publ. Butterworth 1972.
[34] Reactions of small molecules in excited states. Disc. Faraday Soc. *53* (1972).
[35] Levine, R. D.: Theoretical chemistry (ed. Brown). MTP Int. Rev. Sci. Med. Tech. Publ. Butterworth 1972.
[36] George, T. F., Ross, J.: Ann. Rev. Phys. Chem. *24*, 263 (1973).
[37] Bennewitz, H. G., Haerten, R., Müller, G.: Z. Phys. *226* 136 (1969).
[38] Bennewitz, H. G., Gengenbach, R., Haerten, R., Müller, G.: Z. Phys. *226*, 279 (1969).
[39] Bennewitz, H. G., Haerten, R.: Z. Phys. *227*, 399 (1969).
[40] Stolte, S., Reuss, J., Schwartz, H. L.: Abst. VII Int. Conf. Phys. Electronic At. Coll. North-Holland 1971.
[41] Moerkerken, H., Reuss, J.: same Ref. as[40].
[42] Beuhter, R. J., Bernstein, R. B., Kramer, K. H.: J. Amer. Chem. Soc. *88*, 5331 (1966).

43) Beuhter, R. J., Bernstein, R. B.: J. Chem. Phys. *51*, 5305 (1969).
44) Brooks, P. R.: Disc. Faraday Soc. *55*, 299 (1973).
45) Bernstein, R. B., Rulis, A. M.: Disc. Faraday Soc. *55*, 293 (1973).
46) Parson, J. M., Shobatake, K., Lee, Y. T., Rice, S. A.: Disc. Faraday Soc. *55*, 344 (1973).
47) Schafer, T. P., Siska, P. E., Parson, J. M., Tully, F. P., Wong, Y. C., Lee, Y. T.: J. Chem. Phys. *53*, 3385 (1970).
48) Schafer, T. P., Thesis: University of Chicago 1972.
49) McDonald, J. D., Lebreton, P. R., Lee, Y. T., Herschbach, D. R.: J. Chem. Phys. *56*, 769 (1972).
50) Miller, W. B., Safron, S. A., Herschbach, D. R.: J. Chem. Phys. *56*, 3581 (1972).
51) Maltz, C., Weinstein, N. O., Herschbach, D. R.: Mol. Phys. *24*, 133 (1972).
52) Hsu, D. S., Herschbach, D. R.: Disc. Faraday Soc. *55*, 116 (1973).
53) Cheung, J. T., McDonald, J. D., Herschbach, D. R.: Disc. Faraday Soc. *55*, 377 (1973).
54) Moore, C. B., Zittel, P. F.: Ann. Rev. Phys. Chem. *22*, 387 (1971).
55) Moore, C. B.: Science *182*, 541 (1973).
56) Schultz, A., Cruse, H. W., Zare, R. N.: J. Chem. Phys. *57*, 1354 (1972).
57) Dagdigian, P. J., Cruse, H. W., Zare, R. N.: J. Chem. Phys. *62*, 1824 (1975).
58) Cruse, H. W., Dagdigian, P. J., Zare, R. N.: Disc. Faraday Soc. *55*, 277 (1973).
59) Polanyi, J. C.: J. Chem. Phys. *34*, 347 (1961).
60) Polanyi, J. C., Woodall, K. B.: J. Chem. Phys. *56*, 1563 (1972).
61) Anlauf, K. G., Horne, D. S., McDonald, R. G., Polanyi, J. C., Woodall, K. B.: J. Chem. Phys. *57*, 1561 (1972).
62) Polanyi, J. C., Sloan, J. J.: J. Chem. Phys. *57*, 4988 (1972).
63) Hancock, G., Morley, C., Smith, I. W.: Chem. Phys. Lett. *12*, 193 (1971).
64) Freund, S. M., Fisk, G. A., Herschbach, D. R., Klemperer, W.: J. Chem. Phys. *54*, 2510 (1971).
65) Riley, S. J., Herschbach, D. R.: J. Chem. Phys. *53*, 3453 (1970).
66) Mariella, R. P., Herschbach, D. R., Klemperer, W.: J. Chem. Phys. *58*, 3785 (1973).
67) Bennewitz, H. G., Haerten, R., Müller, G.: Chem. Phys. Lett. *12*, 335 (1971).
68) Kasper, J. V., Pimentel, G. C.: Phys. Rev. Lett. *14*, 352 (1965).
69) Parker, H. J., Pimentel, G. C.: J. Chem. Phys. *51*, 91 (1969).
70) Berry, M. J., Pimentel, G. C.: J. Chem. Phys. *53*, 3453 (1970).
71) Coombe, R. D., Pimentel, G. C.: J. Chem. Phys. *59*, 1535 (1973).
72) Molina, M. J., Pimentel, G. C.: IEEE J. Quantum Electron. *9*, 64 (1973).
73) Airey, J. R.: IEEE J. Quantum Electron. *3*, 208 (1967).
74) Lin, M. C.: J. Phys. Chem. *75*, 3642 (1971).
75) King, D. L., Dixon, D. A., Herschbach, D. R.: J. Amer. Chem. Soc. *96*, 3328 (1974).
76) Dixon, D. A., Herschbach, D. R.: J. Amer. Chem. Soc. *97*, 6268 (1975).
77) Muckerman, J. T.: J. Chem. Phys. *56*, 2997 (1972).
78) Blais, N. C., Truhlar, D. G.: J. Chem. Phys. *58*, 1090 (1973).
79) Wilkins, R. L.: J. Chem. Phys. *58*, 3038 (1973).
80) Schatz, G. C., Bowman, J. M., Kuppermann, A.: J. Chem. Phys. *58*, 4023 (1973).
81) Jonathan, N., Melliar-Smith, C. M., Slater, D. H.: Mol. Phys. *20*, 93 (1971).
82) Laidler, K., Polanyi, J. C.: Progr. React. Kinet. *3*, 1 (1965).
83) Polanyi, J. C., Schreiber, J. L.: Kinetics in gas reactions (ed. Eyring), Vol. 6. Acad. Press 1973.
84) Eyring, H., Polanyi, M.: Z. Phys. Chem. B. *12*, 279 1931.
85) Hirschfelder, J. O., Eyring, H., Topley, B.: J. Chem. Phys. *4*, 170 (1936).
86) Evans, M. G., Polanyi, M.: Trans. Faraday Soc. *35*, 178 (1939).
87) Wall, F. T., Hiller, L. A., Mazur, J.: J. Chem. Phys. *29*, 255 (1958).
88) Wall, F. T., Hiller, L. A., Mazur, J.: J. Chem. Phys. *35*, 1284 (1961).
89) Wall, F. T., Porter, R. N.: J. Chem. Phys. *36*, 3256 (1962).
90) Wall, F. T., Porter, R. N.: J. Chem. Phys. *39*, 3112 (1963).
91) Blais, N. C., Bunker, D. L.: J. Chem. Phys. *36*, 2713 (1962).
92) Blais, N. C., Bunker, D. L.: J. Chem. Phys. *39*, 315 (1963).

93) Bunker, D. L., Blais, N. C.: J. Chem. Phys. *41*, 2377 (1964).
94) Polanyi, J. C., Rosner, S. O.: J. Chem. Phys. *38*, 1028 (1963).
95) Kuntz, P. J., Nemeth, E. M., Polanyi, J. C., Rosner, S. D.: J. Chem. Phys. *44*, 1168 (1966).
96) Polanyi, J. C.: Acc. Chem. Res. *5*, 161 (1972).
97) Karplus, M., Porter, R. N., Sharma, R. D.: J. Chem. Phys. *40*, 2033 (1964).
98) Porter, R. N., Karplus, M.: J. Chem. Phys. *40*, 1105 (1964).
99) Karplus, M., Raff, L. M.: J. Chem. Phys. *41*, 1267 (1964).
100) Raff, L. M., Karplus, M.: J. Chem. Phys. *44*, 1212 (1966).
101) Karplus, M., Porter, R. N., Sharma, R. D.: J. Chem. Phys. *43*, 3259 (1965).
102) Polanyi, J. C., Wong, W. H.: J. Chem. Phys. *51*, 1439 (1969).
103) Mok, M. H., Polanyi, J. C.: J. Chem. Phys. *51*, 1451 (1969).
104) Bunker, D. L., Goring, E. A.: Chem. Phys. Lett. *15*, 521 (1972).
105) Harris, R. M., Herschbach, D. R.: Disc. Faraday Soc. *55*, 121 (1973).
106) Bunker, D. L., Blais, N. C.: J. Chem. Phys. *37*, 2713 (1962).
107) Mok, M. H., Polanyi, J. C.: J. Chem. Phys. *53*, 4588 (1970).
108) Morokuma, K., Pedersen, L., Karplus, M.: J. Amer. Chem. Soc. *89*, 5064 (1967).
109) Porter, R. N., Thompson, D. L., Sims, L. B., Raff, L. M.: J. Amer. Chem. Soc. *92*, 3208 (1970).
110) Jaffe, S. B., Anderson, J. B.: J. Chem. Phys. *49*, 2859 (1968).
111) Jaffe, S. B., Anderson, J. B.: J. Chem. Phys. *51*, 1057 (1969).
112) Brumer, P., Karplus, M.: J. Chem. Phys. *58*, 3903 (1973).
113) Brumer, P., Karplus, M.: Faraday Disc. Chem. Soc. *55*, 80 (1973).
114) Loughlin, D. R., Thompson, D. L.: J. Chem. Phys. *59*, 4393 (1973).
115) Montrolland, E. W., Shuler, K. E.: Adv. Chem. Phys. *1*, 361 (1958).
116) Shuler, K. E., in: Chemische Elementarprozesse (ed. Hartmann). Springer-Verlag 1968 and references therein.
117) Ross, J., Mazur, P.: J. Chem. Phys. *35*, 19 (1961).
118) Eliason, M. A., Hirschfelder, J. O.: J. Chem. Phys. *30*, 1426 (1959).
119) Eyring, H. J., Hirschfelder, J. O., Taylor, H. S.: J. Chem. Phys. *4*, 479 (1936).
120) Gioumousis, G., Stevenson, D. P.: J. Chem. Phys. *29*, 294 (1958).
121) Broida, H. P., Polanyi, J. C., Callear, A. B., Zare, R. N., Herschbach, D. R., in: Chemical lasers. Appl. Opt. Suppl. *2* (1965).
122) Shuler, K. E., Carrington, T., Broida, H. P.: same Ref. as[121].
123) Adv. Chem. Phys. *10*: Molecular beams (ed. J. Ross). Interscience Publ. 1965.
124) Secrest, D.: J. Chem. Phys. *62*, 710 (1975).
125) Takayanagi, K.: Suppl. Prog. Theoret. Phys. *25*, 1 (1963).
126) Takayanagi, K.: Adv. At. Molec. Phys. *1*, 149 (1965).
127) Rapp, D., Kassal, T.: Chem. Rev. *69*, 61 (1969).
128) Gordon, R. G.: Meth. Comp. Phys. *10* (1971).
129) Connor, J. N., in: Ann. Rep. A Chem. Soc. (1973) and references therein.
130) Quantum theory (ed. Bates), Vol. I. Acad. Press 1961.
131) Wu, T. Y., Ohmura, T.: Quantum theory of scattering. Prentice Hall 1962.
132) Rodberg, L. S., Thaler, R. M.: Introduction to the quantum theory of scattering. Acad. Press 1967.
133) Herzfeld, K. F., Litowitz, T. A.: Absorption and dispersion of ultrasonic waves. Acad. Press 1959.
134) Cottrell, T. L., McCoubrey, J. C.: Molecular energy transfer in gases. Butterworth 1961.
135) Johnston, H. S.: Gas phase reaction rate theory, Ronald Press 1966.
136) Levine, R. D.: Quantum mechanics of molecular rate processes. Clarendon Press.1969.
137) Rapp, D.: Quantum mechanics. Holt 1971.
138) Child, M. S.: Molecular collision theory. Acad. Press 1974.
139) Levine, R. D., Berstein, R. B.: Molecular reaction dynamics. Clarendon Press 1974.
140) Wolken, G., Karplus, M.: J. Chem. Phys. *60*, 351 (1974).
141) Bowman, J. M., Kuppermann, A.: Chem. Phys. Lett. *12*, 1 (1971).
142) Diestler, D. J., Karplus, M.: J. Chem. Phys. *55*, 5832 (1971).
143) Fong, K. P., Diestler, D. J.: J. Chem. Phys. *56*, 3200 (1972).

144) Marcus, R. A.: Chem. Phys. Lett. *7*, 525 (1970).
145) Miller, W. H.: J. Chem. Phys. *53*, 1949 (1970).
146) Miller, M. H.: J. Chem. Phys. *54*, 5386 (1971).
147) Doll, J. D., George, T. F., Miller, W. H.: J. Chem. Phys. *58*, 1343 (1973).
148) Miller, W. H.: Acc. Chem. Res. *4*, 161 (1971).
149) Miller, W. H.: Adv. Chem. Phys. *25* (1974), and references therein.
150) Light, J. C.: Meth. Comp. Phys. *10* (1971) and references therein.
151) McCullough, E. A., Wyatt, R. E.: J. Chem. Phys. *54*, 3578 (1971).
152) McCullough, E. A., Wyatt, R. E.: J. Chem. Phys. *54*, 3592 (1971).
153) Dugan, J. V., Magee, J. L.: Adv. Chem. Phys. *21*, 207 (1971).
154) La Budde, R. A., Kuntz, P. J., Bernstein, R. B., Levine, R. D.: Chem. Phys. Lett. *19*, 7 (1973).
155) La Budde, R. A., Kuntz, P. J., Bernstein, R. B., Levine, R. D.: J. Chem. Phys. *59*, 6286 (1973).
156) George, T. F., Suplinskas, R. J.: J. Chem. Phys. *51*, 3666 (1969).
157) George, T. F., Suplinskas, R. J.: J. Chem. Phys. *54*, 1037 (1971).
158) George, T. F., Suplinskas, R. J.: J. Chem. Phys. *54*, 1046 (1971).
159) Dugan, J. V., Magee, J. L.: J. Chem. Phys. *58*, 5816 (1973).
160) Pattengill, M. D., Polanyi, J. C.: Chem. Phys. *3*, 1 (1974).
161) Herzfeld, K. F.: J. Chem. Phys. *47*, 743 (1967).
162) Raff, L. M.: J. Chem. Phys. *46*, 520 (1967).
163) Raff, L. M.: J. Chem. Phys. *47*, 1884 (1967).
164) Thommarson, R. L., Berend, G. C.: Int. J. Chem. Kinet. *5*, 629 (1973).
165) Berend, G. C., Thommarson, R. L.: J. Chem. Phys. *58*, 3203 (1973).
166) Berend, G. C., Thommarson, R. L.: J. Chem. Phys. *58*, 3454 (1973).
167) Wilkins, R. L.: J. Chem. Phys. *59*, 698 (1973).
168) Lester, W. A.: J. Chem. Phys. *53*, 1511 (1970).
169) Lester, W. A., Schaefer, J.: J. Chem. Phys. *59*, 3676 (1973).
170) La Budde, R. A., Bernstein, R. B.: J. Chem. Phys. *55*, 5499 (1971).
171) La Budde, R. A., Bernstein, R. B.: J. Chem. Phys. *59*, 3687 (1973).
172) Perry, D. S., Polanyi, J. C.: Can. J. Chem. *50*, 3916 (1972).
173) Douglas, D. J., Polanyi, J. C., Sloan, J. J.: J. Chem. Phys. *59*, 6679 (1973).
174) Perry, D. S., Polanyi, J. C., Wilson, C. W.: Chem. Phys. *3*, 317 (1974).
175) Karplus, M., Porter, R. N.: Disc. Faraday Soc. *44*, 164 (1967).
176) Godfrey, M., Karplus, M.: J. Chem. Phys. *49*, 3602 (1968).
177) Porter, R. N., Kunt, S.: J. Chem. Phys. *52*, 3240 (1970).
178) Brumer, P., Karplus, M.: J. Chem. Phys. *54*, 4955 (1971).
179) Porter, R. N., Sims, L. B., Thompson, D. L., Raff, L. M.: J. Chem. Phys. *58*, 2855 (1973).
180) Anderson, J. B.: J. Chem. Phys. *52*, 3849 (1970).
181) Wilkins, R. L.: J. Chem. Phys. *57*, 912 (1972).
182) Wilkins, R. L.: J. Chem. Phys. *58*, 2326 (1973).
183) Muckerman, J. T.: J. Chem. Phys. *54*, 1155 (1971).
184) Muckerman, J. T., Newton, M. D.: J. Chem. Phys. *56*, 3191 (1972).
185) Muckerman, J. T.: J. Chem. Phys. *57*, 3388 (1972).
186) Landau, L.: Phys. Z. Sow. *2*, 46 (1932).
187) Zener, C.: Proc. Roy. Soc. *A137*, 696 (1932).
188) Nikitin, E. E., in: Chemische Elementarprozesse (ed. Hartmann). Springer-Verlag 1968.
189) Blais, N.: J. Chem. Phys. *49*, 9 (1968).
190) Maier, W. B.: J. Chem. Phys. *54*, 2732 (1971).
191) Tully, J. C., Preston, R. K.: J. Chem. Phys. *55*, 562 (1971).
192) Warshel, A., Karplus, M.: Chem. Phys. Lett. *32*, 11 (1975).
193) Morokuma, K., George, T. F.: J. Chem. Phys. *59*, 1959 (1973).
194) George, T. F., Morokuma, K.: Chem. Phys. *2*, 129 (1973).
195) Jaffe, R. L., George, T. F., Morokuma, K.: Mol. Phys. *28*, 1489 (1974).
196) Jaffe, R. L., Morokuma, K., George, T. F.: J. Chem. Phys. *63*, 3417 (1975).

[197] Unpublished report on the: Workshop on reactions involving two surfaces. Orsay 1975.
[198] Shui, V. H.: J. Chem. Phys. *56*, 4266 (1972).
[199] Shui, V. H., Appleton, J. P., Keck, J. C.: J. Chem. Phys. *57*, 1704 (1972).
[200] Shui, V. H.: J. Chem. Phys. *58*, 4868 (1973).
[201] Clarke, A. G., Burns, G.: J. Chem. Phys. *55*, 4717 (1971).
[202] Clarke, A. G., Burns, G.: J. Chem. Phys. *56*, 4636 (1972).
[203] Clarke, A. G., Burns, G.: J. Chem. Phys. *58*, 1908 (1973).
[204] Wong, W. H., Burns, G.: J. Chem. Phys. *58*, 4454 (1973).
[205] Gelb, A., Kapral, R., Burns, G.: J. Chem. Phys. *59*, 2980 (1973).
[206] Borne, T. B., Bunker, D. L.: J. Chem. Phys. *55*, 4861 (1971).
[207] Kwei, G. H., Boffardi, B. D., Sun, S. F.: J. Chem. Phys. *58*, 1722 (1973).
[208] Roach, A. C., Child, M. S.: Mol. Phys. *14*, 1 (1968).
[209] Bunker, D. L.: J. Chem. Phys. *37*, 393 (1962).
[210] Bunker, D. L.: J. Chem. Phys. *40*, 1946 (1964).
[211] Bunker, D. L., Pattengill, M. D.: J. Chem. Phys. *48*, 772 (1968).
[212] Bunker, D. L., Pattengill, M. D.: J. Chem. Phys. *53*, 3041 (1970).
[213] Bunker, D. L.: J. Chem. Phys. *57*, 332 (1972).
[214] Bunker, D. L., Hase, W. L.: J. Chem. Phys. *59*, 4621 (1973).
[215] Harris, H. H., Bunker, D. L.: Chem. Phys. Lett. *11*, 433 (1971).
[216] Schneider, F. W., Rabinovitch, B. S.: J. Amer. Chem. Soc. *84*, 4215 (1962).
[217] Ting, C. T., Rowland, F. S.: J. Phys. Chem. *74*, 4080 (1970).
[218] Raff, L. M.: J. Chem. Phys. *44*, 1202 (1966).
[219] Kuntz, P. J., Nemeth, E. M., Polanyi, J. C., Wong, W. H.: J. Chem. Phys. *52*, 4654 (1970).
[220] Bunker, D. L., Pattengill, M. D.: Chem. Phys. Lett. *4*, 315 (1969).
[221] Valencich, T., Bunker, D. L.: Chem. Phys. Lett. *20*, 50 (1973).
[222] Wang, I. S., Karplus, M.: J. Amer. Chem. Soc. *95*, 8160 (1973).
[223] Raff, L. M., Stivers, L., Porter, R. N., Thompson, D. L., Sims, L. B.: J. Chem. Phys. *52*, 3449 (1970).
[224] Porter, R. N., Tompson, D. L., Sims, L. B.: J. Amer. Chem. Soc. *92*, 3208 (1970).
[225] Raff, L. M., Tompson, D. L., Sims, L. B., Porter, R. N.: J. Chem. Phys. *56*, 5998 (1972).
[226] Spicer, L. D., Rabinovitch, B. S.: Ann. Rev. Phys. Chem. *21*, 349 (1970).
[227] Henry, J. M., Anderson, J. B., Jaffé, R. L.: Chem. Phys. Lett. *20*, 138 (1973).
[228] Sullivan, J. H.: J. Chem. Phys. *46*, 73 (1967).
[229] Gordon, R. G.: Disc. Faraday Soc. *55* (1973).
[230] Schlessinger, L.: Phys. Rev. *167*, 1411 (1968).
[231] Baker, G. A., Gammel, J. L. (eds.): The Pade approximant in theoretical physics. Acad. Press 1970.
[232] Wall, H. S.: The analytic theory of continued fractions. Van Nostrand 1948.
[233] Walsh, J. L., Ahlberg, J. H., Nilson, E. N.: J. Math. Mech. *11*, 225 (1962).
[234] Ahlberg, J. A., Nilson, E. N., Walsh, J. L.: The theory of splines and their applications. Acad. Press 1967.
[235] Schumaker, L. L.: Theory and applications of spline functions (ed. Greville). Acad. Press 1969.
[236] Sand, A., Weintraub, S.: A book of splines. Wiley 1971.
[237] Sathyamorthy, N., Raff, L. M.: J. Chem. Phys. *63*, 464 (1975).
[238] Bowman, J. M., Kuppermann, A.: Chem. Phys. Lett. *34*, 523 (1975).
[239] Dunfield, L. G., Read, J. F.: J. Chem. Phys. *57*, 2178 (1972).
[240] Gilbert, T. L., Bertoncini, P. J.: J. Chem. Phys. *61*, 3026 (1974).
[241] Gilbert, T. L., Bertoncini, P. J.: Chem. Phys. Lett. *29*, 569 (1974).
[242] Gilbert, T. L., Bertoncini, P. J.: J. Chem. Phys. *62*, 1289 (1975).
[243] Shore, B. W.: J. Chem. Phys. *59*, 6450 (1973).
[244] Horsley, J., Flouquet, F., Chapuisat, X.: Lect. 3rd Colloq. High Resol. Molec. Spectr. (1973).
[245] DeBoor, C.: J. Math. Phys. *41*, 212 (1962).
[246] Adv. Chem. Phys. XXI, Part. II: Kinetics in gas reactions (ed. Laidler).
[247] Salem, L.: J. Amer. Chem. Soc. *96*, 3486 (1974).

[248] Salem, L., Leforestier, C., Segal, G., Wetmore, R.: J. Amer. Chem. Soc. *97*, 479 (1975).
[249] Miller, W. H., George, T. F.: J. Chem. Phys. *56*, 5637 (1972).
[250] Goldstein, H.: Classical mechanics. Addison-Wesley 1959.
[251] Hammersley, J. M., Handscomb, D. C.: Monte-Carlo methods. Methuen 1954.
[252] Kahn, H.: Applications of Monte-Carlo. Rand Corporation Research Memorandum. RM-1237-AEC (1956).
[253] Sizun, M.: Thèse de 3e Cycle. Orsay 1972.
[254] Wigner, E.: Phys. Rev. *40*, 749 (1932).
[255] Fiquet-Fayard, F., Sizun, M., Goursaud, S.: J. de Physique *33*, 669 (1972).
[256] Flouquet, F., Horsley, J., Chapuisat, X.: to be published.
[257] Carrington, T.: J. Chem. Phys. *41*, 2012 (1964).
[258] Horie, T., Kasuga, T.: J. Chem. Phys. *40*, 1683 (1964).
[259] Trautz, M., Winkler, K.: J. prakt. Chem. 2 *104*, 53 (1922).
[260] Baldwin, J. E., Grayston, M. W.: J. Amer. Chem. Soc. *96*, 1629 and 1630 (1974).
[261] Rabinovitch, B. S., Schlag, E. W., Wiberg, K. W.: J. Chem. Phys. *28*, 504 (1958).
[262] Schlag, E. W., Rabinovitch, B. S.: J. Amer. Chem. Soc. *82*, 5996 (1960).
[263] Flowers, M. C., Frey, H. M.: Proc. Roy. Soc. A, *257*, 122 (1960).
[264] Flowers, M. C., Frey, H. M.: Proc. Roy. Soc. A, *260*, 424 (1961).
[265] Frey, H. M., Marshall, D. C.: J. Chem. Soc. 5717 (1963).
[266] Setser, D. W., Rabinovitch, B. S.: J. Amer. Chem. Soc. *86*, 564 (1964).
[267] Willcott III, M. R., Cargle, V. H.: J. Amer. Chem. Soc. *89*, 723 (1967).
[268] Crawford, R. J., Lynch, T. R.: Can. J. Chem. *46*, 1457 (1968).
[269] Berson, J. A., Balquist, J. M.: J. Amer. Chem. Soc. *90*, 7343 (1968).
[270] Carter, W. L., Bergman, R. G.: J. Amer. Chem. Soc. *90*, 7344 (1968).
[271] Bergman, R. G., Carter, W. L.: J. Amer. Chem. Soc. *91*, 7411 (1969).
[272] Willcott III, M. R., Cargle, V. H.: J. Amer. Chem. Soc. *91*, 4310 (1969).
[273] von Doering, W. E., Sachdev, K.: J. Amer. Chem. Soc. *96*, 1168 (1974).
[274] Berson, J. A., Pedersen, L. D., Carpenter, B. K.: J. Amer. Chem. Soc. *97*, 240 (1975).
[275] Berson, J. A., Pedersen, L. D.: J. Amer. Chem. Soc. *97*, 238 (1975).
[276] Bergman, R. G., in: Free radicals (ed. Kochi). Wiley 1973.
[277] Hoffmann, R.: J. Amer. Chem. Soc. *90*, 1475 (1968).
[278] Buenker, R. J., Peyerimhoff, S. D.: J. Phys. Chem. *73*, 1299 (1969).
[279] Siu, A. K. Q., St-John II, W. M., Hayes, E. F.: J. Amer. Chem. Soc. *92*, 7249 (1970).
[280] Hay, P. J., Hunt, W. J., Goddard, W. A., III: J. Amer. Chem. Soc. *94*, 638 (1972).
[281] Benson, S. W.: J. Chem. Phys. *34*, 521 (1961).
[282] Buchwalter, S. L., Closs, G. L.: J. Amer. Chem. Soc. *97*, 3857 (1975).
[283] Hehre, W. J., Stewart, R. F., Pople, J. A.: J. Chem. Phys. *51*, 2657 (1969).
[284] Wright, J. S., Tan, G., Laidler, K. J., Hulse, J. E.: Chem. Phys. Lett. *30*, 200 (1975).
[285] Chapuisat, X., Jean, Y., Salem, L.: Chem. Phys. Lett. *37*, 119 (1976).

Received December 23, 1975

A New Theoretical Look at the Inversion Problem in Molecules

Dr. Dušan Papoušek and Dr. Vladimír Špirko

Department of Molecular Spectroscopy, The J. Heyrovský Institute of Physical Chemistry and Electrochemistry, Czechoslovak Academy of Sciences, 160 00 Prague 6, Czechoslovakia

Contents

1. **Introduction** 60

2. **Molecular Inversion in Ammonia** 62

3. **Vibration–Inversion–Rotation Hamiltonian for Ammonia** 63
3.1. Molecular Reference Configuration and the Molecule-Fixed System of Axes 65
3.2. Classical and Quantum-Mechanical Vibration–Inversion–Rotation Hamiltonian 67
3.3. Extension to NH_2D and ND_2H 70
3.4. Expansion of the Vibration–Inversion–Rotation Hamiltonian 72

4. **Symmetry Classification of the States and the GF Matrix Problem in Ammonia** 76
4.1. Symmetry Classification of the States 76
4.2. GF Matrix Problem for Ammonia 79
4.3. Selection Rules 81

5. **Potential Function of Ammonia and the Calculation of the Vibration–Inversion–Rotation Energy Levels** 85
5.1. Theory of the Centrifugal Distortion in Ammonia 86
5.2. Force Field in $^{14}NH_3$, $^{15}NH_3$, $^{14}ND_3$, $^{14}NT_3$, $^{14}NH_2D$, and $^{14}ND_2H$. 87
5.3. Discussion of the Potential Function of Ammonia 92
5.4. Coriolis Interactions Between ν_2, ν_4, $2\nu_2$, $\nu_2 + \nu_4$, $3\nu_2$ Levels of NH_3. . 93

6. **Molecular Inversion in Other Molecules** 96
6.1. Molecules With Pyramidal Inversion 96
6.2. Molecules With Inversion and Internal Rotation. 98

7. **Conclusions** 99

8. **References** 101

1. Introduction

Although molecular inversion is a phenomenon which theoretically can occur in any nonplanar molecule, from the point of view of vibration-rotation spectroscopy inversion is of significance for relatively few molecules. Nevertheless, molecular inversion is an interesting and important large-amplitude molecular motion. Inversion has pronounced effects on the spectra of certain molecules; experimental as well as theoretical studies of these effects became an important part of the history of molecular spectroscopy. The results of these studies found also important applications, the best-known example being the celebrated NH_3 molecular beam maser.

The nature of molecular inversion can be understood if we consider an operation E* whose effect on the position vectors r_i of all the particles of a molecule (atomic nuclei and electrons) in the space-fixed system of coordinates is defined as

$$\mathrm{E}^* \, r_i = - r_i. \tag{1.1}$$

The operation E* is the element of the Longuet-Higgins' molecular symmetry group of permutation inversion operations[1]. If E* is applied to a molecule with a nonplanar equilibrium configuration of its atomic nuclei, it is the so-called non-completely feasible symmetry operation[1]. In this case, E* transforms an equilibrium configuration A into a symmetrically equivalent equilibrium configuration B which cannot be obtained from A by a rigid rotation in space. Configurations A and B are then separated by a non-zero energy barrier.

The height of this barrier depends on the way we contort the molecule to reach its inversion, *i.e.*, on the path in the configuration space over which we move during inversion. Physical properties of the molecule are determined by the lowest energy barrier which unavoidably must be surmounted if we want to arrive from configuration A to configuration B. We denote this energy difference as the inversion barrier.

If the inversion barrier which separates symmetrically equivalent equilibrium configurations A and B is high enough, all the vibrational wave functions (corresponding to inversion levels below the inversion barrier) have appreciable amplitude only in the neighborhood of the equilibrium configurations A and B. The time period during which a molecule undergoes the inversion is so long that the splitting of energy levels due to the tunneling effect between configurations A and B is very small and cannot be resolved by the spectroscopic techniques which are now available. Such a molecule can be considered as rigid with respect to inversion.

This is the case of most molecules. There are, however, certain molecules in which the inversion barrier is so low that the vibrational wave functions cannot be considered as localized[2]. Frequencies of the transitions between symmetrically equivalent configurations A and B are then high enough for the splitting of energy levels due to the tunneling to be detected experimentally.

The simpliest and most important molecule with a low barrier to inversion is ammonia, NH_3. In its ground electronic state, NH_3 has a pyramidal equilibrium configuration with the geometrical symmetry described by the point group C_{3v} (Fig. 1). Configuration B which is obtained from A by the symmetry operation E* is separated from A by an inversion barrier of about 2000 cm^{-1}. A large amplitude

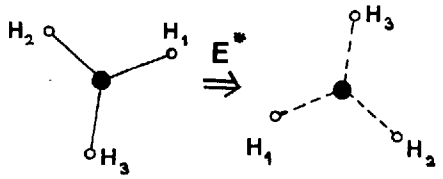

Fig. 1. The effect of inversion, E*, on the equilibrium configuration of ammonia NH_3. Full lines: positions of the H nuclei above the plane of the figure, dotted lines: positions below the plane

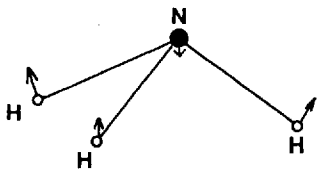

Fig. 2. The ν_2 bending mode of NH_3

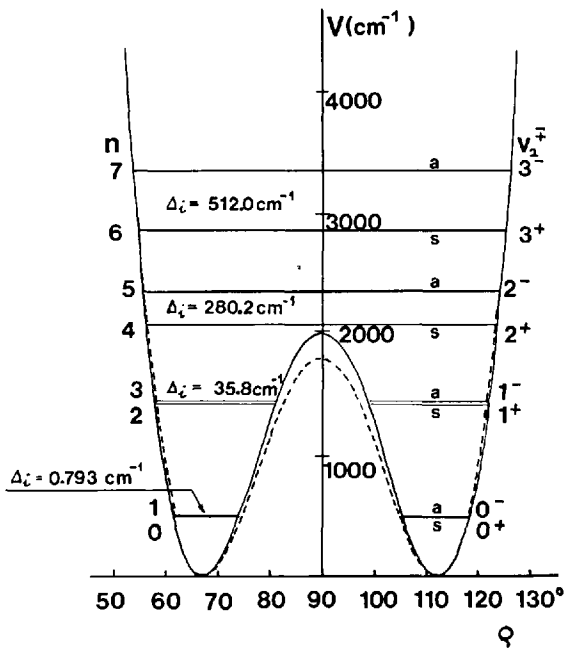

Fig. 3. The double-minimum potential function for NH_3 with the indication of the inversion splittings of the ν_2 energy levels. Full line: effective potential function, dashed line: "true" potential function (Sec. 5.3). Δ_i: inversion splitting; n: labels of the inversion levels according to Bunker[34], $v_2^{\mp}$: quantum numbers of the energy levels of a rigid C_{3v} molecule. Inversion coordinate ρ is defined in Fig. 4

vibrational motion during which this barrier is overcome is the ν_2 bending vibration (Fig. 2). The potential function which describes this motion is a double-minimum function with the minima separated by the inversion barrier (Fig. 3).

Molecular inversion is significant for molecules which can be obtained from NH_3 if we formally substitute the hydrogen nuclei by one or two atoms, as for example NH_2D, ND_2H, NH_2Cl. If we substitute one hydrogen nucleus in NH_3 by a polyatomic group, the new molecule can execute several large-amplitude motions. For example, in methylamine CH_3NH_2, we must consider the wagging vibration which "inverts" the CNH_2 atomic group and in addition the internal rotation of the CH_3 group with

respect to the NH_2 group. In hydrazine, $H_2N \cdot NH_2$, there are two large-amplitude wagging-inversions and one internal rotation. Such molecules possess several symmetrically equivalent equilibrium configurations which are separated by non-zero energy barriers (Section 6.2). In general, we cannot transform one equilibrium configuration of such molecules into another one simply by the operation of inversion, E^*, but by certain well-defined non-completely feasible permutation-inversion operations of the full symmetry group of the molecule[1]. In analogy to the inversion in ammonia, the large-amplitude motions which invert certain non-planar atomic groups in such molecules are also called inversions.

An interesting group of molecules which show an inversion effect related to that observed in ammonia are small ring molecules. Cyclobutane has a four-membered ring with a small potential hump at the planar configuration. A similar situation occurs in trimethylenoxid. Symmetric systems of five-membered rings, such as cyclopentane, have two out-of-plane deformation vibrations (puckering vibrations) which are degenerate. The resulting motion can be considered to rotate around the ring and this type of motion has been called pseudorotation.

Theoretical description of the internal motions in such molecules is a rather complicated problem which still requires further work. Even in the simplest case of ammonia, until recently the theory of the vibration–inversion–rotation states of this molecule had not been worked out in a form which would allow for a systematic analysis of the spectra of this molecule leading to a determination of a reliable potential function.

In Sections 2–5 of the present paper we describe an approach to the ammonia problem which is based on a new vibration–inversion–rotation Hamiltonian developed recently for NH_3 and its isotopic substituents in our lab[3–6]. We concentrate in this paper on the ammonia molecule but the results could be immediately applied to molecules such as NH_2X and NHX_2 or they might be used in extensions of this approach to more complicated molecules with inversion-like motions (Sections 6.1 and 6.2).

2. Molecular Inversion in Ammonia

Ammonia was the first molecule for which the effect of the molecular inversion was studied experimentally and theoretically. Inversion in ammonia was subsequently found to be so important that this molecule played an important role in the history of molecular spectroscopy. Let us recall, for example that microwave spectroscopy started its era with the measurements[7–9] of the frequencies of transitions between the energy levels in the ground vibronic state of NH_3 split by the inversion effect. Furthermore, the first proposal[10] and realization[11, 12] of a molecular beam maser in 1955 was based on the inversion splittings of the energy levels in NH_3. The Nobel Prize which Townes, Basov and Prochorov were awarded in 1964 clearly shows how important this discovery was. Another example of the role which the inversion of ammonia played in the extension of human knowledge is the discovery of NH_3 in the interstellar space by Cheung and his co-workers[13] in 1968, by measuring the

inversion frequencies emitted by the ammonia cloud in Saggitarius B. Ammonia was therefore the first polyatomic molecule found in the interstellar space.

Ammonia has also attracted the attention of theoreticians since the beginning of the application of quantum mechanics to molecular problems. The fact that the tunneling effect does not have any analog in classical mechanics certainly contributed to this interest.

Dennison, Hardy, and Uhlenbeck[14, 15] presented the first quantum mechanical interpretation of the inversion phenomena in ammonia in the early thirties. Fermi[16] was among the first theoreticians to study this problem; his paper on the effect of the centrifugal distortion on the inversion splitting in NH_3 was written in 1932 and after 45 years it is still interesting.

These early papers, as well as most of the theoretical work on the inversion of ammonia that has been done later, have considered the problem of the solution of the Schrödinger equation for a double-minimum potential function in one dimension and the determination of the parameters of such a potential function from the inversion splittings associated with the ν_2 bending mode of ammonia[17]. Such an approach describes the main features of the ammonia spectrum pertaining to the ν_2 bending mode but it cannot be used for the interpretation of the effects of inversion on the energy levels involving other vibrational modes or vibration–rotation interactions.

Until recently, few attempts have been made to extend the theory of the ammonia inversion to account for the dependence of the inversion splittings on the vibrational and rotational quantum numbers [*e.g.*[18]]. These attempts differed not only from the standard approach to the vibration–rotation problem of rigid molecules but also from the approach to the problem of nonrigid molecules with internal rotation [for example[19]].

In the following sections of this paper, we describe a new model Hamiltonian to study the vibration–inversion–rotation energy levels of ammonia. In this model the inversion motion is removed from the vibrational problem and considered with the rotational problem by allowing the molecular reference configuration to be a function of the large amplitude motion coordinate. The resulting Hamiltonian then takes a form which is very close to the standard Hamiltonian used in the study of rigid molecules[19] and allows for a treatment of the inversion motion in a way which is very similar to the formalism developed for the study of molecules with internal rotation [see for example[17]].

3. Vibration–Inversion–Rotation Hamiltonian for Ammonia

In the standard treatment of rigid molecules, we define a rigid reference configuration of the atomic nuclei of the molecule with respect to which we measure the vibrational displacements of the atomic nuclei[19, 20]. It is of course necessary to introduce a set of constraints on these displacements so that external large-amplitude motions (such as translation and overall rotation) are not accounted for as vibrational motions.

Using the procedure described in detail *e.g.* in Chapter 11 of Ref.[20], we arrive at a quantum mechanical Hamiltonian $\mathscr{H}$ which includes the components of the total

angular momentum operator of the molecule, the components of the vibrational angular momentum operator and the potential energy operator V as a function of the normal coordinates of vibration Q. Because the Schrödinger equation for this operator does not lend itself to exact solution, we expand the coefficients[a] $\mu_{\alpha\beta}$ ($\alpha, \beta = x, y, z$) and the potential energy V in a power series in Q. We then treat the Schrödinger equation in different approximations depending upon the accuracy we wish to reach in the theoretical interpretation of the experimental data.

The vibration–rotation Hamiltonian $\mathscr{H}$ is valid irrespective of the magnitude of the amplitudes of vibrations, *i.e.* it could be used in principle to non-rigid molecules as well. There are, however, two main sources of difficulty which arise if we wish to apply $\mathscr{H}$ to non-rigid molecules.

The first problem concerns the expansion of V in the power series in Q. In non-rigid molecules, vibrational wave functions have appreciable amplitude over a wide range of the values of the coordinates describing the large-amplitude motions and we must use very high powers in the polynomial expansion to arrive at a satisfactory description of the potential function of a non-rigid molecule. For example, to describe the double-minimum function of ammonia (Fig. 3), we must use a polynomial expansion of the 10th degree to arrive at about 1% agreement between the calculated and experimental inversion barrier.

The second problem concerns the convergence of the expansion of the coefficients $\mu_{\alpha\beta}$. Until recently this problem has not been studied to the same extent as the effect of the anharmonicity of the large-amplitude vibrations in the expansion of V. However, the role of the large-amplitude motions in the expansion of $\mu_{\alpha\beta}$ may be equally important, especially in the *ab initio* approach to the calculation of the rotational energy levels of a non-rigid molecule [cf.[21]].

In the treatment of non-rigid molecules, we can avoid the above-mentioned difficulties if we define a non-rigid reference configuration of the atomic nuclei which essentially follows the large-amplitude motions. Vibrational displacements measured with respect to the non-rigid reference configuration remain therefore small; the large-amplitude problem is removed from the vibrational part of the Hamiltonian.

This approach has been frequently used in the treatment of molecules with internal rotation. In these molecules, the "top" and "frame" parts of the non-rigid reference configuration follow essentially the internal rotation; internal rotation is not considered as a vibrational motion but rather as a part of the rotational motion described by a new dynamical variable – the angle of internal rotation.

In the following section, we introduce an analogous formalism into the description of the vibration–inversion–rotation states of ammonia. We define a non-rigid reference configuration of the atomic nuclei of the ammonia molecule which follows closely the large amplitude inversion motions of the atomic nuclei. In this way the major part of the anharmonicity due to the inversion motions will be removed from the vibrational problem and accounted for by the large amplitude inversion coordinate ρ.

---

[a] The coefficients $\mu_{\alpha\beta}$ are the elements of the 3x3 matrix which is the inverse to the matrix of the inertia tensor elements defined *e.g.* by Eq. (10) in[20].

3.1. Molecular Reference Configuration and the Molecule-Fixed System of Axes

The reference configuration of the atomic nuclei of the NX_3 molecule (X = H, D, T) is defined by (i) three equal and fixed bond lengths ($\equiv r_0$), (ii) the angle ρ subtended by the NH bond of the reference configuration and the C_3 axis (Fig. 4). We shall require that the molecule-fixed system of axes xyz has its origin at the center of mass, *i.e.*

$$\sum_i m_i a_i(\rho) = 0 \tag{3.1}$$

where $a_i(\rho)$ is the position vector of the ith atomic nucleus of mass m_i. We shall further specify the molecule-fixed system of axes by the requirement that the angular momentum of the reference configuration vanishes in this molecule-fixed axis system, *i.e.*

$$\sum_i m_i \left[a_i(\rho) \times \frac{\mathrm{d}a_i(\rho)}{d\rho} \right] = 0. \tag{3.2}$$

The components of the position vectors $a_i(\rho)$ are then given by

$$\begin{aligned} a_{1x} &= r_0 \sin\rho, \\ a_{2x} &= -\frac{1}{2} r_0 \sin\rho, \\ a_{3x} &= -\frac{1}{2} r_0 \sin\rho, \\ a_{Nx} &= 0, \end{aligned} \tag{3.3.a}$$

$$\begin{aligned} a_{1y} &= 0, \\ a_{2y} &= 3^{1/2}/2 \cdot r_0 \sin\rho, \\ a_{3y} &= -3^{1/2}/2 \cdot r_0 \sin\rho, \\ a_{Ny} &= 0, \end{aligned} \tag{3.3b}$$

$$\begin{aligned} a_{1z} &= (m_N r_0 \cos\rho)/m, \\ a_{2z} &= (m_N r_0 \cos\rho)/m, \\ a_{3z} &= (m_N r_0 \cos\rho)/m, \\ a_{Nz} &= -(3\, m_X r_0 \cos\rho)/m, \end{aligned} \tag{3.3c}$$

where m_X and m_N are the masses of the corresponding atomic nuclei and $m = 3\, m_X + m_N$. The molecule-fixed system of axes xyz is located in the reference configuration as shown in Fig. 4.

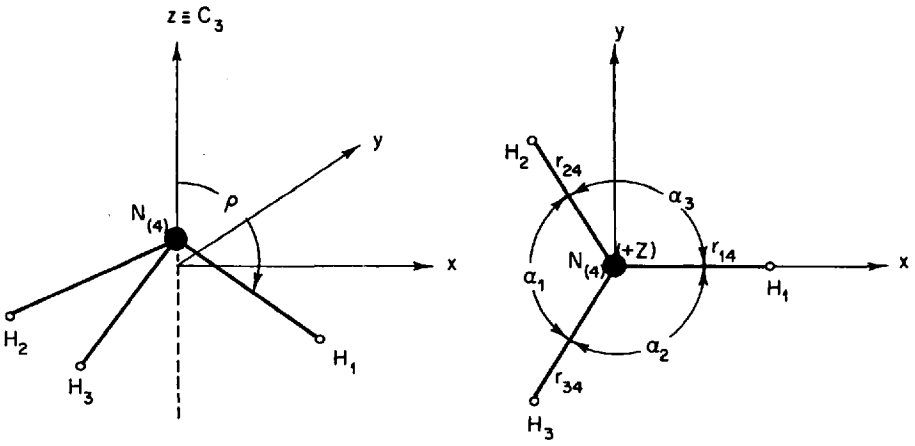

Fig. 4. The numbering of atoms and location of the molecule-fixed axis system in NH_3

We have the following well-known relation between the space-fixed coordinates and the molecule-fixed coordinates of the atomic nuclei for an instantaneous molecular configuration:

$$\boldsymbol{r}_i = \boldsymbol{R} + \mathbf{S}^{-1}(\theta\Phi\chi) \cdot [\boldsymbol{a}_i(\rho) + \boldsymbol{d}_i],\ i = 1,2,\ldots,N \tag{3.4}$$

where $\boldsymbol{r}_i$ is a column matrix of the three coordinates of the ith atomic nucleus in the space-fixed axis system XYZ, $\boldsymbol{R}$ is a column matrix of the three space-fixed coordinates of the origin of the molecule-fixed axis system. The quantity $[\boldsymbol{a}_i(\rho) + \boldsymbol{d}_i]$ is a column matrix of the three instantaneous coordinates of the ith nucleus in the molecule-fixed axis system, the $\boldsymbol{d}_i$'s are the vibrational displacement vectors measured with respect to the reference configuration. The 3 x 3 matrix $\mathbf{S}^{-1}(\theta\Phi\chi)$ of the transformation from the molecule-fixed axis system xyz to the space-fixed axis system XYZ is given explicitly in Appendix I in Ref.[20].

There are $3N + 7$ coordinates on the right sides of Eq. (3.4), *i.e.*, the $3N$ vibrational displacements $d_{i\alpha}$, the three coordinates of the center of mass, the three Euler angles θ, Φ, χ and the angle ρ. Since there are $3N$ coordinates $r_{i\alpha}$ ($i = 1, 2, \ldots, N$; $\alpha = x, y, z$) on the left sides of Eq. (3.4), the $3N$ vibrational displacements $d_{i\alpha}$ are subject to seven constraint equations which further specify the molecule-fixed axis system. We shall use the following set of Eckart and Sayvetz conditions for these constraint equations:

$$\sum_i m_i \boldsymbol{d}_i = 0, \tag{3.5a}$$

$$\sum_i m_i [\boldsymbol{a}_i(\rho) \times \boldsymbol{d}_i] = 0, \tag{3.5b}$$

$$\sum_i m_i \left[\frac{d\boldsymbol{a}_i(\rho)}{d\rho} \cdot \boldsymbol{d}_i\right] = 0. \tag{3.5c}$$

If Eqs. (3.5) are combined with Eq. (3.4), we obtain the following set of equations:

$$\sum_i m_i (r_i - R) = 0, \tag{3.6a}$$

$$\sum_i m_i a_i(\rho) \times [\mathbf{S}(\theta \Phi \chi) \cdot (r_i - R)] = 0, \tag{3.6b}$$

$$\sum_i m_i (da_i/d\rho) \cdot [\mathbf{S}(\theta \Phi \chi) \cdot (r_i - R) - a_i] = 0. \tag{3.6c}$$

If the instantaneous molecular configuration is given by a set of N position vectors r_i ($i = 1, 2, \ldots, N$), then the values of the seven coordinates R, θ, Φ, χ and ρ can be obtained by solving the seven equations (3.6). Consider for example the dependence of the angle $\bar{\rho}$, defined as the angle subtended by the z axis and the NH bond of the instantaneous molecular configuration, on the angle ρ for a motion of the atomic nuclei during which all the instantaneous bond lengths r_{NH} and the instantaneous valence angles remain equal. The following simple relation can be found (between ρ and $\bar{\rho}$) by solving Eqs. (3.6)

$$\cos \rho = (r_{NH}/r_0) \cos \bar{\rho}. \tag{3.7}$$

Eq. (3.7) shows that for a bending motion during which $r_{NH} = r_0$, the reference configuration follows exactly the motion of the instantaneous configuration of the atomic nuclei for all values of ρ in the interval from 0 to π (mod π). Eq. (3.7) implies also that the vibrational displacement vectors d_i in Eq. (3.4) remain small although the molecule exhibits a large-amplitude motion.

3.2. Classical and Quantum-Mechanical Vibration–Inversion–Rotation Hamiltonian

The classical kinetic energy T is defined as

$$2T = \sum_i m_i \dot{r}_i^2 \tag{3.8}$$

where $\dot{r}_i = dr_i/dt$.

If we substitute from Eq. (3.4) for $\dot{r}_i$ and use the various restrictions on the d_i given in Eqs. (3.6), we obtain the following expression for the classical vibration–inversion–rotation energy

$$2T = \sum_{\alpha, \beta = x, y, z, \rho} I_{\alpha\beta} \omega_\alpha \omega_\beta + 2 \sum_{\alpha = x, y, z} \omega_\alpha \sum_i m_i (d_i \times \dot{d}_i)_\alpha + \sum_i m_i \dot{d}_i^2. \tag{3.9}$$

In Eq. (3.9), ω_α ($\alpha = x, y, z$) are the molecule-fixed components of the angular velocity vector of the molecule-fixed axis system in the laboratory-fixed axis system, $\omega_\rho = \dot{\rho}$, $\dot{d}_i = (d/dt) d_i$. The quantities $I_{\alpha\beta}$ ($\alpha, \beta = x, y, z, \rho$) are the elements of the 4x4 matrix of the inertia tensor,

$$I = \begin{bmatrix} I_{xx} & I_{xy} & I_{xz} & I_{x\rho} \\ I_{yx} & I_{yy} & I_{yz} & I_{y\rho} \\ I_{zx} & I_{zy} & I_{zz} & I_{z\rho} \\ I_{\rho x} & I_{\rho y} & I_{\rho z} & I_{\rho\rho} \end{bmatrix} \tag{3.10}$$

where for $\alpha, \beta = x, y, z$

$$I_{\alpha\beta} = \sum_i m_i [\delta_{\alpha\beta}(\boldsymbol{a}_i + \boldsymbol{d}_i) \cdot (\boldsymbol{a}_i + \boldsymbol{d}_i) - (\boldsymbol{a}_i + \boldsymbol{d}_i)_\alpha (\boldsymbol{a}_i + \boldsymbol{d}_i)_\beta], \tag{3.11}$$

$$I_{\alpha\rho} = -2 \sum_i m_i [\frac{d\boldsymbol{a}_i}{d\rho} \times \boldsymbol{d}_i]_\alpha, \tag{3.12}$$

and

$$I_{\rho\rho} = \sum_i m_i \left(\frac{d\boldsymbol{a}_i}{d\rho}\right)^2 - 2 \sum_i m_i \left(\frac{d^2\boldsymbol{a}_i}{d\rho^2}\right) \cdot \boldsymbol{d}_i. \tag{3.13}$$

Let us introduce normal coordinates of vibrations Q_k ($k = 1, 2, \ldots, 3N$) by an orthonormal transformation

$$\begin{bmatrix} \frac{Q}{\overline{Q}} \end{bmatrix} = \begin{bmatrix} \frac{l}{\overline{l}} \end{bmatrix} [\boldsymbol{d}], \tag{3.14}$$

where $\boldsymbol{d}$ is column matrix of the $3N$ mass-weighted vibrational displacements $m_i^{1/2} d_{i\alpha}$ ($i = 1, 2, \ldots, N$; $\alpha = x, y, z$); Q is a column matrix of the genuine normal coordinates $Q_1, Q_2 \ldots, Q_{3N-7}$; $\overline{Q}$ is a column matrix of the seven nongenuine coordinates $Q_{3N-6}, \ldots, Q_{3N}$; l is a $(3N-7)$x$3N$ submatrix of the transformation coefficients $l_{i\alpha,\,k}$ ($k = 1, 2, \ldots, 3N-7$), $\overline{l}$ is a $7 \times 3N$ submatrix of the transformation coefficients $l_{i\alpha,\,s}$ ($s = 3N-6, \ldots, 3N$), which are chosen to be proportional to the coefficients associated with the quantities $d_{i\alpha}$ in the Eckart and Sayvetz conditions (3.5). Thus, $Q_{3N-6}, Q_{3N-5}, \ldots, Q_{3N} = 0$ correspond to the three coordinates of translation, the tree coordinates of rotation, and the coordinate ρ. The requirement which specifies that the Q_k are the normal coordinates of vibration is that the potential energy expansion in Q is diagonal up to the quadratic terms [cf. Eq. (3.23)]

The coefficients $\overline{l}_{i\alpha,\,s}$ ($s = 3N-6, \ldots, 3N$) are in general functions of ρ [see Eqs. (3.5)]. The orthogonality of the genuine normal coordinates Q_k ($k = 1, 2, \ldots, 3N-7$) to the nongenuine normal coordinates Q_s ($s = 3N-6, \ldots, 3N$) then implies that in general the coefficients $l_{i\alpha,\,k}$ ($k = 1, 2, \ldots, 3N-7$) are also functions of ρ.

If we substitute for $\boldsymbol{d}_i$ and $\dot{\boldsymbol{d}}_i$ from the transformation which is the inverse of Eq. (3.14), Eq. (3.9) becomes

$$2T = \sum_{\alpha,\beta = x,y,z,\rho} I'_{\alpha\beta}\omega_\alpha\omega_\beta + \sum_{k=1}^{3N-7} (\dot{Q}_k + \sum_{l,\,\alpha = x,y,z,\rho} \omega_\alpha \zeta^\alpha_{lk} Q_l)^2 \tag{3.15}$$

where

$$I'_{\alpha\beta} = I_{\alpha\beta} - \sum_{k,l,m} \zeta^{\alpha}_{km}\zeta^{\beta}_{lm}Q_kQ_l;\ \alpha, \beta = x, y, z, \rho. \tag{3.16}$$

In Eq. (3.16), the Coriolis constants ζ^{α}_{km} ($\alpha = x, y, z$) are defined as

$$\zeta^{\alpha}_{kl} = -\zeta^{\alpha}_{lk} = \sum_{i} (l_{i\beta,k}\, l_{i\gamma,l} - l_{i\gamma,k}\, l_{i\beta,l});\ \alpha, \beta, \gamma = x, y, z \tag{3.17}$$

and the Coriolis constant ζ^{ρ}_{kl} is given by

$$\zeta^{\rho}_{kl} = -\zeta^{\rho}_{lk} = \sum_{i,\alpha = x,y,z} l_{i\alpha,k}\left(\frac{dl_{i\alpha,l}}{d\rho}\right). \tag{3.18}$$

We can derive the quantum mechanical kinetic energy operator by following, almost exactly, the arguments of Sections 2, 3, and 4 of Chapter 11 in [20]. If we choose the volume element of the Hilbert space to be

$$d\tau = d\rho \sin\theta\, d\theta\, d\Phi d\chi \sum_{k=1}^{3N-7} dQ_k, \tag{3.19}$$

the kinetic energy operator assumes the form

$$2T = \mu^{1/4} \sum_{\alpha,\beta = x,y,z,\rho} (J_\alpha - p_\alpha)\mu_{\alpha\beta}\mu^{-1/2}(J_\beta - p_\beta)\mu^{1/4} + \mu^{1/4} \sum_{k} P_k\mu^{-1/2}P_k\mu^{1/4}. \tag{3.20}$$

In Eq. (3.20), J_α ($\alpha = x, y, z$) are the components of the total angular momentum operator with respect to the molecule-fixed axes. The quantity J_ρ is classically $J_\rho = (\partial T/\partial\omega_\rho)$ and quantum mechanically

$$J_\rho = -i\hbar\,(\partial/\partial\rho). \tag{3.21}$$

The components of the so-called vibrational angular momentum p_α ($\alpha = x, y, z$) and the momentum p_ρ are defined as

$$p_\alpha = \sum_{k,l} \zeta^{\alpha}_{kl}Q_kP_l;\ \alpha = x, y, z, \rho. \tag{3.22}$$

The quantities $\mu_{\alpha\beta}$ ($\alpha, \beta = x, y, z, \rho$) are the elements of the matrix which is the inverse of the 4x4 matrix $[I'_{\alpha\beta}]$; μ is the determinant of the matrix $[\mu_{\alpha\beta}]$.

We have so far considered only the kinetic energy expression. We must also consider the potential energy expression V, which can be expanded for each value of ρ as a Taylor series in the normal coordinates Q_k:

$$V = V_0(\rho) + \sum_k \kappa_k(\rho)Q_k + \frac{1}{2}\sum_k \lambda_k(\rho)Q_k^2 + \text{higher order terms.} \tag{3.23}$$

In Eq. (3.23), $V_0(\rho)$ is the double-minimum inversion potential function of the reference configuration ($Q_1 = Q_2 = \ldots Q_{3N-7} = 0$). The linear force constants $\kappa_k(\rho) = (\partial V/\partial Q_k)\rho$ are not in general zero for all values of ρ, since the reference configuration is not the equilibrium configuration for all values of ρ. The linear as well as the quadratic and higher order force constants must be, of course, considered as the functions of ρ (cf. Section 4.2).

It must be mentioned that our treatment[3, 5, 6] is an extension of the formalism that was originally developed by Hougen, Bunker, and Johns[22] [see also[21, 23]] for the treatment of the large-amplitude bending vibration of triatomic molecules. Moule and Rao[24] have simultaneously with, but independently of us, applied a simplified version of this formalism to an excited electronic state of H_2CO. Sarka, Papoušek, Boháček and Špirko[25–27] [see also [28]] have extended this formalism to tetratomic quasilinear molecules. The Hamiltonian $T + V$ [cf. Eqs. (3.20) and (3.23)] can therefore be applied to any molecule with one large-amplitude bending vibration. We shall discuss the use of this approach to other types of molecules later in Sections 6.1 and 6.2.

3.3. Extension to NH_2D and ND_2H

Discussion in Sections 3.1 and 3.2 is valid for ammonia NX_3 (X = H, D, T). This discussion can be easily extended[5] to asymmetrically substituted ammonia molecules NH_2D or ND_2H.

The reference configuration of the atomic nuclei of NH_2D is defined by (i) three equal and fixed bond lengths ($\equiv r_0$), (ii) the angle ρ subtended by the ND bond of the reference configuration and the axis p which passes through the atomic nucleus N and the center of the equilateral triangle formed by the atomic nuclei H_1, H_2, and D (Fig. 5). All the valence angles α of the reference configuration are defined to be equal, thus

$$(3^{1/2}/2)\,|\sin\rho| = |\sin(\alpha/2)|. \tag{3.24}$$

The molecule-fixed system of axes has its origin at the center of mass of the reference configuration and the z-axis subtends an angle ϵ with the p-axis (Fig. 5). The compo-

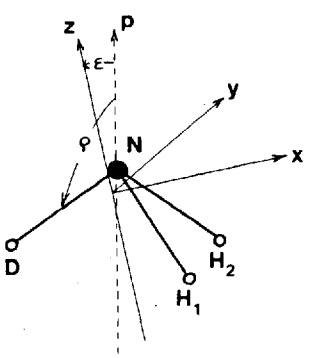

Fig. 5. The numbering of atoms and location of the molecule-fixed axis system for NH_2D. The hydrogen nuclei H_1 and H_2 should be replaced by D_1 and D_2, and D should be replaced by H for NH_2D

nents of the position vectors $a_i(\rho)$ of the ith atomic nucleus in this molecule-fixed axis system are given by

$$a_{1x} = a_{2x} = [(3\,m_D + m_N)/2m]\,r_0 \sin\rho\cos\epsilon + (m_N/m)r_0 \cos\rho \sin\epsilon,$$

$$a_{Dx} = -[(3m_H + m_N)/m]r_0 \sin\rho\cos\epsilon + (m_N/m)r_0 \cos\rho\sin\epsilon, \tag{3.25a}$$

$$a_{Nx} = -[(m_H - m_D)/m]r_0 \sin\rho\cos\epsilon - [(2m_H + m_D)/m]r_0 \cos\rho\sin\epsilon,$$

$$a_{1y} = -(3^{1/2}/2)r_0 \sin\rho,$$

$$a_{2y} = (3^{1/2}/2)r_0 \sin\rho, \tag{3.25b}$$

$$a_{Dy} = 0,$$

$$a_{Ny} = 0,$$

$$a_{1z} = a_{2z} = -[(3m_D + m_N)/2m]r_0 \sin\rho\sin\epsilon + (m_N/m)r_0 \cos\rho\cos\epsilon,$$

$$a_{Dz} = [(3m_H + m_N)/m]r_0 \sin\rho\sin\epsilon + (m_N/m)]\,r_0 \cos\rho\cos\epsilon, \tag{3.25c}$$

$$a_{Nz} = [(m_H - m_D)/m]r_0 \sin\rho\sin\epsilon - [(2m_H + m_D/m)]\,r_0 \cos\rho\cos\epsilon,$$

where m_H, m_N, and m_D are the masses of the atomic nuclei H, N, and D, respectively, and $m = 2m_H + m_D + m_N$. Equation (3.2) can be used to calculate the relationship between the angle ρ and ϵ; we obtain

$$d\epsilon/d\rho = u_1/(u_2 + u_3 \sin^2\rho), \tag{3.26}$$

where

$$u_1 = m_N(m_D - m_H),$$

$$u_2 = m_N(2m_H + m_D), \tag{3.27}$$

$$u_3 = \frac{3}{2}m_H(3m_D - m_N).$$

Equation (3.26) can be integrated to give

$$\epsilon(\rho) = \frac{u_1}{[u_2(u_2 + u_3)]^{1/2}} \arctan\left[\left(\frac{u_2 + u_3}{u_2}\right)^{1/2} \tan\rho\right] + \text{const}, \tag{3.28}$$

where the integration constant may be arbitrarily chosen so that $\epsilon = 0$ for the value of the parameter $\rho = 0$ (*i.e.*, const = 0). Note that for NH_3 Eq. (3.28) gives the identity $\epsilon = 0$ for all values of ρ (cf. Section 3.1).

The vibration–inversion–rotation Hamiltonian then assumes the same form as in Eq. (3.20); $\mu_{\alpha\beta}$, μ and V are of course different functions of ρ and Q.

3.4. Expansion of the Vibration–Inversion–Rotation Hamiltonian

The exact vibration–inversion–rotation Hamiltonian $\mathscr{H} = T + V$ [Eqs. (3.20) and (3.23)] is, of course, too complicated to work with directly. Analogously as in the standard treatment of the vibration–rotation states of rigid molecules[29, 30], we can expand $\mathscr{H}$ in terms of the normal coordinates of vibration. This makes it possible to use various approximations to $\mathscr{H}$ which are manageable numerically.

Let us first rearrange $\mathscr{H}$ into the following form:

$$\mathscr{H} = \frac{1}{2} \sum_{\alpha,\beta=x,y,z,\rho} \mu_{\alpha\beta} (J_\alpha - p_\alpha)(J_\beta - p_\beta) - \frac{1}{2} \sum_{\alpha,\beta=x,y,z,\rho} (p_\alpha \mu_{\alpha\beta})(J_\beta - p_\beta) +$$

$$+ \frac{1}{2} \sum_{\alpha=x,y,z,\rho} (J_\rho \mu_{\rho\alpha})(J_\alpha - p_\alpha) + \frac{1}{2} \mu^{1/4} \left\{ \sum_{\alpha\beta=x,y,z,\rho} [p_\alpha \mu_{\alpha\beta} \mu^{-1/2} (p_\beta \mu^{1/4})] - \right.$$

$$- \sum_{\alpha=x,y,z,\rho} [p_\alpha \mu_{\alpha\rho} \mu^{-1/2} (J_\rho \mu^{1/4})] - \sum_{\alpha=x,y,z,\rho} [J_\rho \mu_{\rho\alpha} \mu^{-1/2} (p_\alpha \mu^{1/4})] +$$

$$\left. + [J_\rho \mu_{\rho\rho} \mu^{-1/2} (J_\rho \mu^{1/4})] \right\} + \frac{1}{2} \sum_k P_k^2 + \frac{1}{8} \mu^{-1} \sum_k (P_k^2 \mu) - \frac{5}{32} \mu^{-2} \sum_k (P_k \mu)^2 +$$

$$+ V(\rho, Q). \tag{3.29}$$

In rearranging the Hamiltonian we used the fact that the operators J_α ($\alpha = x, y, z$) commute with all other operators in Eq. (3.29). In Eq. (3.29), the operators p_α, J_ρ, P_k operate only within the brackets in expressions like $(p_\alpha \mu_{\alpha\beta})$, $(J_\rho \mu_{\rho\alpha})$, $(P_k^2 \mu)$ *etc.*

We expand the inverse moment of the inertia matrix as a power series in the vibrational normal coordinates[31]

$$\mu_{\alpha\beta} = \mu^0_{\alpha\beta} + \sum_k X_k^{\alpha\beta} Q_k + \sum_{k,l} Y_{kl}^{\alpha\beta} Q_k Q_l + \ldots; \alpha, \beta = x, y, z, \rho . \tag{3.30}$$

Let us consider the case of NX_3 (X = H, D, T). From our choice of the reference configuration [Eqs. (3.11)–(3.13)] we have [b] $\mu^0_{\alpha\beta} = \delta_{\alpha\beta} \mu^0_{\alpha\beta}$, and the expressions for $X_k^{\alpha\beta}$ and $Y_{kl}^{\alpha\beta}$ take a simple form:

$$X_k^{\alpha\beta} \left[\equiv (\partial \mu_{\alpha\beta} / Q_k)_\rho \right] = - a_k^{\alpha\beta} \mu^0_{\alpha\alpha} \mu^0_{\beta\beta}, \tag{3.31a}$$

$$Y_{kl}^{\alpha\beta} \left[\equiv - \frac{1}{2} (\partial^2 \mu_{\alpha\beta} / \partial Q_k \partial Q_l)_\rho \right] = \frac{3}{8} \sum_{\epsilon=x,y,z,\rho} (a_k^{\alpha\epsilon} a_l^{\beta\epsilon} + a_l^{\alpha\epsilon} a_k^{\beta\epsilon}) \mu^0_{\alpha\alpha} \mu^0_{\beta\beta} \mu^0_{\epsilon\epsilon}, \tag{3.31b}$$

[b] Tensor $\mu^0_{\alpha\beta}$ is diagonal because the reference configuration of the NH_3 molecule defined in Section 3.2 is a symmetric top not only for the equilibrium configuration (point group C_{3v}) but also for every value of the angle ρ in the interval from 0 to π (with mod π).

where

$$a_k^{\alpha\beta} = (\partial I_{\alpha\beta}/\partial Q_k)_\rho \tag{3.32}$$

are the derivatives of the instantaneous inertia tensor $I_{\alpha\beta}$, evaluated at the reference configuration.

Expansion (3.31) can be substituted into the right side of Eq. (3.29) and maintaining only terms of order of magnitude $\kappa^2 T_v$ [at $J = 10$ for $v_1 = v_3 = v_4 = 0$, cf. Ref.[21] for determining the orders of magnitude in Eq. (3.29)] we have for the kinetic energy operator

$$T = T_i^0 + T_r^0 + T_{\text{Cent}} + T_{\text{Cor}} + T_{\text{vib}}, \tag{3.33}$$

where

$$T_i^0 = \frac{1}{2}\mu_{\rho\rho}^0 J_\rho^2 + \frac{1}{2}(J_\rho \mu_{\rho\rho}^0) J_\rho + \frac{1}{2}(\mu^0)^{1/4}\left\{ J_\rho \mu_{\rho\rho}^0 (\mu^0)^{-1/2} \cdot [J_\rho (\mu^0)^{1/4}] \right\} + U_0(\rho), \tag{3.34}$$

$$T_r^0 = \frac{1}{2}\mu_{xx}^0 (J_x^2 + J_y^2) + \frac{1}{2}\mu_{zz}^0 J_z^2, \tag{3.35}$$

$$T_{\text{Cent}} = \frac{1}{2} \sum_{\alpha,\beta=x,y,z,\rho} [\sum_k X_k^{\alpha\beta} Q_k + \sum_{k,l} Y_{kl}^{\alpha\beta} Q_k Q_l] J_\alpha J_\beta +$$

$$+ \frac{1}{2} \sum_{\alpha=x,y,z,\rho} [\sum_k (J_\rho X_k^{\rho\alpha}) Q_k + \sum_{k,l} (J_\rho Y_{kl}^{\rho\alpha}) Q_k Q_l] J_\alpha, \tag{3.36}$$

$$T_{\text{Cor}} = -\frac{1}{2} \sum_{\alpha=x,y,z,\rho} \mu_{\alpha\alpha}^0 (J_\alpha p_\alpha + p_\alpha J_\alpha) - \frac{1}{2}(J_\rho \mu_{\rho\rho}^0) p_\rho, \tag{3.37}$$

$$T_{\text{vib}} = \frac{1}{2}\sum_k P_k^2 + \frac{1}{2} \sum_{\alpha=x,y,z,\rho} \mu_{\alpha\alpha}^0 p_\alpha^2. \tag{3.38}$$

In Eqs. (3.36) and (3.38), k and l take on the values 1, 3a, 3b, 4a, 4b [see Eq. (4.2)]. The term $U_0(\rho)$ in Eq. (3.34) consists of that part of $\frac{1}{2}\mu^{1/4} \sum [P_k \mu^{-1/2} (P_k \mu^{1/4})]$ having order of magnitude $\kappa^2 T_v$. The explicit expression for $U_0(\rho)$ is

$$U_0(\rho) = \frac{\hbar^2}{8}\left\{ a_1^{xx} a_1^{zz} \mu_{xx}^0 \mu_{zz}^0 + a_1^{xx} a_1^{\rho\rho} \mu_{xx}^0 \mu_{\rho\rho}^0 + \frac{1}{2} a_1^{zz} a_1^{\rho\rho} \mu_{zz}^0 \mu_{\rho\rho}^0 - \right.$$

$$- \frac{1}{4}(a_1^{zz})^2 (\mu_{zz}^0)^2 - \frac{1}{4}(a_1^{\rho\rho})^2 (\mu_{\rho\rho}^0)^2 - 2 \sum_{t=3,4} [(a_{tb}^x)^2 \mu_{xx}^0 \mu_{\rho\rho}^0 +$$

$$\left. + (a_{ta}^{xz})^2 \mu_{xx}^0 \mu_{zz}^0 + (a_{ta}^{xx})^2 (\mu_{xx}^0)^2] \right\}. \tag{3.39}$$

We have included certain terms from the expansion of $\mu_{\rho\alpha}$ in the third term on the right side of Eq. (3.29) in Eqs. (3.36) and (3.38) although their contribution is

probably below the order of our approximation. It can be verified that this must be done if we want to preserve the Hermitian properties of the centrifugal distortion operator T_{Cent} and of the Coriolis operator T_{Cor} [Eqs. (3.36) and (3.37)]. For example, operators $X_k^{\rho\alpha} Q_k J_\alpha J_\rho$ in Eq. (3.36) are not Hermitian.

We shall discuss briefly the physical meaning of various terms which occur in the expansion of our Hamiltonian and the corresponding approximations. The simpliest approximation to $\mathscr{H}$ is obtained when all the small-amplitude vibrational coordinates Q_k ($k = 1, 3a, 3b, 4a, 4b$) are put equal to zero. We shall call this Hamiltonian the zeroth-order inversion–rotation Hamiltonian, or the rigid bender Hamiltonian. It follows from Eqs. (3.23) and (3.33)–(3.38) that it can be written in the following form:

$$\mathscr{H}^0_{\mathrm{ir}} = \mathscr{H}^0_{\mathrm{i}} + T^0_{\mathrm{r}} \tag{3.40}$$

where $\mathscr{H}^0_{\mathrm{i}} = [T^0_{\mathrm{i}} - U^0(\rho)] + V_0(\rho)$. In the expression for T^0_{i} and T^0_{r} [Eqs. (3.34) and (3.35)], $\mu^0_{\alpha\alpha} = 1/I^0_{\alpha\alpha} (\alpha = x, y, z, \rho)$; the explicit expression for $I^0_{\alpha\alpha}$ are as follows:

$$I^0_{xx} = I^0_{yy} \left[\equiv \sum_i m_i (a^2_{iy} + a^2_{iz})\right] = 3m_{\mathrm{H}} r_0^2 \left[(m_{\mathrm{N}}/m) \cos^2\rho + \frac{1}{2} \sin^2\rho\right], \tag{3.41}$$

$$I^0_{zz} \left[\equiv \sum_i m_i (a^2_{ix} + a^2_{iy})\right] = 3m_{\mathrm{H}} r_0^2 \sin^2\rho, \tag{3.42}$$

$$I^0_{\rho\rho} \left[\equiv \sum_i m_i (\partial a_i/\partial\rho)^2\right] = 3m_{\mathrm{H}} r_0^2 \left[\cos^2\rho + (m_{\mathrm{N}}/m) \sin^2\rho\right]. \tag{3.43}$$

Consider briefly now the Schrödinger equation for the zeroth-order inversion Hamiltonian $\mathscr{H}^0_{\mathrm{i}}$:

$$\mathscr{H}^0_i \psi^0_i(\rho) = E^0_i \psi^0_i(\rho). \tag{3.44a}$$

This equation does not have a simple analytical solution but it can be solved by the numerical integration technique which will be discussed in Section 5.2. After solving this equation we can obtain the eigenvalues and eigenvectors of the inversion states of ammonia in the ground "vibrational" state, and, hence, we can obtain the required inversion splittings in the ν_2 states of ammonia. The important difference between this treatment and all other previous treatments of the one-dimensional Schrödinger equation for the NH_3 molecule lies in the fact that in this treatment the large-amplitude motion is considered in the kinetic part as well as in the potential energy part of the Hamiltonian.

From Eqs. (3.40) and (3.35) it is obvious that the inversion–rotation wave functions $\psi^0_{ir}(\theta, \Phi, \chi, \rho)$ of NH_3 which are the eigenfunctions of the operator $\mathscr{H}^0_{ir}$, can be written as a product of the rigid-rotor symmetric top wave functions depending on the Euler angles θ, Φ, χ and the inversion wave functions, depending on the variable ρ. Integration of the Schrödinger equation

$$(\mathscr{H}^0_{ir} - E^0_{ir})\, \psi^0_{ir}(\theta, \Phi, \chi, \rho) = 0 \tag{3.44b}$$

over θ, Φ and χ then leads to the following equation:

$$\left\{ \mathscr{H}_i^0 + (\hbar^2/2)\,\mu_{xx}^0[J(J+1) - k^2] + (\hbar^2/2)\,\mu_{zz}^0 k^2 \right\} \psi_{Jk}^0(\rho) = E_{ir}^0 \psi_{Jk}^0(\rho). \qquad (3.45)$$

The wave functions $\psi_{Jk}^0(\rho)$ in Eq. (3.45) depend on ρ (as the dynamic variable) and on the rotational quantum numbers J and k (as parameters).

After solving Eq. (3.45) we can obtain the eigenvalues and eigenvectors of the inversion–rotation states of ammonia in the ground "vibrational" state; *i.e.* we can calculate – in the rigid bender approximation – the rotational dependence of the inversion splittings in the ν_2 states of ammonia. Note that the J and k dependent terms in the Schrödinger equation [Eq. (3.45)] represent a modification of the double-minimum potential function $V_0(\rho)$ for each rotational state J, k (see further Sections 5.1 and 5.2).

Up to the second order of approximation, we can obtain the vibration–inversion–rotation energy levels and the corresponding wave functions by solving the Schrödinger equation

$$(T + V)\,\psi_{\text{vir}}\,(Q; \rho, \theta, \Phi, \chi) = 0. \qquad (3.46)$$

The solutions of Eq. (3.46) are therefore the inversion–rotation states of ammonia in the ground as well as in the excited vibrational states, calculated in the so-called non-rigid bender approximation.

The operator T_{Cent} which appears in the kinetic energy operator T [Eq. (3.36)] involves certain terms which are formally the same as the centrifugal-distortion operators in a rigid molecule of a C_{3v} symmetry[30, 32]. In our case, however, the coefficients $X_k^{\alpha\beta}$ and $Y_{kl}^{\alpha\beta}$ must be considered as functions of ρ. Furthermore, in the centrifugal distortion operator T_{Cent} in Eq. (3.36) there are several J_ρ containing terms which do not appear in the theory of centrifugal distortion in a rigid C_{3v} molecule. In the theory of a rigid molecule, these terms would account for certain effects of the higher order than $\kappa^2 T_v$. In our case they become lower order terms because of the anharmonicity of the large amplitude inversion motion. T_{Cent} also contains certain terms which describe the vibration–inversion–rotation interaction between the ν_2 inversion states and the doubly degenerate ν_4 vibrational states (see Section 5.4 for details).

In Eq. (3.37), T_{Cor} is the Coriolis operator for the interaction between the vibrational states ν_1, ν_3 and ν_4 in NH_3 [the first term on the right side of Eq. (3.37)]; the operator $(J_\rho \mu_{\rho\rho}^0) p_\rho$ has the meaning of a quartic potential constant. T_{vib} in Eq. (3.38) is the operator of the vibrational kinetic energy where $\mu_{\alpha\alpha}^0$ are of course considered as functions of ρ.

The application of $\mathscr{H}_{\text{vir}}$ to the analysis of the vibrational–inversion–rotation spectra of ammonia will be discussed in detail in Sections 5.1–5.4. Here we mention only that if the interaction between the inversion, vibration and rotation states is neglected, the overall wave function ψ_{vir} can be written as a product of the harmonic oscillator wave functions $\psi_{v_k}^0$, the inversion wave function $\psi_i(\rho)$, and the symmetric rotor wave function $S_{JkM}(\theta, \Phi) \exp(ik\chi)$:

$$\psi_{\text{vir}} = [\psi_{v_1}^0 \psi_{v_3}^0 \psi_{v_4}^0]\,[\psi_i(\rho)]\,[S_{JkM}(\theta, \Phi) \exp(ik\chi)]. \qquad (3.47)$$

We have so far considered the expansion of the vibration–inversion–rotation Hamiltonian $\mathscr{H}$ for the symmetrically substituted molecules NX_3 (X = H, D, T). For NH_2D or ND_2H, the treatment must be modified in an obvious way[5]. Because of the lower symmetry of the reference configuration of NH_2D with respect to that of NH_3, the matrix $[\mu^0_{\alpha\beta}]$ is not diagonal for NH_2D but contains the off-diagonal element μ^0_{xz}. For example, in the rigid bender approximation, T^0_i remains formally the same but T^0_r becomes

$$T^0_r = \frac{1}{2}\mu^0_{xx}J^2_x + \frac{1}{2}\mu^0_{yy}J^2_y + \frac{1}{2}\mu^0_{xz}(J_xJ_z + J_zJ_x). \tag{3.48}$$

Note that T^0_r in Eq. (3.48) is not diagonal in the rotational quantum number k, and we cannot use Eq. (3.45) for the calculation of the inversion–rotation energy levels of NH_2D in the rigid-bender approximation (Section 5.2).

4. Symmetry Classification of the States and the GF Matrix Problem in Ammonia

Before we apply the formalism developed in Section 3 to the vibration–inversion–rotation spectra of ammonia, we shall discuss in this section certain group theoretical problems concerning the classification of the states of ammonia, the construction of the symmetry coordinates, the symmetry properties of the molecular parameters, and the *GF* matrix problem for the ammonia molecule.

4.1. Symmetry Classification of the States

Ammonia is an interesting molecule also from the group-theoretical point of view. It has been recognized since the beginnings of the applications of group theory to molecular spectra that the C_{3v} point group which characterizes the geometrical symmetry of NH_3 does not give full information on the symmetry properties of its quantum states. Instead of the C_{3v} group, the D_{3h} group has been used for the classification of the states of NH_3. However, the general theoretical principles pertaining to the use of the D_{3h} group of ammonia have been presented much later in the fundamental paper of Longuet-Higgins[1] on the symmetry groups of nonrigid molecules.

Following Longuet-Higgins[1], the full symmetry group of NH_3 is the group of the permutations[c] and permutation inversion of the identical atomic nuclei:

$$\mathbf{E},\ \{(123),\ (132)\},\quad \{(12)^*, (13)^*, (23)^*\} \tag{I}$$

$$\mathbf{E}^*, \{(123)^*, (132)^*\},\ \{(12),\ (13),\ (23)\} \tag{II}$$

where for example (123) is the cyclic permutation of the hydrogen nuclei numbered according to Fig. 1, E* is the operation of inversion defined by Eq. (1.1), and for

[c] We permute the positions and spins of the identical atomic nuclei.

example (123)* is the permutation (123) followed by inversion E*. This group is isomorphic to the D_{3h} point group on the basis of the following one-to-one correspondence between the permutation–inversion group (PI group) operations and the point group operations: $\mathbf{E} \leftrightarrow \mathbf{E}$, $(123) \leftrightarrow C_3$, $(12)^* \leftrightarrow \sigma_v$, $\mathbf{E}^* \leftrightarrow \sigma_h$, $(123)^* \leftrightarrow \mathbf{S}_3$, $(12) \leftrightarrow \mathbf{C}_2$. Note that the elements in the row (I) are the completely feasible elements of the Longuet-Higgins group[1] because only rigid rotations of the equilibrium configuration are connected with their application; they form a subgroup of the D_{3h} group which is isomorphic with the C_{3v} group. On the other hand, all the elements in the row (II) are non-completely feasible because they transform the equilibrium configuration into a symmetrically equivalent configuration which is separated from the original one by the inversion barrier.

The PI group operations are defined by their effect on the space-fixed coordinates of the atomic nuclei and electrons. Since our molecular wavefunctions are written in terms of the vibrational coordinates, the Euler angles and the angle ρ, we must first determine the effect of the PI group operations on these variables. In the case of inversion this can lead to certain problems both in the understanding of the concepts of molecular symmetry and in the proper use of group theoretical methods in the classification of the states of ammonia.

We shall use Eqs. (3.6) first to find the effect of the PI group operations on the Euler angles θ, Φ, χ and on the angle ρ. This will make it possible to find the effect of the PI group operations on the small vibrational displacements d_i. The effect of $\mathbf{E}^*$ on the space-fixed coordinates r_i is defined by Eq. (1.1). It can easily be verified[3] that if a set of values θ, Φ, χ, ρ is a solution of Eqs. (3.6) for a molecular configuration defined by a set of position vectors r_i ($i = 1, 2, \ldots, N$), then for a molecular configuration defined by a set of position vectors $-r_i$ ($i = 1, 2, \ldots, N$), the solution of Eqs. (3.6) is $\theta, \Phi, \chi-\pi, \pi-\rho$.

The functions $\psi_i^0(\rho)$ are of two types [cf. Fig. 72 in Ref.[33]]: either $\psi_i^0(\rho) = + \psi_i^0(\pi-\rho)$ or $\psi_i^0(\rho) = - \psi_i^0(\pi-\rho)$ where $0 \leqslant \rho < \pi$. Let us denote the first type of inversion function as $\psi_i^+(\rho)$, the second type as $\psi_i^-(\rho)$.

By considering the effect of the $\mathbf{E}^*$ operation it is obvious that

$$\mathbf{E}^* \psi_i^+(\rho) = + \psi_i(\rho), \quad \mathbf{E}^* \psi_i^-(\rho) = - \psi_i^-(\rho). \tag{4.1}$$

The effects of all the PI group operations on the Euler angles θ, Φ, χ and the angle ρ are summarized in Table 1. Fig. 6 is the illustration of the symmetry classification of the rotational levels in the ground state of the NH_3 molecule.

Let us consider now the effect of the PI group operations on the small vibrational coordinates. Instead of the Cartesian coordinates d_i it is convenient to introduce the three stretching coordinates r_{14}, r_{24}, r_{34} and the three bending coordinates $\alpha_1, \alpha_2, \alpha_3$ (Fig. 4), and a set of vibrational symmetry coordinates constructed from these stretch and bend coordinates

$$\begin{aligned}
S_1 &= 3^{-1/2} \cdot (r_{14} + r_{24} + r_{34}), & S_{4a} &= 6^{-1/2} (2\alpha_1 - \alpha_2 - \alpha_3), \\
S_{3a} &= 6^{-1/2} \cdot (2r_{14} - r_{24} - r_{34}), & S_{4b} &= 2^{-1/2} (\alpha_2 - \alpha_3). \\
S_{3b} &= 2^{-1/2} \cdot (r_{24} - r_{34}),
\end{aligned} \tag{4.2}$$

Table 1. Transformation of θ, Φ, χ, ρ and of the stretch and bend coordinates of NH_3 by the symmetry operations of the permutation-inversion group D_{3h}.

Variables	E E	C_3 (123)	σ_v (23)*	σ_h E*	S_3 (123)*	C_2 (23)
θ	θ	θ	$\pi - \theta$	θ	θ	$\pi - \theta$
Φ	Φ	Φ	$\pi + \Phi$	Φ	Φ	$\pi + \Phi$
χ	χ	$\chi - (2\pi/3)$	$\pi - \chi$	$\chi - \pi$	$\chi + (\pi/3)$	$-\chi$
ρ	ρ	ρ	ρ	$\pi - \rho$	$\pi - \rho$	$\pi - \rho$
r_{14}	r_{14}	r_{34}	r_{14}	r_{14}	r_{34}	r_{14}
r_{24}	r_{24}	r_{14}	r_{34}	r_{24}	r_{14}	r_{34}
r_{34}	r_{34}	r_{24}	r_{24}	r_{34}	r_{24}	r_{24}
α_1	α_1	α_3	α_2	α_1	α_3	α_2
α_2	α_2	α_1	α_1	α_2	α_1	α_1
α_3	α_3	α_2	α_3	α_3	α_2	α_3

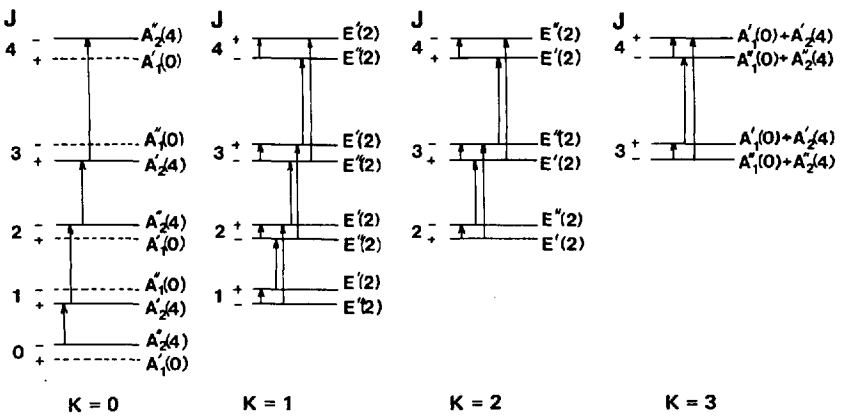

Fig. 6. Symmetry classification of the rotational levels in the ground state of NH_3. Arrows: inversion and inversion–rotation transitions allowed by selection rules discussed in Section 4.3. *Numbers in parenthesis behind the species symbols:* spin statistical weights

The stretch and bend coordinates transform by the symmetry operations as given in Table 1, thus the symmetry coordinates S_i form the basis of a reducible representation

$$\Gamma(S_i) = A_1' + 2E' \tag{4.3}$$

(see Table 2).

In Fig. 6 and in the following discussion, the ± label attached to an energy level denotes the parity of the *overall* wave function with respect to inversion, E*. By symmetric (s) and antisymmetric (a) we always mean the parity of the *inversion* wave function $\psi_i(\rho)$ with respect to E*. We shall denote the inversion states by the quantum number $v_2^{\pm}$ which corresponds to the vibrational quantum number of the ν_2 bend-

ing mode in a rigid C_{3v} molecule. The symbol v_2^+ denotes always the lower component, v_2^- the upper component of the inversion doublet (Fig. 3).

Bunker[34] has recently introduced a different labeling of the inversion states according to the number of nodes v_{inv} of the inversion function $\psi_i(\rho)$. Thus, the 0^+ label corresponds to $v_{inv} = 0$, 0^- to 1, 1^+ to 2 etc. (Fig. 3). The notation of Bunker allows one to label the energy levels by their symmetry and to determine the vibration and rotation selection rules in a very straightforward way[34]. We feel, however, that for high inversion barriers and especially for the inversion states below the inversion barrier it is more natural to use the old labeling (but we may be too conservative in this respect).

The symmetry group of NH_2D (ND_2H) is the C_{2v} group of the permutations and permutation-inversions of the elements E, (12), E*, and (12)*. By the same arguments as described above for NH_3 we find that the symmetry coordinates for NH_2D form the basis of a reducible representation[5]

$$\Gamma(S_i) = 3A_1 + 2B_2. \tag{4.4}$$

4.2. GF Matrix Problem for Ammonia

The potential energy V can be expanded for each value of ρ as a Taylor series in the symmetry coordinates S_1, S_3, S_4 (for NH_3)

$$V = V_0(\rho) + \sum_n F_n(\rho) S_n + \frac{1}{2} \sum_{m,n} F_{mn}(\rho) S_m S_n + \ldots \tag{4.5}$$

The linear[d] and quadratic force constants F_n and F_{mn} are written as a Fourier expansion

$$F_n(\rho) = \sum_{t=0}^{\infty} [k_{c,n}^{(t)} \cos(t\rho) + k_{s,n}^{(t)} \sin(t\rho)], \tag{4.6}$$

$$F_{mn}(\rho) = \sum_{t=0}^{\infty} [K_{c,mn}^{(t)} \cos(t\rho) + K_{s,mn}^{(t)} \sin(t\rho)], \tag{4.7}$$

where t is an integer. The species of the symmetry coordinates is either A_1' or E' (Table 2) and the species of $\sin(t\rho)$ and $\cos(t\rho)$ are A_1' and A_2'' for t odd and A_2'' and A_1' for t even. Since the potential energy V must be invariant with respect to all the symmetry operations it holds that

$$k_{c,m}^{(t)} = K_{c,mn}^{(t)} = 0 \quad \text{for } t \text{ odd}, \tag{4.8}$$

---

[d] Because of the high symmetry of the reference configuration in ammonia NX_3 (X = H, D, T), the only non-vanishing linear force constant is $F_1(\rho)$.

Tabel 2. The symmetry species of the operators and of the wave functions in the D_{3h} group of NH_3

Quantity	Species	Quantity	Species
$\sin\rho$	A_1'	S_1	A_1'
$\cos\rho$	A_2''	(S_{3a}, S_{3b})	E'
$\sin 2\rho$	A_2''	(S_{4a}, S_{4b})	E'
$\cos 2\rho$	A_1'	$\xi^x_{1,3b}$	A_2''
$\psi_i^+(\rho)$	A_1'	$\xi^x_{1,4b}$	A_2''
$\psi_i^-(\rho)$	A_2''	$\xi^z_{3a,\,3b}$	A_1'
(J_x, J_y)	E''	$\xi^z_{4a,\,4b}$	A_1'
(p_x, p_y)	E''	$\xi^z_{3a,\,4b}$	A_1'
J_z	A_2'	$\xi^x_{3a,\,4b}$	A_2''
J_ρ	A_2''	$\xi^\rho_{3a,\,4a}$	A_2''
p_z	A_2'	μ_Z	A_1''
p_ρ	A_2''	(μ_x, μ_y)	E'
		μ_z	A_2''

$$k^{(t)}_{s,n} = K^{(t)}_{s,mn} = 0 \quad \text{for } t \text{ even.} \tag{4.9}$$

The elements of the kinematic matrix G in the representation of the symmetry coordinates [Eqs. (4.2)] are as follows:

$$\begin{aligned} G_{11} &= \mu_H + (1 + 2\cos\alpha)\mu_N, \\ G_{33} &= \mu_H + (1 - \cos\alpha)\mu_N, \\ G_{34} &= \mu_N (1 - \cos\alpha)^2/(r_0 \sin\alpha), \\ G_{44} &= (1 - \cos\alpha)\,[(1 - \cos\alpha)^2 \mu_N + (2 + \cos\alpha)\mu_H]/(r_0^2 \sin^2\alpha) \end{aligned} \tag{4.10}$$

where α is the instantaneous value of the bond angle; it holds that

$3^{1/2} \cdot |\sin\rho|/2 = |\sin\alpha/2|$ and $\mu_H = 1/m$, $\mu_N = 1/m_N$.

The standard GF matrix problem[20] can be written as[22]

$$GFL = L\Lambda, \tag{4.11}$$

where Λ is a diagonal matrix of $\lambda_k(\rho)$ from Eq. (3.23) and L is the square matrix of the eigenvectors which transform the five symmetry coordinates S [(Eqs. (4.2)] into the five normal coordinates $Q_1, Q_{3a}, Q_{3b}, Q_{4a}, Q_{4b}$

$$S = LQ. \tag{4.12}$$

The elements of the eigenvectors L in Eq. (4.12) are totally symmetric[3]. However, the elements of the eigenvectors in Eq. (3.14) are of the species A_1' for $l_{ix,k}$ and $l_{iy,k}$, while that of $l_{iz,k}$ is A_2'' [see[3]].

For NH_3, the non-vanishing Coriolis parameters defined by Eqs. (3.17) and (3.18) are then the following:

$$\zeta^x_{1,3b} = -\zeta^y_{1,3a};\ \zeta^x_{1,4b} = -\zeta^y_{1,4a};\ \zeta^x_{3a,4b} = -\zeta^x_{4a,3b} = \zeta^y_{3a,4a} = -\zeta^y_{3b,4b};\ \zeta^z_{3a,3b};\ \zeta^z_{4a,4b};$$
$$\zeta^z_{3a,4b} = -\zeta^z_{3b,4a};\ \zeta^\rho_{3a,4a} = \zeta^\rho_{3b,4b}.$$

Note that the Coriolis constants ζ^x, ζ^y, and ζ^ρ are not totally symmetric (Table 2); this is illustrated also by Figs. 7a und 7b.

This discussion can be easily extended to NH_2D or ND_2H [see partly Ref.[5]].

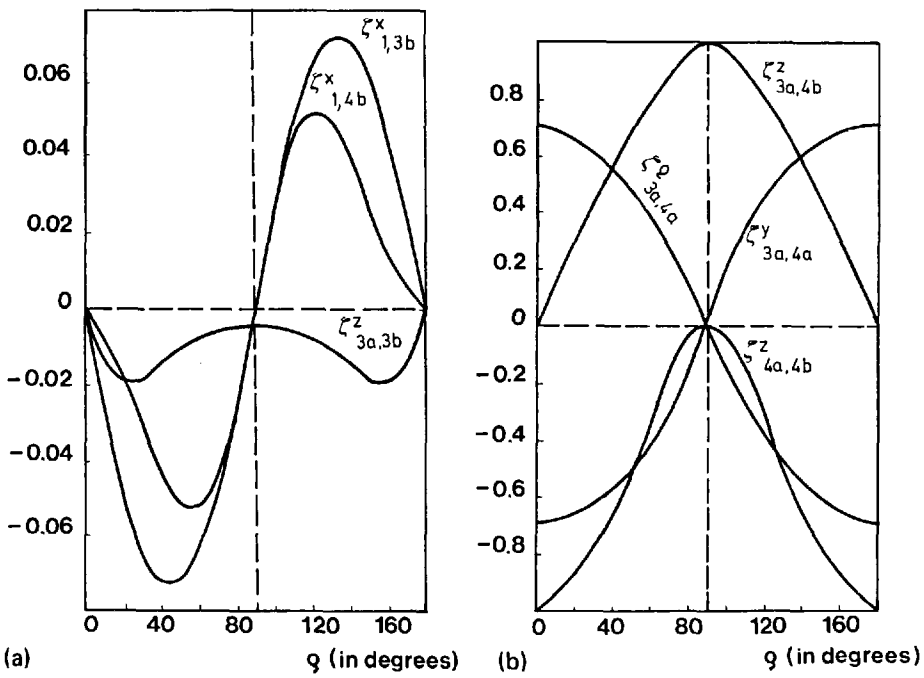

Fig. 7a, b. (a) The dependence of the Coriolis constants $\zeta^x_{1,3b}$, $\zeta^x_{1,4b}$, and $\zeta^z_{3a,3b}$ on the inversion coordinate ρ for NH_3. Calculated from the force field in Table 3
(b) The dependence of the Coriolis constants $\zeta^z_{3a,4b}$, $\zeta^\rho_{3a,4a}$, $\zeta^y_{3a,4a}$, and $\zeta^z_{4a,4b}$ on the inversion coordinate ρ for NH_3. Calculated from the force field in Table 3

4.3. Selection Rules

Let us denote by μ_Z the component of the electric dipole moment vector with respect to the space-fixed axis Z. A transition between vibration–inversion–rotation energy levels of ammonia is allowed by selection rules if

$$\langle \psi'_{\mathrm{vir}} | \mu_Z | \psi''_{\mathrm{vir}} \rangle \neq 0. \tag{4.13}$$

The component μ_Z belongs to the species A_1'' in the D_{3h} group because μ_Z is not changed by pure permutations and it changes sign by permutation–inversion operations (Section 4.1). The overall symmetry selection rule therefore allows transitions only between vibration–inversion–rotation states with opposite parity with respect to the operation of inversion (cf. Fig. 6).

To derive the selection rules for the allowed transitions between vibration, inversion and rotation states, we must express μ_Z in terms of the components μ_α ($\alpha = x, y, z$) of the dipole moment vector with respect to the molecule-fixed axes $x\,y\,z$, *i.e.*

$$\langle \psi'_{vir} | \mu_Z | \psi''_{\mathrm{vir}} \rangle = \sum_{\alpha=x,y,z} \langle \psi'_i(\rho)\psi'_v(Q) | \mu_\alpha | \psi''_i(\rho)\psi''_v(Q) \rangle \cdot$$

$$\cdot \langle \psi'_r(\theta\Phi\chi) | \lambda_{Z\alpha} | \psi''_r(\theta\Phi\chi) \rangle. \tag{4.14}$$

In Eq. (4.14), μ_α ($\alpha = x, y, z$) must be considered as functions of the normal coordinates Q and the inversion coordinate ρ; $\lambda_{Z\alpha}$ are the direction cosines between the molecule and space-fixed system of axes which are functions of the Euler angles θ, Φ, χ only.

By standard treatment[32–34] we find the following selection rules for NH_3:
Pure inversion transitions:

$$+ \leftrightarrow -, \Delta J = 0, \quad \Delta k = 0; \Delta v = 0.$$

Inversion–rotation transitions:

$$+ \leftrightarrow -, \Delta J = \pm 1, \Delta k = 0; \Delta v = 0.$$

Vibration–inversion–rotation transitions:

Parallel band: $+ \leftrightarrow -, \Delta J = 0, \pm 1; \Delta k = 0; \Delta v \neq 0.$
Perpendicular band: $+ \leftrightarrow -, \Delta J = 0, \pm 1; \Delta k = \pm 1; \Delta v \neq 0.$

Because μ_z is antisymmetric and (μ_x, μ_y) are symmetric with respect to inversion, E^*, (Table 2), selection rules for allowed transitions in the parallel band are $s \leftrightarrow a$ while they are $s \leftrightarrow s, a \leftrightarrow a$ in the perpendicular band (Fig. 8).

From these selection rules, only the $+ \leftrightarrow -$ rule is strictly valid. In addition to these rules, perturbation allowed transitions are possible in ammonia. For example, the ground vibrational–inversion state of NH_3 is mixed by a higher-order vibrational–rotational interaction[35] with the doubly degenerate ν_4 level (Fig. 8). As a result of these mixings, there are the following transitions allowed by these interactions (see Fig. 8)

$$\Delta J = \pm 1, \Delta k = \pm 3, s \leftrightarrow s, a \leftrightarrow a, \Delta v = 0.$$

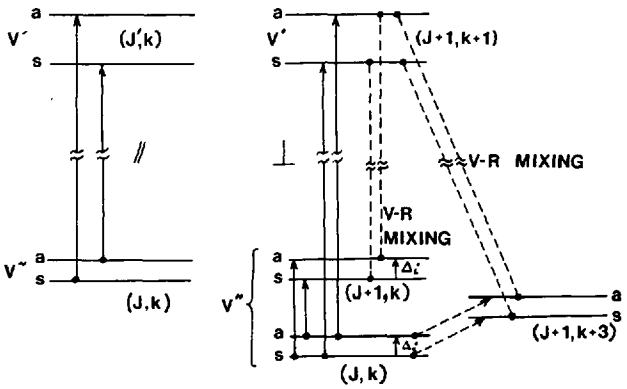

Fig. 8. Allowed transitions for the parallel (∥) and perpendicular (⊥) vibration–inversion–rotation bands in NH_3. System of levels on the right side of the figure illustrates a vibration–rotation mixing of the ground vibrational state with the ν_4 degenerate state

For ammonia $^{14}NH_3$, we have predicted (cf. Section 5.2) the frequency of the $a(2, \pm 2) \leftarrow a(1, \mp 1)$ transition to be 867.7 GHz, that of $a\,(8,8) \leftarrow a(7,5)$ to be 554.8 GHz, *i.e.* they should appear in the submillimeter wave region. Although their intensity should be very small ($\gamma \approx 10^{-7}\,cm^{-1}$), the submillimeter spectrometer built by Krupnov *et al.*[36] using the acoustic detector might have been able to detect these transitions. In a search for the weak transitions, the fact could be used that the frequency separation of the $a(J+1, k \pm 3) \leftarrow a(J, k)$ and $s(J+1, k \pm 3) \leftarrow (J, k)$ transitions can be determined with microwave accuracy from the known inversion frequencies in the ground vibrational state of ammonia (see Fig. 8).

The measurements of these "forbidden" transitions would provide important information on rotational constants for ammonia; these transitions are also of astrophysical interest[35]. Equally important and interesting would be a study of the "forbidden" vibration–inversion–rotation transitions in the infrared region [similar to that described recently by Maki *et al.* [37] for phosphine PH_3].

Discussion of selection rules must be modified for NH_2D (ND_2H) because they are asymmetric top molecules[38]. The convention for inertia moments in asymmetric tops is $I_a < I_b < I_c$. We shall use the symbol $J_{K_{-1}K_1}$ to label the rotational energy levels of NH_2D (ND_2H); K_{-1} is the quantum number in the limit of the prolate symmetric top ($I_b \rightarrow I_c$); K_1 is the quantum number of the oblate symmetric top ($I_b \rightarrow I_a$).

The inversion wave functions $\psi_i^+(\rho)$ of NH_2D (ND_2H) belong[5] to the A_1 species $\psi_i^-(\rho)$ to B_1. The species of the rotational wave functions can be found by standard methods[19]; they are given for the lowest inversion–rotation levels of NH_2D (ND_2H) in Fig. 9.

The species of the component of the electric dipole moment μ_Z along a space fixed Z axis is A_2 in the C_{2v} group, thus the overall selection rule for the allowed vibration–inversion–rotation transitions can be written as

$$\Gamma' \times \Gamma'' \in A_2 .$$

According to this rule, transitions between the energy levels of the same inversion doublets are not allowed in NH_2D and ND_2H (cf. Fig. 9), that is, there is no pure inversion spectrum in these molecules.

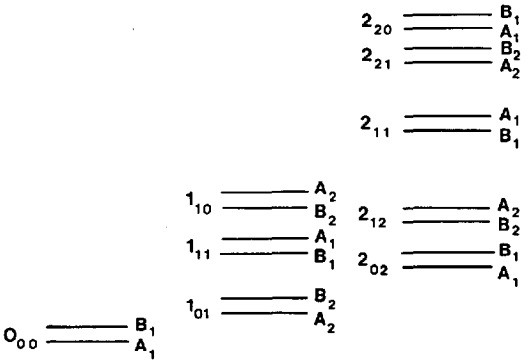

Fig. 9. Symmetry classification of the rotational levels of NH_2D (ND_2H) in the A_1 vibrational state. Species for the B_2 vibrational state can be obtained from the direct product of the species in this figure with the species B_2

The symmetry of the components μ_a, μ_b, μ_c determines the selection rules for the *a*, *b*, *c* type of transitions. Since μ_a and μ_b are invariant with respect to $\mathbf{E}^*$, selection rules for the *a*- and *b*-type transitions are $s \leftrightarrow s, a \leftrightarrow a$ (Fig. 10). The component μ_c is antisymmetric with respect to $\mathbf{E}^*$, thus we have the selection rule $s \leftrightarrow a$ for *c*-type transitions (Fig. 10).

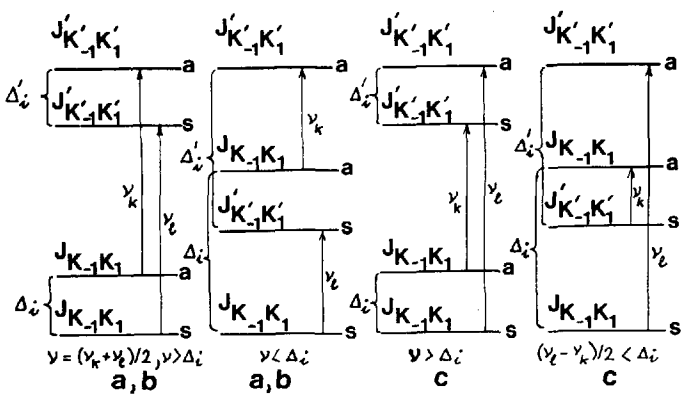

Fig. 10. Allowed *a*, *b*, and *c*-type transitions between the inversion doublets of NH_2D (ND_2H)

In the limit case of a prolate symmetric top $I_b = I_c$ and the dipole moment changes along the symmetry axis. Thus, the *a*-type transitions give rise to parallel bands with the following selection rules:

$\Delta J = 0, \pm 1; \Delta K_{-1} = 0, \Delta K_1 = \pm 1.$

The b-type transitions give rise to perpendicular bands in both limiting cases and the selection rules are

$$\Delta J = 0, \pm 1; \Delta K_{-1} = \pm 1, \Delta K_1 = \pm 1.$$

The c-type transitions give rise to perpendicular bands in the prolate symmetric top limit and to parallel bands in the oblate symmetric top limit. Selection rules are then

$$\Delta J = 0, \pm 1; \Delta K_{-1} = \pm 1, \Delta K_1 = 0.$$

The electric dipole moment vector μ subtends an angle of approximately 10° with the symmetry axis z ($\leftrightarrow c$) in NH_2D (ND_2H); in the equilibrium configuration there is a nonzero component μ_X. Most prominent in vibration–inversion–rotation spectra of NH_2D and ND_2H are therefore the c-type transitions; in NH_2D there are also a-type transitions ($x \leftrightarrow a$), in ND_2H the b-type transitions ($x \leftrightarrow b$).

5. Potential Function of Ammonia and the Calculation of the Vibration–Inversion–Rotation Energy Levels

As was already mentioned in Section 3.4, we can calculate the vibration–inversion–rotation energy levels of ammonia by solving the Schrödinger equation [Eq. (3.46)]. We are of course primarily interested in the determination of the potential function of ammonia from the experimental frequencies of transitions between these levels (Fig. 11), *i.e.* we must solve the "inverse" eigenvalue problem [Eq. (3.46)].

Our second order Hamiltonian in Eq. (3.46) describes the effects of the large-amplitude inversion motion in the potential as well as in the kinetic energy part of the operator, and the effects of the centrifugal distortion and Coriolis interactions. The Schrödinger equation [Eq. (3.46)], however, is not yet amenable to a direct numerical treatment and we have to develop an effective vibration–inversion–rotation Hamiltonian which would allow for a numerical treatment of this problem.

We shall proceed as follows. We shall first diagonalize the Schrödinger problem [Eq. (3.46)] with respect to the vibrational and rotational quantum numbers (Section 5.1). We arrive in this way at a Schrödinger equation in the variable ρ with an effective potential function for each vibration–rotation state. A least squares procedure that includes the numerical integration of the Schrödinger equation for this effective Hamiltonian will be used to determine the harmonic force field and the double-minimum inversion potential function for ($^{14}NH_3$, $^{15}NH_3$), ($^{14}ND_3$, $^{14}NT_3$) and NH_2D, ND_2H (Section 5.2).

Because there is a close coincidence between certain inversion levels in NH_3 and the excited vibrational levels pertaining to the doubly degenerate ν_4 vibrational modes (Fig. 11), and these levels interact by a Coriolis coupling effect, a special numerical treatment is required in this case (Section 5.4).

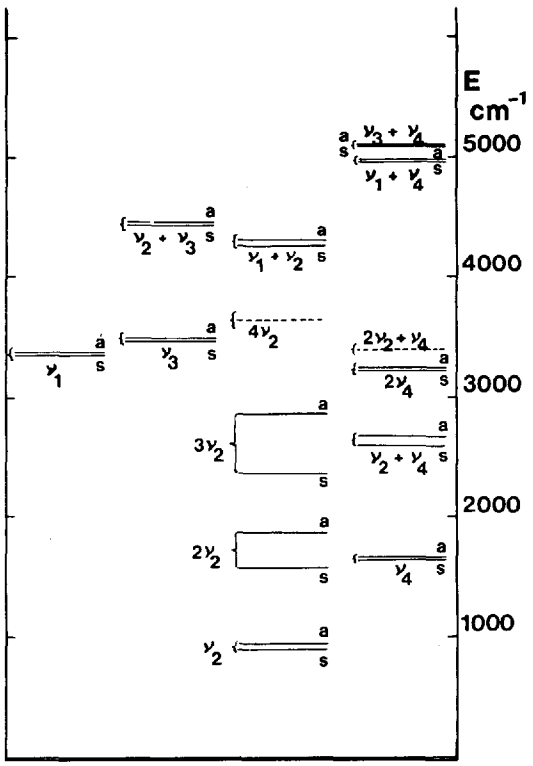

Fig. 11. The lowest vibration and inversion energy levels in NH_3. [From Ref.[6], courtesy of Academic Press]

5.1. Theory of the Centrifugal Distortion in Ammonia

Let us consider the diagonalization of the centrifugal distortion operator T_{Cent} [Eq. (3.36)] with respect to the vibrational and rotational states using second order perturbation theory. If the interaction between the inversion, vibration and rotation states is neglected, the overall wave function ψ_{vir} can be written as described by Eq. (3.47). Up to the second order of approximation we have to consider all the matrix elements of the operators containing $X_k^{\alpha\beta}$ which are off-diagonal in the vibrational states and the diagonal elements of the operators containing $Y_{kk}^{\alpha\beta}$.

Using second-order perturbation theory and evaluating the matrix elements of the vibrational and rotational operators occuring in our simplified Hamiltonian $\mathscr{H} = T + V$, we obtain the following effective vibration–inversion–rotation Hamiltonian[6] for NH_3:

$$\mathscr{H}_{\text{vir}} = \mathscr{H}_{\text{vir}}^{(N)} + \mathscr{H}'_{\text{vir}}, \tag{5.1}$$

where

$$\mathscr{H}_{\text{vir}}^{(N)} = \left\{ \frac{1}{2}(\mu_{\rho\rho}^0 + \Delta_1) J_\rho^2 + \frac{1}{2}(J_\rho \mu_{\rho\rho}^0) J_\rho \right\} + \left\{ \sum_k \lambda_k (v_k + d_k/2) + \right.$$

$$\left. + \frac{1}{2}(\mu^0)^{1/4} [J_\rho \mu_{\rho\rho}^0 (\mu^0)^{-1/2} (J_\rho (\mu^0)^{1/4})] + V_0(\rho) + U_0(\rho) + f(\rho) + \right.$$

$$+\frac{\hbar^2}{2}(\mu^0_{xx}+\Delta_2+\Delta_3)[J(J+1)-K^2]+\frac{\hbar^2}{2}(\mu^0_{zz}+\Delta_4+\Delta_5)K^2-$$

$$-D_J J^2(J+1)^2-D_{JK}J(J+1)K^2-D_K K^4\Big| \tag{5.2}$$

and

$$\mathscr{H}'_{\text{vir}}=\Phi_1 J_\rho+\Phi_2 J_\rho^3+\Phi_3 J_\rho^4. \tag{5.3}$$

The coefficients $\lambda_k (k = 1, 3, 4)$ are defined by Eq. (3.23); and D_J, D_{JK}, and D_K have the same formal dependence on the derivatives of the moments of inertia with respect to the normal coordinates ($a_k^{\alpha\beta}$) as that of a rigid C_{3v} symmetric top[32], only now the $a_k^{\alpha\beta}$ are functions of ρ. Similarly, terms $\Delta_i (i = 1, 2, \ldots, 5)$ represent a ρ-dependent modification of $\mu^0_{\rho\rho}$ and of the rotational constants; Δ_2 and Δ_4 involve the same functions of $X_k^{\alpha\beta}$ and $Y_{kk}^{\alpha\beta}$ ($\alpha, \beta = x, y, z$) as the corresponding corrections to the rotational constants A, B and C in a rigid C_{3v} molecule[32]; $f(\rho)$, Δ_1, Δ_3 and Δ_5 involve some additional terms[6] which come from the operators in Eq. (3.36) containing J_ρ (Δ_1 is a ρ-dependent function of the vibrational and rotational quantum numbers[6]). Care must be taken in this treatment of the fact that J_ρ operates not only on the inversion functions $\psi_i(\rho)$ but also on $X_k^{\alpha\beta}$. Terms coming from the latter effect appear in Φ_1, Φ_2 and Φ_3 but we have found[6] that their contribution is practically negligible and $\mathscr{H}'_{vir}$ will not be considered in further discussion.

We have used the Numerov-Cooley method of numerical integration[4] to solve the Schrödinger equation

$$\mathscr{H}^{(N)}_{\text{vir}}\psi^{(N)}_{\text{vir}}(\rho)=E^{(N)}_{\text{vir}}\psi^{(N)}_{\text{vir}}(\rho). \tag{5.4}$$

The term containing J_ρ in the first composite brackets on the right side of Eq. (5.2) can be removed[6, 22] by changing the volume element $d\rho$ to $I^0_{\rho\rho}\,d\rho$. The terms in the second composite brackets represent the effective potential function for each vibrational–rotational state.

5.2. Force Field in $^{14}NH_3$, $^{15}NH_3$, $^{14}ND_3$, $^{14}NT_3$, $^{14}NH_2D$, and $^{14}ND_2H$

In Section 4.2. we have mentioned that we can write

$$V=V_0(\rho)+\sum_n F_n(\rho)S_n+\frac{1}{2}\sum_{m,n}F_{mn}(\rho)S_mS_n+\frac{1}{6}\sum_{m,n,s}F_{mns}(\rho)S_mS_nS_s+\ldots \tag{5.5}$$

where the symmetry coordinates S_m, S_n etc., are geometrically defined curvilinear internal displacement coordinates [see Eqs. (4.2)] and the ρ-dependent force constants are the 1st, 2nd, and 3rd etc. derivatives of V with respect to the coordinates taken at equilibrium for a given value of ρ. The double-minimum potential function $V_0(\rho)$ is supposed (in agreement with physical experience) to be of the form

$$V_0(\rho) = \frac{1}{2}\bar{k}(\rho - \pi/2)^2 + a\exp[-\bar{b}(\rho - \pi/2)^2][1 + h^2(\rho - \pi/2)^2]^{-1} + c(\rho - \pi/2)^4 \quad (5.6)$$

where $\bar{k}, a, \bar{b}, h$ and c are adjustable parameters.

We can see from Eqs. (3.5) [see also Appendix in Ref.[21]] that the force constants F_n, F_{mn} etc., are generally mass dependent quantities. To arrive at the isotopically invariant potential function we must therefore express these quantities in terms involving mass independent valence force constants and to fit these to experimental spectra [cf.[21]]. For ammonia, this would represent a really formidable numerical problem. Taking into account the proposed limits of our model, the fact that we are mainly interested in the inversion–rotation structure of the spectra, we have overcome the above mentioned difficulties in the following way [see[6] for details]: (i) all the anharmonic force constants in Eq. (5.5) were neglected (ii) the ρ-dependent contributions to the harmonic force constants F_{mn} [see Eq. (4.7)] were neglected (iii) the least squares fit of the double-minimum potential function parameters and the ρ-independent harmonic force constants F^0_{mn} were performed for "light" isotopes ($^{14}NH_3$, $^{15}NH_3$) and "heavy" isotopes ($^{14}ND_3$, $^{14}NT_3$) separately.

Although these approximations of the real potential function (significantly reducing the amount of numerical calculations) are rather rough, we were still able, as we shall see, to explain all features of the inversion–rotation spectra of all low-lying vibrational and inversion states and to arrive at an only slightly mass dependent double-minimum potential function (Section 5.3).

We have done basically two kinds of determination of the potential function of ammonia. In the rigid bender approximation, we solved the "inverse" eigenvalue

Table 3. Potential function of ammonia

Parameter[1])	($^{14}NH_3$, $^{15}NH_3$)[2])	($^{14}ND_3$, $^{14}NT_3$)[2])	NH_2D[3])	ND_2H[3])
F^0_{11}(N.m^{-1})	704.82	695.23		
F^0_{33}(N.m^{-1})	703.52	703.59		
F^0_{34}(N.m^{-1})	− 26.71	− 19.92		
F^0_{44}(N.m^{-1})	65.85	65.39		
$\bar{k}\cdot10^{18}$(J)	1.8272[4])	1.8475[4])	1.775	1.87
$a\cdot10^{18}$(J)	0.4542	0.4614	0.4444	0.4799
$\bar{b}$	− 3.1887	− 3.1708	−3.2835	−3.1228
$h^2\cdot10^3$	− 3.45[4])	− 1.37[4])	0[4])	0[4])
$c\cdot10^{20}$(J)	− 1.55[4])	0.000[4])	0[4])	0[4])

[1]) Conversion factors: N.m^{-1} = 10^{-2} mdyn. Å^{-1}, J = 10^7 erg.

[2]) Calculated in the non-rigid bender approximation with the constrained value r_0 = 1.0116 Å for the N-H internuclear distance[6]).

[3]) Calculated in the rigid bender approximation with the constrained value r_0 = 1.0156 Å for the N-H and N-D internuclear distances[5]).

[4]) Constrained value.

Table 4. Experimental and calculated energy levels of ammonia (in cm^{-1})

	$^{14}NH_3$		$^{15}NH_3$		$^{14}ND_3$		$^{14}NT_3$	
$\|v_1v_2v_3v_4)$	Exp.	Calc.	Exp.	Calc.	Exp.	Calc.	Exp.	Calc.
00^+00	*0.0000*	*0.0000*	*0.0000*	*0.0000*	*0.0000*	*0.0000*	*0.0000*	*0.0000*
00^-00	0.7934[1]	0.7942	0.7577[4]	0.7576	0.0531[6]	0.0539	0.0102[8]	0.0102
01^+00	932.44 [2]	933.05	927.727 [5]	929.41	745.7[2]	745.1	656.37[9]	652.33
01^-00	968.04 [2]	967.97	962.915 [5]	963.09	749.4[7]	748.6	657.19[9]	653.10
02^+00	1602.0 [3]	1602.19		1596.42	1359 [7]	1362		1230.5
02^-00	1882.16 [3]	1882.53		1871.81	1429 [7]	1431		1251.6
03^+00	2383.46 [2]	2384.69		2370.63	1830 [7]	1831.5		1657.7
03^-00	2895.48 [2]	2893.17		2874.68	2106.6[7]	2108.8		1816.7
04^+00	3442 [3]	3456.84		3434.16	2482 [3]	2482		2125.2
04^-00		4054.27		4027.26	2876 [3]	2872		2424.6
1^+000	3495.47	3495.93	3493.86	3492.61		2490.70		2063.27
					2490.9		2050.4	
1^-000	3496.43	3496.87	3494.77	3493.50		2490.77		2063.28
001^+0	3589.31	3589.14	3579.65	3579.89		2641.62		2240.08
					2641.4		2240.4	
001^-0	3590.06	3589.88	3580.40	3580.60		2641.67		2240.09
0001^+	1681.36	1681.45	1676.05	1677.94		1220.55		1017.89
					1220.6		1017.9	
0001^-	1681.78	1681.86	1676.47	1678.33		1220.57		1017.90

[1]) Ref.[32].
[2]) Ref.[39].
[3]) Ref.[44].
[4]) Ref.[45].
[5]) Ref.[46].
[6]) Ref.[47].
[7]) Ref.[40].
[8]) Ref.[48].
[9]) Ref.[41].

problem described by Eq. (3.44a), *i.e.* we determined the double-minimum potential function parameters from the experimental inversion energy levels $0^{\pm 1}$, $1^{\pm}$, $2^{\pm}$, ... With these parameters, we have calculated the inversion–rotation energy levels by the numerical integration of Eq. (3.45).

In the non-rigid bender approximation, we solved the "inverse" eigenvalue problem described by Eq. (5.4), *i.e.* we determined the potential function parameters given in Table 3 for NX_3 (X = H, D, T). We have used the experimental infrared frequencies of transitions from the ground state to the ν_2, $2\nu_2$, $3\nu_2$, and $4\nu_2$ inversion states and the "zero-order" frequencies of vibrations (Table 4). The "zero-order" frequencies have been obtained from the observed fundamental frequencies of $^{14}NH_3$ [Ref.[39]], $^{14}ND_3$ [Ref.[40]], $^{14}NT_3$ [Refs.[41, 42]] and $^{15}NH_3$ [Ref.[43]] corrected for anharmonicity in a semiempirical way[6].

We could of course attempt to adjust a potential function of ammonia using Eq. (5.4) in a least squares fit to the data extended to a set of energy levels with $J \neq 0$, $k \neq 0$. However, it seems better to adjust a minimum number of potential function parameters using the vibration and inversion data alone and to check the validity of our model by comparing the calculated vibration–inversion–rotation transition frequencies with the observed data[6].

Agreement between the calculated and experimental data can be seen in Table 4 and is illustrated by Figs. 12–15. As could be expected, the non-rigid bender approximation gives better results than the rigid bender approximation. For example, the near coincidence is very well reproduced of the R-branch transition frequencies for a given J, which is a typical feature of the $1^- \leftarrow 0^+$ transition in the ν_2 infrared band of NH_3 (Fig. 14). The absence of this effect in the $1^+ \leftarrow 0^-$ transition (Fig. 15) shows the importance of a theoretical model which considers separately the symmetric and antisymmetric components of inversion levels.

For NH_2D and ND_2H, only the rigid bender approximation has been used so far in the determination of the double-minimum potential function parameters[5]

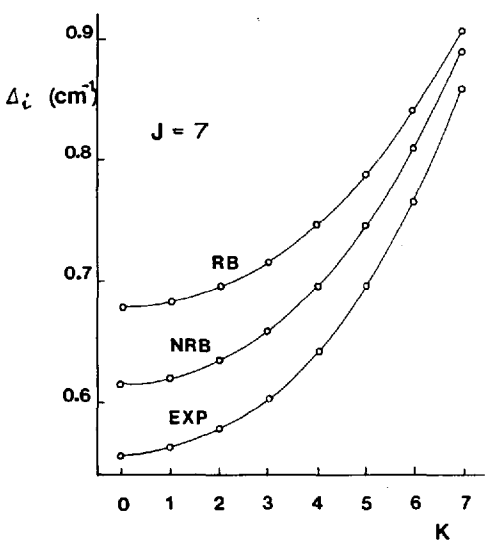

Fig. 12. The dependence of the ground-state inversion splitting Δ_i on the rotational quantum number K for $J = 7$ in $^{14}NH_3$. RB, rigid bender approximation; NRB: non-rigid bender approximation; EXP: experimental data[32]. [From Ref.[6], courtesy of Academic Press]

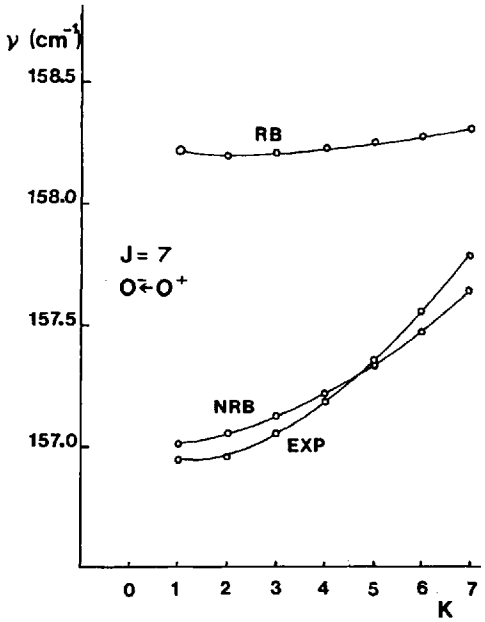

Fig. 13. Dependence of the inversion–rotation frequencies in $^{14}NH_3$ on the rotational quantum number K ($0^- \leftarrow 0^+$ transitions) at $J = 7$. RB: rigid bender approximation; NRB: non-rigid bender approximation; EXP: experimental data[56]. [From Ref.[6], courtesy of Academic Press]

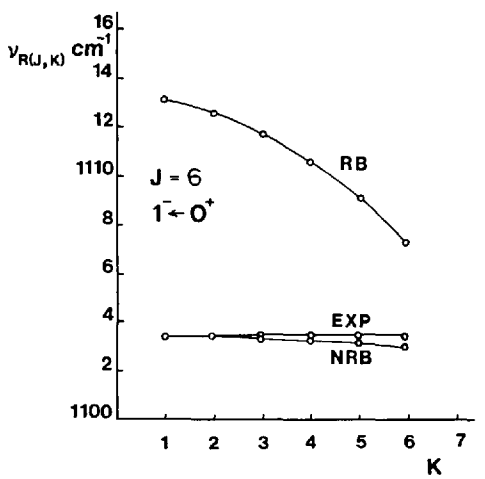

Fig. 14. Frequencies of the $R\ (J, K)$ lines in the $1^- \leftarrow 0^+$ transitions of $^{14}NH_3$ at $J = 6$. RB: rigid bender approximation; NRB: non-rigid bender approximation; EXP: experimental data[39, 57]. [From Ref.[6], courtesy of Academic Press]

(Table 3). A better adjustment of the parameters would be possible only after high-resolution measurements on the $n\nu_2$ inversion states as well as on the excited vibrational states in NH_2D and ND_2H molecules become available.

In calculating the inversion–rotation energy of NH_2D (ND_2H), we must first integrate the Schrödinger equation

$$[T_i^0 + V_0(\rho) + (\hbar^2/2)\,\mu_{zz}^0 k^2]\,\psi_{i,k}(\rho) = E_{i,k}^0 \psi_{i,k}^0(\rho) \tag{5.7}$$

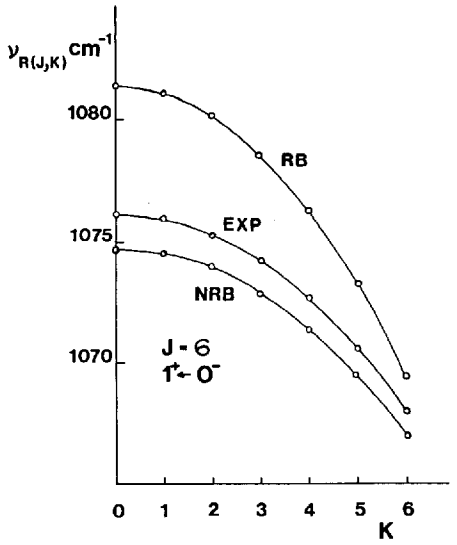

Fig. 15. Frequencies of the R (J, K) lines in the $1^+ \leftarrow 0^-$ transitions of $^{14}NH_3$ at $J = 6$. RB: rigid bender approximation; NRB: non-rigid bender approximation; EXP: experimental data[38, 57].
[From Ref.[6], courtesy of Academic Press]

by using the Numerov-Cooley technique, with the $V_0(\rho)$ potential function determined by a fit to the $n\nu_2$ inversion energy levels[5] for $J = k = 0$. The product wave functions $\psi^0_{ik} \cdot S_{Jkm}(\theta, \Phi)$ are then used as functions generating the basis in which the matrix elements of the remaining rotational operators are formed. The inversion–rotation energy levels of the asymmetric tops NH_2D (ND_2H) are then obtained by the diagonalization of the suitably truncated energy matrix[5, 22, 23].

5.3. Discussion of the Potential Function of Ammonia

There is one important point concerning the height of the inversion barrier in ammonia which has not been discussed explicitly in our paper[6]. We have an effective mass-dependent potential energy function in the Schrödinger equation [Eq. (5.2)] for each vibrational and rotational state. For $J = k = 0$, this potential contribution $\Sigma \lambda_k (v_k + d_k/2)$, and a pseudopotential term in Eq. (5.2). The main mass dependent contribution to this effective potential function is given by the vibrational term (see Table 5). We can also see from the Table 5 that $V_0(\rho)$ is only slightly mass dependent. It must be emphasized that the barrier height which is calculated from $V_0(\rho)$ in the non-rigid bender approach should be considered as the "true" barrier to inversion in ammonia. The value of this barrier (Table 5) is considerably lower than that obtained in the rigid bender approximation.

We have so far not discussed explicitly the path over which the atomic nuclei move during the inversion of a real molecule. Our reference configuration was defined in Section 3.2 with the assumption that the bond lengths do not change during the inversion motion. If we were to choose a different path, the fit to experimental data would lead in general to a different double-minimum potential function $V_0(\rho)$. Obviously physical intuition which is involved in considerations of the inversion path should be supported in further developments by quantum chemical calculations.

Table 5. "True" and effective inversion barriers in different isotopic species of ammonia (in cm^{-1})

Parameter	$^{14}NH_3$	$^{15}NH_3$	$^{14}ND_3$	$^{14}NT_3$	$^{14}NH_2D$	$^{14}ND_2H$
$\Delta\overline{V_i}$ (see[1])	2023.0	– [2]	1978.6	– [2]	2003.7	1976.0
ΔV_i (see[3])	1806.2	1806.2	1814.5	1814.5	– [2]	– [2]
$E_v(\rho = 0) - E_v(\rho_e)$ (see[4])	219.0	217.2	171.9	151.2	– [2]	– [2]
Pseudopotential	1.9	2.0	0.4	−0.1	– [2]	– [2]
ΔV_i^{eff} (see[5])	2027.1	2025.4	1986.8	1965.6	– [2]	– [2]
ρ_e	111.89°	111.89°	111.81°	111.81°	– [2]	– [2]
ρ_0	112.43°	112.42°	112.23°	112.18°	112.30°	112.27°

[1]) Rigid bender approximation.
[2]) Has not been calculated.
[3]) Non-rigid bender approximation (cf. Table 3).
[4]) Contribution to the effective inversion barrier from the vibrational terms.
[5]) Effective inversion barrier.

5.4. Coriolis Interactions Between $\nu_2, \nu_4, 2\nu_2, \nu_2 + \nu_4, 3\nu_2$ Level of NH_3

Coriolis interactions between the $\nu_2, \nu_4, 2\nu_2, \nu_2 + \nu_4, 3\nu_2$, etc. sequence of energy levels in NH_3 (Figs. 11 and 16) represent an interesting example of vibration–rotation interactions in a non-rigid molecule. Certain effects of this interaction have been observed in the microwave[49, 50] and high resolution infrared spectra[39, 51–53] and

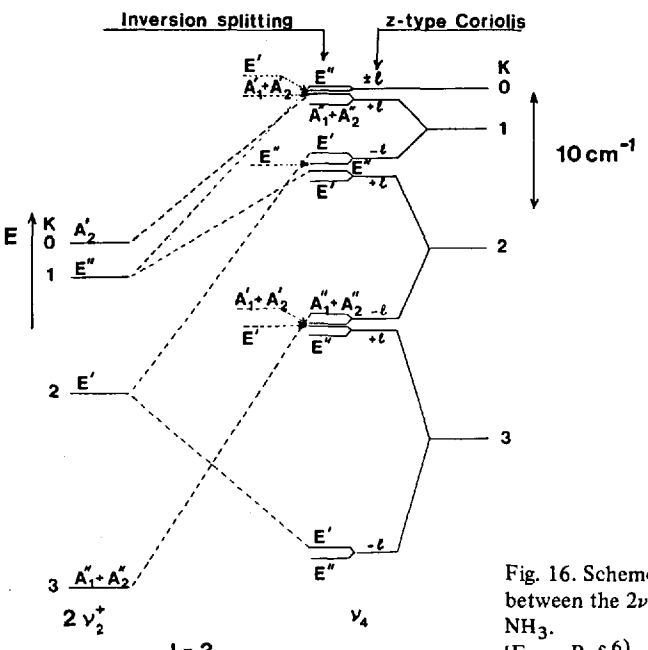

Fig. 16. Scheme of the Coriolis interaction between the $2\nu_2^+$ and ν_4^- energy levels in NH_3.
[From Ref.[6], courtesy of Academic Press]

analyzed using the standard theory for a C_{3v} rigid molecule[39, 49, 50]. An effect of this interaction which has not been mentioned in previous papers[39, 49–53] is the anomalous rotational dependence of the inversion splittings in the ($\pm l$) components of the doubly degenerate ν_4 vibrational level[6] (Fig. 17).

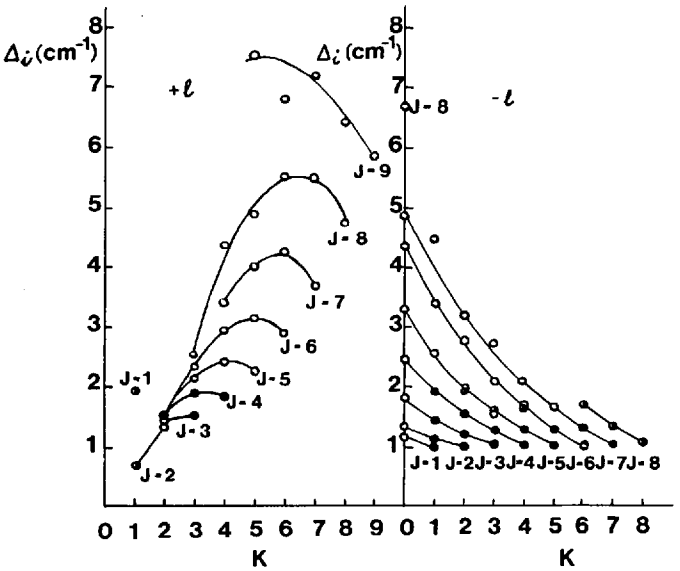

Fig. 17. The dependence of the observed inversion splittings on the rotational quantum number K in the $\pm l$ components of the doubly degenerate ν_4 vibration state in $^{14}NH_3$.
[From Ref.[6], courtesy of Academic Press]

In our theoretical description of the vibration–inversion–rotation states of ammonia, the operator which is responsible for these interactions in ammonia appears formally in the centrifugal distortion operator defined in Eq. (3.36). It can be written as

$$\mathscr{H}_{2,4} = -(\mathrm{i}/2)\,[X^{\gamma\rho}_{4a} J_\rho + \tfrac{1}{2}(J_\rho X^{\gamma\rho}_{4a})]\,(Q_4^- J_+ - Q_4^+ J_-) \tag{5.8}$$

where $Q_4^\pm = Q_{4a} \pm \mathrm{i}Q_{4b}$, $J_\pm = J_x \pm \mathrm{i}J_y$. Because of the coincidence between the $2\nu_2$ and ν_4 levels (Figs. 11 and 16), this operator causes a strong coupling between the inversion motion and the doubly degenerate Q_4 vibrational mode.

Because the approximation described by Eq. (3.47) fails if the inversion and vibrational wave functions are strongly mixed, the Coriolis operator defined by Eq. (5.8) cannot be treated by the numerical methods described in Sections 5.1 and 5.2. Instead of the perturbation treatment described in Section 5.1, we must use a variational approach in which the energy levels are calculated as eigenvalues of an energy matrix; the off-diagonal elements of this matrix are the matrix elements of the Coriolis operator[6] $\mathscr{H}_{2,4}$.

The energy matrix of this interaction is an infinite matrix but we have found that for the calculation of the $2\nu_2$ and ν_4 energy levels it is sufficient to work with a 7x7 matrix for each value of the rotational quantum number J. In the notation $|v_2^{\pm}, v_4^l 4; J, k\rangle$, the off-diagonal matrix elements of $\mathscr{H}_{2,4}$ connect the following states (see Fig. 16):

$$|3^{\pm}, 0^0; J, k\rangle, |1^{\mp}, 1^{+1}; J, k+1\rangle, |1^{\mp}, 1^{-1}; J, k-1\rangle, |0^{\mp}, 1^{+1}; J, k+1\rangle,$$
$$|2^{\pm}, 0^0; J, k\rangle, |0^{\mp}, 1^{-1}; J, k-1\rangle, |1^{\pm}, 0^0; J, k\rangle.$$

Thus, for each value of J we have two 7x7 matrices, one connecting symmetric $n\nu_2$ states with the antisymmetric states $(n\nu_2 + \nu_4)$ and *vice versa* (Fig. 16). For special values of the rotational quantum numbers J, k, instead of a 7x7 matrix we have smaller blocks[6]. This factorization is the analog of the factorization of the matrices describing Coriolis interactions in a C_{3v} rigid molecule[54, 55] and can be used for a qualitative interpretation of the anomaly in Fig. 17. For example, the $J' = K'$ levels in the $-l$ component of the ν_4 level have basically the ground-state character of the rotational dependence of the inversion-splitting (Fig. 17) because they are obtained from the 1x1 block and therefore are unperturbed.

Inversion splittings in the ($\pm l$) components of the ν_4 level calculated by the diagonalization of the energy matrices[6] are shown in Fig. 18. The calculated in-

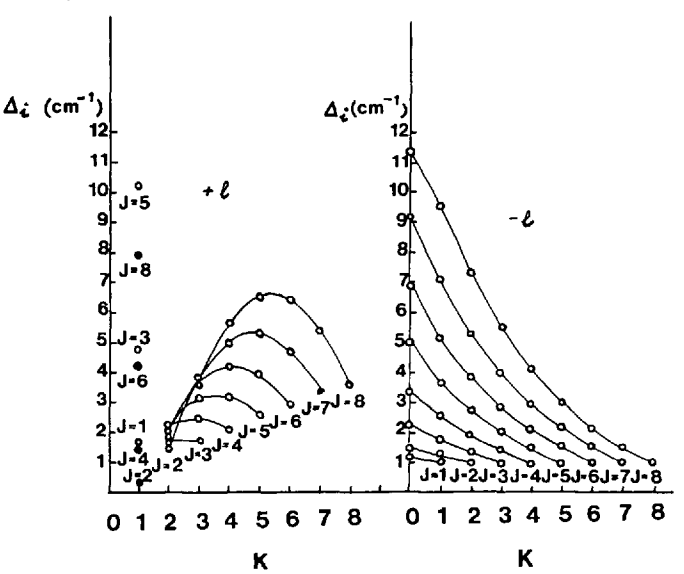

Fig. 18. Calculated dependence of the inversion frequencies on the rotational qunatum number K in the $\pm l$ componentes of the ν_4 vibrational state in $^{14}NH_3$. For $K \neq 1$, the inversion frequencies are equal to the inversion splittings. Full dots: $K = 1$ in the $+l$ level indicate the calculated "reversal" of the inversion doublets by the "giant" l-type doubling effect[6].
[From Ref.[6], courtesy of Academic Press]

version splittings are larger than the experimental values, especially in the $-l$ component, but the peculiarity of this effect is well described. We found that the calculated values of the splitting are not sensitive to the physically acceptable variation of our potential function[6]. It seems that effects higher than those considered in this paper should be introduced to improve the agreement.

6. Molecular Inversion in Other Molecules

We shall discuss in this section large-amplitude motions which are either inversion as in ammonia, or are related to this type of motion. We shall concentrate on the so-called pyramidal inversion which occurs in molecules with tricoordinate atom whose stable position is not in the plane defined by the three atoms directly bounded to it.

We shall divide these molecules into two categories: (i) molecules with one large amplitude motion (inversion) which will be dealt with in Section 6.1 (ii) molecules with inversion and internal rotation (Section 6.2). Only such molecules will be considered, where the inversion barrier is low enough that inversion splittings can be resolved by microwave or infrared spectroscopy. As for the pyramidal inversion with higher barriers, description of the methods for determination of the barrier heights and the chemical consequences of the existence of the so-called invertomers, the reader is referred to review papers[58, 59].

Molecules where inversion could occur by a regrouping of the atomic nuclei by a mechanism different from that for pyramidal inversion and could be detected by spectroscopical methods now available, will not be dealt with in this paper. At the present time, experimental detection of the inversion splittings in these molecules is a challenge to experimentalists and we have to wait some time before convincing results are presented. For example, Ozier *et al.* [60] reported the resolution of the splitting between the two inversion levels of methane CH_4 by a molecular-beam magnetic resonance radiofrequency method. Hougen[61], however, in a group-theoretical discussion of this problem has shown that no information on the inversion splitting was obtained from experiments of this type. A theoretical discussion of some other molecules which are candidates for experimental studies of the inversion splittings can be found *e.g.* in Ref.[62].

We shall also not deal in our paper with the large amplitude ring puckering and pseudorotation in small ring molecules. Molecular dynamics of these motions and the determination of the barriers of pseudorotation from microwave and infrared spectra have been the subject of a great number of papers; this problem has been recently reviewed in the monography[63].

6.1. Molecules With Pyramidal Inversion

Phosphine, PH_3, is the simpliest molecule next to ammonia, NH_3, with pyramidal inversion. An inversion doubling has long been suspected in PH_3. Costain and

Sutherland[64] predicted an observable (140 kHz) tunneling inversion in the ground vibrational state of PH_3, on the basis of their calculated inversion barrier of 6000 cm^{-1}. However, subsequent quantum chemical calculations have predicted [see [58]] a much higher barrier (between 10 000 and 14 000 cm^{-1}). A molecular-beam electric resonance spectrometer has been used[65] to measure the ground state inversion splitting in PH_3. It was found that the inversion splitting must be lower than the resolution of the spectrometer (1 kHz). Similarly, in a high-resolution infrared study of the $4\nu_2$ band of PH_3, Maki *et al.* [37] found that the splitting of this level must be less than 0.02 cm^{-1}.

We are now working on a prediction of the inversion splittings of the highly excited $n\nu_2$ energy levels in PH_3, using an inversion barrier calculated quantum mechanically and the theoretical model for molecular inversion described in Sections 2–5. A high-resolution laser spectroscopy investigation of these levels may lead to a resolution of their splittings.

The amino group in simple amides normally takes a nonplanar configuration at equilibrium, and thus executes an inversion-type motion with a double-minimum potential function. The barrier height is in most cases low enough to allow a resolution of the splittings of inversion energy levels by microwave or high-resolution infrared spectroscopy (Table 6). Formamide, H_2NCOH and thioformamide, H_2NCSH might

Table 6. Inversion barriers (in cm^{-1})

Molecule	Inversion barrier	Refs.
$^{14}NH_3$, $^{15}NH_3$	1806	6)
$^{14}ND_3$, $^{14}NT_3$	1814	6)
PH_3	10 000–14 000	58)
H_2CO [see[1])]	360	24)
NH_2Cl	< 4000	66)
H_2NCN	710	67)
H_2NCOH	≈ 0	68)
H_2NCSH	≈ 0	69)
CH_3NH_2	1688	70)
CH_3NHCl	2520	71)
$(CH_3)_2NH$	1540	72)
$C_2H_5NCH_3$	1820	73)
$H_2N \cdot NH_2$	2620	74)
$H_2N \cdot NO_2$	< 2000	75)

[1]) Formaldehyde in the $\tilde{A}^1A_2$ excited electronic state[24].

be exceptional cases of nearly zero potential barrier to the amino inversion[68, 69].

Theoretical treatment of molecular inversion described in Sections 2–5 could be immediately applied to monochloramine, NH_2Cl, or easily extended to cyanamide, H_2NCN. However, further experimental work is required for these molecules, especially in the infrared region, before such a treatment could be really successful (cf. Section 5.2 for a similar situation in NH_2D and ND_2H).

6.2. Molecules With Inversion and Internal Rotation

In the methylamine molecule, CH_3NH_2, there are two large-amplitude internal motions: (i) internal rotation of the CH_3 group about its own symmetry axis with respect to the NH_2 group (ii) wagging vibration of the NH_2 group which is called inversion in analogy to the inversion in ammonia (Fig. 19). As a result of this, the methylamine molecule has a two-dimensional six-minimum potential. The six conformations of methylamine CH_3NH_2 corresponding to the six potential minima are symmetrically equivalent. Each energy level of methylamine therefore splits into

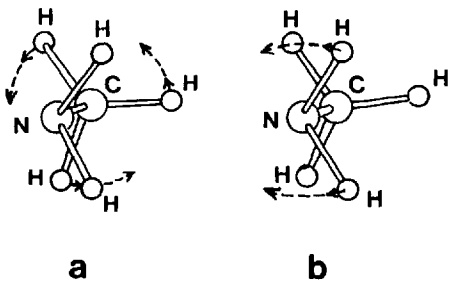

Fig. 19a, b. Internal rotation (a) and the wagging-inversion (b) motion in methylamine, CH_3NH_2

a doublet due to internal rotation; the components of this doublet are designated by A (non-degenerate) and E (doubly degenerate). This component further splits into a doublet due to inversion.

The infrared and especially microwave spectra of methylamine and its deuterated species have been studied in considerable detail [see paper[76] for further references]. The potential barriers to internal rotation and inversion are both relatively high [Table 6; internal rotation barrier is 684 cm^{-1} in the ground state[77] of CH_3NH_2] but the splittings of the energy levels are measurable.

It would be possible to develop a vibration–inversion–internal rotation–overall rotation Hamiltonian for methylamine by starting from a vibration–rotation Hamiltonian in which the dependence of the $\mu_{\alpha\beta}$ elements and V on both the internal rotation and inversion is put in explicitly (cf. Sections 2–5). The diagonalization of this Hamiltonian would require the numerical integration of a two-dimensional Schrödinger equation which is certainly a very difficult problem. We have done some preliminary investigations of the possibility of the extension of the Numerov-Cooley technique of numerical integrations of differential equations to two-dimensional Schrödinger equation[78]. Although it is possible to find an efficient algorithm[78] for the solution of this problem, numerical instability of the procedure seems to remain the basic difficulty. Nevertheless, we believe that with the availability of fast computers with high arithmetic precision, the solution of this important problem will be possible in the near future.

Another interesting example of a molecule with amino inversion and internal rotation is hydrazine, $H_2N \cdot NH_2$ (Fig. 20). In hydrazine, there are three large amplitude motions: (i) two wagging vibrations of the NH_2 groups which may be

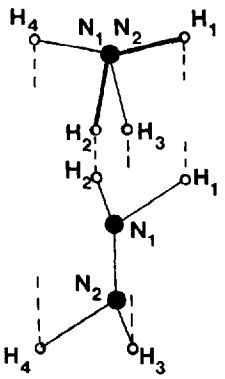

Fig. 20. The structure of the hydrazine molecule

called symmetric and antisymmetric wagging-inversions (ii) internal rotation of one of the NH_2 group with respect to the other NH_2 group.

The equilibrium angle of internal rotation of one of the amino groups in the hydrazine molecule with respect to the other is almost exactly 90° (Fig. 20). This means that inversion of an amino group leads almost exactly to a symmetrically equivalent equilibrium configuration. In methylamine, on the contrary, an internal rotation is required, after the inversion of the amino group takes place, to reach an equilibrium configuration [see paper[74)] for a nice physical discussion of this problem and for further references].

Therefore, the coupling between the inversion and internal rotation may be neglected in a good approximation in the hydrazine molecule, while this is not the case in the methylamine molecule. In this approximation, the potential function of the two wagging-inversion motions in hydrazine is a two-dimensional four-minimum potential. Due to tunneling between the four equivalent equilibrium conformations, of the four inversion sublevels in each vibrational state, one is symmetric (A), another antisymmetric (B), and the other two degenerate (E) with respect to the C_4 symmetry axis.

We have already reported[79)] our attempt to extend the theoretical treatment described in Sections 2–5 to the hydrazine molecule. As for the application of the treatment to experimental data, the situation is analogous to that described above for methylamine.

7. Conclusions

In this section, we shall compare briefly the approach to molecular spectra using the Hamiltonian described in this paper with the standard approach[19, 20)]. Such a comparison is useful because it shows future trends and problems in the theoretical interpretation of vibration–rotation spectra of molecules.

In the standard treatment, we can develop an effective Hamiltonian which can be used in the precise parametrization of the energy levels [see, *e.g.*, Refs.[80, 81)]].

However, molecular parameters obtained in this way are often only effective quantities without physical significance. Furthermore, if the molecule executes large-amplitude vibrations, the number of these parameters becomes unmanageably large.

On the other hand, the Hamiltonian described in this paper does not lend itself to a parametrization of the experimental data with a precision approaching the requirements of the high-resolution spectroscopy. However, if one wants to use these data as fully as possible to obtain physically reliable information on the potential function, then an approach such as described in this paper is required. Determination of the value of the inversion barrier in ammonia which is approximately by 200 cm^{-1} lower than the value determined previously (Section 5.3) shows on the importance of such approach.

Acknowledgements. Much of the work described in this paper was carried out in collaboration with Dr. J. M. R. Stone during his stay in Prague at the Royal Society – Czechoslovak Academy of Sciences Exchange Fellow [Refs. [3, 6]] and in collaboration with V. Danielis [Ref.[5]]. We are also grateful to Professor P. M. Hierl from the Department of Chemistry, University of Kansas, U.S.A., for the critical perusal of the manuscript.

Note Added in Proof:

During the preparation of this manuscript for print, two interesting papers appeared which have a close relation to certain problems discussed in this review. M.S. Child [Mol. Phys. *31*, 1031 (1976)] has shown that it is possible to construct a classical integral representation for the wavefunction such that the barrier penetration can be described in terms of an analytical continuation of classical mechanics into the complex time plane [W.H. Miller, Adv. Chem. Phys. *25*, 69 (1974)] (cf. Section 2 of the present review).

D. Laughton, S. M. Freund, and T. Oka (private communication) detected for the first time two $\Delta k = \pm 3$ "forbidden" vibration-rotation transitions in the ν_2 band of $^{14}NH_3$ using infrared microwave two-photon spectroscopy and laser Stark spectroscopy (cf. Section 4.3). This has made it possible to obtain the C_0 rotational constant of 6.2280 ± 0.0008 cm^{-1}.

8. References

1) Longuet-Higgins, H. C.: Mol. Phys. *6*, 445 (1963).
2) Watson, J. K. G.: Canad. J.Phys. *43*, 1996 (1965).
3) Papoušek, D., Stone, J. M. R., Špirko, V.: J. Mol. Spectrosc. *48*, 17 (1973).
4) Špirko, V., Stone, J. M. R., Papoušek, D.: J. Mol. Spectrosc. *48*, 38 (1973).
5) Danielis, V., Papoušek, D., Špirko, V., Horák, M.: J. Mol. Spectrosc. *54*, 339 (1975).
6) Špirko, V., Stone, J. M. R., Papoušek, D.: J. Mol. Spectrosc. *60*, 159 (1976).
7) Cleeton, C. E., Williams, N. H.: Phys. Rev. *45*, 234 (1934).
8) Good, W. E.: Phys. Rev. *70*, 213 (1946).
9) Bleaney, B., Penrose, R. P.: Nature *157*, 339 (1946).
10) Basov, N. G., Prochorov, A. M.: Zhurnal Eksp. Teoret. Fiz. *27*, 431 (1954).
11) Gordon, J. P., Zeiger, H. Z., Townes, C. H.: Phys. Rev. *99*, 1264 (1955).
12) Vuylsteke, A. A.: Am. J. Phys. *27*, 554 (1959).
13) Cheung, A. C., Rank, D. M., Townes, C. H., Thornton, D. D., Welch, W. J.: Phys. Rev. Letters *21*, 1701 (1968).
14) Dennison, D. M., Hardy, J. D.: Phys. Rev. *39*, 938 (1932).
15) Dennison, D. M., Uhlenbeck, G. E.: Phys. Rev. *41*, 313 (1932).
16) Fermi, E.: Nuovo Cimento *9*, 277 (1932).
17) Wollrab, J. E.: Rotational spectra and molecular structure. New York: Academic Press 1967.
18) Weeks, W. T., Hecht, K. T., Dennison, D. M.: J. Mol. Spectrosc. *8*, 30 (1962).
19) Allen, Jr., H. C., Cross, P. C.: Molecular vib-rotors. New York: J. Wiley and Sons 1963.
20) Wilson, Jr., E. B., Decius, J. C., Cross, P. C.: Molecular vibrations. New York: McGraw Hill 1955.
21) Hoy, A. R., Bunker, P. R.: J. Mol. Spectrosc. *52*, 439 (1974).
22) Hougen, J. T., Bunker, P. R., Johns, J. W. C.: J. Mol. Spectrosc. *34*, 136 (1970).
23) Bunker, P. R., Stone, J. M. R.: J. Mol. Spectrosc. *41*, 310 (1972).
24) Moule, D. C., Rao, Ch. V. S. R.: J. Mol. Spectrosc. *45*, 120 (1973).
25) Sarka, K., Papoušek, D., Boháček, I.: First International Seminar on High Resolution Infrared Spectroscopy, Prague, 1970.
26) Sarka, K.: J. Mol. Spectrosc. *38*, 545 (1971).
27) Boháček, I., Danielis, V., Papoušek, D., Špirko. V.: J. Mol. Structure, in preparation.
28) Stone, J. M. R.: J. Mol. Spectrosc. *54*, 1 (1975).
29) Nielsen, H. H.: Rev. Mod. Phys. *23*, 90 (1951).
30) Mills, I. A.: Vibration–rotation structure in asymmetric- and symmetric-top molecules. In: Molecular spectroscopy: modern research, Rao, K. Narahari, Mathews, C. W. (eds.). New York: Academic Press 1972.
31) Watson, J. K. G.: Mol. Phys. *15*, 479 (1968).
32) Gordy, W., Cook, R. L.: Microwave molecular spectra. New York: Interscience Publishers 1970.
33) Herzberg, G.: Molecular spectra and molecular structure. II. Infrared and Raman spectra of polyatomic molecules. Princeton: Van Nostrand 1959.
34) Bunker, P. R.: Practically everything you ought to know about the molecular symmetry group. New York: M. Dekker 1976.
35) Oka, T., Shimizu, F. O., Shimizu, T., Watson, J. K. G.: Astrophys. J. *165*, L15 (1971).
36) Belov, S. P., Burenin, A. V., Gershtein, L. I., Korolochin, V. V., Krupnov, A. F.: Optika i Spektroskopia *35*, 295 (1973).
37) Maki, A. G., Sams, R. L., Olson, W. B.: J. Chem. Phys. *58*, 4502 (1973).
38) De Lucia, F. C., Helminger, P.: J. Mol. Spectrosc. *54*, 200 (1975).
39) Garing, J. S., Nielsen, H. H., Rao, K. N.: J. Mol. Spectrosc. *3*, 496 (1959).
40) Benedict, W. S., Plyrer, E. K.: Canad. J. Phys. *35*, 1235 (1957).
41) Rao, K. N., Brim, W. W., Hoffman, J. M., Jones, L. H., McDowell, R. S.: J. Mol. Spectrosc. *7*, 362 (1961).
42) Jones, L. H., Brim, W. W., Rao, K. N.: J. Mol. Spectrosc. *11*, 389 (1963).

43) Duncan, J. L.: unpublished data.
44) Coon, J. B., Naugle, N. W., McKenzie, R. D.: J. Mol. Spectrosc. *20*, 107 (1966).
45) Schnabell, E., Torring, T., Wilke, W.: Z. Phys. *188*, 167 (1965).
46) Shimizu, F. O., Shimizu, T.: J. Mol. Spectrosc. *36*, 94 (1970).
47) Herrman, G.: J. Chem. Phys. *29*, 875 (1958).
48) Helminger, P., De Lucia, F. C., Gordy, W., Morgan, H. W., Staats, P. A.: Phys. Rev. *A 9*, 12 (1974).
49) Cohen, E. A., Poynter, R. L.: J. Mol. Spectrosc. *53*, 131 (1974).
50) Kwan, Y. Y., Cohen, E. A.: J. Mol. Spectrosc. *58*, 54 (1975).
51) Walker, R. E., Hochheimer, B. F.: J. Mol. Spectrosc. *34*, 500 (1970).
52) Weber, W. H., Maker, P. D., Yeung, K. F., Peters, C. W.: Appl. Opt. *13*, 1431 (1974).
53) Johns, J. W. C., McKellar, A. R. W., Trombetti, A.: J. Mol. Spectrosc. *55*, 131 (1975).
54) Di Lauro, C., Mills, I. M.: J. Mol. Spectrosc. *21*, 386 (1966).
55) Sarka, K., Papoušek, D., Rao, K. N.: J. Mol. Spectrosc. *37*, 1 (1971).
56) Dowling, J. M.: J. Mol. Spectrosc. *27*, 527 (1968).
57) Curtis, J. B., Stout, D., Yin, P. K. L., Rao, K. N.: to be published.
58) Rank, A., Allen, L. C., Mislow, K.: Angew. Chem. Int. Edit. *9*, 400 (1970).
59) Mislov, K.: Trans. New York Acad. Sci. Series II, *35*, 227 (1973).
60) Ozier, I., Yi, P., Khosla, A., Ramsey, N. F.: Phys. Rev. Letters *24*, 642 (1970).
61) Hougen, J. T.: J. Chem. Phys. *55*, 1122 (1971).
62) Ovchinnikov, Yu. V., Ionov, S. P.: Soviet Physics JETP *26*, 385 (1968).
63) Kroto, H. W.: Molecular rotation spectra. London – New York – Sidney – Toronto: J. Wiley and Sons 1975.
64) Costain, C., Sutherland, G.: J. Phys. Chem. *56*, 321 (1952).
65) Davies, P. B., Neumann, R. M., Wofsy, S. C., Klemperer, W.: J. Chem. Phys. *55*, 3564 (1971).
66) Cazolli, G., Lister, D. G.: J. Mol. Spectrosc. *45*, 467 (1973).
67) Tyler, J. K., Sheridan, J., Costain, C. C.: J. Mol. Spectrosc. *43*, 248 (1972).
68) Hirota, E., Sugisaki, R., Nielsen, C. J., Sørensen, G. O.: J. Mol. Spectrosc. *49*, 251 (1974).
69) Sugisaki, R., Tanaka, T., Hirota, E.: J. Mol. Spectrosc. *49*, 241 (1974).
70) Tsuboi, M., Hirakawa, A. Y., Tamagaka, K.: J. Mol. Spectrosc. *22*, 272 (1967).
71) Mirri, A. M., Caminali, W.: J. Mol. Spectrosc. *47*, 204 (1973).
72) Wollrab, J. E., Laurie, V. W.: J. Chem. Phys. *48*, 5058 (1968).
73) Penn, R. E., Boggs, J. E.: J. Mol. Spectrosc. *47*, 340 (1973).
74) Hamada, Y., Hirakawa, A. Y., Tamagake, K., Tsuboi, M.: J. Mol. Spectrosc. *35*, 420 (1970).
75) Tyler, J. K.: J. Mol. Spectrosc. *11*, 39 (1963).
76) Tamagake, K., Tsuboi, M.: J. Mol. Spectrosc. *53*, 189 (1974).
77) Takagi, K., Kojima, T.: J. Phys. Soc. Japan *30*, 1145 (1971).
78) Špirko, V.: IIIrd International Seminar on High Resolution Infrared Spectroscopy, Prague 1974.
79) Papoušek, D., Danielis, V.: IInd International Seminar on High Resolution Infrared Spectroscopy, Prague 1972.
80) Watson, J. K. G.: J. Chem. Phys. *46*, 1935 (1967).
81) Steenbeckeliers, G., Bellet, J.: J. Mol. Spectrosc. *45*, 10 (1973).

Received April 27, 1976

Ion Solvation in Mixed Solvents

Dr. Hermann Schneider

Max-Planck-Institut für Biophysikalische Chemie, Postfach 968, D-3400 Göttingen

Contents

I. Introduction 105

II. The Free Energy of Transfer of Single Ions 106
a) Experimental Evaluation of Free Energies of Transfer 107
b) Estimation of the Single Ion Free Energy of Transfer 108
1. Treatments Based on the Born Model 108
2. Reference Solutes 109
3. Real Free Energy of Solvation 110
4. The Assumption of Negligible Liquid Junction Potential 110
5. Spectroscopic Methods 111

III. Complex Formation of Solvent Molecules with Ions 116
a) Coordination Model of Ion Solvation and the Ionic Free Energy of Transfer 117
b) Experimental Evaluation of Coordination and of Formation Constants of Ion-Solvent Complexes 122
1. Potentiometric Titration 124
2. Electrolytic Conductance 124
3. The Solubility of Electrolytes in Mixed Solvents 127
4. Optical Spectroscopy 128
5. Nuclear Magnetic Resonance 128
6. Thermodynamic Properties of Transfer for Single Ions in Mixed Solvents 111

IV. Transference Numbers 133
a) A Binary Electrolyte in a Single Solvent 134
1. The Hittorf Reference System 135
2. The Washburn Reference System 135
b) An Electrolyte in a Binary Solvent Mixture 136
1. The Velocity of One Solvent Component as Reference Velocity . . 136
2. The Barycentric Velocity v_m of the Solvent Mixture as Reference Velocity 137

3. The Velocity of "Free" Solvent as Reference Velocity 138
4. The Mean Molar Velocity $\overline{v}$ of the Solvent Mixture as Reference Velocity 139
c) Experimental Determination of Solvent Transport in Mixed Solvent Electrolyte Solutions 141
1. The Hittorf Transference Method 141
2. The Electromotive Force Method 142

V. References 145

I. Introduction

The behavior of electrolyte solutions is determined by three factors: ion-ion interaction, ion-solvent interaction or ion solvation, and solvent-solvent interaction. The energetic contributions are decreasing in the sequence cited. Each factor is by itself composed of several contributions, the more differentiated the representation is.

In dilute electrolyte solutions ion-ion interaction as function of electrolyte concentration is fully explained by the Debye-Hückel-Onsager theory and its further development. The contribution of ion solvation is noticed, if, for instance, the mobilities at infinite dilution of an ion in different solvent media or as function of ionic radii as considered. Up till now the calculation of that dependence has been only rather approximate[1]. An improvement is quite probable, though, theoretically very involved if the solvent is not regarded as a continuum, but the number and arrangement of solvent molecules in the primary solvation shell of an ion is taken into consideration. Also the lifetime of molecules in the solvation shell must be known. Beyond this region a continuum model of ion-solvent interaction may be sufficient to account for the contributions of solvent molecules in the second or third sphere.

In aqueous electrolyte solutions ion hydration has been studied extensively. With the exception of studies using NMR technique[2] or Taube's isotopic dilution method[3] or also X-ray diffraction technique[4] of concentrated electrolyte solutions, the hydration numbers are not always integral numbers which quite often represent deviations of experimental data from results of a theoretical description of an equilibrium property. Therefore, these hydration numbers depend on the solution property studied.

Much more direct evidence of ion solvation has been deduced from studies on electrolytes in mixed solvents. Originally used as an easy way to change the dielectric constant of a solvent medium, the employment of mixed solvents enables us today to study not only preferential solvation of ions by one or the other solvent component, but experimental results point to integer solvation numbers or coordination numbers, also of univalent ions. Under favorable conditions it is possible to observe in a mixed solvent medium the stepwise replacement of one solvent component in the ion solvation shell by molecules of the more strongly interacting component. In addition, there are a large number of effects specific for electrolytes in mixed solvents which can be less directly attached to single ion properties. For example, in binary solvent systems with an upper critical solution temperature, as in mixtures of water and acetonitrile[5], this temperature is changed by adding a small amount of electrolyte. If cation and anion are preferentially solvated by the same solvent component (homoselective solvation) the phase separation temperature of the solvent mixture is shifted to higher temperatures. On the other hand, with heteroselective solvation of an electrolyte, when one ion is preferentially solvated by one solvent component and the counterion by the second component, the upper critical solution temperature decreases by adding that electrolyte.

The treatment of all those properties of electrolyte solutions, where selective solvation of ions in mixed solvents may play a major role, would result in an accumulation of data hard to follow up. Therefore, only those theoretical treatments of ion solvation have been mentioned in the following whose results have been used to

analyse experimental data, that is mainly the Born equation and its modifications. Theories which apply only to ions in mixed solvents are the electrostatic theory of solvent sorting by ions deduced by Debye and McAuley[6] and adopted to salting in-salting out experiments. Furthermore, the thermodynamic treatment of mixed fluids in an electrostatic field applied to the calculation of preferential solvation in mixed solvents by Padova[7], and Hall's[8] explanation of the primary medium effect for individual ionic species using the Kirkwood-Buff theory of solutions, enable a more detailed interpretation of ion-solvent interactions. Yet, these treatments can be applied to specific systems successfully only when composition and extent of the solvation shell of individual ions in mixed solvents is elucidated in detail.

Therefore, three subjects have been treated: the free energy of transfer of individual ions between two solvent media, solvation numbers and the composition of the solvation shell, and the transport of a solvent component in a mixed solvent electrolyte solution.

II. The Free Energy of Transfer of Single Ions

The free energy of solvation of an uncharged species as well as the related enthalpy and entropy quantities are experimentally accessible. The evaluation of the corresponding properties for single ions is only possible with the help of an extra-thermodynamic assumption. This also holds for the free energy of transfer of neutral combinations of ions and the related thermodynamic quantities.

The standard free energies of solvation G_i^0 of ions i are in the range of -400 to -4000 kJ/mole. But the difference in free energies of solvation of individual ions in two solvents ($'$ and $''$), the free energy of transfer $\Delta G_{t,i}^0$

$$\Delta G_{t,i}^0 = G_i^{0''} - G_i^{0'} \tag{1}$$

is always much smaller. The reason for a procedure which adopts non-thermodynamic models to obtain "thermodynamic" quantities, is the assurance that the use of a multiplicity of assumptions as different as possible, will converge towards single ion properties which enable the comparison of the behavior of single ions in different media.

A well known example is the establishment of solvent-independent ion activity scales (*e.g.* pH). Furthermore, in electroanalytical chemistry and preparative chemistry it would be favorable not only to be able to predict the behavior of certain systems in a new solvent from the knowledge in some other solvent (most often water), but in advance also to use single ion properties to prepare mixed solvent media in which each ion interacts with the medium in a manner aspired.

Besides the standard free energy of transfer $\Delta G_{t,i}^0$ also the medium activity coefficient or transfer activity coefficient γ_i^* is used quite often to relate the ion activities a_i' and a_i'' of an ion referred to the standard states in the two solvents ($'$and $''$):

$$a_i' = m_i\gamma_i', \quad a_i'' = m_i\gamma_i'' \tag{2}$$

γ_i is the familiar activity coefficient which is unity at zero molality, γ_i' in solvent (′) and γ_i'' in solvent (″). Now, the activity of ion i in the second solvent (″) is related to the standard state in the primary solvent (′) through the medium activity coefficient γ_i^*:

$$a_i' = a_i''\gamma_i^* = m_i\gamma_i''\gamma_i^* \tag{3}$$

The relationship between medium activity coefficient and the free energy of transfer in the standard state is:

$$\Delta G_{t,i}^0 = RT \ln \gamma_i^* \tag{4}$$

Several excellent articles[9, 15] have recently been published in which the thermodynamic properties of single ions in aqueous and non-aqueous solvents have been treated thoroughly. Therefore, only a short survey over a) the experimental methods and b) the assumptions for the determination of the free energy of transfer of single ions shall be presented.

a) Experimental Evaluation of Free Energies of Transfer

There are three experimental methods which are used most often to determine the free energy of transfer of electrolytes and neutral combinations of ions.

1. From the solubilities ($a_{\pm sat}'$ and $a_{\pm sat}''$) of a strong electrolyte in two media (′ and ″) follow its free energy of transfer ΔG_t^0 using Eqs. (3) and (4).

$$\Delta G_t^0 = 2\,RT \ln \frac{a_{\pm sat}'}{a_{\pm sat}''} \tag{5}$$

This relation holds only if both saturated solutions are in equilibrium with the same solid phase. Solvate formation in one and/or the other medium necessitates a correction[10].

2. The primary medium effect of an electrolyte can also be calculated from the standard potentials of a galvanic cell. The difference of the standard electromotive forces $E^{0\prime}$ and $E^{0\prime\prime}$ of the galvanic cells

$$\mathrm{M}\,\Big|\begin{matrix}\mathrm{MX}\\ \\ \mathrm{S}'\end{matrix}\Big|\,\mathrm{X}\,\Big|\begin{matrix}\mathrm{MX}\\ \\ \mathrm{S}''\end{matrix}\Big|\,\mathrm{M} \tag{A}$$

with solvent media S′ and S″ is proportional to the free energy of transfer:

$$\Delta G_t^0 = F(E^{0\prime\prime} - E^{0\prime}) \tag{6}$$

3. The total vapour pressure of a binary solvent mixture and the composition of the vapour change on addition of electrolytes. Grunwald *et al.*[16] deduced the fol-

lowing relation for the derivation of the standard molal free energy of transfer ΔG_t^0 of an electrolyte (molality m)

$$\frac{1}{RT}\frac{d(\Delta G_t^0)}{dx_1} = \frac{1000}{M_{12}}\left[\frac{\partial \ln \alpha_1/\alpha_2}{\partial m}\right]_{x_1} - 2\left[\frac{\partial \ln \gamma_\pm}{\partial x_1}\right]_m + 2\,m\,\frac{M_1 - M_2}{M_{12}}\left[\frac{\partial \ln \gamma_\pm}{\partial m}\right]_{x_1} \quad (7)$$

with the solvent components 1 and 2, the mole fraction $x_1 = 1 - x_2$, the molecular weights M_1 and M_2, and $M_{12} = x_1M_1 + x_2M_2$. α_1 is the ratio of the fugacity of component 1 in the presence of solute to the fugacity in the absence of solute, both at composition x_1. If $\partial(\Delta G_t^0)/\partial x_1$ is known as function of mole fraction, the free energy of transfer ΔG_t^0 may be evaluated by integration with one pure component as Refs.[17,18].

b) Estimation of the Single Ion Free Energy of Transfer

The free energy of transfer of an electrolyte is an additive function for cation and anion. The separation of the experimental quantities into single ion terms even in an approximate manner will be of practical importance as mentioned before. Several models are in use and lately a great number of single ion free energies of transfer have been determined[9,10]. Yet, on principle, the free energy of transfer for only one charged species between two solvent media S′ and S″ need to be established, whereupon the free energies for transferring other ions from S′ to S″ become calculable from free energies of transfer for uncharged combinations of ions obtainable with e.m.f. measurements or solubility determinations. The various models, used to estimate single ions' free energy of transfer, are presented in a short version, because several detailed articles have been published about each method.

1. Treatments Based on the Born Model

The electrostatic contribution to the free energy of transfer of a charged species i between two solvents of different dielectric constant (ϵ) is the electrostatic interaction of a charged sphere i (charge z, radius r_i) with the dielectric continua of the two solvents. Born produced the following equation:

$$\Delta G_{t,i,el}^0 = RT\ln\ \gamma_{i,el}^* = \frac{Nz^2e^2}{2\,r_i}\left(\frac{1}{\epsilon''} - \frac{1}{\epsilon'}\right) \quad (8)$$

with Avogadro number N, electron charge e. This equation is of great importance, for it enables the estimation of the behavior of ions in different media, though the "macroscopic" dielectric constant is used for calculation. Dielectric saturation or other types of interactions contributing to $\Delta G_{t,i}^0$ are neglected and wrong predictions are known.

As the non-electrostatic part of $\Delta G^0_{t,i}$ cannot be calculated in as simple a manner as $\Delta G^0_{t,i,el}$, several extrapolation procedures using the Born equation in a modified form have been used.

Izmailov *et al.*[19] and Feakins *et al.*[20] plotted the free energies of transfer between water and another solvent medium for halogen acids (HX) and alkali-metal chlorides (MCl) as function of the reciprocal radius of the counterions. Extrapolation to $r^{-1} = 0$ leads to the free energy of transfer of the common ion of a series: $\Delta G^0_t(H^+)$ or $\Delta G^0_t(Cl^-)$. Later on, Alfenaar and de Ligny[21] determined the non-electrostatic contribution to ΔG^0_t from the solubilities of analogous uncharged species of the same radius (as *e.g.* noble gases) and extrapolated the free energy of transfer of an electrolyte corrected by the non-electrostatic contribution of the variable counterion as function of the reciprocal radius to $r^{-1} = 0$. The authors attempted, furthermore, to improve the method by adding to the electrostatic and non-electrostatic terms of ΔG^0_t further terms proportional to r^{-2} and r^{-3}, which account for ion-dipole and ion-quadrupole interactions[22].

Plots of the diverse ΔG^0_t functions versus r^{-1} often fail to be linear, complicating the long range extrapolation, and if the plot is linear[12] the slope differs from the theoretical slope deduced from the Born equation. This discrepancy was eliminated by adding constant increments δ_+ and δ_- to the crystal radii, as was shown by Latimer *et al.*[23] and Strehlow *et al.*[24].

But in general, the Born equation in its original form is used quite often to estimate the electrostatic contribution to the free energy of transfer of large ions[25] and entities which consist of an ion with several solvent molecules[26].

2. Reference Solutes

Rubidium scale: Pleskov[27] proposed to use the standard electrode potential of Rb/Rb^+ in different solvents as a medium independent reference. Due to the large radius and low polarizability of the rubidium ion the solvation energies should be low. The approximation $\Delta G^0_t(Rb^+) = 0$ was improved by Strehlow[24], who took into consideration the contribution calculated by the Born equation in its form modified with the additive radius increment. Strehlow *et al.*[25] studied several redox systems and finally selected ferrocene-ferricinium$^+$ (foc/fic$^+$) and cobaltocene-cobalticinium (coc/cic$^+$) as being suitable. Ferrocene and cobaltocene are complexes of two cyclopentadienyl anions with Fe^{2+} and Co^{2+}, respectively. The assumption on which the application is based, is the solvent independence of $[\Delta G^0_t(foc) - \Delta G^0_t(fic^+)]$ or of the respective combination for coc/cic$^+$. This assumption works all the better the larger the species and the lower the charge, which is centered in the middle of the species. The same condition applies to bisbiphenylchromium (O, I), a redox system first studied by Schroer and Vlček[28] and adopted by Gutmann *et al.*[29]. Other redox reference systems have also been proposed but applied only sporadically[30, 31].

Recently reference electrolytes have been used to estimate medium effects. The assumption is based on a simple picture, *i.e.*, the ionic free energies of transfer of an uni-univalent electrolyte which is composed of large ions of equal size and similar surface, are the same for cation and anion. A reference electrolyte was used for the first time by Grunwald *et al.*[16, 32], namely, tetraphenylphosphonium-tetraphenyl-

borate (Ph_4PBPh_4). Later on Popovych *et al.*[33] proposed triisoamylbutylammonium-tetraphenylborate ($TABBPh_4$) and Alexander and Parker[34] employed tetraphenylarsonium-tetraphenylborate (Ph_4AsBPh_4) extensively. The medium effects are determined by solubility measurements[9, 10].

3. Real Free Energy of Solvation

While $\Delta G^0_{t,i}$ is the difference of the free energies of solvation of charged species i in two different solvent media, the direct transport of i from one solvent across the surfaces into the other solvent is described by the difference of real free energies of solvation, *i.e.*, the real free energy of transfer $\Delta\alpha^0_i$ which is directly measurable.

$$\Delta\alpha^0_i = \Delta G^0_{t,i} + z_i F\chi \tag{9}$$

where z_i is the ionic charge. χ is the difference of the surface potentials of the solvents. The real free energy of transfer of chloride ion has been determined by Parsons *et al.*[35] in several water – non-aqueous solvent mixtures. In some mixtures χ remains nearly constant over a large range of mole fraction up to the pure non-aqueous components as deduced from the surface composition. In this range the variation of $\Delta\alpha^0_{Cl}$ reflects the variation of $\Delta G^0_t(Cl^-)$.

4. The Assumption of Negligible Liquid Junction Potential

Parker and Alexander[36] treated the galvanic cell (B) with liquid junction

Ag	$AgClO_4$ (0.01 m) S′	TEA PIC (0.1 m) S_b	$AgClO_4$ (0.01 m) S″	Ag	(B)

to determine free energies of transfer of Ag^+ between different solvents S′ and S″. The bridge solvent S_b may be either S′ or S″ or any other solvent which supports the intention to reduce the voltage contribution of the liquid junctions between the electrode compartments. Tetraethylammonium picrate (TEA PIC) was chosen because the ions are bulky and preferential solvation may be neglected. The mobilities of TEA^+ and PIC^- are very similar in a variety of solvents[37]. The electromotive force of cell (B) is given, following Scatchard[38]

$$E_+ = \frac{RT}{F} \ln \frac{a''_{Ag^+}}{a'_{Ag^+}} - \frac{1}{F} \int_{a'}^{a''} \left[\Sigma \frac{t^{(m)}_+}{z_+} d \ln \mu_+ + \Sigma \frac{t^{(m)}_-}{z_-} d \ln \mu_- + \Sigma_k \tau^{(m)}_k d \ln \mu_k \right] \tag{10}$$

In this formula the mass of the solvent is used as a reference. The activities, a, of all ions are referred to the same standard state. $\tau^{(m)}_k$ is the reduced transference number of component k. The sum of the three terms within the brackets is extended over all

cationic and anionic constituents and over all solvent components (k) in cell (B). As the concentration of TEA PIC is much larger than that of $AgClO_4$, $t_+^{(m)}$ may be replaced by t_{TEA} and $t_-^{(m)}$ by t_{PIC}. The integrals over the cationic and anionic contributions to the liquid junction potential may be replaced by

$$\left(\frac{0.5}{F}\,\Delta\mu_{TEA} - \frac{0.5}{F}\,\Delta\mu_{PIC}\right)$$

because approximately $t_{TEA} = t_{PIC}$ holds. $\Delta\mu_{TEA}$ and $\Delta\mu_{PIC}$ are the differences in chemical potential of TEA^+ and PIC^- between S'' and S'. These differences should be independent of the bridge solvent used. The solvent-transport term was shown to be small, with the exception of the combinations: S' = acetonitrile, S'' = dimethylsulphoxide, S_b = formamide and arrangements using S'' = water, methanol or formamide and various bridge solvents. Otherwise, the agreement within measurements with different bridge solutions was remarkably good (±15 mV and better[37]). As the first term in Eq. (10) is proportional to RT/F ln $\gamma_\ddagger$, the medium activity coefficients evaluated with other methods were used to obtain the liquid junction potential. The authors found it to be negligible, except in the special cases mentioned before. Cells similar to (B) have been used also with other electrodes.

5. Spectroscopic Methods

While in the methods treated before ion solvation represents the sum of various terms of ion-solvent interaction, spectroscopic methods are mainly, if at all, sensitive to the immediate environment of an ion. Due to this the coordination model, representing the primary solvation shell, is not only used for highly charged ions[2, 3] but also for univalent ions. The precise results of the direct ion-solvent interactions made it possible to evaluate equilibrium constants describing the composition in the solvation shell of an ion in mixed solvents. Therefore, the estimation of single ion free energies of transfer from spectroscopic measurements is the subject of several recent efforts and is theme of Part III.

6. Thermodynamic Properties of Transfer for Single Ions in Mixed Solvents

Alot of information about the free energies of transfer of single ions between pure solvents has been accumulated. Less numerous are determinations in mixed solvents, and the ionic enthalpies of transfer and entropies of transfer as function of mole fraction are known as an exception only. In Table 1 ions and solvent mixtures are listed for which free energies of transfer and some other thermodynamic quantities have been determined.

Results based on different assumptions have been compared critically several times, especially comprehensively for mixed solvent systems by Parker *et al.*[9, 34], Parsons *et al.*[35] and Popovych[10]. As an example, the free energy of transfer of Cl^- in aqueous acetone is plotted versus mole fraction in Fig. 1. The curve with BPC(O/I) as reference was calculated from Cl^- (foc/fic$^+$)[14] and a comparison of BPC(O/I) with coc/cic$^+$ [39]. As has been shown elsewhere[25], ΔG_t^0 values are independent of the reference, irrespective of whether foc/fic$^+$ or coc/cic$^+$ is chosen.

Table 1. Free energies of transfer and some other thermodynamic properties of transfer for single ions in mixed solvents

Ions	Thermodynamic quantity	Method	Footnotes
Methanol-water			
Na^+, K^+, Cl^-, Br^-, I^-	ΔH_t^0	–	[1]
H^+, Li^+, Na^+, K^+, Cl^-, Br^-, I^-	ΔG_t^0	Extr.	[2, 3]
H^+, Li^+, Na^+, K^+, Rb^+, Cs^+, Me_4N^+, Et_4N^+, Pr_4N^+, Bu_4N^+, fic$^+$, Cl^-, Br^-, I^-, ClO_4^-	ΔG_t^0	Extr.	[4, 5]
H^+, Li^+, Na^+, K^+, Rb^+, Cs^+, Cl^-, Br^-, I^-	$\Delta\alpha_t^0$	–	[6]
H^+, Li^+, Na^+, K^+, Rb^+, Cs^+, Ag^+, Me_4N^+, Pr_4N^+, Bu_4N^+, fic$^+$, Ba^{2+}, Sr^{2+}, Cd^{2+}, Zn^{2+}, OH^-, Cl^-, Br^-, I^-, ClO_4^-	ΔG_t^0	$\Delta G_t(H_{11}O_5^+)$	[7, 8]
H^+, Na^+, OH^-, Cl^-	ΔG_t^0	$Ph_4As^+ = BPh_4^-$	[23]
Ethanol-water			
Na^+, K^+, Cl^-, Br^-, I^-	ΔH_t^0	–	[1]
H^+, K^+, Cl^-, (picrate)$^-$	ΔG_t^0	$TAB^+ = BPh_4^-$	[9, 10]
H^+	ΔG_t^0	foc/fic$^+$	[11]
Ag^+, Cl^-, Br^-, I^-, SCN^-	ΔG_t^0	foc/fic$^+$	[12]
H^+	ΔG_t^0	–	[13]
Iso-propanol – water			
H^+, Cl^-	ΔG_t^0	$\Delta G_t^0(H_{11}O_5^+)$	[8]
t-Butylalcohol – water			
H^+, Cl^-, Br^-, I^-	ΔG_t^0	Extr.	[14]
Ethylene glycol-water			
H^+, Li^+, Na^+, K^+, Cl^-, Br^-, I^-	ΔG_t^0	Extr.	[15]
H^+, Cl^-, Br^-, I^-	ΔG_t^0, ΔH_t^0	Extr.	[16]
Cl^-	$\Delta\alpha_t^0$	–	[17]
H^+, Li^+, Na^+, K^+, OH^-, Cl^-, Br^-, I^-	ΔG_t^0, ΔH_t^0	$\Delta G_t^0(H_{11}O_5^+)$	[18]
Glycerol-water			
H^+, Cl^-, Br^-, I^-	ΔG_t^0	Extr.	[19]
H^+, Cl^-, Br^-, I^-	ΔG_t^0	$\Delta G_t^0(H_{11}O_5^+)$	[8]
Acetic acid-water			
H^+, Cl^-, Br^-, I^-	ΔG_t^0	Extr.	[20]
Dioxan-water			
H^+, Li^+, Na^+, K^+, Rb^+, Cs^+, Me_4N^+, Ph_4P^+, OH^-, Cl^-, Br^-, I^-, NO_3^-, ClO_4^-, BPh_4^-,  SO_3^-	$\frac{d(\Delta G_t^0)}{dx_{H_2O}}$	$Ph_4P^+ = BPh_4^-$	[21]
Li^+, Na^+, Me_4N^+, OH^-, Cl^-, Br^-	ΔG_t^0	$Ph_4As^+ = BPh_4^-$ $\Delta G_t^0(Me_4N^+) = 0$	[22, 23]
Cl^-	$\Delta\alpha_t^0$		[17]
H^+, Li^+, Na^+, K^+, Rb^+, Cs^+, OH^-, Cl^-, Br^-, I^-	ΔG_t^0	Extr.	[24]

Table 1 (continued)

Ions	Thermodynamic quantity	Method	Footnotes
Formamide-water			
Cl^-	$\Delta\alpha_t^0$	–	[17]
Urea-water			
H^+, Cl^-, Br^-, I^-	ΔG_t^0	Extr.	[25]
Acetonitrile-water			
Ag^+	ΔG_t^0	foc/fic$^+$	[26]
H^+, Ag^+, Cl^-, Br^-, I^-, SCN^-	ΔG_t^0	foc/fic$^+$	[11,12]
H^+, OH^-	ΔG_t^0	$\Delta G_t^0(Me_4N^+) = 0$	[23]
Na^+, Ag^+, Cu^+, Cu^{2+}, Fe^{2+}, Fe^{3+}, Cl^-	ΔG_t^0	n.l.j.p.	[27]
Dimethylsulphoxide-water			
H^+, Cl^-, Br^-, I^-	ΔG_t^0	Extr.	[28]
H^+, Tl^+, Ag^+, Cl^-, I^-, N_3^-, (acetate)$^-$, (benzoate)$^-$, SO_4^{2-}	ΔG_t^0	foc/fic$^+$	[29,30]
Cl^-	$\Delta\alpha_t^0$	–	[17]
H^+, Me_4N^+, OH^-	ΔG_t^0	PhAs$^+$ = BPh_4^- $\Delta G_t^0(Me_4N^+) = 0$	[23]
H^+, Li^+, Na^+, K^+, Rb^+, Cs^+, OH^-, Cl^-, Br^-, I^-	ΔG_t^0	Extr.	[31]
Ag^+, Cu^{2+}	ΔG_t^0	n.l.j.p.	[27]
N,N-dimethylformamide – water			
Ag^+, Cl^-, Br^-, I^-, SCN^-	ΔG_t^0	foc/fic$^+$	[12]
Acetone-water			
Ag^+, Cl^-, Br^-, I^-, SCN^-	ΔG_t^0	foc/fic$^+$	[12]
H^+	ΔG_t^0	foc/fic$^+$	[11]
H^+, Cl^-, Br^-, I^-	ΔG_t^0	Extr.	[32]
Cl^-	$\Delta\alpha_t^0$	–	[17]
H^+, K^+, Rb^+, Cs^+, Ag^+, Me_4N^+, Pr_4N^+, Bu_4N^+, fic$^+$, Cl^-, Br^-, I^-	ΔG_t^0	$\Delta G_t^0(H_{11}O_5^+)$	[8]
Propylene carbonate-water			
H^+, Li^+, Na^+, K^+, Rb^+, Cs^+, Ag^+, Tl^+	ΔG_t^0	foc/fic$^+$	[33]
Ethylene carbonate-water			
Ag^+, Cl^-, Br^-, I^-, I_3^-	ΔG_t^0	foc/fic$^+$	[34]
Tetrahydrofurane-water			
Ag^+, Cl^-, Br^-, I^-, SCN^-	ΔG_t^0	foc/fic$^+$	[12]
Li^+, Na^+, Ag^+, NH_4^+, Me_4N^+, Pr_4N^+, Bu_4N^+, Hex_4N^+, $Hept_4N^+$, Ph_4As^+, F^-, Cl^-, Br^-, I^-, NO_3^-, ClO_3^-, ClO_4^-, BPh_4^-	$\frac{d(\Delta G_t^0)}{dx_{H_2O}}$		[35]
Na^+, Cl^-	ΔG_t^0		[35]

Table 1 (continued)

Ions	Thermo-dynamic qunatity	Method	Foot-notes
Dimethylsulphoxide-methanol			
H^+, Ag^+, Cl^-, I^-, (acetate)$^-$, $AgCl_2^-$, SO_4^{2-}	ΔG_t^0	foc/fic$^+$	36, 37)
Acetonitrile-methanol			
Ag^+	ΔG_t^0	n.l.j.p.	27)
Dimethylsulphoxide-propylene carbonate			
Tl^+, Cd^{2+}, Pb^{2+}	ΔG_t^0	coc/cic$^+$	38)
Dimethylsulphoxide-acetonitrile			
Na^+	ΔG_t^0	n.l.j.p.	27)
Propylene carbonate-acetonitrile			
Ag^+, Cu^+, Cu^{2+}	ΔG_t^0	n.l.j.p.	27)
Acetone-acetonitrile			
Ag^+	ΔG_t^0	n.l.j.p.	27)

Abbreviations: extr. = extrapolation (methods); n.l.j.p. = negligible liquid junction potential

1) Krestov, G. A., Klopov, V. J.: Zh. Struk. Khim. *5*, 829 (1964).
2) Feakins, D., Watson, P.: J. Chem. Soc. 4735 (1963).
3) Feakins, D., in: "Physico-chemical processes in mixed aqueous solvents", F. Franks (ed.), p. 71. London: Heinemann Educational Books Ltd. 1967.
4) Alfenaar, M., de Ligny, C. L.: Rec. Trav. Chim. *86*, 929 (1967).
5) Bax, D., de Ligny, C. L., Remijnse, A. G.: Rec. Trav. Chim. *91*, 452, 965 (1972).
6) Case, B., Parsons, R.: Trans. Faraday Soc. *63*, 1224 (1967).
7) Wells, C. F.: J. C. S., Faraday I *69*, 984 (1973).
8) Wells, C. F.: J. C. S., Faraday I *70*, 694 (1974).
9) Popovych, O., Dill, A. J.: Anal. Chem. *41*, 456 (1969).
10) Popovych, O.: Crit. Rev. Anal. Chem. *7*, 73 (1970).
11) Vedel, J.: Ann. Chim. *2*, 335 (1967).
12) Barraqué, C., Vedel, J., Trémillon, B.: Bull. Soc. Chim. France, 3421 (1968).
13) Gutbezahl, B., Grunwald, E.: J. Amer. Chem. Soc. *75*, 559, 565 (1953).
14) Bose, K., Das, A. K., Kundu, K. K.: J. C. S., Faraday I, *71*, 1838 (1975).
15) Kundu, K. K., Rakshit, A. K., Das, M. N.: Electrochim. Acta *17*, 1921 (1972).
16) Kundu, K. K., Jana, D., Das, M. N.: Electrochim. Acta *18*, 95 (1973).
17) Parsons, R., Rubin, B. I.: J. C. S., Faraday I, *70*, 1636 (1974).
18) Wells, C. F.: J. C. S., Faraday I, *71*, 1868 (1975).
19) Khoo, K. H.: J. C. S., Faraday I, *68*, 554 (1972).
20) Bennetto, H. P., Feakins, D., Turner, D. J.: J. C. S. A, 1211 (1966).
21) Grunwald, E., Baughman, G., Kohnstam, G.: J. Amer. Chem. Soc. *82*, 5801 (1960).
22) Villermaux, S., Baudot, V., Delpuech, J. J.: Bull. Soc. Chim. France, 1781 (1972); 815 (1974).
23) Villermaux, S., Delpuech, J. J.: Bull. Soc. Chim. France, 2534 (1974).
24) Bennetto, H. P., Feakins, D., in: "Hydrogen-bonded solvent systems", (A. K. Covington and P. Jones, eds.) London: Taylor & Francis Ltd. 1968.
25) Kundu, K. K., Mazumdar, K.: J. C. S., Faraday I, *71*, 1422 (1975).

Footnotes to Table 1 (continued)

[26]) Koepp, H. M., Wendt, H., Strehlow, H.: Z. Elektrochem., Ber. Bunsenges. physik. Chem. *64*, 483 (1960);
Strehlow, H.: "Electrode potentials in non-aqueous solvents", in: The chemistry of non-aqueous solvents (J. J. Lagowski, ed.). New York: Academic Press 1966.
[27]) Cox, B. G., Parker, A. J., Waghorne, W. E.: J. Phys. Chem. *78*, 1731 (1974).
[28]) Khoo, K. H.: J. Chem. Soc., *A*, 2932 (1971).
[29]) Courtot-Coupez, J., Le Démézet, M., Laouenan, A., Madec, C.: J. Electroanal. Chem. *29*, 21 (1971).
[30]) El-Harakany, A. A., Schneider, H.: J. Electroanal. Chem. *46*, 255 (1973).
[31]) Das, A. K., Kundu, K. K.: J. C. S., Faraday I, *70*, 1452 (1974).
[32]) Bax, D., de Ligny, C. L., Remijnse, A. G.: Rec. Trav. Chim. *91*, 1225 (1972).
[33]) L'Her, M., Morin-Bozec, D., Courtot-Coupez, J.: J. Electroanal. Chem. *55*, 133 (1974); *61*, 99 (1975).
[34]) Cabon, J. Y., L'Her, M., Courtot-Coupez, J.: J. Electroanal. Chem. *64*, 219 (1975).
[35]) Treiner, C., Bocquet, J. F., Chemla, M.: J. Chim. Phys. *70*, 472 (1973);
Treiner, C.: J. Chim. Phys. *70*, 1183 (1973);
Treiner, C., Finas, P.: J. Chim. Phys. *71*, 67 (1974).
[36]) Madec, C., Courtot-Coupez, J.: J. Electroanal. Chem. *54*, 123 (1974).
[37]) Rodehüser, L., Schneider, H.: Z. Physik. Chem., N. F., *100*, 119 (1976).
[38]) Massaux, J., Duyckaerts, G.: J. Electroanal. Chem. *59*, 311 (1975).

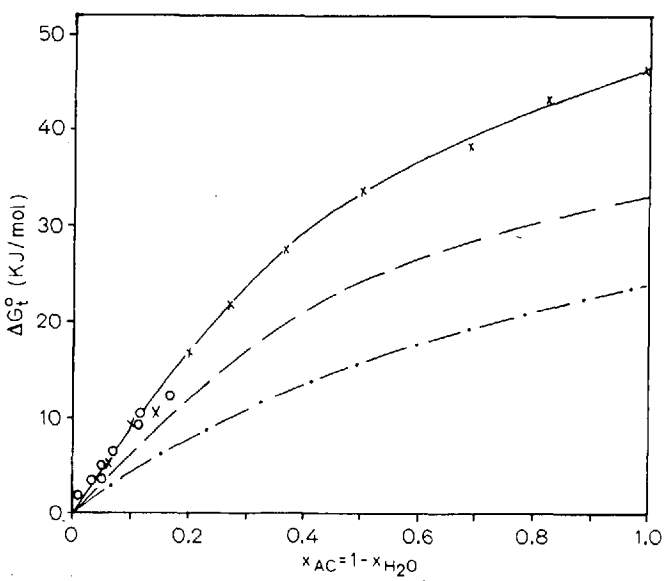

Fig. 1. Free energies of transfer of Cl^- in acetone-water mixtures at 25 °C.
o Wells[26]; x Barraque *et al.*[47]; – – – $\Delta G_t^0(Cl^-) - \{\Delta G_t^0(BPC) - \Delta G_t^0(foc/fic^+)\}$[39]; –·–·– Parsons *et al.*[35]

The agreement between BPC(O/I), foc/fic$^+$, and Parson's data is not remarkably good. For example a deviation of $\Delta G_t^0(Cl^-)$ referred to foc/fic$^+$ reference couple in highly aqueous acetone solutions was already mentioned previously in the case of other highly aqueous solvent mixtures[35, 40]. This has been claimed to be due to specific interactions between ferrocinium$^+$ [41, 42] and for ferrocene[43] with water.

The variation of the free energy of transfer of single ions with mole fraction is sometimes indicative of the thermodynamic properties of the solvent mixtures[44, 45]. For instance, in mixtures of methanol and of dioxan with water the solvent molecules are more basic than in water[12, 20].

Sometimes the Born equation (8) has been used to eliminate the effect of changing dielectric constant with solvent composition[45]. Due to the uncertainties connected with the application of the Born equation to special problems, this treatment will only rarely give results which may be more easily interpreted in terms of the structure of the solvent mixture.

Generally, in mixtures of protic solvents with aprotic solvents and especially in mixtures of two aprotic solvents the dependence of $\Delta G^0_{t,i}$ on composition is fixed by the transfer free energy of ion i between both pure solvent components. For cations quite often the sign of $d^2(\Delta G^0_{t,+})/dx_2^2$ is opposite to that of $\Delta G^0_{t,+}(x_2 = 1)$[25, 39, 46–49], if $\Delta G^0_{t,+}(x_2 = 1) < 0$. That means, $\Delta G^0_{t,+}$ decreases on addition of component 2, because the cation is preferentially solvated by solvent component 2. If, on the other hand, $\Delta G^0_{t,+}(x_2 = 1) > 0$, the solvent 2 changes $\Delta G^0_{t,+}$ only drastically when the mixture is composed mainly out of solvent component 2; that men as, $d^2(\Delta G^0_{t,+})/dx_2^2 > 0$[25, 39, 46–49]. In the case of anions, these relations only hold sometimes[46]. This is due to the higher sensitivity of anion solvation to solvent structure, *e.g.* to hydrogen bonding. Nevertheless, the combination of $d^2(\Delta G^0_{t,-})/dx_2^2 < 0$ and $\Delta G^0_{t,-}(x_2 = 1) > 0$ is also observed quite often[47–49].

An outstanding exception is the solvation of ions in dimethylsulphoxide (DMSO)-water mixtures. While in dimethylsulphoxide $\Delta G^0_t(Ag^+)$ related to water is negative, in highly aqueous DMSO mixtures Ag^+ is preferentially hydrated[46, 50–52]. The change of preferential solvation of an ion with solvent composition has also been noticed for other ions[53, 54]. This behavior can be attributed to the "stabilization" of the hydrogen-bonded water structure by DMSO[55].

The enthalpy of transfer ΔH^0_t of electrolytes and single ions i will be much more sensitive to the solvent structure than ΔG^0_t. As an example the thermodynamic properties for transfer of alkalimetal chlorides between water and 20% dioxan-water[12] should be mentioned. In the determination of $\Delta G^0_{t,i}$ and $\Delta H^0_{t,i}$ the increase in the number of experiments is not the only problem (mole fraction and temperature must be varied). But a large experimental accuracy is necessary for the evaluation of $\Delta G^0_{t,i}$ and $\Delta H^0_{t,i}$, whereas, less precise data may give a valuable indication to $\Delta G^0_{t,i}$ being positive or negative.

III. Complex Formation of Solvent Molecules with Ions

On treating ion solvation it is useful to differentiate between primary and secondary solvation shell or between chemical and physical solvation, respectively[56]. The electrostatic calculation of ion solvation is quite often less accurate because specific ion-solvent interactions have to be considered. In the primary solvation shell specific ion-solvent interactions are of much more importance than those with solvent molecules

in the secondary solvation shell. The energetic contribution of these regions can be taken into account satisfactorily by the coulombic interactions of an ion with the solvent represented as a continuous dielectric medium. Fortunately, there are experimental results which show that the specific ion-solvent interactions for different ions and various solvents are similar, and semiquantitative predictions are reliable. An example is the donicity which was introduced by Gutmann[57] for the reaction enthalpy (ΔH) of 1 : 1 complex formation of a polar solvent molecule (electron-pair donor) with antimony(V) chloride (electron-pair acceptor) in 1,2-dichloroethane. The donicity scale is a very useful means for estimating the strength of ion-solvent interaction in different solvents.

Solvation equilibria have often been used to explain acid-base equilibria in mixed solvents[11, 58] and solvent extraction experiments[59, 60]. Recently, the change in the behavior of cations in a solvent of low donicity on addition of a stronger donor solvent was studied with different methods. Corresponding experiments have been performed with anions. Already in 1960 Grunwald *et al.*[61] deduced a relation between the free energy of solvation of a solute in a mixed solvent on the one hand, and the free energy contributions of the various forms of solvated species on the other hand. Grunwald applied this formula to alkali-metal ions in aqueous dioxan solutions. Later on, Covington *et al.*[62] and Cox *et al.*[46] treated the free energy of transfer of an ion between a mixed solvent and its pure compounds, using a coordination model for the contribution of the primary solvation shell.

a) Coordination Model of Ion Solvation and the Ionic Free Energy of Transfer

A solution of n_I moles of an ionic species I in a mixture of two solvents A and B with n_A moles of A and n_B moles of B shall be considered. In dilute solutions ion-pair formation can be neglected. The free energy G of the solution is given by:

$$G = n_I \bar{G}_I + n_A \bar{G}_A + n_B \bar{G}_B \tag{11}$$

Following Grunwald's[61] treatment to derive a formula for the free energy of transfer of ion I in terms of the contribution of solvated ions and of solvent composition, we start with the equilibrium

$$I_{00} + (n - i)\,A + i\,B \rightleftharpoons I\,A_{n-i}\,B_i \tag{12}$$

I_{00} represents those ions which are unsolvated. n is the coordination number which is most often equal to the number of solvent molecules in the primary solvation shell. Free energy terms are marked with a prime, if they refer to actual ionic and molecular species. Equilibrium (12) is described by

$$\bar{G}'_{00} + (n - i)\,\bar{G}'_A + i\,\bar{G}'_B = \bar{G}'_{n-i,i} \tag{13}$$

With Φ'_{00}, the fraction of solute in the unsolvated form I_{00}, and with $\Phi'_{n-i,i}$, the fraction of n_I as $I\,A_{n-i}\,B_i$, one obtains:

$$\Phi'_{00} + \sum_{i=0}^{n} \Phi'_{n-i,i} = 1 \tag{14}$$

The ions in the unsolvated form I_{00} are used in the following as a reference to compare the free energies of solvation of I in various media and to derive free energies of transfer. The contribution of I_{00} is eliminated in the following and Φ' is later on replaced by Φ, which refers only to solvated ionic species.

Multiplication of Eq. (13) by $\Phi'_{n-i,i}$ and summation over i gives

$$(1 - \Phi'_{00})\,\overline{G}'_{00} + \overline{G}'_A \sum_{i=0}^{n} (n-i)\,\Phi'_{n-i,i} + \overline{G}'_B \sum_{i=0}^{n} i\,\Phi'_{n-i,i}$$

$$= \sum_{i=0}^{n} \Phi'_{n-i,i}\,\overline{G}'_{n-i,i} \tag{15}$$

With

$$\Phi'_{n-i,i} = \frac{[I\,A_{n-i}\,B_i]}{[I_{00}] + [I\,A_n] + [I\,A_{n-1}\,B] + \ldots + [I\,B_n]} \tag{16}$$

we can show that the mean solvation numbers λ_A and λ_B are dependent on $\Phi_{n-i,i}$, a new, more evident fraction scale

$$\Phi_{n-i,i} = \frac{[I\,A_{n-i}\,B_i]}{[I\,A_n] + [I\,A_{n-1}\,B] + \ldots + [I\,B_n]} \tag{17}$$

in the following way:

$$\lambda_A = \sum_{i=0}^{n} (n-i)\,\Phi_{n-i,i} = \frac{\sum_{i=0}^{n} (n-i)\,\Phi'_{n-i,i}}{1 - \Phi'_{00}} \tag{18a}$$

and

$$\lambda_B = \sum_{i=0}^{n} i\,\Phi_{n-i,i} = \frac{\sum_{i=0}^{n} i\,\Phi'_{n-i,i}}{1 - \Phi'_{00}} \tag{18b}$$

Additionally, it is

$$\sum_{i=0}^{n} \Phi_{n-i,i}\,\overline{G}'_{n-i,i} = \frac{\sum_{i=0}^{n} \Phi'_{n-i,i}\,\overline{G}'_{n-i,i}}{1 - \Phi'_{00}} \tag{18c}$$

Applying Eqs. (18), the following equation results from Eq. (15)

$$\bar{G}'_{00} + \lambda_A \bar{G}'_A + \lambda_B \bar{G}'_B = \sum_{i=0}^{n} \Phi_{n-i,i}\, \bar{G}'_{n-i,i} \tag{19}$$

The free energy G of the solution may now be written in terms of actual ionic species:

$$G = (n_A - n_I \lambda_A)\, \bar{G}'_A + (n_B - n_I \lambda_B)\, \bar{G}'_B + n_I \sum_{i=0}^{n} \Phi_{n-i,i}\, \bar{G}'_{n-i,i} \tag{20}$$

With Eq. (19) the last equation reduces to

$$G = n_I \bar{G}'_{00} + n_A \bar{G}'_A + n_B \bar{G}'_B \tag{21}$$

Comparison of Eqs. (11) and (21) gives

$$\bar{G}'_{00} = \bar{G}_I, \quad \bar{G}'_A = \bar{G}_A, \quad \bar{G}'_B = \bar{G}_B \tag{22}$$

Grunwald *et al.*[61, 63] showed that the partial molar free energy of the solute I is the same as that of the fraction of unsolvated I. Also, the partial molar free energy of the solvent components treated as formal quantity or as solvated species is independent of the solute. The following relations

$$\bar{G}'_{00} = \bar{G}_I = G_I^0 + RT \ln n_I = G'^0_{00} + RT \ln (n_I\, \Phi'_{00}) \tag{23a}$$

$$\bar{G}'_{n-i,i} = G'^0_{n-i,i} + TT \ln (n_I\, \Phi_{n-i,i}) \tag{23b}$$

are used, and with n_I approaching zero (superscript o) one obtains with (19):

$$G_I^0 = \sum_{i=0}^{n} \Phi^0_{n-i,i}\, G'^0_{n-i,i} + RT \sum_{i=0}^{n} \Phi^0_{n-i,i} \ln \Phi^0_{n-i,i} - \lambda_A^0 \bar{G}_A - \lambda_B^0 \bar{G}_B \tag{24}$$

This equation is equal to Eq. (53) of Grunwald's[61] paper and corresponds to Eq. (4) in Covington's[62] treatment (part 2).

$\bar{G}_A$ and $\bar{G}_B$ depend on the mole fraction $x_A = 1 - x_B$ and on the activity coefficients f_A and f_B which are given the value one in the following:

$$\bar{G}_A = G_A^0 + RT \ln x_A f_A \tag{25}$$

$$\bar{G}_B = G_B^0 + RT \ln x_B f_B$$

It follows from Eq. (24):

$$x_A = 1: \quad G_I^0(x_A = 1) = G'^0_{n,0} - nG_A^0 \tag{26}$$

$$x_A = 0: \quad G_I^0(x_A = 0) = G'^0_{0,n} - nG_B^0 \tag{27}$$

The free energy to transfer I from A to B is the difference of Eq. (27) minus Eq. (26):

$$\Delta G_t^0(\text{tot}) = G_I^0(x_A = 0) - G_I^0(x_A = 1) = G'^0_{0,n} - G'^0_{n,0} - n(\bar{G}_B^0 - \bar{G}_A^0) \tag{28}$$

The free energy of transfer between the solvent mixture (x_A) and pure solvent A is calculated using Eqs. (24) to (26):

$$\begin{aligned}\Delta G_t^0 &= G_I^0(x_A) - G_I^0(x_A = 1) \\ &= \sum_{i=0}^{n} \Phi_{n-i,i}^0 (G_{n-i,i}'^0 - G_{n,0}'^0 + iG_A^0 - iG_B^0) \\ &\quad + RT \sum_{i=0}^{n} \Phi_{n-i,i}^0 \ln \Phi_{n-i,i}^0 - RT \sum_{i=0}^{n} (n-i)\, \Phi_{n-i,i}^0 \ln x_A \\ &\quad - RT \sum_{i=0}^{n} i\Phi_{n-i,i}^0 \ln x_B\end{aligned} \tag{29}$$

Following Covington *et al.*[62], a simplification of Eqs. (28) and (29) is possible, if $G_{n-i,i}'^0$ is assumed to consist of three terms:

$$G_{n-i,i}'^0 = (G_{n-i,i}'^0)^{int} + (G_{n-i,i}'^0)^{coord} + (G_{n-i,i}'^0)^{elec} \tag{30}$$

The first term on the right hand side refers to the bare ion and disappears because we are engaged in differences of free energies. The second term refers to the coordination model of ion-solvent interaction in the primary solvation shell and the third term takes into account long range interactions. The last contribution may be approximated by the electrostatic interaction of a charged species with the solvent. The radius of the charged species is equal to that of the solvated ion (*e.g.*, ionic radius + diameter of the solvent molecules in the primary solvation shell).

The constant β_i of the equilibrium

$$I A_n + i B \rightleftharpoons I A_{n-i} B_i + i A \tag{31}$$

$$\beta_i = \frac{[I A_{n-i} B_i]\,[A]^i}{[I A_n]\,[B]^i} \tag{32}$$

is related to the coordination term of the free energy:

$$-RT \ln \beta_i = (G_{n-i,i}'^0)^{coord} - (G_{n,0}'^0)^{coord} + iG_A^0 - iG_B^0 \tag{33}$$

Now Eqs. (29), (30) and (33) lead to the equation:

$$\begin{aligned}\Delta G_t^0 = G_I^0(x_A) - G_I^0(x_A = 1) &= -RT \sum_{0}^{n} \Phi_{n-i,i}^0 \ln \left[\frac{\beta_i\,[B]^i}{\Phi_{n-i,i}^0\,[A]^i}\right] \\ &\quad - n\,RT \ln x_A + \sum_{0}^{n} \Phi_{n-i,i}^0 (G_{n-i,i}'^0)^{elec} - (G_{n,0}'^0)^{elec}\end{aligned} \tag{34}$$

The first term in the last equation can be simplified with the help of the consecutive equilibria of stepwise replacement of solvent component A by component B:

$$\begin{array}{ccc} IA_n + B & \overset{K_1}{\rightleftharpoons} & IA_{n-1}B + A \\ \vdots & & \vdots \\ IA_{n-i+1}B_{i-1} + B & \overset{K_i}{\rightleftharpoons} & IA_{n-i}B_i + A \\ \vdots & & \vdots \\ IA_1B_{n-1} + B & \overset{K_n}{\rightleftharpoons} & IB_n + A \end{array} \tag{35}$$

Now it is

$$[IA_{n-i}B_i] = K_i[IA_{n-i+1}B_{i-1}]\frac{[B]}{[A]} = \beta_i \frac{[B]^i}{[A]^i}[IA_n] \tag{36}$$

with

$$\beta_i = K_1K_2 \ldots K_i$$

With Eq. (32) one obtains from Eq. (34)

$$\Delta G_t^0 = -RT \ln \left[1 + \sum_{i=1}^{n} \beta_i \frac{[B]^i}{[A]^i}\right] - n\,RT \ln x_A + \sum_{0}^{n} \Phi_{n-i,i}^0 (G_{n-i,i}'^0)^{elec} - (G_{n,0}'^0)^{elec} \tag{37}$$

The last equation is identical with Eq. (16) found by Cox *et al.*[46], if the electrostatic contribution is neglected and x_A, x_B are volume fractions.

A relation for the free energy of transfer between $x_A = 1$ and $x_A = 0$ follows from Eq. (28) with Eqs. (30) and (33):

$$\Delta G_t^0(tot) = -RT \ln \beta_n + (G_{0,n}'^0)^{elec} - (G_{n,0}'^0)^{elec} \tag{38}$$

Cox et al.[46] and Manahan *et al.*[70] performed potentiometric titrations and calculated the equilibrium constants for the complexes formed between Ag^+ or Cu^+ and some ligand molecules (solvent B). Several solvents (A) were used as reaction medium. Table 2 contains the cumulative equilibrium constants β_i. The free energy of transfer $\Delta G_t^0(tot)$ was calculated with Eq. (38), whereby the electrostatic contribution was neglected. $\Delta G_t^0(tot)$ has been compared with ΔG_t^0 values, estimated from the assumption of negligible liquid junction potential in a galvanic cell similar to cell (B). As one can see in Table 2, the agreement between the two sets of values is excellent. Similarly, the free energies of transfer in mixtures of the solvents A and B (mentioned in Table 2), once calculated from Eq. (37) and once estimated from the assumption of n.l.j.p., are also in convincing agreement.

That means, it is possible to calculate reliable ΔG_t^0 values from equilibrium constants for ion-solvent complex formation. If, in case of cations, the ligand (solvent B)

is a much stronger Lewis base (high donicity) than solvent A, the equilibrium constants can be determined in very dilute solutions of the cation and of component B. Then, Eq. (37) enables one to calculate the free energy of transfer of an ion from solvent A to solvent mixtures of A and B, and even to the pure solvent B. The results in Table 2 show that the influence of the solvent outside the coordination sphere is small.

b) Experimental Evaluation of Coordination Numbers and of Formation Constants of Ion-Solvent Complexes

In general, the complex of an ion with a charged ligand is much stronger than the complex of an ion with a solvent molecule as ligand. Therefore, much less information about ion-solvent complex equilibria exists, though the experimental methods and the theoretical discussion adopted for this problem are the same as those used for complexes with charged ligands. To increase the strength of interactions between an ion and the molecules of a special solvent one always intends to perform the experiments in media which interact to a lesser degree with the given ion. An extremum of this intention is the determination of complex formation between ions and solvent molecules in the gas phase by mass spectroscopy[64]. The stepwise growth of ion-solvent clusters in the gas phase supported the attempt to explain the solvation, also of univalent ions in liquids, to some extent by the arrangement of an integer number (coordination number) of solvent molecules around an ion. However even before gas phase experiments were conducted, the formation of ion solvent complexes had been studied. In a series of fundamental experiments Bjerrum *et al.*[65] used potentiometric and spectroscopic methods to determine formation constants of ion solvent complexes. Later on other procedures were used with success by other workers. The study of ion solvent interaction was especially stimulated by the fact that nuclear magnetic resonance (NMR) became a common tool in chemistry and physical chemistry.

The most comprehensive information about ion-solvent complex formation follows from potentiometric titrations and some NMR measurements. This applies to NMR studies with solutions of ions like aluminum(III), gallium(III), beryllium(II) or magnesium(II) which interact so strongly with the molecules of several dipolar solvents that the lifetime of the molecules in the solvation shell is very long. Then the solvent exchange kinetics is slow enough to observe in the NMR spectrum of the solvent separate lines for coordinated solvent molecules and for free solvent.

More often, only the first or second equilibrium constant follows from electrochemical and spectroscopic measurements. NMR studies of solutions with monovalent ions in mixtures of two solvent components which interact rather differently with the ion sometimes show a break in the chemical shift plotted versus concentration. The slope of the curve changes near a solvent to ion ratio which obviously represents a coordination number.

In the following only some rather instructive examples of ion-solvent coordination shall be presented. Solvation of the proton in terms of complex formation has been studied extensively[11, 58, 66] and very detailed information has been accumulated[67, 68]. But this special subject has not been taken into consideration.

Table 2. Cumulative constants of ion solvation equilibria and free energies of transfer between solvent A and solvent B[46)]

Ion	Solvent A	Ligand (solvent B)	$\log \beta_1$	$\log \beta_2$	$\log \beta_3$	$\log \beta_4$	ΔG_t^0 (Eq. 38[2])) (kcal/mole)	ΔG_t^0 n.l.j.p. (kcal/mole)
Ag^{+1})	MeOH	MeCN	2.4	3.8	5.0		− 6.8	− 6.3
Ag^{+1})	Me_2CO	MeCN	2.3	4.1	5.5		− 7.5	− 7.3
Ag^{+1})	$MeNO_2$, E_tNO_2	MeCN	2.4	5.4	7.8	9.6	−13.1	−12.4
Ag^{+1})	H_2O	MeCN	2.0	3.4			− 4.6	− 4.2
Ag^+	PC	MeCN	3.0	5.2	6.9		− 9.4	− 9.5
Ag^+	PC	DMSO	3.3	5.9	7.9	9.5	−12.9	−12.9
Cu^{+1})	H_2O	MeCN		6.5	8.0		−10.9	−11.5

[1]) Ref.[70)].
[2]) The electrostatic terms of Eq. (38) have been neglected.

1. Potentiometric Titration

Larson and Iwamoto[69] determined the interaction of small amounts of water in nitromethane with Cu^{2+} by voltammetric studies. The dependence of the half-wave potential for the Cu^{2+}/Cu^{+} wave on water concentration was analysed to deduce the stepwise formation constants K_i of the complex species $[Cu(H_2O)_i]^{2+}$. The constants are in good agreement with those evaluated from spectroscopic measurements.

But in principle, the change of potential with water concentration should be referred to a reference redox couple being independent on solvent composition. Thus, from potentiometric titrations of an aqueous $AgNO_3$ solution with acetonitrile (AN) Koepp, Wendt and Strehlow[25] deduced the first and second overall formation constant of $[Ag(CH_3CN)]^{+}$ and $[Ag(CH_3CN)_2]^{+}$, respectively. In this study the potential of the silver electrode was referred to the ferrocene-ferricinium^{+} redox system. By this method any liquid junction potential effects are eliminated. Manahan and Iwamoto[70] polarographically determined the overall formation constants β_i of acetonitrile with Ag^{+} and with Cu^{+} in various solvents. Some of the data have been taken by Cox *et al.*[46] to calculate ΔG_t^0(tot) in Table 2. Luehrs *et al.*[71–73] obtained in the same way the formation constants of Ag^{+} with N,N-dimethylformamide (DMF), with dimethylsulphoxide (DMSO) and with hexamethylphosphoramide (HMPA) in various solvents. In Table 3 some of the results have been arranged in such a way that the interaction of Ag^{+} with the various ligands can be compared in the same solvent. The complexes of AN with Ag^{+} are much stronger than those with the other ligands and are due to the specific interaction between nitriles and the silver ion. But excepting AN the strength of the complexes increases with increasing donor strength[57] from DMF over DMSO to HMPA. With HMPA steric hindrance must be taken into account. The formation constants in methanol are in the mean smaller than those in 2-butanol, which solvates Ag^{+} less strongly. Also here water plays a special role. Complexes of DMF, DMSO, and HMPA with Ag^{+} could not be detected in water. But in aqueous dioxan solution the formation of DMSO-complexes with Ag^{+} were observed. This is in agreement with free energy of transfer data and NMR chemical shift experiments in aqueous DMSO solutions[52]. At low concentrations, DMSO strengthens the water structure[55] and Ag^{+} is preferentially hydrated.

Izutsu *et al.*[74] studied the complexing of Na^{+} in acetonitrile solution with various protic and aprotic solvents using an ion-sensitive glass electrode. Parker's assumption of negligible liquid junction potential with an tetraethylammonium picrate salt bridge was adopted and found to be valid, even when water was added. The formation constants increased in the order: methanol $<$ H_2O $<$ DMF $<$ N,N-dimethylacetamide $\sim$ DMSO $<$ HMPA.

2. Electrolytic Conductance

The electrical conductivities of electrolyte solutions and the ion-pair association constant are both very sensitive to ion solvation and permit the calculation of solvation constants.

D'Aprano and Fuoss[75] found that in dilute solution of Me_4NBr and $(n\text{-}Bu)_4NBr$ in acetonitrile the conductance changes if p-nitroaniline is added. The change could

Table 3. Formation constants β_i of $[AgB_i]^+$ complexes ($Ag^+ + iB \rightleftharpoons [AgB_i]^+$)

Solvent	Ligand (B)	log β_1	log β_2	log β_3	log β_4	Ref.
Methanol	AN	1.1	1.2	1.2	–	70)
Methanol	DMF	−0.36 ± 0.02	−0.3 ± 0.1	–	–	71)
Methanol	DMSO	0.00 ± 0.10	0.15 ± 0.10	–	–	72)
Methanol	HMPA	−0.2 ± 0.1	0.2 ± 0.1	–	–	73)
2-Butanol	AN	1.0	1.4	1.3	–	70)
2-Butanol	DMF	0.36 ± 0.05	0.3 ± 0.1	–	–	71)
2-Butanol	DMSO	0.08 ± 0.10	0.73 ± 0.10	0.65 ± 0.10	–	72)
2-Butanol	HMPA	0.68 ± 0.10	0.97 ± 0.10	0.3 ± 0.10	1.48 ± 0.10	73)
Water	AN	0.43 ± 0.3	0.47 ± 0.3	–	–	25)
Water	AN	0.7	0.8	–	–	70)
Water	DMF, DMSO, HMPA	–	–	–	–	71–73)
70% dioxan	DMSO	−0.05 ± 0.10	−0.40 ± 0.20	--	–	72)

not be rationalized by taking into account the change in concentration and in dielectric constant. The effect may be explained in a simple way, if ion-dipole association between Br^- and p-nitroaniline (dipole moment 6.32 D) increases the dissociation of ion pairs. The effects are larger when nitrophenols (meta and para) are added to dilute solutions of quarternary ammonium salts[76].

In case of ionophores the formation of ion pairs is dependent on the electrical charge e, the dielectric constant ϵ and the center-to-center distance a. The association constant K_A was calculated for rigid charged spheres with diameter a in a dielectric continuum[77]

$$K_A = K_0 \exp(e^2/a\,\epsilon\,kT) \tag{39}$$

Many examples of systems have been studied which are in agreement with Eq. (39) and where a plot of ln K_A versus $1/\epsilon$ is linear. But, again and again, salt-solvent systems were found with a non-linear dependence of ln K_A on $1/\epsilon$ and even with slopes of the wrong sign. Fuoss *et al.*[78] selected several special systems where the sphere-in-continuum model fails. The association constant of tetrabutylammonium picrate in acetonitrile-dioxan mixtures is much larger than K_A in mixtures of p-nitroaniline-dioxan. The difference is attributed to the formation of a dipole solvate between the picrate ion and p-nitroaniline.

More quantitative information about solvation equilibria resulted when the association of picric acid was studied in mixtures of acetonitrile (AN) with several hydroxylic solvents (water, MeOH, EtOH) and in water-EtOH mixtures. The dependence of ln K_A on $1/\epsilon$ is in no case linear and with two binary solvent systems (AN–MeOH, AN–EtOH) ln K_A even increases with ϵ. Fuoss *et al.*[78] introduced a conductance association constant K_Λ as a factor. The strange behavior of the systems studied were attributed to specific solvation of HPi by the hydroxylic solvents (base B). The following reaction scheme was assumed to hold.

$$HPi + nB \overset{K_S}{\rightleftharpoons} BH^+ \cdot B_{n-1}\,Pi^-$$

$$BH^+ \cdot B_{n-1}\,Pi^- \overset{K_A}{\rightleftharpoons} BH^+ + B_{n-1}\,Pi^-$$

The association constant K_Λ determined by experiment is related to K_A and to the concentration of base B in the following way:

$$K_\Lambda = K_A[1 + (1/K_S B^n)] \tag{40}$$

The analysis of the experimental data with Eq. (40) gave n = 4, and $K_S = 4.0 \times 10^{-7}$ (MeOH and EtOH), $K_S = 2.5 \times 10^{-5}$ (H_2O).

The competition between ion-pair formation and ion-ligand association was utilized to determine the hydration constant of NO_3^- in acetonitrile[79]. The relative association constant K_A^0/K_A of $AgNO_3$ in solutions of acetonitrile with small amounts of water was found to depend linearly on the water concentration. K_A^0 is the association constant of $AgNO_3$ in anhydrous acetonitrile. As Ag^+ is preferentially solvated by acetonitrile even in highly aqueous solvents[25, 70], the hydration of NO_3^-

$$NO_3^- + H_2O \overset{K_{1-}}{\rightleftharpoons} NO_3^- \cdot H_2O$$

effects a decrease of the ion-pair concentration. The experimental association constants were analysed using the relation between K_A and K_{1-}

$$K_A^0/K_A = 1 + K_{1-}[H_2O] \tag{41}$$

with the result: $K_{1-} = 1.7\ M^{-1}$.

The addition of polar molecules to electrolyte solutions effects a much larger change in conductance if low dielectric solvents are employed[80]. In a series of papers Gilkerson *et al.*[81] studied the ion-molecule interaction of tertiary and quarternary ammonium cations with Lewis bases in low dielectric solvents, like o-dichlorobenzene, chlorobenzene or 1,2-dichloroethane. The change of the ion-pair association constant with concentration of an additive L was attributed to the formation of 1 : 1 cation-molecule complexes:

$$M^+ + L \rightleftharpoons ML^+, \quad K_{1+} = [ML^+]/[M^+][L]$$

The ions are highly associated into ion pairs and due to this the Shedlovsky conductance equation[82] is applicable. Thus, the experiments are easily analysed. An equation analogous to Eq. (41)

$$\frac{K_A^0}{K_A} = 1 + K_{1+}[L] \tag{42}$$

was fitted to the experimental data. Only in some instances the existence of $[ML_2^+]$ had to be considered. The temperature dependence of K_A permitted the calculation of ΔH and ΔS[81h, 81k]. In the same way the association of alkali-metal cations with triphenylphosphine oxide in tetrahydrofurane was studied[81j]. In general, the experiments show that the dipole moments of the ligands, in addition to their basicities, are important in determining the extent of ion-ligand association. Furthermore, the association of tri-n-butylammonium cation with a group of ligand molecules in o-dichlorobenzene leads to a simple functional dependence between K_{1+} and free energy of transfer values[81i].

3. The Solubility of Electrolytes in Mixed Solvents

Chantooni and Kolthoff[83, 84] derived equations which permit the calculation of hydration constants of cations and anions from the solubility products of slightly soluble salts in solutions of acetonitrile with various concentrations of water. The ionic solubility of a salt was determined by measuring the conductance. The water concentration of the acetonitrile solution was always less than 1 M. The total ionic solubility product was expanded in powers of the water concentration. The coefficients are related to the individual ionic hydration constants and were evaluated by

curve fitting procedures. Li^+, Na^+, Cl^-, NO_3^- and several organic anions were found to form mono- and dihydrates. This elegant method has been applied only rarely[85,107].

4. Optical Spectroscopy

Spectroscopic studies, intended to obtain a better understanding of the state of solvation of ions in mixed solvents, have been carried out for a long time. Bjerrum and Jørgensen[86, 87] interpreted the change in spectral intensity in terms of ion hydration when the concentration of water in non-aqueous solutions of transition metal ions was changed gradually. Larson and Iwamoto[69] were able to determine all six hydration constants of aquo-copper(II) complexes in nitromethane from the absorption band of water[88]. The absorption spectrum of Cu^{2+}, which changes with decreasing amount of water in acetone and ethanol, was interpreted as being due to the successive replacement of two water molecules of the Cu^{2+} hydration shell by two molecules of either acetone or ethanol[89]. In a comprehensive publication Kuntz and Cheng[90] used infrared spectroscopy to study the solvation of univalent ions by water and methanol in a number of polar aprotic solvents. The evaluation of ionic solvation constants from spectral absorption experiments are not always straightforward.

5. Nuclear Magnetic Resonance

Since NMR has been introduced as a new method to study electrolyte solutions the knowledge of ion solvent interaction has advanced remarkably.

As we are engaged in solvation equilibria, only chemical shift data shall be discussed and the relaxation times T_1 and T_2 will not be taken into consideration. Furthermore, to clarify the process, the chemical shift experiments are separated into two classes which differ in the magnitude of solvent exchange kinetics. In solutions of a few ions, *e.g.*, Al^{3+}, Ga^{3+}, Be^{2+} and Mg^{2+}, in a number of donor solvents, the lifetime, τ, of the solvent protons in the solvation shell is sufficiently long ($\tau >$ ca. 10^{-4} sec), for two signals to be observed. With respect to resonance measurements of the ion nucleus the long lifetime of solvating molecules sometimes has the effect that several lines for an ion in a mixed solvent system may be observed at the same time. In the other class of experiments the exchange kinetic is fast ($\tau <$ ca. 10^{-4} sec) and only one signal can be observed.

If the lifetime of solvent molecules in the solvation shell of a cation is longer than 0.1 msec, the solvation number n of the cation follows directly from the area of the NMR line for the coordinated molecules. In pure solvents, n is equal to 6 for Al^{3+}, Ga^{3+}, Mg^{2+} and equal to 4 for Be^{2+} [2, 91, 92]. In mixed solvents the mean number $\bar{n}$ of molecules of a solvent component coordinating a cation depends on the composition of the mixture. In mixtures of water and polar aprotic solvents Al^{3+} is preferentially hydrated[92]. In water-dimethylsulphoxide the line of DMSO molecules in the primary solvation shell of Al^{3+} is clearly separated from the line of free DMSO[93] and the mean coordination number $\bar{n}$ is accessible. $\bar{n}$ depends on the mole fraction $x_{H_2O} = 1 - x_{DMSO}$ in an unexpected manner: Al^{3+} is preferentially solvated by water at $x_{H_2O} > 0.8$ and by DMSO at $x_{H_2O} < 0.8$. This special behavior of DMSO-

water mixtures has already been discussed in previous sections.

Olander *et al.*[94] determined the solvation constants of the equilibria

$$Al(DMSO)_{6-(i-1)}(H_2O)_{i-1}^{3+} + H_2O \overset{K_i}{\rightleftharpoons} Al(DMSO)_{6-i}(H_2O)_i + DMSO$$

from the mean coordination number $\bar{n}$ by a procedure introduced by Bjerrum[65]. Delpuech *et al.*[95] adopted the same method to calculate solvation equilibrium constants for Al^{3+} and Be^{2+} in aqueous mixtures of organophosphorus solvents. Generally, the accuracy of $\bar{n}$ and, therefore, of K_i is limited by the overlap of the lines for bound and free molecules. Under favorable conditions all ionic species which are differing in the composition of the coordination shell can be observed separately, and all K_i values result from the integration of the various lines of coordinated molecules. The ^{1}H-NMR spectra of solutions with a behavior like this have been observed for $Al(ClO_4)_3$-water-acetonitrile[97], $Mg(ClO_4)_2$-water-acetone[98, 99] and $Al(ClO_4)_3$-DMSO-DMF-nitromethane. In the last example nitromethane acts merely as an inert diluent. In the ^{31}P-NMR spectra of the system $BeCl_2$-hexamethylphosphoramide-water[95] and in the ^{27}Al-NMR spectra of the systems $Al(ClO_4)_3$-DMF-DMSO-nitromethane[100] and $Al(ClO_4)_3$-trimethylphosphate-DMSO-nitromethane[101] all different solvates could be observed as separate lines.

If the exchange of solvent molecules is fast ($\tau < 10^{-4}$ sec) the dependence of the chemical shift δ on electrolyte concentration, solvent composition and temperature is interpreted in terms of ion solvation. The chemical shift difference δ of the solvent protons in the presence and absence of an electrolyte is, generally, assumed to be the sum of three contributions:

$$\delta = p^+\delta^+ + p^-\delta^- + p^0\delta^0 \qquad (43)$$

p^+, p^- and p^0 are the fractions of solvent molecules in the cationic solvation shell, in the anionic solvation shell and of those in the bulk solvent. δ^+, δ^- and δ^0 are the chemical shifts of molecules surrounding the cation, the anion and in the bulk solvent. In dilute electrolyte solutions δ^0 is the chemical shift of the molecules in solution with zero concentration of electrolyte. Different methods have been applied to estimate either $p^+\delta^+$ or $p^-\delta^-$ in mixed solvents which permits the calculation of solvation numbers over the total range of mole fraction[46, 102]. If the solvents differ remarkably in their strength to solvate an ion, the coordination number results directly out of the graph of δ versus the ratio of moles coordinating solvent to moles electrolyte. The slope of the curve changes appreciably when the mole ratio is roughly equal to the coordination number. Some results are collected in Table 4. The influence of counterions can be neglected when they are large and interact much weaker with the coordinating solvent. Thus, no break could be observed for $(n\text{-}Bu)_4NClO_4$ with DMSO in PC[105], though $LiClO_4$ as well as $(n\text{-}Bu)_4Br$ effect a change in the slope of the chemical shift graph near a 4 : 1 ratio.

Cogly, Butler and Grunwald[107] were the first who determined solvation equilibrium constants from chemical shift measurements. The chemical shifts of water in propylene carbonate containing various salts were extrapolated to zero water concentration. The dependence of the chemical shift of water at infinite dilution in PC

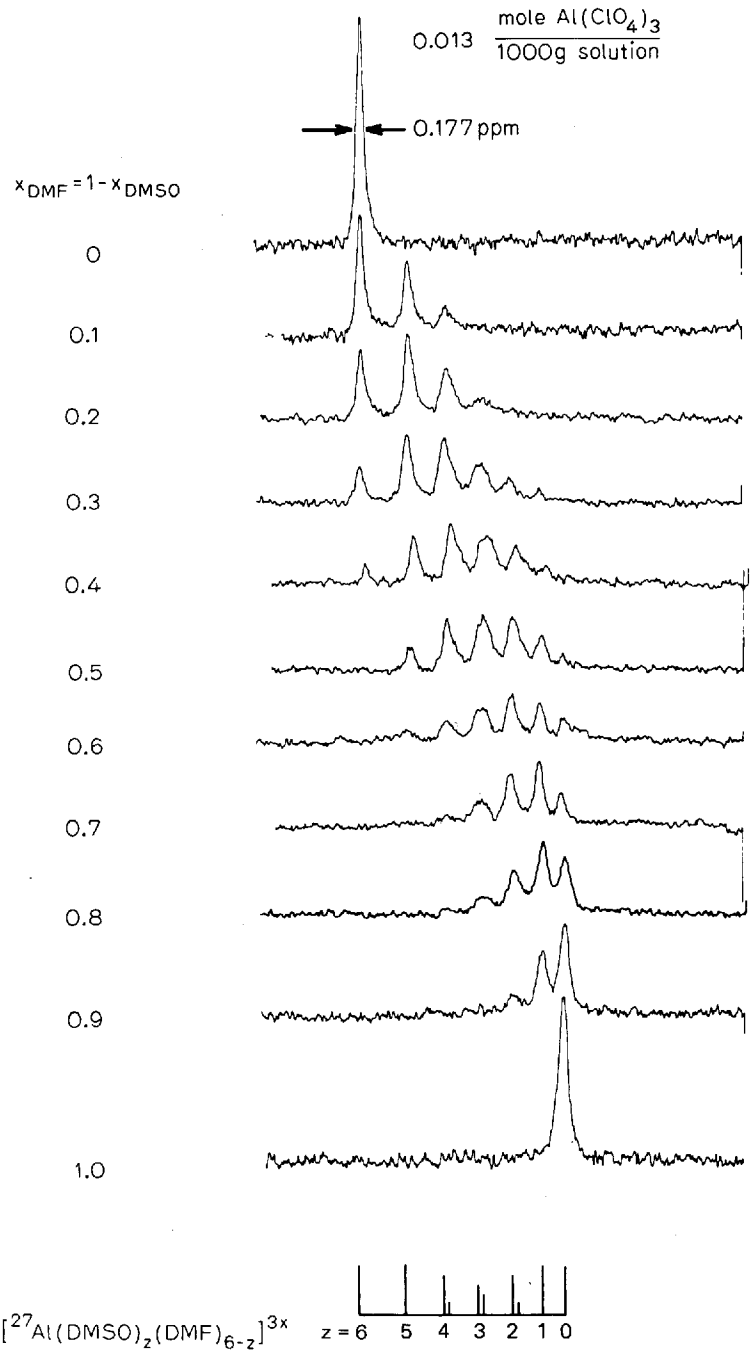

Fig. 2. ^{27}Al-NMR spectra of $Al(ClO_4)_3$ solutions in mixtures of DMSO and DMF in nitromethane

Table 4. Coordination numbers from mole ratio studies

Mole ratios	Electrolyte	Solvent	Method	Ref.
Acetone : $Li^+ \cong 4.4 : 1$	$LiClO_4$, LiI	Nitromethane	^{1}H-NMR, IR	104d)
Acetone : $Li^+ \cong 4 : 1$	$LiClO_4$, LiI	Nitromethane	^{23}Na-NMR	106)
PC : $Li^+ \cong 4.2 : 1$	$LiClO_4$	Nitromethane	^{1}H-NMR	105)
DMSO : $Li^+ \cong 2 : 1$	$LiClO_4$, LiI	1-Pentanol	^{1}H-NMR	104a)
1M2PY : $Li^+ \cong 2 : 1$ and 4 : 1	$LiClO_4$	Dioxan	fir	104b)
1M2PY : $Li^+ \cong 4.5 : 1$	$LiClO_4$, LiI	Dioxan	^{1}H-NMR	104b)
DMSO : $Na^+ \cong 1 : 1$	NaI	1-Pentanol	^{1}H-NMR	104a)
DMSO : $Na^+ \cong 6 : 1$	$NaAlBu_4$	Dioxan	^{1}H-NMR	104b)
1M2PY : $Na^+ \cong 4 : 1$	$NaAlBu_4$	Dioxan	^{1}H-NMR	104b)
THF : $Na^+ \cong 1 : 1$	$NaAlBu_4$	Cyclohexane	^{1}H-NMR	103)
DE : $Na^+ \cong 1 : 1$	$NaAlBu_4$	Cyclohexane	^{1}H-NMR	103)
DMSO : $NH_4^+ \cong 2 : 1$	NH_4SCN	1-Pentanol	^{1}H-NMR	104a)
DMSO : $Ag^+ \cong 4 : 1$	$AgClO_4$	PC	^{1}H-NMR	52)
DMSO : $Ag^+ \cong 4.0 : 1$	$AgClO_4$	Nitromethane	^{1}H-NMR	105)
PC : $Br^- \cong 4 : 1$	Bu_4NBr	Nitromethane	^{1}H-NMR	105)
PC : $I^- \cong 3.6 : 1$	Bu_4NI	Nitromethane	^{1}H-NMR	105)

DE = diethylether
1M2PY = 1-methyl-2-pyrrolidone
PC = propylene carbonate
THF = tetrahydrofurane

on salt concentration was analysed and under mild extra-thermodynamic assumptions the molal association constants for several univalent ions with water were evaluated. They are in good agreement with the solvation constants from solubility measurements. The formation constants for mono-, di- and trihydrates of Li^+ could be derived. This publication has stimulated a lot of further investigations[108–116].

In order to simplify the determination of free energies of transfer, Covington *et al.*[62] deduced a relation between ΔG_t^0 and the chemical shifts of ions. It is well known that the chemical shift of alkali metal and halide ions in mixed solvents (*e.g.* A and B) is not at all linearly dependent on the mole fraction $x_B = 1 - x_A$[117]. If the chemical shift, δ, at infinite dilution is assumed to be an additive function of the contribution δ_i of all ionic species, which differ in the composition of A and B in the primary solvation shell, Eq. (44) is a relation between the chemical and with the distribution of the different ionic solvates I A_{n-i} B_i [Eqs. (12) and (17)]

$$\delta = \sum_{i=0}^{n} \Phi_{n-i,i}^0 \, \delta_i \tag{44}$$

As the chemical shifts δ_i are mainly sensitive to the immediate environment of the ion, it is obvious that the intrinsic shifts δ_i of the various solvated species depend on the fraction of B in the solvation shell,

$$\delta_i = \frac{i}{n} \delta_B \tag{45}$$

δ_B is the chemical shift difference of the ion at infinite dilution in pure B and in pure A. $\Phi^0_{n-i,i}$ depends on the stepwise formation constants K_i [Eq. (35)] and the activity ratio $y = [B]/[A]$. As the solvent exchange is fast in all systems studied and only one mean resonance line can be observed, the n equilibrium constants K_i are unknown. Therefore, it is reasonable to suppose that the individual equilibrium constants are related entirely to statistical requirements. Thus, the n equilibrium constants are replaced by one constant $\beta_n = K_1 \cdot K_2 \ldots K_n$ [Eq. (32)]

$$K_i = \beta_n^{1/n} \frac{n + 1 - i}{i} \tag{46}$$

If one considers Eqs. (17), (36), (44), and (45),

$$\frac{\delta}{\delta_B} = \frac{\beta_n^{1/n} y}{1 + \beta_n^{1/n} y} \tag{47}$$

A simple rearrangement of Eq. (47) leads to

$$\beta_n = \left(\frac{\delta}{\delta_B - \delta} \frac{[A]}{[B]} \right)^n \tag{48}$$

Eq. (47) has been used to determine β_n from a plot of $1/\delta$ versus $1/y$[62, 117].

One obtains a relation between ΔG_t^0 and the infinite dilution shift δ, if the first term on the right hand side of Eq. (37) is simplified under the assumption that the relative concentrations of all individual ionic species correspond to the statistical distribution,

$$1 + \sum_{i=1}^{n} \beta_i \frac{[B]^i}{[A]^i} = \left(1 + \beta_n^{1/n} \frac{[B]}{[A]} \right)^n \tag{49}$$

Combining Eqs. (37), (48) and (49),

$$\Delta G_t^0 = -n\,RT \ln \frac{\delta_B}{\delta_B - \delta} - n\,RT \ln x_A + \sum_{i=0}^{n} \Phi^0_{n-i,i} (G'^0_{n-i,i})^{elec} - (G'^0_{n,0})^{elec} \tag{50}$$

This equation corresponds to Eq. (28) of Covington *et al.*[62] (Part 2), who found that ΔG_t^0 values from electrochemical and spectroscopic experiments agree satisfactorily in mixtures of isodielectric solvents. Relations between ΔG_t^0 and δ have also been treated which involve change of solvation number and nonstatictical distribution of the solvated species[62].

IV. Transference Numbers

In electrolyte solutions the transference or transport number of an ion is often defined as the fraction of the current which it transports. But ion-pair formation or stepwise dissociation is the normal behavior and the effects observed, a moving boundary, or the change in concentration in an electrode compartment during a Hittorf experiment is the only information available; therefore one has to use the term ion constituent instead of the term ion as shown by Noyes and Falk[118] and also by Spiro[119]. The ion constituents of an electrolyte are the ion-forming portions of the electrolyte molecule. In the following we are interested in ion-solvent interactions in mixed solvents. With few exceptions the dielectric constant of nonaqueous solvents is smaller than that of water and full dissociation of electrolytes is the exception. However, the influence of ion association on the solvent transport is neglected, for the contribution of ion pairs is, in general, small and taking it into consideration, the experimental accuracy has to be much better than to-days methods offer. While the ionic association constant is a well known quantity only at low electrolyte concentrations, the solvent transport numbers are obtainable by experiment only at higher electrolyte concentrations.

Transference numbers are quantities which are treated in the thermodynamics of irreversible processes. In a continuous system, the average velocity v_i of a species i related to a reference velocity ω, describes the diffusional motion of the species i. The diffusion current density J_i represents in moles/cm^2 sec the flow of species i in unit time perpendicular to a surface of unit area which by itself is moving with velocity ω[120].

$$J_i = c_i (v_i - \omega) \tag{51}$$

where c_i is the concentration of species i in moles per liter. Treating transference numbers, the fixation of the reference velocity ω is quite important. In text books of thermodynamics of irreversible processes[120, 121], it is shown that the reference velocity ω may be chosen such that the following relations

$$\omega = \Sigma\, w_i\, v_i \tag{52}$$

$$\Sigma\, \omega_i = 1 \tag{53}$$

hold. The summation comprises all species i which one wants to consider. ω_i are normalized weight factors.

The transference number t_i is the fraction of the total electric current density I carried by the i-th ion relative to the reference system chosen:

$$t_i = \frac{z_i F J_i}{I} = \frac{z_i F c_i (v_i - \omega)}{I} \tag{54}$$

where F is the Faraday constant. The total electric current density is

$$I = \Sigma\, z_i F J_i \tag{55}$$

where the summation is over all charged species. Now, from (54) and (55) follows:

$$\Sigma t_i = 1 \tag{56}$$

With Eqs. (51) and (55) one obtains

$$I = \Sigma z_i F c_i v_i \tag{57}$$

because of the condition for electric neutrality $\Sigma z_i c_i = 0$. As it is obvious from Eq. (57), the total electric current is independent of the reference velocity chosen.

In electrolyte solutions with neutral solutes or with two or more solvent components, the flow of uncharged molecules in electrical transport experiments had to be taken into consideration. It is useful to introduce a reduced transference number τ_i. For one Faraday, τ_i moles of species i, charged (ion constituent) or uncharged, are transferred in the direction of positive current. The reduced transference numbers τ_i are defined as

$$\tau_i = \frac{F J_i}{I} \tag{58}$$

The relation between τ_i of a charged species i and its transference number t_i is

$$t_i = z_i \tau_i \tag{59}$$

In the literature, several different notations for t_i and τ_i have been used. Today, the terms transport number and transference number are used for t_i side by side[122]. Staverman[123] introduced the terms "reduced electrical transport number" for τ_i and "electrical transport number" for t_i. Scatchard[38] called τ_i a transference number and t_i a transport number, while Agar[124] introduced the notation Washburn number if τ_i is referred to one of the uncharged components. The solvent transference number Δ, which was introduced by C. Wagner[125], is a reduced transference number with the reference system fixed to the sum of moles of all solvent components. "Elektrische Lösungsmittelüberführung", $L^{(*)}$, (electrolytic solvent transport)[120, 126] originates in the proposal of Nernst[127] to discriminate between solvent molecules in the solvation shell of the ions and the "free" solvent. $L^{(*)}$ is a reduced transference number referred to the motion of the free solvent. Inspection of Eqs. (54) and (57) shows that τ_i depends on the reference system used. This will be shown in the following section in more detail.

a) A Binary Electrolyte in a Single Solvent

Following Haase's treatment[120], the transference numbers t_i of the ions (i = +, −) of a binary electrolyte in a single solvent 1 (*e.g.* water) shall be discussed with respect to the Hittorf reference system and the Washburn reference system.

1. The Hittorf Reference System

In this system the reference velocity chosen is the velocity v_1 of the solvent. With $\omega = v_1$ [Eq. (52)] and $\omega_1 = 1$ [Eq. (53)] the diffusion current density of the solvent $J_1^{(1)}$ is zero and

$$J_i^{(1)} = z_i F (v_i - v_1) \quad (i = +, -) \tag{60}$$

The index 1 for the sole solvent has been used to facilitate the comparison with mixed solvents. The transference number

$$t_i^{(1)} = \frac{z_i F J_i}{I} \tag{61}$$

is the well known Hittorf transference number.

2. The Washburn Reference System

The interaction of ions with solvent molecules suggests a more detailed picture in which during electrolysis the cations are transporting n_{1+} solvent molecules into the cathode compartment and the anions n_{1-} solvent molecules out of that region into the opposite direction. The residual molecules of the solvent, which remain unaffected by the ion movement, are regarded as "free". $n_{1i} = n_{1+}$, n_{1-} are total solvation numbers of the ions which differ from those in Chapter III. The transference numbers $t_i^{(*)}$ referred to the free solvent (index *) are called "true" transference numbers[120]. The diffusion current density $J_i^{(*)}$ referred to the velocity $v_1^{(*)}$ of the free solvent results from Eq. (51):

$$J_i^{(*)} = c_i (v_i - v_1^{(*)}) \qquad (i = +, -) \tag{62}$$

The "true" transference number $t_i^{(*)}$ follows from (54) and (62)

$$t_i^{(*)} = \frac{z_i F J_i^{(*)}}{I} = \frac{z_i F c_i (v_i - v_1^{(*)})}{I} \tag{63}$$

The velocity v_1 of the total solvent is related to the velocity $v_1^{(*)}$ of the free solvent by[120]

$$v_1 c_1 = v_1^{(*)} c_1^{(*)} + \Sigma n_{1i} c_i v_i \tag{64}$$

The summation is over all ionic species i (i = +, −). With

$$c_1 = c_1^{(*)} + \Sigma n_{1i} c_i \tag{65}$$

one obtains from (64)

$$c_1(v_1 - v_1^{(*)}) = \Sigma\, n_{1i}\, c_i (v_i - v_1^{(*)}) \tag{66}$$

Now, the reduced transference number τ_1 [Eq. (58)] of the solvent

$$\tau_1^{(*)} = \frac{F\, J_1^{(*)}}{I} = \frac{F\, c_1 (v_1 - v_1^{(*)})}{I} \tag{67}$$

can be expressed as a function of the solvation numbers. With (63) and (66) one obtains

$$\tau_1^{(*)} = \Sigma\, n_{1i}\, \frac{t_i^{(*)}}{z_i} = n_{1+}\, \frac{t_+^{(*)}}{z_+} + n_{1-}\, \frac{t_-^{(*)}}{z_-} \equiv L_1^{(*)} \tag{68}$$

The reduced transference number of the solvent is equal to the electrolytic solvent transport $L_1^{(*)}$ and may be calculated numerically only if $t_i^{(*)}$ or n_{1i} are known from other experiments. With Eqs. (60), (61), (63) and (66) a relation between $t_i^{(1)}$ and $t_i^{(*)}$ may be calculated:

$$\begin{aligned} \frac{t_i^{(1)}}{t_i^{(*)}} &= \frac{v_i - v_1}{v_i - v_1^{(*)}} = 1 - \frac{v_1 - v_1^{(*)}}{v_i - v_1^{(*)}} \\ &= 1 - \frac{z_i\, c_i\, \Sigma\, n_{1i}\, c_i (v_i - v_1^{(*)})}{c_1\, t_i^{(*)}\, I/F} \end{aligned} \tag{69}$$

From Eqs. (63) and (68) now results

$$t_i^{(1)} = t_i^{(*)} - \frac{z_i\, c_i}{c_1}\, \Sigma\, n_{1i}\, \frac{t_i^{(*)}}{z_i} = t_i^{(*)} - \frac{z_i\, c_i}{c_1}\, L_1^{(*)} \tag{70}$$

b) An Electrolyte in a Binary Solvent Mixture

As before, the binary electrolyte is assumed to be fully dissociated. The subscripts used are i = +, – for the ions and k = 1, 2 for the solvent components. n_{1i} and n_{2i} are the (four) solvation numbers.

1. The Velocity of One Solvent Component as Reference Velocity

Reference velocity $\omega = v_k$

With k = 1, the transference number $t_i^{(1)}$ follows directly from Eq. (54) on substituting $\omega = v_1$:

$$t_i^{(1)} = \frac{z_i\, F\, c_i (v_i - v_1)}{I} \tag{71}$$

The reduced transference number $\tau_2^{(1)}$ of solvent component 2 is

$$\tau_2^{(1)} = \frac{F\, c_2 (v_2 - v_1)}{I} = w_2 \tag{72}$$

With k = 2, the reference velocity is equal to the velocity of solvent component 2, $\omega = v_2$, and one obtains analogously

$$t_i^{(2)} = \frac{z_i F\, c_i (v_i - v_2)}{I} \tag{73}$$

and

$$\tau_i^{(2)} = \frac{F\, c_1 (v_1 - v_2)}{I} = w_1 \tag{74}$$

The reduced transference numbers $\tau_2^{(1)}$ and $\tau_1^{(2)}$ are the Washburn numbers w_2 and w_1 introduced by Agar[124]. In his discussion the movement of a neutral solute is treated with respect to the solvent. Later on, Feakins[128] used Washburn numbers to explain the solvent transport in mixtures of two solvent components when the solvent mole fraction is varied between 0 and 1.

Since the total electric current density I is independent of the reference velocity

$$I = \Sigma\, z_i F\, c_i (v_i - v_2) = \Sigma\, z_i F\, c_i (v_i - v_1) \tag{75}$$

one may easily derive relations between the transference numbers and the Washburn numbers in the two reference systems:

$$\frac{w_1}{c_1} = -\frac{w_2}{c_2} \tag{76}$$

and

$$\frac{t_i^{(1)}}{z_i} - \frac{t_i^{(2)}}{z_i} = \frac{c_i}{c_2} w_2 = -\frac{c_i}{c_1} w_1 \tag{77}$$

Eq. (76) is a relation first deduced by Feakins[128].

2. The Barycentric Velocity v_m of the Solvent Mixture as Reference Velocity

If after termination of a Hittorf transference experiment the changes in concentration in the electrode compartments are referred to a fixed weight of solvent, the reference velocity $\omega = v_m$ is equal to

$$v_m = \frac{c_1 v_1 M_1 + c_2 v_2 M_2}{c_1 M_1 + c_2 M_2} \tag{78}$$

with M_1, M_2 the molecular weights of the solvent components. Eq. (78) follows from Eq. (52) with the weight factors $\omega_k = c_k M_k/(c_1 M_1 + c_2 M_2)$. From Eqs. (54) and (58) follows

$$t_i^{(m)} = \frac{z_i F c_i (v_i - v_M)}{I} \quad (i = +, -) \tag{79}$$

and

$$\tau_k^{(m)} = \frac{F c_k (v_k - v_M)}{I} \quad (k = 1, 2) \tag{80}$$

As one can see immediately it is

$$\tau_i^{(m)} M_1 = -\tau_2^{(m)} M_2 \tag{81}$$

and from Eqs. (74) and (80) follows, *e.g.*

$$\tau_1^{(m)} = w_1 \frac{c_2 M_2}{c_1 M_1 + c_2 M_2} \tag{82}$$

and a similar combination adopting Eqs. (76) and (81). Only two out of several relations between $t_i^{(m)}$ and $t_i^{(k)}$ are

$$\frac{t_i^{(m)}}{z_i} = \frac{1}{z_i} \frac{c_1 M_1 t_i^{(1)} + c_2 M_2 t_i^{(2)}}{c_1 M_1 + c_2 M_2} \tag{83}$$

$$= \frac{t_i^{(1)}}{z_i} - \frac{c_i M_2 w_2}{c_1 M_1 + c_2 M_2} \tag{84}$$

This relation was first deduced by Feakins[128].

3. The Velocity of "Free" Solvent as Reference Velocity

With

$$c_k v_k = c_k^{(*)} v_k^{(*)} + \Sigma n_{ki} c_i v_i \tag{85}$$

and $(k = 1, 2)$

$$c_k = c_k^{(*)} + \Sigma n_{ki} c_i \tag{86}$$

where the summation is over the ions $(i = +, -)$, one obtains

$$c_k (v_k - v_k^{(*)}) = \Sigma n_{ki} c_i (v_i - v_k^{(*)}) \tag{87}$$

a relation which was used previously to introduce the solvent transport number $L_k^{(*)}$ in an electrolyte solution with only one solvent component. A consequence of the assumption that one can differentiate between solvent molecules which are solvating the charged species, and "free" solvent molecules, which remain unaffected by the passage of the current, is the equality

$$v_1^{(*)} = v_2^{(*)} \tag{88}$$

This identity means that the reference velocity ω is equal to the "free" solvent velocities of both components.

$$\omega = v_1^{(*)} = v_2^{(*)} = v^{(*)} \tag{89}$$

The transference numbers $t_i^{(*)}$

$$t_i^{(*)} = \frac{z_i F c_i (v_i - v^{(*)})}{I} \qquad (i = +, -) \tag{90}$$

and the reduced transference numbers $\tau_k^{(*)}$ of the solvent components k, where $\tau_k^{(*)}$ is equal to the "electrolytic solvent transport" $L_k^{(*)}$ of the solvent components [compare Eq. (68)]

$$\tau_k^{(*)} = \frac{F c_k (v_k - v_k^{(*)})}{I} = L_k^{(*)} \qquad (k = 1, 2) \tag{91}$$

may be used to deduce several relations with corresponding quantities of other reference systems. As an example, only the following connection shall be cited

$$L_2^{(*)} = \frac{c_2}{c_1} (L_1^{(*)} - w_1) \tag{92}$$

4. The Mean Molar Velocity $\bar{v}$ of the Solvent Mixture as Reference Velocity

If after the termination of a Hittorf experiment the concentration changes are referred to a fixed number of total moles of solvent molecules, the reference velocity is given by

$$\omega = \bar{v} = \frac{c_1 v_1 + c_2 v_2}{c_1 + c_2} \tag{93}$$

All quantities referred to $\bar{v}$ are labelled with a horizontal bar. The relation between

$$\bar{t}_i = \frac{z_i F c_i (v_i - \bar{v})}{I} \qquad (i = +, -) \tag{94}$$

and $t_i^{(m)}$ shows that the difference is negligible, if $M_1 \cong M_2$:

$$\bar{t}_i = t_i^{(m)} - \frac{z_i c_i c_2 (M_2 - M_1)}{(c_1 + c_2)(c_1 M_1 + c_2 M_2)} \tau_1^{(2)} \tag{95}$$

The reduced transference number $\bar{\tau}_1$ of solvent component k = 1

$$\bar{\tau}_1 = \frac{F c_1 (v_1 - \bar{v})}{I} \tag{96}$$

is easily brought into connection with the electrolytic solvent transport $\tau_k^{(*)}$, if $v_1^{(*)}$ and $v_2^{(*)}$ are added to or substracted from $(v_1 - \bar{v})$. With the Eqs. (93) and (91) it follows

$$\bar{\tau}_1 = x_2 L_1^{(*)} - x_1 L_2^{(*)} = -\bar{\tau}_2 \equiv -\Delta \tag{97}$$

This solvent transference number Δ was first introduced by Strehlow and Koepp[129]. With Eq. (68) one obtains

$$\Delta = x_1 \Sigma n_{2i} \frac{t_i^{(*)}}{z_i} - x_2 \Sigma n_{1i} \frac{t_i^{(*)}}{z_i} \quad (i = +, -) \tag{98}$$

For a uni-univalent electrolyte Δ depends on the four solvation numbers n_{1+}, n_{1-}, n_{2+}, and n_{2-} in the following way

$$\Delta = (x_1 n_{2+} - x_2 n_{1+}) t_+^{(*)} - (x_1 n_{2-} - x_2 n_{1-}) t_-^{(*)} \tag{99}$$

In the solvation shell of the cation, *e.g.* the excess of solvent component 2 over the respective concentration of 2, if the composition of the solvation shell is like that of the bulk, is given by[129]

$$n_{2+}^* = x_2 \left(\frac{n_{2+}}{x_2} - \frac{n_{1+}}{x_1} \right) \tag{100}$$

Similarly, the excess concentration of component 1 in the solvation shell of the anions is

$$n_{1-}^* = x_1 \left(\frac{n_{1-}}{x_1} - \frac{n_{2-}}{x_2} \right) \tag{101}$$

x_1, x_2 are the mole fractions of the solvents. With Eqs. (99), (100) and (101) one finds[129]

$$\Delta = x_1 x_2 \left[\frac{n_{2+}^*}{x_2} t_+^{(*)} + \frac{n_{1-}^*}{x_1} t_-^{(*)} \right] \tag{102}$$

Δ is the concentration change of species 2 in the cathode compartment during a Hittorf experiment in the mean molar velocity reference system. As can be shown using Eqs. (82), (92) and (97), the following relations also hold

$$\Delta = x_1 w_2 = -x_2 w_1 \tag{103}$$

which was found by Spiro[130] and

$$\Delta = x_1 \tau_2^{(m)} - x_2 \tau_1^{(m)} \tag{104}$$

A relation between Washburn number w_1, *e.g.* and solvation numbers follows from Eqs. (91), (92) and (68)

$$w_1 = \frac{t_+^{(*)}}{z_+}\left(n_{1+} - \frac{c_1}{c_2} n_{2+}\right) - \frac{t_-^{(*)}}{z_-}\left(n_{1-} - \frac{c_1}{c_2} n_{2-}\right) \tag{105}$$

For a uni-univalent electrolyte one obtains with Eqs. (100) and (101)

$$w_1 = t_+^{(*)} n_{1+}^* - t_-^{(*)} n_{1-}^* \tag{106}$$

when n_{1+}^* and n_{1-}^* are the number of moles of component 1, transported from cation and anion, relative to component 2 per Faraday.

c) Experimental Determination of Solvent Transport in Mixed Solvent Electrolyte Solutions

Two methods have been used to obtain Washburn numbers w_2, w_1 or solvent transference numbers Δ.

1. The Hittorf Transference Method

During a Hittorf transference experiment in a mixed solvent electrolyte solution, the concentration of the electrolyte as well as the composition of the solvent changes in the electrode compartments. The determination of the solvent transport requires detailed analysis of the electrode compartment. This has been done using refractive index or density measurements[129, 131–133]. As the time of electrolysis is limited, the variation in solvent composition is at most 1%. The solvent transference number is largest in the case of heteroselective solvation when the cation is preferentially solvated by one component, the anion by the other. Δ is a function of four solvation numbers as shown by Eq. (99). With the assumption of a monotonic dependence of the solvation numbers on solvent composition and with reasonable maximum solvation numbers, all solvation numbers can be estimated semiquantitatively under favorable conditions. This has been done by Strehlow and Koepp[129] for $AgNO_3$ in H_2O–CH_3CN mixtures. In agreement with numerous experiments with this system[134] Ag^+ is more strongly solvated by CH_3CN, and NO_3^- more strongly by water.

Heteroselective solvation was also found in the system $ZnCl_2$–N_2H_4–H_2O[132]. The values of Δ remain much smaller in the case of insignificant selective solvation or of homoselective solvation. Further experiments have been performed in mixtures of water with methanol[131, 133] and acetonitrile[132].

2. The Electromotive Force Method

The solvent transport may also be obtained using emf measurements. As shown by Scatchard[38], the electromotive force of a concentration cell with transport may be expressed as

$$\frac{EF}{RT} = \frac{E_0' F}{RT} - \Sigma \nu_i' \ln a_i' - \int_{a'}^{a''} \Sigma \tau_i \, d \ln a_i - \Sigma \nu_i'' \ln a_i'' - \frac{E_0'' F}{RT} \tag{107}$$

$'$ and $''$ denote the region of the two half-cells. E_0' and E_0'' are the standard potentials of the two electrodes. a_i is the activity of species i and τ_i its reduced transference number. ν_i' and ν_i'' moles of species i are formed on passing one Faraday.

Feakins *et al.*[128, 135] used concentration cells with transference to get Washburn numbers. As water is nearly always the one component of the solvent mixtures used, in the following the abbreviation W and S for water and the non-aqueous solvent, respectively, shall be used. The emf of the cell (C)

$$\mathrm{Ag - AgCl} \left| \begin{array}{c|c} \mathrm{MCl}(a_\pm') & \mathrm{MCl}(a_\pm'') \\ \mathrm{W}(a_W') & \mathrm{W - S}(a_W'', a_S'') \end{array} \right| \mathrm{AgCl - Ag} \tag{C}$$

follows from Eq. (107), whereby $E_0' = E_0''$ and $\nu_0' = -1$, $\nu_0'' = +1$. Solvent S is assumed to be stationary and used as reference.

$$E_- \frac{F}{RT} = \ln a_-' - \ln a_-'' - \int_{a'}^{a''} \left\{ \frac{t_+^{(S)}}{z_+} d \ln a_+ + \frac{t_-^{(S)}}{z_-} d \ln a_- + w_W \, d \ln a_W \right\} \tag{108}$$

With

$$\ln a_-' - \ln a_-'' = - \int_{a'}^{a''} d \ln a_- \tag{109}$$

one obtains

$$E_- = \frac{2\,RT}{F} \int_{a_\pm''}^{a_\pm'} t_+^{(S)} \, d \ln a_\pm + \frac{RT}{F} \int_{a_W''}^{a_W'} w_W \, d \ln a_W \tag{110}$$

where a_W is the activity of water in one half cell (a_W') or the other (a_W''). A corresponding equation holds if water is used as reference. Since $a_\pm$ is referred to the standard state in one special solvent (*e.g.* water), the free energy of transfer of MX must be known from independent measurements (*e.g.* from the emf of a cell without transference) to calculate the Washburn number. Furthermore, $t_+^{(S)}$ is set equal to the Hittorf transference number which is reasonable within experimental accuracy.

$a_\pm''$ was adjusted to be approximately equal to $a_\pm'$ and the first term of Eq. (110)

could be neglected if the variation of the transference number $t_+^{(S)}$ was small. Otherwise a change of t_+ over the region of the liquid junction was taken into consideration[128, 135]. In dilute solutions, a_W is practically independent of the electrolyte concentration and w_W could be calculated from the second integral in Eq. (110).

Washburn numbers of hydrochloric acid and of alkali-metal halides have been determined in mixtures of water with methanol[128, 135, 137, 139, 140], ethanol[140], glycerol[141, 142], dimethylsulphoxide[138, 143] and dioxan[135, 136]. w_W depends on the "excess" hydration numbers of cation and anion and the transference number [Eq. (106)]. Therefore, in several systems the dependence of w_W on mole fraction shows maxima and minima. Only in the case of marked heteroselective solvation a simple dependence on solvent composition is obvious.

Another way of determining the solvent transport by emf measurements has been proposed by C. Wagner[125]. The two half cells contain two solvent mixtures of similar composition which are both saturated with a sparingly soluble salt, *e.g.* a silver salt AgX. Though the chemical potential of AgX is the same throughout the galvanic cell with transport, the emf is different from zero since the chemical potential of the solvent is different in the two half cells and Δ moles of the non-aqueous solvent component are transported into the cathode compartment per Faraday.

With the mean molar velocity $\bar{v}$ of the solvent mixture as reference velocity the reduced transference number of the non-aqueous component is equal to Δ, as shown in Eq. (97).

The emf E_+ of the cell

$$\mathrm{Ag}\left|\begin{array}{l|l}\mathrm{AgX(sat)} & \mathrm{AgX(sat)}\\ \mathrm{W-S}(a'_W, a'_S) & \mathrm{W-S}(a''_W, a''_S)\end{array}\right|\mathrm{Ag} \qquad \text{(D)}$$

follows from Eq. (107) with $E'_0 = E''_0$ and $\nu'_+ = +1$, $\nu''_+ = -1$,

$$E_+ \frac{F}{RT} = -\ln a'_+ - \int_{a'}^{a''} \left\{ \bar{t}_+ \, d\ln a_+ - \bar{t}_- \, d\ln a_- + \bar{\tau}_W \, d\ln a_W + \bar{\tau}_S \, d\ln a_S \right\} + \ln a''_+ \qquad (111)$$

and

$$E_+ = -\frac{2RT}{F}\int_{a'_\pm}^{a''_\pm} \bar{t}_- \, d\ln a_\pm - \frac{RT}{F}\int_{a'}^{a''} \left\{ \bar{\tau}_W \, d\ln a_W + \bar{\tau}_S \, d\ln a_S \right\} \qquad (112)$$

With saturated solutions the first term is zero and only the second term has to be treated.

With $\bar{\tau}_S = \Delta = -\bar{\tau}_W$ and the Gibbs-Duhem equation

$$x_W d\mu_W + x_S d\mu_S = 0 \qquad (113)$$

where x_W, x_S are the mole fractions of water and the non-aqueous component S, it follows from Eq. (112)

$$E_+ = -\frac{RT}{F}\int_{a'_S}^{a''_S}\frac{\Delta}{1-x_S}\,d\ln a_S \qquad (114)$$

Using the activity coefficient f_S of the non-aqueous component,

$$d\ln a_S = d\ln x_S + d\ln f_S \qquad (115)$$

for small differences between x'_S and x''_S the integral in Eq. (114) may be replaced by its average value:

$$E_+ \cong -\frac{RT}{F}\frac{(x''_S - x'_S)\,\Delta}{(1-x_S)\,x_S}\left(1+\frac{\partial\ln f_S}{\partial\ln x_S}\right) \qquad x_S = \frac{1}{2}(x'_S + x''_S) \qquad (116)$$

Cell (D) has been used several times to determine the solvent transference number Δ of the sparingly soluble salt Ag_2SO_4 in the binary solvent mixtures: acetonitrile-water[144], dimethylsulphoxide-water[50] and dimethylsulphoxide-methanol[145]. In Fig. 3 the solvent transference number of Ag_2SO_4 is plotted versus $x_{DMSO} = 1 - x_{MeOH}$. Additionally, the Washburn number w_{DMSO} has been calculated using Eq. (97) and is also plotted versus x_{DMSO}. With $x_{DMSO} \to 1$ the Washburn number w_{DMSO} tends versus 4 and, though w_{DMSO} is quite different from the coordination number of Ag^+ from nmr chemical shift measurements[39], the agreement of the results indicates that the contribution of the sulphate ion is of minor importance.

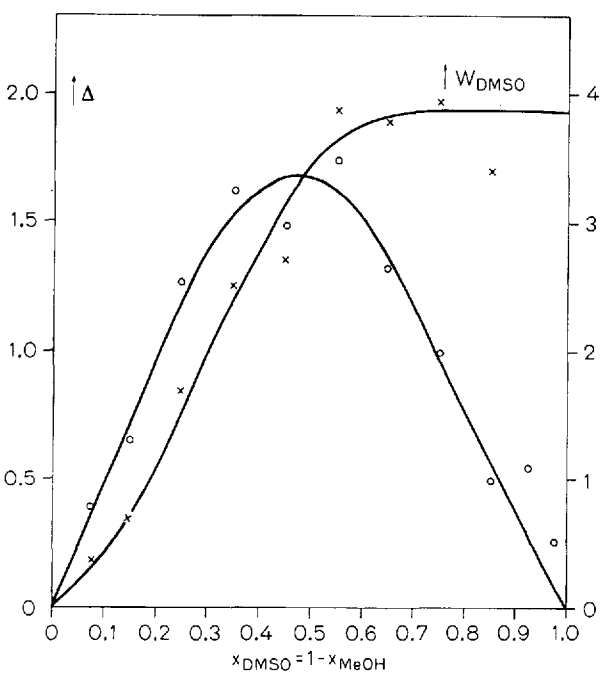

Fig. 3. Solvent transport number, Δ, and Washburn number, w_{DMSO}, for Ag_2SO_4 in methanol-DMSO mixtures at 25 °C

V. References

[1] Zwanzig, R.: J. Chem. Phys. *52*, 3625 (1970).
[2] Fratiello, A., in: Progr. inorg. chem. (ed. J. O. Edwards), Vol. 17, pp. 57–92. New York: Interscience 1972.
[3] Taube, H.: Electron transfer reactions of complex ions in solution, pp. 6–10. New York: Academic Press 1970.
[4] Safford, G. J., Leung, P. S., in: Techniques of electrochemistry (eds. E. Yeager and A. J. Salkind), Vol. 2, pp. 173–289. New York: J. Wiley & Sons 1973.
[5] Moolel, M., Schneider, H.: Z. physik. Chem., N. F. *74*, 237 (1971);
Benter, G., Schneider, H.: Ber. Bunsenges. physik. Chem. *77*, 997 (1973).
[6] Debye, P., McAulay, J.: Physik. Z. *26*, 22 (1925).
[7] Padova, J.: J. Phys. Chem. *72*, 796 (1968);
Padova, J. I., in: Modern aspects of electrochemistry (eds. B. E. Conway and J. O'M. Bockris), Vol. 7, pp. 1–82. London: Butterworths 1972.
[8] Hall, D. G.: Trans. Faraday Soc. *67*, 2516 (1971); J. C. S. Faraday, II *68*, 25 (1972); *69*, 1391 (1973).
[9] Parker, A. J., Alexander, R.: J. Amer. Chem. Soc. *90*, 3313 (1968);
Cox, B. G., Hedwig, G. R., Parker, A. J., Watts, D. W.: Austral. J. Chem. *27*, 477 (1974).
[10] Popovych, O.: Crit. Rev. Anal. Chem. *1*, 73 (1970).
[11] Kolthoff, I. M.: Pure and Appl. Chem. *25*, 305 (1971).
[12] Feakins, D., Bennetto, H. P.: Hydrogen-bonded solvent systems (eds. A. K. Covington and P. Jones), p. 235. London: Taylor & Francis 1968.
[13] Bates, R. G., in: Hydrogen-bonded solvent systems (eds. A. K. Covington and P. Jones), pp. 49–86. London: Taylor & Francis 1968.
Bates, R. G., in: Solute-solvent interaction (eds. J. F. Coetzee and C. D. Ritchie), p. 46–96. New York: Marcel Dekker 1969.
[14] Trémillon, B.: Chemistry in non-aqueous solvents. Dordrecht-Holland: D. Reidel Publ. Comp. 1974.
[15] Bauer, D., Breant, M., in: Electroanalytical chemistry (ed. A. J. Bard), Vol. 8, pp. 282–348. New York: Marcel Dekker 1975.
[16] Grunwald, E., Bacarella, A. L.: J. Amer. Chem. Soc. *80*, 3840 (1958);
Grunwald, E., Baughman, G., and Kohnstam, G.: J. Amer. Chem. Soc. *82*, 5801 (1960).
[17] Villermaux, S., Baudot, V., Delpuech, J. J.: Bull. Soc. Chim. France *1972*, 1781;
Rat, J. C., Villermaux, S., Delpuech, J. J.: Bull. Soc. Chim. France *1974*, 815;
Villermaux, S., Delpuech, J. J.: Bull. Soc. Chim. France 2534, 2541 (1974).
[18] Treiner, C., Bocquet, J. F., Chemla, M.: J. Chim. Phys. *70*, 472 (1973);
Treiner, C.: J. Amer. Chem. Soc. *70*, 1183 (1973);
Treiner, C., Finas, P.: J. Amer. Chem. Soc. *71*, 67 (1974).
[19] Izmailov, N. A.: Dokl. Akad. Nauk. SSSR *127*, 104 (1959); *149*, 884, 1103, 1364 (1963); Zh. Fiz. Khim. *23*, 639, 647 (1949).
[20] Feakins, D., Watson, P.: J. Chem. Soc. 4686, 4734 (1963).
[21] Alfenaar, M., De Ligny, C. L.: Rec. Trav. Chim. *86*, 929 (1967).
[22] Bax, D., De Ligny, C. L., Alfenaar, M.: J. Amer. Chem. Soc. *91*, 452 (1972).
[23] Latimer, W. M., Pitzer, K. S., Slansky, C. M.: J. Chem. Phys. *7*, 108 (1939).
[24] Strehlow, H.: Z. Elektrochem., Ber. Bunsenges. physik. Chem. *56*, 827 (1952);
Strehlow, H., in: The chemistry of non-aqueous solvents (ed. J. J. Lagowski), Vol. 1, Chapter 4. New York: Academic Press 1966.
[25] Koepp, H.-M., Wendt, H., Strehlow, H.: Z. Elektrochem., Ber. Bunsenges. physik. Chem. *64*, 483 (1960).
[26] Wells, C. F.: J. C. S. Faraday I *69*, 984 (1973); *70*, 694 (1974); *71*, 1868 (1975).
[27] Pleskov, W. A.: Usp. Chim. *16*, 254 (1947).
[28] Schroer, H. P., Vlček, A. A.: Z. anorg. Chem. *334*, 205 (1964).

[29] Gutmann, V., Wychera, E.: Inorg. Nucl. Chem. Letters *2*, 257 (1966);
Gutmann, V., Schmid, R.: Monatsh. Chem. *100*, 2113 (1969).
[30] Nelson, J. V., Iwamoto, R. T.: Anal. Chem. *33*, 1795 (1961); *35*, 867 (1963).
[31] Case, B., Hush, N. S., Parsons, R., Poever, M.: J. Electroanal. Chem. *10*, 360 (1965).
[32] Grunwald, E., in: Electrolytes (ed. B. Pesce), p. 62. Oxford: Pergamon Press 1962.
[33] Popovych, O.: Anal. Chem. *38*, 558 (1966).
[34] Alexander, R., Parker, A. J.: J. Amer. Chem. Soc. *89*, 5539 (1967).
[35] Parsons, R., Rubin, B. T.: J. C. S. Faraday I *70*, 1636 (1974).
[36] Parker, A. J., Alexander, R.: J. Amer. Chem. Soc. *90*, 3313 (1968).
[37] Alexander, R., Parker, A. J., Sharp, J. H., Waghorne, W. E.: J. Amer. Chem. Soc. *94*, 1148 (1972).
[38] Scatchard, G.: J. Amer. Chem. Soc. *75*, 2883 (1953).
[39] Behr, B., Gutknecht, J., Schneider, H., Stroka, J.: in preparation.
[40] Duschek, O., Gutmann, V.: Monatsh. Chem. *104*, 990 (1973).
[41] Diggle, J. W., Parker, A. J.: Electrochim. Acta *18*, 975 (1973).
[42] Alfenaar, M.: J. Phys. Chem. *79*, 2200 (1975).
[43] Coetzee, J. F., Campion, J. J.: J. Amer. Chem. Soc. *89*, 2513 (1967).
[44] L'Her, M., Morin-Bozec, D., Courtot-Coupez, J.: J. Electroanal. Chem. *55*, 133 (1974).
Cabon, J. Y., L'Her, M., Courtot-Coupez, J.: J. Amer. Chem. Soc. *64*, 219 (1975).
[45] Kundu, K. K., Rakshit, A. K., Das, M. N.: Electrochim. Acta, *17*, 1921 (1972);
Bose, K., Das, A. K., Kundu, K. K.: J. C. S. Faraday I *71*, 1838 (1975).
[46] Cox, B. G., Parker, A. J., Waghorne, W. E.: J. Phys. Chem. *78*, 1731 (1974).
[47] Barraqué, C., Vedel, J., Trémillon, B.: Bull. Soc. Chim. France *1968*, 3421.
[48] Massaux, J., Duyckaerts, G.: J. Electroanal. Chem. *59*, 311 (1975).
[49] Madec, C., Courtot-Coupez, J.: J. Electroanal. Chem. *54*, 123 (1974).
[50] El-Harakany, A. A., Schneider, H.: J. Electroanal. Chem. *46*, 255 (1973).
[51] Courtot-Coupez, J., Le Démézet, M., Laouenan, A., Madec, C.: J. Electroanal. Chem. *29*, 21 (1971).
[52] Clausen, A., El-Harakany, A. A., Schneider, H.: Ber. Bunsenges. physik. Chem. *77*, 994 (1973).
[53] Thomas, S., Reynolds, W. L.: Inorg. Chem. *9*, 78 (1970).
[54] Frankel, S., Stengle, T. R., Langford, C. H.: Canad. J. Chem. *46*, 3183 (1968).
[55] Safford, G., Schaffer, P. C., Leung, P. S.: J. Chem. Phys. *40*, 2140 (1967).
[56] Bockris, J. O'M., Reddy, A. K. N.: Modern electrochemistry, Vol. 1, pp. 117–132. New York: Plenum Press 1970.
[57] Gutmann, V.: Coordination chemistry in non-aqueous solutions. Wien: Springer 1968.
[58] King, E. J.: Acid-base equilibria, Oxford: Pergamon Press 1965.
[59] Marcus, M., Kertes, A. S.: Ion exchange and solvent extraction of metal complexes. New York 1969.
[60] Widmer, H. M.: Chimia *26*, 229 (1972).
[61] Grunwald, E., Baugham, G., Kohnstam, G.: J. Amer. Chem. Soc. *82*, 5801 (1960) (appendix).
[62] Covington, A. K., Lilley, T. H., Newman, K. E., Porthouse, G. A.: J. C. S. Faraday I *69*, 963 (1973) (Part 1);
Covington, A. K., Newman, K. E., Lilley, T. H.: J. C. S. Faraday I *69*, 973 (1973), (Part 2);
Covington, A. K., Lantzke, I. R., Thain, J. M.: J. C. S. Faraday I *70*, 1869 (1974) (Part 3);
Covington, A. K., Thain, J. M.: J. C. S. Faraday I *70*, 1879 (1974) (Part 4);
Covington, A. D., Covington, A. K.: J. C. S. Faraday I *71*, 831 (1975).
[63] Leffler, J. E., Grunwald, E.: Rates and equilibria of organic reactions. New York: J. Wiley 1963.
[64] Kebarle, P., in: Ions and ion pairs in organic reactions (ed. M. Szwarc), Vol. 1, pp. 27–83. New York: Wiley-Interscience 1972; J. Amer. Chem. Soc. *96*, 3359 (1974).
[65] Bjerrum, J., Nielson, E. J.: Acta Chem. Scand. *2*, 297 (1948);
Bjerrum, J., Lamm, C. G.: Acta Chem. Scand. *4*, 997 (1950);
Bjerrum, J.: Metal Ammine Formation in aqueous solution, P. Haase and Son, Copenhagen, 1957.

66) Davies, M. M.: Acid-base behavior in aprotic organic solvents, Nat. Bur. Standards Monograph *1968*, 105.
67) Kolthoff, I. M., Chantooni, Jr., M. K.: J. Amer. Chem. Soc. *90*, 3320 (1968).
Chantooni, Jr., M. K., Kolthoff, I. M.: J. Amer. Chem. Soc. *92*, 2236 (1970).
68) Kondo, Y., Tokura, N.: Bull. Chem. Soc. Japan *45*, 818 (1972).
69) Larson, R. C., Iwamoto, R. T.: Inorg. Chem. *1*, 316 (1962).
70) Manahan, S. E., Iwamoto, R. T.: J. Electroanal. Chem. *14*, 213 (1967).
71) Luehrs, D. C.: J. Inorg. Nucl. Chem. *33*, 2701 (1971).
72) Luehrs, D. C., Nicholas, R. W., Hamm, D. A.: J. Electroanal. Chem. *29*, 417 (1971).
73) Luehrs, D. C.: J. Inorg. Nucl. Chem. *34*, 791 (1972).
74) Izutsu, K., Nomura, T., Nakamura, T., Kazama, H., Nakajima, S.: Bull. Chem. Soc. Japan *47*, 1657 (1974).
75) D'Aprano, A., Fuoss, R. M.: J. Phys. Chem. *67*, 1722 (1963).
76) Treiner, C., Quintin, M., Fuoss, R. M.: J. Chim. Phys. *63*, 320 (1966).
77) Fuoss, R. M., Accascina, F.: Electrolytic conductance. New York: Interscience 1959.
78) D'Aprano, A., Fuoss, R. M.: J. Phys. Chem. *67*, 1871 (1963); *73*, 223, 400 (1969).
79) Moolel, M., Schneider, H.: to be published.
80) Witschonke, C. R., Kraus, C. A.: J. Amer. Chem. Soc. *69*, 2472 (1947).
81) a) Ralph, E. R., Gilkerson, W. R.: J. Amer. Chem. Soc. *86*, 4783 (1964);
b) Ezell, J. B., Gilkerson, W. R.: J. Phys. Chem. *68*, 1581 (1964);
c) Gilkerson, W. R., Ralph, E. R.: J. Amer. Chem. Soc. *87*, 175 (1965);
d) Gilkerson, W. R., Ezell, J. B.: J. Amer. Chem. Soc. *87*, 3812 (1965);
e) Ezell, J. B., Gilkerson, W. R.: J. Phys. Chem. *72*, 144 (1968);
f) Ezell, J. B., Gilkerson, W. R.: J. Amer. Chem. Soc. *88*, 3486 (1966);
g) Gilkerson, W. R., Ezell, J. B.: J. Amer. Chem. Soc. *89*, 808 (1967);
h) Flora, H. B., Gilkerson, W. R.: J. Amer. Chem. Soc. *92*, 3273 (1970);
i) Aitken, H. W., Gilkerson, W. R.: J. Amer. Chem. Soc. *95*, 8551 (1973);
j) Flora, H. B., Gilkerson, W. R.: J. Phys. Chem. *77*, 1421 (1973);
k) Junker, M. L., Gilkerson, W. R.: J. Amer. Chem. Soc. *97*, 493 (1975).
82) Shedlovsky, T.: J. Franklin Inst. 275 (1938).
83) Chantooni, Jr., M. K., Kolthoff, I. M.: J. Amer. Chem. Soc. *89*, 1582 (1967).
84) Chantooni, Jr., M. K., Kolthoff, I. M.: J. Amer. Chem. Soc. *92*, 2236 (1970).
85) Benoit, R. L., Lam, S. Y.: J. Amer. Chem. Soc. *96*, 7385 (1974).
86) Bjerrum, J., Jørgensen, C. K.: Acta Chem. Scand. *7*, 951 (1953).
87) Jørgensen, C. K.: Acta Chem. Scand. *8*, 175 (1954).
88) Minc, S., Libus, W.: Roczniki Chem. *29*, 1073 (1955).
89) Friedman, N. J., Plane, R. A.: Inorg. Chem. *2*, 11 (1963).
90) Kuntz, J. D., Cheng, C. J.: J. Amer. Chem. Soc. *97*, 4852 (1975).
91) Lincoln, S. F.: Coord. Chem. Rev. *6*, 309 (1971).
92) Covington, A. K., Lilley, T. H., in: Specialist periodical reports: electrochemistry, Vol. 1, pp. 42–53. London: Chemical Society 1970.
93) Thomas, S., Reynolds, W. L.: Inorg. Chem. *9*, 78 (1970).
94) Olander, D. P., Marinelli, R. S., Larson, R. C.: Anal. Chem. *41*, 1097 (1969).
95) Delpuech, J. J., Peguy, A., Khaddar, M. R.: J. Electroanal. Chem. *29*, 31 (1971).
96) Delpuech, J. J., Peguy, A., Khaddar, M. R.: J. Magn. Res. *6*, 325 (1972).
97) Supran, L. D., Sheppard, N.: J. C. S., Chem. Comm. *1967*, 832.
98) Green, R. D., Sheppard, N.: J. C. S. Faraday II *68*, 821 (1972).
99) Toma, F., Villemín, M., Thiéry, J. M.: J. Phys. Chem. *77*, 1294 (1973).
100) Gudlin, D., Schneider, H.: J. Magn. Res. *16*, 362 (1974).
101) Benter, G.: Thesis, Göttingen, 1975.
102) Schneider, H., Strehlow, H.: Z. Physik. Chem., N.F. *49*, 44 (1966).
103) Schaschel, E., Day, M. C.: J. Amer. Chem. Soc. *90*, 503 (1968).
104) a) Maxey, B. W., Popov, A. I.: J. Amer. Chem. Soc. *90*, 4470 (1968);
b) Wuepper, J. L., Popov, A. I.: J. Amer. Chem. Soc. *91*, 4352 (1969);
c) Wuepper, J. W., Popov, A. I.: J. Amer. Chem. Soc. *92*, 1493 (1970);
d) Wong, M. G., McKinney, W. J., Popov, A. I.: J. Phys. Chem. *75*, 56 (1971).

105) Yeager, H. L., Fedyk, J. D., Parker, R. J.: J. Phys. Chem. *77*, 2407 (1973).
106) Popov, A. I., in: Non-aqueous solutions (ed. V. Gutmann), p. 273. London: Butterworths 1975; Pure and Appl. Chem. *41*, 275 (1975).
107) Cogley, D. R., Butler, J. N., Grunwald, E.: J. Phys. Chem. *75*, 1477 (1971).
108) Stockton, G. W., Martin, J. S.: J. Amer. Chem. Soc. *94*, 6921 (1972).
109) Green, R. D., Martin, J. S.: J. Amer. Chem. Soc. *90*, 3659 (1968).
110) Martin, J. S., Hayami, J. J., Lemieux, R. U.: Canad. J. Chem. *46*, 3263 (1968).
111) Green, R. D., Martin, J. S., McG. Cassie, W. B., Hyne, J. B.: Canad. J. Chem. *47*, 1639 (1969).
112) Benoit, R. L., Buisson, C.: Inorg. Chim. Acta *7*, 256 (1973).
113) Benoit, R. L., Lam, S. Y.: Canad. J. Chem. *53*, 2683 (1975).
114) Haas, Y., Navon, G.: J. Phys. Chem. *76*, 1449 (1972).
115) Barcza, L., Pope, M. T.: J. Phys. Chem. *77*, 1795 (1973).
116) Barcza, L., Pope, M. T.: J. Phys. Chem. *78*, 168 (1974).
117) Greenberg, M. S., Popov, A. I.: Spectrochim. Acta *31A*, 697 (1975).
118) Noyes, A. A., Falk, K. G.: J. Amer. Chem. Soc. *33*, 1436 (1911).
119) Spiro, M.: J. Chem. Educ. *33*, 464 (1956).
120) Haase, R.: Thermodynamics of irreversible processes. Reading, Massachusetts: Addison-Wesley Publ. Comp. 1969.
121) de Groot, S. R., Mazur, P.: Non-equilibrium thermodynamics. Amsterdam: North-Holland Publ. Comp. 1962.
122) Spiro, M.: Determinations of transference numbers, in: Physical methods of organic chemistry (ed. A. Weissberger), Vol. IV, pp. 3049–3111. New York: Interscience 1960.
123) Staverman, A. J.: Trans. Faraday Soc. *48*, 176 (1952).
124) Agar, J. N., in: The structure of electrolytic solutions (ed. W. J. Hamer), p. 200. New York: Wiley 1959.
125) Wagner, C., in: Advances in electrochemistry and electrochemical engineering (eds. P. Delahay and C. W. Tobias), Vol. 4, pp. 1–46. New York: Wiley-Interscience 1966.
126) Haase, R.: Z. Elektrochem., Ber. Bunsenges. physik. Chem. *62*, 279 (1958).
127) Nernst, W.: Gött. Nachr. *1900*, 68.
128) Feakins, D.: J. Chem. Soc. *1961*, 5308.
129) Strehlow, H., Koepp, H.-M.: Z. Elektrochem., Ber. Bunsenges. physik. Chem. *62*, 373 (1958).
130) Spiro, M., in: Physical chemistry of organic solvent systems (eds. A. K. Covington and T. Dickinson), pp. 630–633. London: Plenum Press 1973.
131) Schneider, H., Strehlow, H.: Z. Elektrochem., Ber. Bunsenges. physik. Chem. *66*, 309 (1962);
132) Schneider, H., Strehlow, H.: Ber. Bunsenges. physik. Chem. *69*, 674 (1965).
133) Viehweger, U., Emons, H.-H.: Z. anorg. allgem. Chem. *383*, 183 (1971).
134) Strehlow, H., Schneider, H.: Pure and Applied Chemistry *25*, 327 (1971).
135) Feakins, D., Lorimer, J. P.: J. C. S., Faraday I *70*, 1888 (1974).
136) Feakins, D., Lorimer, J. P.: J. C. S., Chem. Comm. *1971*, 646.
137) Feakins, D., Khoo, K. K., Lorimer, J. P., Voice, P. J.: J. C. S., Chem. Comm. *1972*, 1336.
138) Feakins, D., Hickey, B. E., Lorimer, J. P.. O'Shaughnessy, D. A., Voice, P. J.: J. Electroanal. Chem. *54*, 443 (1974).
139) Alfenaar, M., De Ligny, C. L., Remijnse, A. G.: Rec. Trav. Chim. *86*, 986 (1967).
140) De Ligny, C. L., Remijnse, A. G., van der Veen, N. G.: J. Electroanal. Chem. *45*, 488 (1973).
141) Khoo, K. H.: J. C. S., Faraday I *69*, 1313 (1973).
142) Khoo, K. H.: Austral. J. Chem. *26*, 1797 (1973).
143) Khoo, K. H., Chee-Yan, C.: J. C. S., Faraday I *71*, 446 (1975).
144) Schneider, H., in: Solute-solvent interaction (eds. J. F. Coetzee and C. D. Ritchie), pp. 313–315. New York: Marcel Dekker 1969.
145) Rodehüser, L., Schneider, H.: Z. physik. Chem., N.F. *100*, 119 (1976).

Received January 7, 1976

Author Index Volumes 26 - 68

The volume numbers are printed in italics

Albini, A., and Kisch, H.: Complexation and Activation of Diazenes and Diazo Compounds by Transition Metals. *65*, 105–145 (1976).

Altona, C., and Faber, D. H.: Empirical Force Field Calculations. A Tool in Structural Organic Chemistry. *45*, 1–38 (1974).

Anderson, J. E.: Chair-Chair Interconversion of Six-Membered Rings. *45*, 139–167 (1974).

Anet, F. A. L.: Dynamics of Eight-Membered Rings in Cyclooctane Class. *45*, 169–220 (1974).

Ariëns, E. J., and Simonis, A.-M.: Design of Bioactive Compounds. *52*, 1–61 (1974).

Aurich, H. G., and Weiss, W.: Formation and Reactions of Aminyloxides. *59*, 65–111 (1975).

Bardos, T. J.: Antimetabolites: Molecular Design and Mode of Action. *52*, 63–98 (1974).

Barnes, D. S., see Pettit, L. D.: *28*, 85–139 (1972).

Bauer, S. H., and Yokozeki, A.: The Geometric and Dynamic Structures of Fluorocarbons and Related Compounds. *53*, 71–119 (1974).

Baumgärtner, F., and Wiles, D. R.: Radiochemical Transformations and Rearrangements in Organometallic Compounds. *32*, 63–108 (1972).

Bernauer, K.: Diastereoisomerism and Diastereoselectivity in Metal Complexes. *65*, 1–35 (1976).

Boettcher, R. J., see Mislow, K.: *47*, 1–22 (1974).

Brandmüller, J., and Schrötter, H. W.: Laser Raman Spectroscopy of the Solid State. *36*, 85–127 (1973).

Bremser, W.: X-Ray Photoelectron Spectroscopy. *36*, 1–37 (1973).

Breuer, H.-D., see Winnewisser, G.: *44*, 1–81 (1974).

Brewster, J. H.: On the Helicity of Variously Twisted Chains of Atoms. *47*, 29–71 (1974).

Brocas, J.: Some Formal Properties of the Kinetics of Pentacoordinate Stereoisomerizations. *32*, 43–61 (1972).

Brunner, H.: Stereochemistry of the Reactions of Optically Active Organometallic Transition Metal Compounds. *56*, 67–90 (1975).

Buchs, A., see Delfino, A. B.: *39*, 109–137 (1973).

Bürger, H., and Eujen, R.: Low-Valent Silicon. *50*, 1–41 (1974).

Butler, R. S., and deMaine, A. D.: CRAMS – An Automatic Chemical Reaction Analysis and Modeling System. *58*, 39–72 (1975).

Caesar, F.: Computer-Gas Chromatography. *39*, 139–167 (1973).
Čársky, P., and Zahradník, R.: MO Approach to Electronic Spectra of Radicals. *43*, 1–55 (1973).
Chandra, P.: Molecular Approaches for Designing Antiviral and Antitumor Compounds. *52*, 99–139 (1974).
Chapuisat, X., and Jean, Y.: Theoretical Chemical Dynamics: A Tool in Organic Chemistry. *68*, 1–57 (1976).
Christian, G. D.: Atomic Absorption Spectroscopy for the Determination of Elements in Medical Biological Samples. *26*, 77–112 (1972).
Clark, G. C., see Wasserman, H. H.: *47*, 73–156 (1974).
Clerc, T., and Erni, F.: Identification of Organic Compounds by Computer-Aided Interpretation of Spectra. *39*, 91–107 (1973).
Clever, H.: Der Analysenautomat DSA-560. *29*, 29–43 (1972).
Connors, T. A.:Alkylating Agents. *52*, 141–171 (1974).
Craig, D. P. and Mellor, D. P.: Discriminating Interactions Between Chiral Molecules. *63*, 1–48 (1976).
Cram, D. J., and Cram, J. M.: Stereochemical Reaction Cycles. *31*, 1–43 (1972).
Gresp, T. M., see Sargent, M. V.: *57*, 111–143 (1975).

Dauben, W. G., Lodder, G., and Ipaktschi, J:: Photochemistry of β,γ-Unsatuared Ketones. *54*, 73–114 (1974).
DeClercq, E.: Synthetic Interferon Inducers. *52*, 173–198 (1974).
Degens, E. T.: Molecular Mechanisms on Carbonate, Phosphate, and Silica Deposition in the Living Cell. *64*, 1–112 (1976).
Delfino, A. B., and Buchs, A.: Mass Spectra and Computers. *39*, 109–137 (1973).
DeMaine, A. D., see Butler, R. S.: *58*, 39–72 (1975).
DePuy, C. H.: Stereochemistry and Reactivity in Cyclopropane Ring-Cleavage by Electrophiles. *40*, 73–101 (1973).
Devaquet, A.: Quantum-Mechanical Calculations of the Potential Energy Surface of Triplet States. *54*, 1–71 (1974).
Dimroth, K.: Delocalized Phosphorus-Carbon Double Bonds. Phosphamethincyanines, λ^3-Phosphorins and λ^5-Phosphorins. *38*, 1–150 (1973).
Döpp, D.: Reactions of Aromatic Nitro Compounds *via* Excited Triplet States. *55*, 49–85 (1975).
Dougherty, R. C.: The Relationship Between Mass Spectrometric, Thermolytic and Photolytic Reactivity. *45*, 93–138 (1974).
Dryhurst, G.: Electrochemical Oxidation of Biologically-Important Purines at the Pyrolytic Graphite Electrode. Relationship to the Biological Oxidation of Purines. *34*, 47–85 (1972).
Dürr, H.: Reactivity of Cycloalkene-carbenes. *40*, 103–142 (1973).
Dürr, H.: Triplet-Intermediates from Diazo-Compounds (Carbenes). *55*, 87–135 (1975).
Dürr, H., and Kober, H.: Triplet States from Azides. *66*, 89–114 (1976).
Dürr, H., and Ruge, B.: Triplet States from Azo Compounds. *66*, 53–87 (1976).

Dugundji, J., and Ugi, I.: An Algebraic Model of Constitutional Chemistry as a Basis for Chemical Computer Programs. *39*, 19–64 (1973).

Eglinton, G., Maxwell, J. R., and Pillinger, C. T.: Carbon Chemistry of the Apollo Lunar Samples. *44*, 83–113 (1974).
Eicher, T., and Weber, J. L.: Structure and Reactivity of Cyclopropenones and Triafulvenes. *57*, 1–109 (1975).
Erni, F., see Clerc, T.: *39*, 139–167 (1973).
Eujen, R., see Bürger, H.: *50*, 1–41 (1974).

Faber, D. H., see Altona, C.: *45*, 1–38 (1974).
Fietzek, P. P., and Kühn, K.: Automation of the Sequence Analysis by Edman Degradation of Proteins and Peptides. *29*, 1–28 (1972).
Finocchiaro, P., see Mislow, K.: *47*, 1–22 (1974).
Fischer, G.: Spectroscopic Implications of Line Broadening in Large Molecules. *66*, 115–147 (1976).
Fluck, E.: The Chemistry of Phosphine. *35*, 1–64 (1973).
Flygare, W. H., see Sutter, D. H.: *63*, 89–196 (1976).
Fowler, F. W., see Gelernter, H.: *41*, 113–150 (1973).
Freed, K. F.: The Theory of Raditionless Processes in Polyatomic Molecules. *31*, 105–139 (1972).
Fritz, G.: Organometallic Synthesis of Carbosilanes. *50*, 43–127 (1974).
Fry, A. J.: Stereochemistry of Electrochemical Reductions. *34*, 1–46 (1972).

Ganter, C.: Dihetero-tricycloadecanes. *67*, 15–106 (1976).
Gasteiger, J., Gillespie, P., Marquarding, D., and Ugi, I.: From van't Hoff to Unified Perspectives in Molecular Structure and Computer-Oriented Representation. *48*, 1–37 (1974).
Geick, R.: IR Fourier Transform Spectroscopy. *58*, 73–186 (1975).
Geist, W., and Ripota, P.: Computer-Assisted Instruction in Chemistry. *39*, 169–195 (1973).
Gelernter, H., Sridharan, N. S., Hart, A. J., Yen, S. C., Fowler, F. W., and Shue, H.-J.: The Discovery of Organic Synthetic Routes by Computer. *41*, 113–150 (1973).
Gerischer, H., and Willig, F.: Reaction of Excited Dye Molecules at Electrodes. *61*, 31–84 (1976).
Gillespie, P., see Gasteiger, J.: *48*, 1–37 (1974).
Gleiter, R., and Gygax, R.: No-Bond-Resonance Compounds, Structure, Bonding and Properties. *63*, 49–88 (1976).
Guibé, L.: Nitrogen Quadrupole Resonance Spectroscopy. *30*, 77–102 (1972).
Gundermann, K.-D.: Recent Advances in Research on the Chemiluminescence of Organic Compounds. *46*, 61–139 (1974).
Gust, D., see Mislow, K.: *47*, 1–22 (1974).
Gutman, I., and Trinajstić, N.: Graph Theory and Molecular Orbitals. *42*, 49–93 (1973).
Gutmann, V.: Ionic and Redox Equilibria in Donor Solvents. *27*, 59–115 (1972).
Gygax, R., see Gleiter, R.: *63*, 49–88 (1976).

Haaland, A.: Organometallic Compounds Studied by Gas-Phase Electron Diffraction. *53*, 1–23 (1974).
Häfelinger, G.: Theoretical Considerations for Cyclic (pd) π Systems. *28*, 1–39 (1972).
Hariharan, P. C., see Lathan, W. A.: *40*, 1–45 (1973).
Hart, A. J., see Gelernter, H.: *41*, 113–150 (1973).
Hartmann, H., Lebert, K.-H., and Wanczek, K.-P.: Ion Cyclotron Resonance Spectroscopy. *43*, 57–115 (1973).
Hehre, W. J., see Lathan, W. A.: *40*, 1–45 (1973).
Hendrickson, J. B.: A General Protocol for Systematic Synthesis Design. *62*, 49–172 (1976).
Hengge, E.: Properties and Preparations of Si-Si Linkages. *51*, 1–127 (1974).
Henrici-Olivé, G., and Olivé, S.: Olefin Insertion in Transition Metal Catalysis. *67*, 107–127 (1976).
Herndon, W. C.: Substituent Effects in Photochemical Cycloaddition Reactions. *46*, 141–179 (1974).
Höfler, F.: The Chemistry of Silicon-Transition-Metal Compounds. *50*, 129–165 (1974).

Ipaktschi, J., see Dauben, W. G.: *54*, 73–114 (1974).

Jacobs, P., see Stohrer, W.-D.: *46*, 181–236 (1974).
Jahnke, H., Schönborn, M., and Zimmermann, G.: Organic Dyestuffs as Catalysts for Fuel Cells. *61*, 131–181 (1976).
Jakubetz, W., see Schuster, P.: *60*, 1–107 (1975).
Jean, Y., see Chapuisat, X.: *68*, 1–57 (1976).

Jørgensen, C. K.: Continuum Effects Indicated by Hard and Soft Antibases (Lewis Acids) and Bases. *56*, 1–66 (1975).
Julg, A.: On the Description of Molecules Using Point Charges and Electric Moments. *58*, 1–37 (1975).

Kaiser, K. H., see Stohrer, W.-D.: *46*, 181–236 (1974).
Khaikin, L. S., see Vilkow, L.: *53*, 25–70 (1974).
Kisch, H., see Albini, A.: *65*, 105–145 (1976).
Kober, H., see Dürr, H.: *66*, 89–114 (1976).
Kompa, K. L.: Chemical Lasers. *37*, 1–92 (1973).
Kratochvil, B., and Yeager, H. L.: Conductance of Electrolytes in Organic Solvents. *27*, 1–58 (1972).
Krech, H.: Ein Analysenautomat aus Bausteinen, die Braun-Systematic. *29*, 45–54 (1972).
Kühn, K., see Fietzek, P. P.: *29*, 1–28 (1972).
Kutzelnigg, W.: Electron Correlation and Electron Pair Theories. *40*, 31–73 (1973).

Lathan, W. A., Radom, L., Hariharan, P. C., Hehre, W. J., and Pople, J. A.: Structures and Stabilities of Three-Membered Rings from *ab initio* Molecular Orbital Theory. *40*, 1–45 (1973).

Lebert, K.-H., see Hartmann, H.: *43*, 57–115 (1973).
Lodder, G., see Dauben, W. G.: *54*, 73–114 (1974).
Luck, W. A. P.: Water in Biologic Systems. *64*, 113–179 (1976).
Lucken, E. A. C.: Nuclear Quadrupole Resonance. Theoretical Interpretation. *30*, 155–171 (1972).

Mango, F. D.: The Removal of Orbital Symmetry Restrictions to Organic Reactions. *45*, 39–91 (1974).
Maki, A. H., and Zuclich, J. A.: Protein Triplet States. *54*, 115–163 (1974).
Margrave, J. L., Sharp., K. G., and Wilson, P. W.: The Dihalides of Group IVB Elements. *26*, 1–35 (1972).
Marius, W., see Schuster, P.: *60*, 1–107 (1975).
Marks, W.: Der Technicon Autoanalyzer. *29*, 55–71 (1972).
Marquarding, D., see Gasteiger, J.: *48*, 1–37 (1974).
Maxwell, J. R., see Eglinton, G.: *44*, 83–113 (1974).
Mead, C. A.: Permutation Group Symmetry and Chirality in Molecules. *49*, 1–86. (1974).
Meier, H.: Application of the Semiconductor Properties of Dyes Possibilities and Problems. *61*, 85–131 (1976).
Meller, A.: The Chemistry of Iminoboranes. *26*, 37–76 (1972).
Mellor, D. P., see Craig, D. P.: *63*, 1–48 (1976).
Michl, J.: Physical Basis of Qualitative MO Arguments in Organic Photochemistry. *46*, 1–59 (1974).
Minisci, F.: Recent Aspects of Homolytic Aromatic Substitutions. *62*, 1–48 (1976).
Mislow, K., Gust, D., Finocchiaro, P., and Boettcher, R. J.: Stereochemical Correspondence Among Molecular Propellers. *47*, 1–22 (1974).

Nakajima, T.: Quantum Chemistry of Nonbenzenoid Cyclic Conjugated Hydrocarbons. *32*, 1–42 (1972).
Nakajima, T.: Errata. *45*, 221 (1974).
Neumann, P., see Vögtle, F.: *48*, 67–129 (1974).

Oehme, F.: Titrierautomaten zur Betriebskontrolle. *29*, 73–103 (1972).
Olivé, S., see Henrici-Olivé, G.: *67*, 107–127 (1976).

Papoušek, D., and Špirko, V.: A New Theoretical Look at the Inversion Problem in Molecules. *68*, 59–102 (1976).
Pearson, R. G.: Orbital Symmetry Rules for Inorganic Reactions from Perturbation Theory. *41*, 75–112 (1973).
Perrin, D. D.: Inorganic Medicinal Chemistry. *64*, 181–216 (1976).
Pettit, L. D., and Barnes, D. S.: The Stability and Structure of Olefin and Acetylene Complexes of Transition Metals. *28*, 85–139 (1972).
Pignolet, L. H.: Dynamics of Intramolecular Metal-Centered Rearrangement Reactions of Tris-Chelate Complexes. *56*, 91–137 (1975).
Pillinger, C. T., see Eglinton, G.: *44*, 83–113 (1974).
Pople, J. A., see Lathan, W. A.: *40*, 1–45 (1973).

Puchelt, H.: Advances in Inorganic Geochemistry. *44*, 155–176 (1974).
Pullman, A.: Quantum Biochemistry at the All- or Quasi-All-Electrons Level. *31*, 45–103 (1972).

Quinkert, G., see Stohrer, W.-D.: *46*, 181–236 (1974).

Radom, L., see Lathan, W. A.: *40*, 1–45 (1973).
Rice, S. A.: Conjectures on the Structure of Amorphous Solid and Liquid Water. *60*, 109–200. (1975).
Rieke, R. D.: Use of Activated Metals in Organic and Organometallic Synthesis. *59*, 1–31 (1975).
Ripota, P., see Geist, W.: *39*, 169–195 (1973).
Rüssel, H. and Tölg, G.: Anwendung der Gaschromatographie zur Trennung und Bestimmung anorganischer Stoffe/Gas Chromatography of Inorganic Compounds. *33*, 1–74 (1972).
Ruge, B., see Dürr, H.: *66*, 53–87 (1976).

Sargent, M. V. and Cresp, T. M.: The Higher Annulenones. *57*, 111–143 (1975).
Schäfer, F. P.: Organic Dyes in Laser Technology. *61*, 1–30 (1976).
Schneider, H.: Ion Solvation in Mixed Solvents. *68*, 103–148 (1976).
Schönborn, M., see Jahnke, H.: *61*, 133–181 (1976).
Schrötter, H. W., see Brandmüller, J.: *36*, 85–127 (1973).
Schuster, P., Jakubetz, W., and Marius, W.: Molecular Models for the Solvation of Small Ions and Polar Molecules. *60*, 1–107 (1975).
Schutte, C. J. H.: The Infra-Red Spectra of Crystalline Solids. *36*, 57–84 (1973).
Scrocco, E., and Tomasi, J.: The Electrostatic Molecular Potential as a Tool for the Interpretation of Molecular Properties. *42*, 95–170 (1973).
Sharp, K. G., see Margrave, J. L.: *26*, 1–35 (1972).
Shue, H.-J., see Gelernter, H.: *41*, 113–150 (1973).
Simonetta, M.: Qualitative and Semiquantitative Evaluation of Reaction Paths. *42*, 1–47 (1973).
Simonis, A.-M., see Ariëns, E. J.: *52*, 1–61 (1974).
Smith, S. L.: Solvent Effects and NMR Coupling Constants. *27*, 117–187 (1972).
Špirko, V., see Papoušek, D.: *68*, 59–102 (1976).
Sridharan, N. S., see Gelernter, H.: *41*, 113–150 (1973).
Stohrer, W.-D., Jacobs, P., Kaiser, K. H., Wiech, G., and Quinkert, G.: Das sonderbare Verhalten elektronen-angeregter 4-Ringe-Ketone. – The Peculiar Behavior of Electronically Exited 4-Membered Ring Ketones. *46*, 181–236 (1974).
Stoklosa, H. J., see Wasson, J. R.: *35*, 65–129 (1973).
Suhr, H.: Synthesis of Organic Compounds in Glow and Corona Discharges. *36*, 39–56 (1973).
Sutter, D. H., and Flygare, W. H.: The Molecular Zeeman Effect. *63*, 89–196 (1976).

Thakkar, A. J.: The Coming of the Computer Age to Organic Chemistry. Recent Approaches to Systematic Synthesis Analysis. *39*, 3–18 (1973).
Tölg, G., see Rüssel, H.: *33*, 1–74 (1972).

Tomasi, J., see Scrocco, E.: *42*, 95–170 (1973).
Trinajstić, N., see Gutman, I.: *42*, 49–93 (1973).
Trost, B. M.: Sulfuranes in Organic Reactions and Synthesis. *41*, 1–29 (1973).
Tsuji, J.: Organic Synthesis by Means of Transition Metal Complexes: Some General Patterns. *28*, 41–84 (1972).
Turley, P. C., see Wasserman, H. H.: *47*, 73–156 (1974).

Ugi, I., see Dugundji, J.: *39*, 19–64 (1973).
Ugi, I., see Gasteiger, J.: *48*, 1–37 (1974).

Veal, D. C.: Computer Techniques for Retrieval of Information from the Chemical Literature. *39*, 65–89 (1973).
Vennesland, B.: Stereospecifity in Biology. *48*, 39–65 (1974).
Vepřek, S.: A Theoretical Approach to Heterogeneous Reactions in Non-Isothermal Low Pressure Plasma. *56*, 139–159 (1975).
Vilkov, L., and Khainkin, L. S.: Stereochemistry of Compounds Containing Bonds Between Si, P, S, Cl, and N or O. *53*, 25–70 (1974).
Vögtle, F., and Neumann, P.: [2.2] Paracyclophanes, Structure and Dynamics. *48*, 67–129 (1974).
Vollhardt, P.: Cyclobutadienoids. *59*, 113–135 (1975).

Wänke, H.: Chemistry of the Moon. *44*, 1–81 (1974).
Wagner, P. J.: Chemistry of Excited Triplet Organic Carbonyl Compounds. *66*, 1–52 (1976).
Wanczek, K.-P., see Hartmann, K.: *43*, 57–115 (1973).
Wasserman, H. H., Clark, G. C., and Turley, P. C.: Recent Aspects of Cyclopropanone Chemistry. *47*, 73–156 (1974).
Wasson, J. R., Woltermann, G. M., and Stoklosa, H. J.: Transition Metal Dithio- and Diselenophosphate Complexes. *35*, 65–129 (1973).
Weber, J. L., see Eicher, T.: *57*, 1–109 (1975).
Weiss, A.: Crystal Field Effects in Nuclear Quadrupole Resonance. *30*, 1–76 (1972).
Weiss, W., see Aurich, H. G.: *59*, 65–111 (1975).
Wentrup, C.: Rearrangements and Interconversion of Carbenes and Nitrenes. *62*, 173–251 (1976).
Werner, H.: Ringliganden-Verdrängungsreaktionen von Aromaten-Metall-Komplexen. *28*, 141–181 (1972).
Wiech, G., see Stohrer, W.-D.: *46*, 181–236 (1974).
Wild, U. P.: Characterization of Triplet States by Optical Spectrocsopy. *55*, 1–47 (1975).
Wiles, D. R., see Baumgärtner, F.: *32*, 63–108 (1972).
Willig, F., see Gerischer, H.: *61*, 31–84 (1976).
Wilson, P. W., see Margrave, J. L.: *26*, 1–35 (1972).
Winnewisser, G., Mezger, P. G., and Breuer, H. D.: Interstellar Molecules. *44*, 1–81 (1974).
Wittig, G.: Old and New in the Field of Directed Aldol Condensations. *67*, 1–14 (1976).

Woenckhaus, C.: Synthesis and Properties of Some New $NAD^{\oplus}$ Analogues. *52*, 199–223 (1974).

Woltermann, G. M., see Wasson, J. R.: *35*, 65–129 (1973).

Wrighton, M. S.: Mechanistic Aspects of the Photochemical Reactions of Coordination Compounds. *65*, 37–102 (1976).

Yeager, H. L., see Kratochvil, B.: *27*, 1–58 (1972).

Yen, S. C., see Gelernter, H.: *41*, 113–150 (1973).

Yokozeki, A., see Bauer, S. H.: *53*, 71–119 (1974).

Yoshida, Z.: Heteroatom-Substituted Cyclopropenium Compounds. *40*, 47–72 (1973).

Zahradník, R., see Čársky, P.: *43*, 1–55 (1973).

Zeil, W.: Bestimmung der Kernquadrupolkopplungskonstanten aus Mikrowellenspektren. *30*, 103–153 (1972).

Zimmermann, G., see Jahnke, H.: *61*, 133–181 (1976).

Zoltewicz, J. A.: New Directions in Aromatic Nucleophilic Substitution. *59*, 33–64 (1975).

Zuclich, J. A., see Maki, A. H.: *54*, 115–163 (1974).